KGS
OF
93-60

STRATIGRAPHY, PETROLOGY, DIAGENESIS, AND DEPOSITIONAL ENVIRONMENTS OF THE PENNSYLVANIAN (MISSOURIAN) CHANUTE SHALE, SOUTHEASTERN KANSAS, NORTHEASTERN OKLAHOMA

by

Sonia I. Fernández

A thesis submitted in partial fulfillment
of the requirements for the Master of
Science degree in Geology
in the Graduate College of
The University of Iowa

August 1993

Thesis supervisor: Associate Professor Robert L. Brenner

KANSAS GEOLOGICAL SURVEY
OPEN-FILE REPORT 93-60

STRATIGRAPHY, PETROLOGY, DIAGENESIS, AND DEPOSITIONAL ENVIRONMENTS OF THE PENNSYLVANIAN (MISSOURIAN) CHANUTE SHALE, SOUTHEASTERN KANSAS, NORTHEASTERN OKLHAOMA

By

S. I. Fernandez

Disclaimer

The Kansas Geological Survey does not guarantee this document to be free from errors or inaccuracies and disclaims any responsibility or liability for interpretations based on data used in the production of this document or decisions based thereon. This report is intended to make results of research available at the earliest possible date, but is not intended to constitute final or formal publications.

Kansas Geological Survey
1930 Constant Avenue
University of Kansas
Lawrence, KS 66047-3726

Graduate College
The University of Iowa
Iowa City, Iowa

CERTIFICATE OF APPROVAL

MASTER'S THESIS

This is to certify that the Master's thesis of

Sonia I. Fernández

has been approved by the Examining Committee for the thesis requirement for the Master of Science degree in Geology at the August 1993 graduation.

Thesis committee: Robert Bremner
Thesis supervisor

Philip D Heckel
Member

Greg Ludvigson
Member

ACKNOWLEDGMENTS

I would like to thank Dr. Lynn Watney, John French, and the people of the Kansas Geological Survey for their help during field work and sample collection of this study. I would also like to thank Dr. Robert L. Brenner, Dr. Luis González, Dr. P. H. Heckel, the Department of Geology at The University of Iowa, Dr. Greg Ludvigson and the Iowa Geological Survey for their help, support and helpful comments during the project.

Special thanks to Héctor M. Ruiz for bearing with me during the hard times.

ABSTRACT

The Upper Pennsylvanian (Missourian) Chanute Shale consists of the lower Chanute, the Thayer Coal and the upper Chanute members. Deposited in fluvial to transitional paralic environments during a marine transgression, the lower Chanute represents fluvial channels grading into a fluvially-dominated delta, whereas the upper Chanute represents a funnel-shaped estuarine environment. Isolith and isopach maps show the thickest deposits are located in the south, within the Noxie channels area, thinning towards the north and west from the outcrop belt. The source of sediments for both members are the Ouachita Mountains, south to southeast of the study area.

The Chanute consists of coarse silt to medium-grained quartz arenites, sublitharenites, subarkoses, litharenites, feldspathic litharenites, to quartz, lithic and feldspathic wackes, that were exposed to strong diagenetic alterations in the meteoric and compactional regimes. Precipitation of early silica and calcite cements, formation of secondary porosity, chemical alteration of framework grains, and precipitation of authigenic clays and cements are some of the diagenetic features of the Chanute Shale. Many of the diagenetic changes observed in the late diagenesis of the Chanute sandstones are related to acidic compactional waters from adjacent shales and coals.

TABLE OF CONTENTS

Page

LIST OF FIGURES vii

LIST OF TABLES xi

CHAPTER I INTRODUCTION 1
- Previous work 3
- Tectonic setting 6
- Objectives 11
- Methods 11
  - Field work 11
  - Sample analysis 12
  - Well log analysis 13

CHAPTER II STRATIGRAPHY 14
- Stratigraphic overview 14
- The Chanute Shale and the cyclothem concept 24
- Subsurface relationships 28
  - Characterization of the Chanute interval in geophysical well logs 28
  - Thickness variations in the Chanute Shale interval 40
  - Sandstone distribution in the Chanute Shale 46
  - The Thayer Coal and associated (possible) marine horizon 51

CHAPTER III LITHOFACIES 56
- Definition of lithofacies 56
  - Interbedded fine sandstone and silty clay shale 56
  - Massive channeled sandstones 58
  - Gray, fissile, clayey shale 58
  - Silty shale 58
  - Mottled blocky mudstone 59
  - Coal 59

Thinly-bedded, thinly-laminated, micaceous sandstone....60
Carbonate cemented, contorted, fine micaceous sandstone....60
Interlaminated siltstone and shale....61
Lithofacies distribution....61

CHAPTER IV DEPOSITIONAL ENVIRONMENTS....64
Introduction....64
Lithofacies depositional environments....64
Interbedded fine sandstone and silty shale....64
Massive channeled sandstones....66
Silty shale....67
Blocky mudstone and coal....67
Interlaminated siltstone and shale....69
Thinly-bedded, thinly-laminated, micaceous sandstone, and carbonate cemented, contorted sandstone....70
The lower Chanute....70
The upper Chanute....78
Paleogeography....82

CHAPTER V SANDSTONE PETROGRAPHY....85
Introduction....85
Detrital constituents....85
Monocrystalline quartz....85
Polycrystalline quartz....87
Feldspars....87
Plagioclase....87
Orthoclase....88
Microcline....88
Perthite....88
Micas....91
Chert....91
Rock fragments....95
Carbonate skeletal fragments....98
Glauconite, pyrite, and heavy minerals....98
Organic matter....98
Authigenic minerals....99
Quartz overgrowths....99

Iron-oxide....99
Carbonate cements....101
Calcite cement....101
Ankerite....101
Dolomite....104
Clays....104
Porosity....107
Petrographic characteristics of the Noxie sandstone....107
Petrographic characteristics of the Cottage Grove sandstone....109
Cathodoluminescence....112

CHAPTER VI DIAGENESIS....113
Diagenetic characteristics of sandstones in the Chanute Shale....113
Secondary porosity....113
Early silica cementation....114
Dissolution and chemical alteration of labile grains....118
Precipitation of late kaolinite....123
Compaction....126
Chloritization of biotite and clays....127
Early Calcite Cement....128
Late calcite, dolomite and ankerite....129
Late diagenetic events....132
Paragenesis of the diagenetic events in the Chanute sandstones....134

CHAPTER VII SUMMARY AND CONCLUSIONS....142

APPENDIX I WELL-LOG DATA....145

APPENDIX II POINT COUNTS....179

APPENDIX III STRATIGRAPHIC COLUMNS....199

APPENDIX IV MICROPROBE DATA....213

REFERENCES CITED....216

LIST OF FIGURES

Figure Page

1. Idealized Kansas cyclothem....2
2. Location map of study area....4
3. Generalized stratigraphic column of the Chanute Shale and adjacent units....5
4. Pennsylvanian tectonic features in Kansas and Oklahoma....8
5. Sandstone exposure of the Noxie channels at the top of the Allin Hill outcrop, west of Coffeyville, Kansas....17
6. Thayer Coal and underclay exposed along the road south of Independence, Kansas....19
7. South Independence outcrop....20
8. Shale, underclay and Thayer Coal exposed at the Thayer Dam outcrop....21
9. Slabby Cottage Grove sandstone exposed at the top of the Thayer Dam outcrop....22
10. The slabby Cottage Grove sandstone towards the west of Thayer dam grades laterally into contorted beds towards the east of the dam....23
11. Contact between the Chanute Shale and the Iola Limestone exposed at the underpass of old US 169 and US 169....25

12. Location map of the geophysical well logs used in this study of the Chanute Shale. 29

13. Example of well log signatures for the Chanute Shale and surrounding units. 30

14. Proposed revision of Pennsylvanian (Missourian) stratigraphic nomenclature Kansas and Oklahoma. 32

15. Location map for cross sections through the study area. 34

16. Cross section through the Chanute Shale from Oklahoma (south) to Kansas (north). 35

17. Cross section through the Chanute Shale from east to west, across the northern part of the study area. 36

18. Cross section through the Chanute Shale from east to west, across the southern part of the study area. 37

19. Example of Chanute Shale well log signature. 38

20. Isopach map of the entire Chanute Shale interval. 41

21. Isopach of lower Chanute. 44

22. Isopach map of the upper Chanute. 45

23. Structural map of the base of the Chanute Shale 47

24. Isolith of the Noxie sandstone, lower Chanute. 48

25. Isolith of the Cottage Grove sandstone, upper Chanute. 50

26. Isolith of the Thayer Coal and the Chanute's marine horizon. 52

27. Cross section through the Chanute Shale from south to north, across the southern part of the study area 54

28. Relationships between sandstone characteristics, log signature, and depositional environment....57

29. Rhythmically spaced interlaminations in core Gaddy #1....62

30. Proposed depositional model for the Chanute Shale; A, B, C, D, E, F....73

31. Monocrystalline quartz (Q) in the Chanute sandstones....86

32. Microcline feldspar (M) showing partial dissolution along preferred twins....89

33. Perthite (P), SRF, and polycrystalline quartz (QP) grains in the Noxie sandstone....90

34. Biotite grain (B) in the Chanute sandstone showing partial chemical alteration to chlorite and clay....92

35. Detrital chlorite fragment (C) in the Chanute Shale....93

36. Chert fragment (C) showing a clear grain boundary around the interlocking quartz crystals....94

37. Metamorphic rock fragment (MRF), chert (C) and a foliated clay chip (schistose MRF). in the Chanute sandstones....96

38. Igneous rock fragments (IRF) in the Chanute consists of polymineralic (granitic) grains....97

39. Boxwork structures of iron-oxide are common in outcrop and core samples, with secondary porosity very often observed....100

40. The iron-oxide boxwork structures are observed in association with carbonates (ankerite: A) only in core samples....102

41. Poikilotopic calcite cement (C) is usually found in very small patches in the Chanute sandstones both in outcrop and in cores 103

42. Stained ankerite (A). 105

43. Kaolinite "books" (K) filling available pore space in the Chanute samples 106

44. Compositions of the Chanute Shale sandstones and wackes. 108

45. Concave convex contacts between quartz grains in the Chanute sandstones are common but not pervasive 110

46. Thin and discontinuous quartz overgrowths on detrital quartz grains (Q) 115

47. Plagioclase (PL) showing partial dissolution of preferred twins, and chemical alteration to sericite 119

48. Schistose MRF, SRF, and biotite (B) showing partial dissolution and chemical alteration of the detrital grains into clays 120

49. Kaolinite (K) and ankerite (A) filling a rhizome in a core sample of the Cottage Grove sandstone 124

50. When stained with a mix of potassium ferricyanide and alizarin red, ankerite (A) stains deep navy blue. 130

51. Boxwork iron-oxide structures (B) in the Chanute sandstones 133

52. Paragenetic diagram for the Chanute Shale sandstones. 135

53. Diagenetic model for the Chanute Shale sandstones; A, B, C, D. 136

LIST OF TABLES

Table		Page
1.	Tops and bottoms of the Chanute Shale members.	147
2.	Thicknesses and sand counts of the Chanute Shale members.	160
3.	Point counts of the Chanute Shale core and outcrop samples	180
4.	Microprobe data of the Chanute Shale sandstones	214

CHAPTER I
INTRODUCTION

The cyclic nature of the carbonate/siliciclastic platform deposits of the Midcontinent has been studied by geologists for over 60 years. These alternating sequences of thin limestones and siliciclastic units are thought to be the result of transgressive and regressive events. These sea level changes are related to the waxing and waning of the glaciers in Gondwana from Late Mississippian trough Middle Permian (Heckel, 1980; Bunker and others, 1988). Three types of cyclic patterns, better known as cyclothems, have been recognized; the Appalachian, the Illinois, and the Kansas cyclothems (Klein and Willard, 1989). The idealized "Kansas cyclothem" (Figure 1) is constituted by four main lithologic elements, although locally not all of them are present. These elements are: 1) The middle (transgressive) limestone, 2) the core shale, 3) the upper (regressive) limestone, and 4) the outside (nearshore) shale (Heckel, 1977). The characteristics of the Chanute Shale, the subject of this study, match those of the outside (nearshore) shale component of the idealized "Kansas Cyclothem."

Exposures of the Chanute Shale are found along the Pennsylvanian outcrop belt in northeastern Oklahoma, eastern

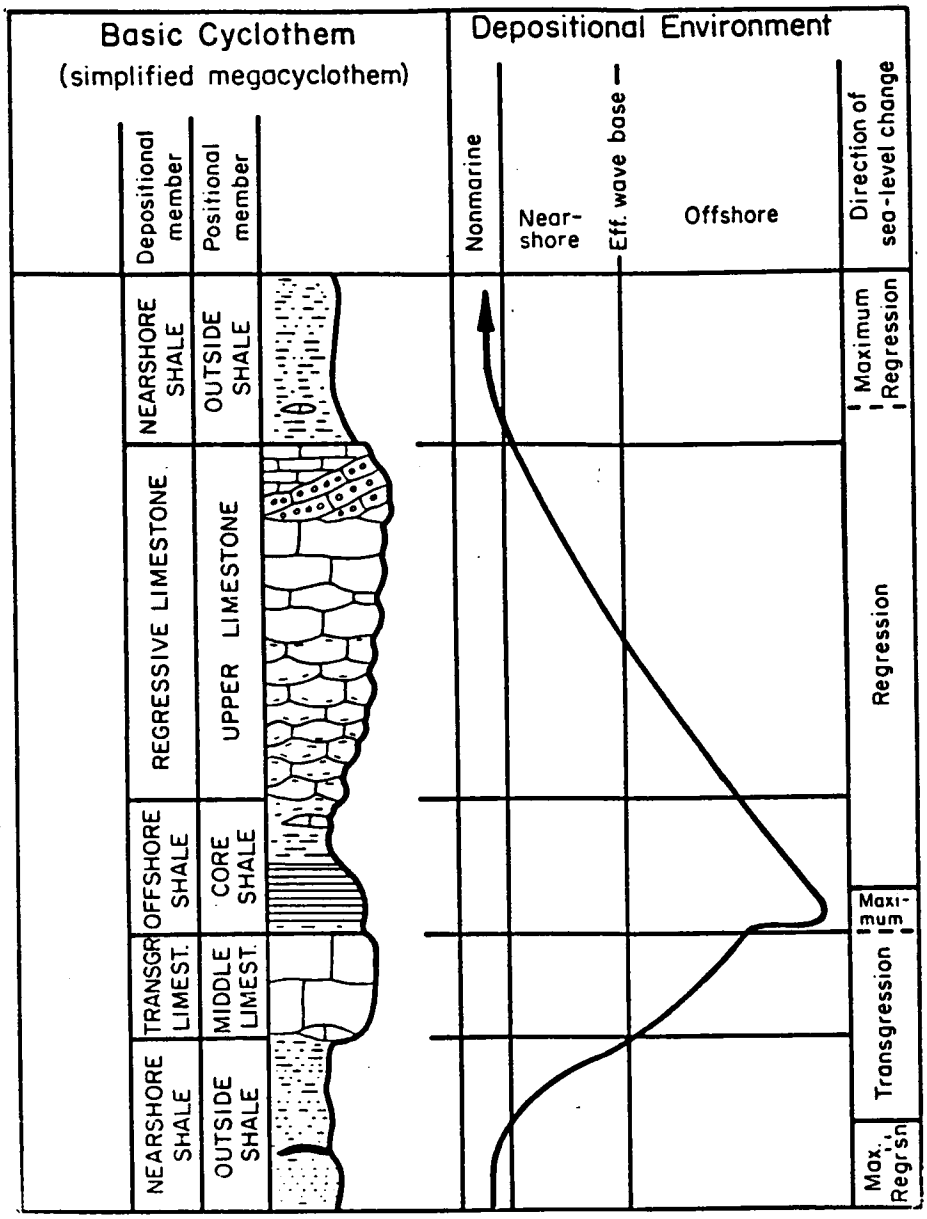


Figure 1. Idealized Kansas cyclothem, (modified from Heckel 1977).

Kansas, northwestern Missouri, southern Iowa, and southeastern Nebraska. The Chanute Shale is composed of fluvially derived sandstones, shales, and a thin coal in the area covered by this study, which includes northeastern Oklahoma and southeastern Kansas (Figure 2). This study focuses on 12 exposures along the Chanute outcrop belt, shown as squares in Figure 2, and two cores (circles) through the unit in Montgomery and Wilson counties Kansas, and geophysical well-logs from approximately 500 wells drilled throughout the study area.

Previous work

Initially described by Haworth and Kirk in 1894, the Chanute Shale was defined as the siliciclastic unit directly overlying the Drum Limestone (now known to be the Dewey Limestone in this region; Heckel, ms. in review) and directly underlying the Iola Limestone (Figure 3). Miscorrelation of the Iola by Haworth and Bennet in 1908 led to confusion and errors in the nomenclature and correlation of Missourian strata in the Midcontinent. Further work by Newell (1935) and Moore (1936; 1948) helped to correct most of these errors, thus correctly correlating the Iola, and Chanute formations northward. Newell (1935) named the upper sandstone body in the Chanute as the Cottage Grove member of the Chanute Shale, while Moore (1937) referred to the Noxie sandstone as "the prominent sandstone that forms the lower part of the Chanute." Schoewe (1944) studied the coal resources of the Thayer coal bed of the Chanute Shale in eastern Kansas. In this study, stratigraphic and

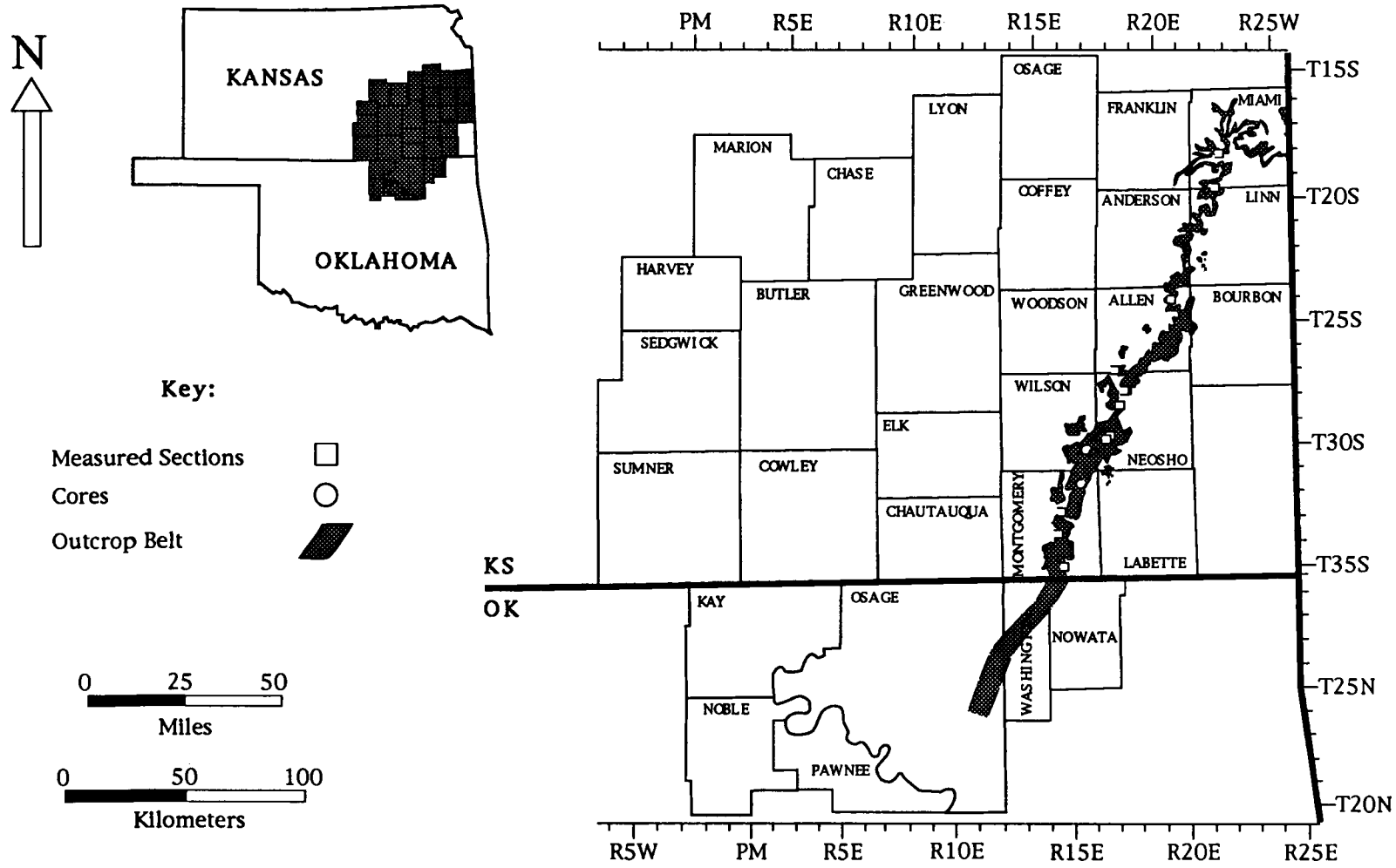


Figure 2. Location map of study area.

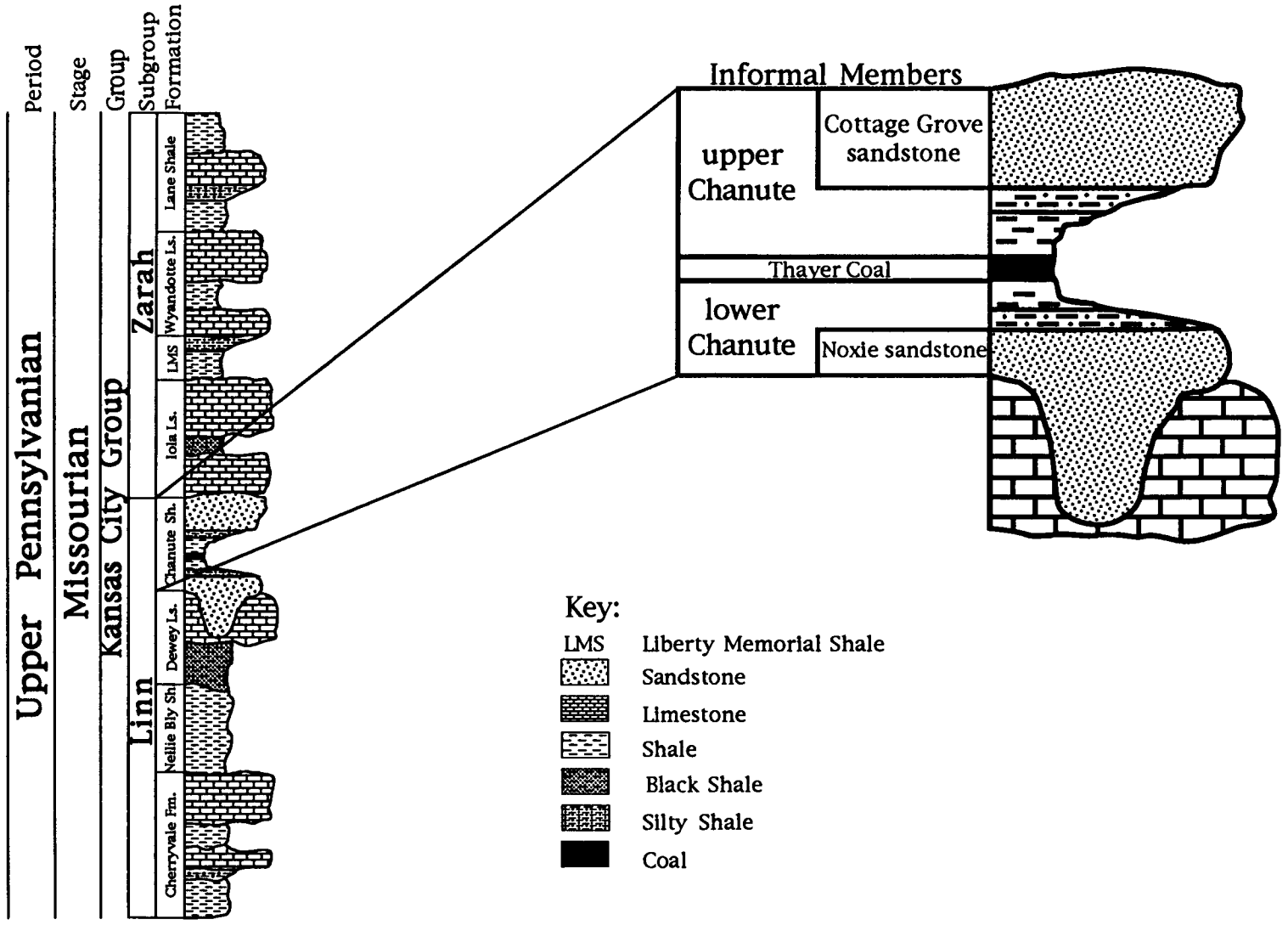


Figure 3. Generalized stratigraphic column of the Chanute Shale and adjacent units.

production information from the Thayer coal of the Chanute was disclosed. Continued studies by Condra (1949), Welp and others (1957), Oakes (1959),.and Hershey and others (1960) delineated the extent of the unit in other states and provided a basic description of its characteristics in outcrop. In a ground-water resource study, Seevers (1969) reported "an exposure of the Cottage Grove sandstone of the Chanute Formation topographically higher than the Iola limestone possibly as a result of limestone deposition around a mass of thickened sandstone" in Linn County, Kansas. This study also added some new information on the depositional environments of some of the Chanute members. More recent studies on the Chanute include a thesis in 1970 by Haggiaggi (Kansas University) on the stratigraphy and depositional environments of the Chanute, a study on depositional environments by Fruit and Elmore (1988) in the western subsurface, and a revision of Missourian stratigraphy by Heckel, (ms in review) which clarifies some recently recognized stratigraphic problems within the unit. The present study addresses the stratigraphy, petrographic characteristics, diagenetic history, and the depositional environments of parts of the Chanute Shale in southern Kansas, and adjacent Oklahoma.

Tectonic setting

The late Paleozoic collision between Laurussia and Gondwana marked a profound change in the tectonic framework of the Midcontinent. The pre-Absaroka unconformity (Sloss, 1963; North American sequences) represents this change where renewed uplift of

pre-existing structural features and erosional stripping of uplifted strata led to the development of a geologically complex land surface (Bunker and others, 1988).

The present thickness trends of Mississippian deposits reflect the extensive pre-Absaroka uplift and erosional event, especially in structurally positive features such as the Nemaha uplift and the Cambridge arch-Central Kansas uplift (Figure 4). As a result, Pennsylvanian strata (Morrowan through Missourian) onlap Precambrian to Late Mississippian rocks in the Midcontinent (Rascoe, and Adler, 1983). Two positive features, the Ouachita mountains and the Amarillo-Wichita-Arbuckle mountains, were formed during the late Early Pennsylvanian orogeny by folding and thrusting of previously deposited sediments of the older Ouachita basin and uplift of basement rocks respectively, resulting in the formation of two major negative features to the north, the Arkoma foredeep and the Anadarko intracratonic foreland basin. Both basins received great thicknesses of siliciclastic sediments from the nearby uplifted regions (Rascoe, and Adler, 1983) promoting further subsidence. The Arkoma basin joins northward with the Cherokee shelf, which is bordered by three structural features; the Nemaha uplift to the west-northwest, the Bourbon arch to the north and the Ozark uplift to the east. To the west of the Nemaha uplift two basins are present, the Salina basin on the north, and the Sedgwick basin towards the south. The Sedgwick basin merges south with the Anadarko basin. Both the Salina and the Sedgwick basins are bordered to the west by the Central Kansas

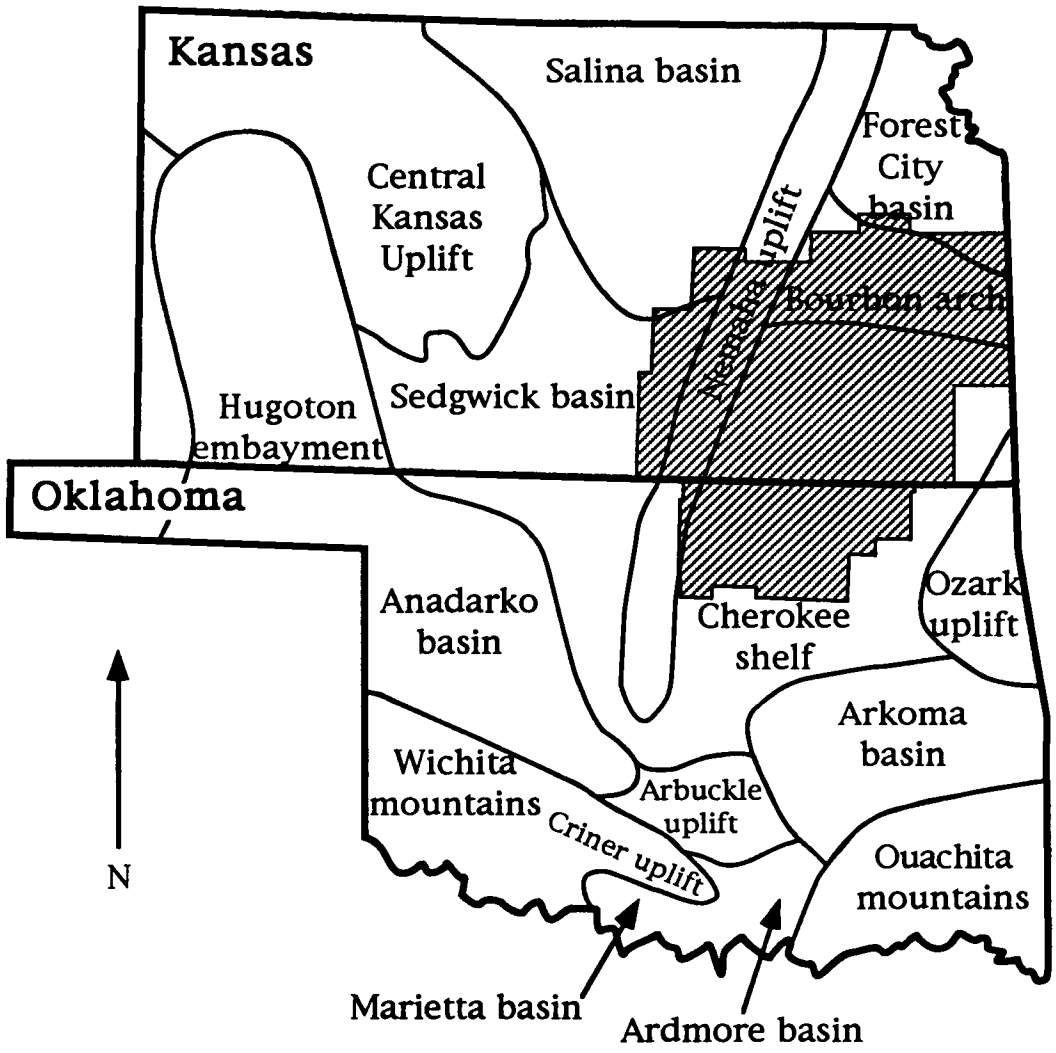


Figure 4. Pennsylvanian tectonic features in Kansas and Oklahoma. Study area is shaded (modified from Lardner, 1984, Merriam, 1963).

uplift and were formed at a period of increased structural activity during the Middle Pennsylvanian.

As a result of the Late Paleozoic orogenic event, the Arkoma Basin became the main depocenter for Ouachita-derived sediments by Middle to Late Pennsylvanian time. Atokan erosion of the Ouachita mountains led to the deposition of thick flysch assemblages along the southern margin of the basin (Arbenz, 1989). By late Atokan time (Middle Pennsylvanian) the flysch basin had filled up and sedimentation became shallow marine and ultimately fluvial. Occasionally, sediments reached the northern Cherokee shelf area in the Desmoinesian of the Arkoma Basin (Arbenz, 1989). Towards the southwest, the Anadarko Basin was little affected by this clastic influx but underwent a series of episodic carbonate shelf margin progradations and retreats (Watney, and others, 1989).

Towards the north, Middle Pennsylvanian faulting along the Humboldt Fault Zone occurred also as a result of the collision between the North American craton and the South American continent during the Late Paleozoic. This event gave rise to the Nemaha uplift, a reactivation of the older southeast Nebraska arch (Bunker and others, 1988). The uplift continued to have moderate positive relief until overlapped by Missourian (Upper Pennsylvanian) strata (Bunker and others, 1988). The Bourbon arch, which separates the Cherokee shelf from the northern Forest City basin formed as a result of differential subsidence of both basins. The Bourbon arch is a broad feature with little closure, and low structural relief. Poorly

defined, it trends northwestward from Bourbon, through Allen, Anderson, Coffey, Lyon and Chase counties (Stewart, 1975). The arch ceased to divide the basins by the end of the Atokan (Middle Pennsylvanian) when fluvially-derived sediments filled the basins and overlapped the structure by Desmoinesian time (upper part of Middle Pennsylvanian; Brenner, 1989) but regained moderate relief after compaction of these sediments took place. Recent evidence suggests that the feature continued affecting the deposition of units as young as Missourian in age (Price et al., 1985, this study),. The Nemaha uplift and the Central Kansas uplift continued to be topographic highs until Late Pennsylvanian when they were overlapped by the Kansas City Group (post Hertha) as a result of a decrease in differential subsidence rates for both the Forest City and Salina basins (Bunker and others, 1988). The widespread lateral continuity of the Upper Pennsylvanian cyclothems of the Midcontinent reflect the relative tectonic stability of the area during that time (Bunker and others, 1988).

Pennsylvanian siliciclastic sources included four positive areas: 1) the ancestral Rockies to the West, 2) the Marathon Ouachita Mountains to the South, 3) Canadian Shield sources to the North, and 4) alluvial-deltaic sediments that prograded into the Midcontinent from Appalachian sources during Desmoinesian times (Bunker and others, 1988, Houseknecht, 1993). Subsidence of the foreland basins was primarily of flexural origin (Bally, 1989) with varied average rates between 0.3 m. (1 ft.)/ka in the basin to less than 0.05 m. (0.17

ft.)/ka on the northern shelf (Watney and others, 1989). The subsidence of the foredeep (Arkoma Basin) was primarily controlled by the Atokan orogenic activity of the folded thrust belt (the Ouachitas) that peaked during the orogenic phase and diminished by Missourian time (Watney and others, 1989).

Objectives

The objectives of this project include the following; determination of the areal extent and overall geometry of the Chanute Shale in southeastern Kansas and adjacent Oklahoma, interpretation of the facies relationships and depositional environments of the unit, determination of petrographic and diagenetic characteristics of the Chanute sandstone units, their relationship with the depositional history and provenance, and determination of the stratigraphic relationships between the Chanute Shale and adjacent units and their relation to the cyclicity of the siliciclastic deposits in the Midcontinent.

Methods

Field work

Vertical sections were measured and samples of the Chanute Shale were collected from 12 exposures in southeastern Kansas and northeastern Oklahoma. Sampling and description of cores from two wells provided by the Kansas Geological Survey was also carried out during this part of the investigation. Analysis of outcrop and core samples included documentation of composition, textures, and

sedimentary structures present in the sandstone bodies of the Chanute Formation. Areal extent of the formation on the surface was also documented from the 12 exposures analyzed within the outcrop belt (Figure 2).

Sample analysis

Sandstone composition was determined from 56 thin sections made from outcrop and core samples. Samples were impregnated with blue dyed epoxy resin prior to thin section preparation to distinguish true porosity from artifact porosity produced by the grinding process. The thin sections were examined using a petrographic light microscope to describe the petrographic characteristics (i.e., mineralogy, porosity) of the unit. A total of 300 points per thin section (Appendix 2) were counted to determine the percentages of each component in the sandstone bodies. Thin sections containing carbonates were stained using a mix of potassium ferricyanide and alizarin red to determine certain aspects of carbonate composition. More detailed examination of the carbonates was accomplished using an ARL-SEMQ electron microprobe at the Department of Geological and Atmospheric Sciences, Iowa State University. Samples used for this analysis were carbon-coated micro-polished thin sections from outcrops and cores. Additional analysis of cements and diagenetic alterations were performed using cathodoluminescence petrography with a Nuclide ELM 2A model cathodoluminoscope.

Well log analysis

Analysis and interpretation of geophysical well-logs (provided by the Kansas Geological Survey) were used to determine the subsurface areal extent and features of the Chanute Shale such as thickness, lithologic variation, lateral continuity, and overall geometry. Approximately 500 Gamma Ray-Neutron Density well logs (Appendix 1) were used for these purposes. Sand counts were performed using the "shale baseline technique" (Brenner and McHargue, 1988) in which 100% shale and 100% sandstone lines are drawn on the well log along their corresponding values. A third line is drawn, which approximates the percentage of clean sand based on core data from the unit in question. In this study, a 60% line was used to differentiate the sands from the shale in the Chanute interval. The well-log data collected from the study was used to generate isopachs and isoliths of the members of the Chanute Shale. These maps are discussed in detail in following chapters.

CHAPTER II

STRATIGRAPHY

Stratigraphic overview

Named after exposures around Chanute in Neosho County, Kansas, the Chanute Shale is a formation in the Kansas City Group, Missourian Stage (Upper Pennsylvanian Series) of the Pennsylvanian System (Figure 3) overlying the Dewey Limestone and underlying the Iola Limestone (Heckel, ms. in review). Although Chanute Shale is the formal name of this unit in Kansas, it contains a considerable amount of sandstone. Chanute Formation is used formally for the same interval in Missouri and Nebraska. The Chanute interval comprises three subdivisions in Kansas: the lower Chanute, the Thayer Coal, and the upper Chanute. The Chanute Shale includes sandstones and shales separated by a coal unit (Thayer Coal) named after the town of Thayer in Neosho Co., Kansas (Figure 3). The lower Chanute consists of the Noxie sandstone (now considered an informal name: Heckel, ms. in review) locally at the base, silty shale, shale, and occasionally an underclay underneath the Thayer Coal. The upper Chanute consists of shale and silty shale, with the Cottage Grove sandstone (now considered an informal name: Heckel, ms. in review) capping the unit. Since the study area lies predominantly in

Kansas and adjacent counties in northeastern Oklahoma (Figure 2), Kansas terminology is used in this study.

In the southern part of the study area (Montgomery County, Kansas), the Noxie sandstone, at the base of the lower Chanute, consists of nested sandstone channels up to 88 ft (26.8 m) or more in thickness (Schoewe, 1944). In Neosho County, at the type section of the Chanute Shale, the Noxie interval is represented by a thin 10 ft (3.1 m) shale unit (Heckel, ms. in review). The overlying Thayer Coal is generally about 1 foot (0.3 m) thick, but is reported to range from 2.4 ft (0.73 m) in Montgomery County to a thin "veneer" around the Kansas City area (Schoewe, 1944). The upper Chanute is mostly represented by the Cottage Grove sandstone, which ranges from about 7 ft (2.1 m) thick in Allen County, just north of Chanute, to 15-30 ft (4.6 - 9.1 m) in Linn and Miami counties in Kansas (Heckel, ms. in review). The Cottage Grove also thickens southward from the type section, ranging from 70 ft (21.3 m) in Wilson County, Kansas to about 160 ft (48.8 m) in Montgomery County, Kansas (Schoewe, 1944).

The Chanute Shale lies conformably above the Dewey Limestone (Heckel, ms. in review) in southeastern Kansas and northeastern Oklahoma. Around the Kansas-Oklahoma border, where the Dewey has been removed by erosion, the Chanute overlies the Nellie Bly Formation, a name recently extended into Kansas by Heckel (ms. in review) for siliciclastic deposits below the Dewey Limestone and above the Drum Limestone. At the measured section

in Allin Hill, along US. 166 west of Coffeyville (SW, SW, sec. 32, T34S, R16E; Appendix 3), the Dewey Limestone is cut out by Noxie channel sandstones, which begin to appear about 23.3 ft (7.1 m) above the base of this section (Appendix 3). In this section, the base of the Chanute is the base of the sandstone beds, because the conglomeratic limestone lens, which incorporates eroded fragments of the Dewey Limestone and usually underlie the sandstones is currently covered. The Noxie sandstones are fine-grained, micaceous, limonite stained, thinly-bedded, and thinly-laminated, with some ripples, and are interbedded with silty shale and shales. Coaly fragments, and pyritic concretions are also present in parts of these sandstones. Channels can be seen clearly at the top of the outcrop (Figure 5, Appendix 3). The sandstones in these channels have the same characteristics as the sandstones underneath them but are better cemented (less friable) and show some plane laminations. The total exposure of the Chanute (lower member only) in this outcrop is 35.5 ft (10.6 m).

The Chanute Shale thins southward in northern Oklahoma beyond the southern edge of the Noxie sandstone channel complex (Heckel, ms. in review). Crossing the Kansas-Oklahoma border, into Nowata county Oklahoma, exposures of the lower Chanute (mainly the Noxie sandstone) can be followed along the "Noxie road", close to the remnants of the town of Noxie, Oklahoma (W line, sec. 30, T29N, R15E). Noxie sandstones are exposed at the bottom of Opossum Creek and can be followed up to the top of the hill located at the southwest corner of section 30. At least 122 ft (36.6 m) of Noxie is



Figure 5. Sandstone exposure of the Noxie channels at the top of the Allin Hill outcrop, west of Coffeyville, Kansas.

exposed along this road but no section was measured.

The Thayer Coal has been reported to occur as far south as Osage County, Oklahoma (Oakes, 1952). A good outcrop of the Thayer Coal and the underclay beneath it, is exposed along the road south of the town of Independence, Montgomery Co., Kansas (NE, NE, SE, sec. 24, T33S, R15E; Figure 6, Appendix 3). In this section (South Independence), about 1.64 ft (0.5 m) of coal is underlain by gray clayey shale, grayish brown silty shale, and a poorly developed underclay. The coal is blocky and dull in overall appearance, but shiny on fresh surfaces, with sulfur and iron-oxide concentrations along fractures. The coal is overlain by silty shale grading upward into fine-grained sandstone (Cottage Grove, Figure 7).

A thick section of almost the entire Chanute Shale interval was measured near Thayer, close to the Thayer dam (SW, NW, NW, sec. 30, T29S, R18E; Figure 8). This section shows about 19.68 ft (6 m) of clayey shale grading upward into an underclay, overlain by the Thayer Coal (0.98 ft, 0.3 m thick), with silty shale and the Cottage Grove sandstone on top. The Cottage Grove here (Figure 9) is a slabby, thinly-bedded, very fine-grained, organic-rich, micaceous, and well-cemented sandstone. The slabby sandstone grades laterally into contorted beds towards the east, on the northwestern side of City Lake (Figure 10), which grade upward into parallel strata towards the top of the section. North of Chanute, Kansas, the contact between the upper Chanute and the Iola Limestone is exposed at the underpass of US 169 and the old US 169. In this section (North

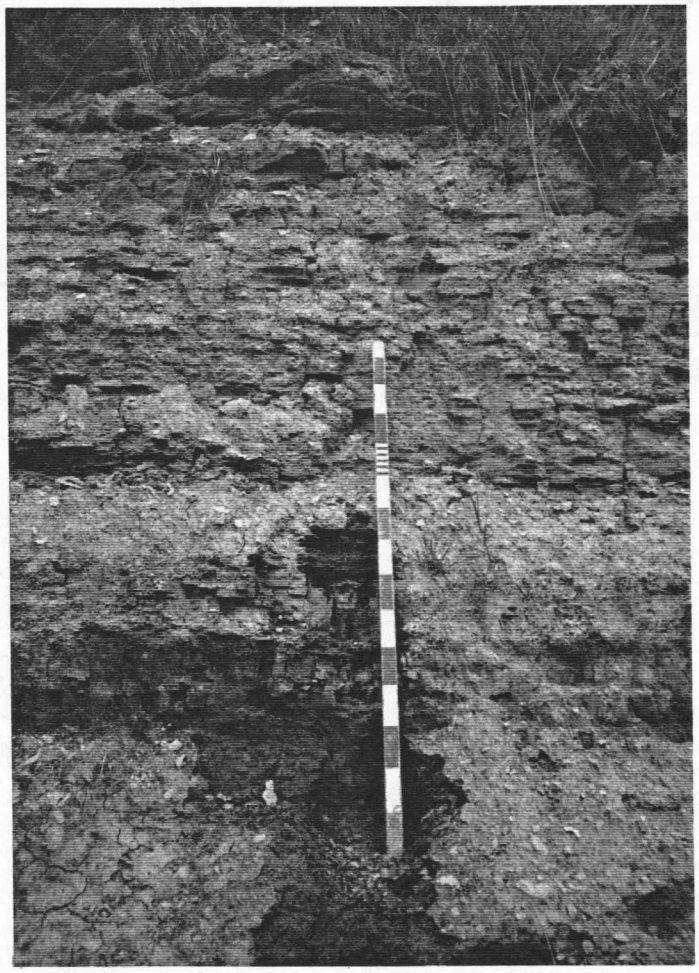


Figure 6. Thayer Coal and underclay exposed along the road south of Independence, Kansas.

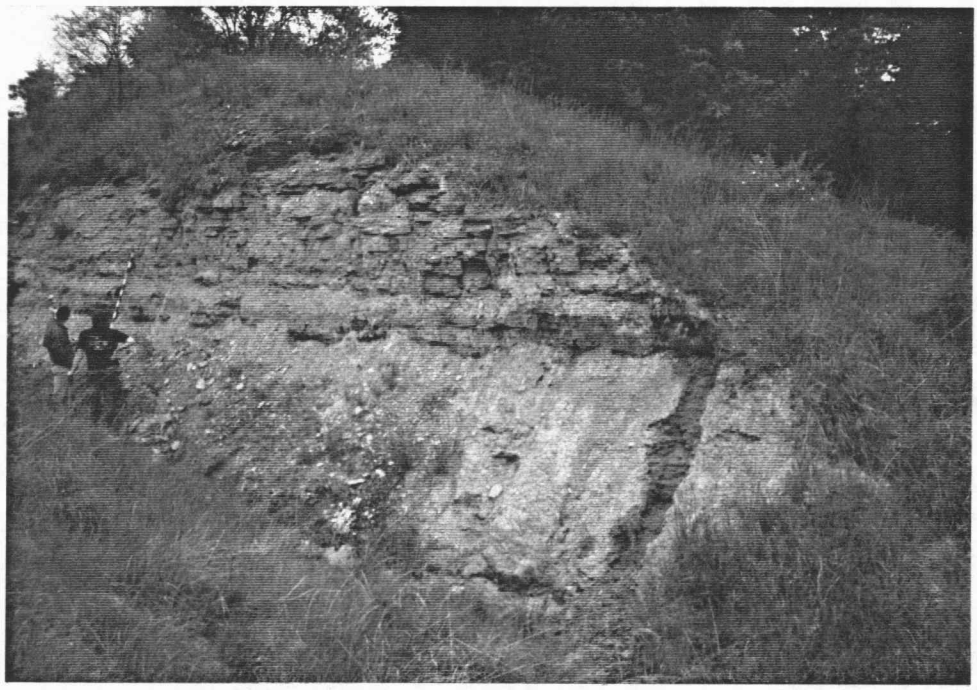


Figure 7. South Independence outcrop. The Thayer Coal grades upward into a silty shale and thinly-bedded sandstones of the Cottage Grove.



Figure 8. Shale, underclay and Thayer Coal exposed at the Thayer Dam outcrop. The slabby Cottage Grove sandstone can be seen on top.



Figure 9. Slabby Cottage Grove sandstone exposed at the top of the Thayer Dam outcrop.

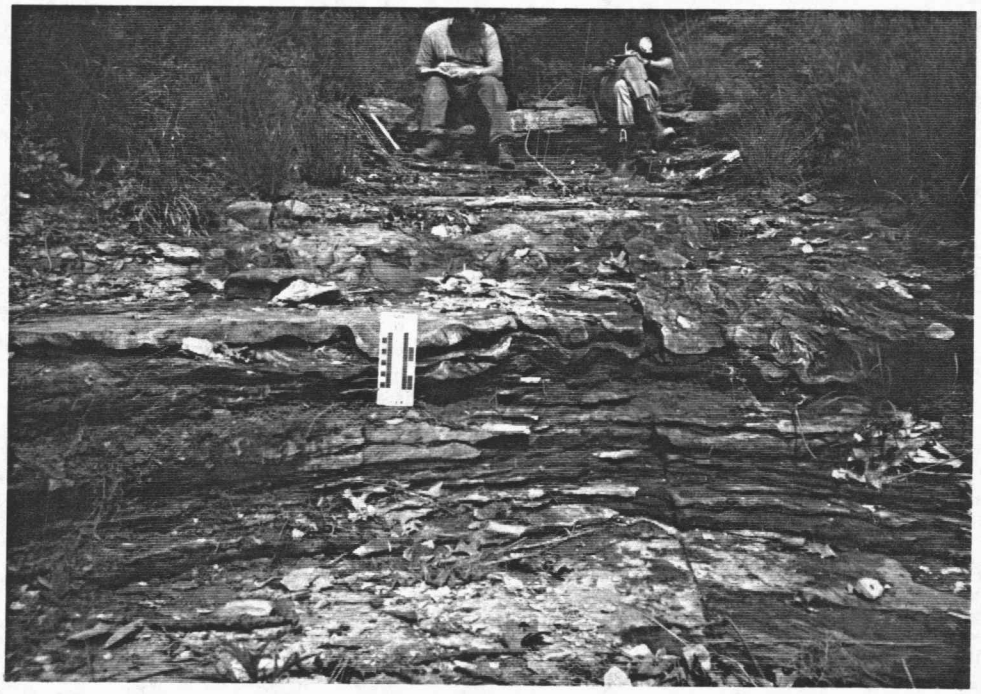


Figure 10. The slabby Cottage Grove sandstone towards the west of Thayer dam grades laterally into contorted beds towards the east of the dam.

Chanute, Appendix 3), organic-rich shale of the upper Chanute is in sharp contact with the Iola Limestone above (Figure 11). The Cottage Grove sandstone is absent in this area.

The Chanute Shale is thickest in the southern part of the study area. From northeastern Oklahoma into Montgomery county, Kansas, the Noxie sandstone constitutes most of the lower Chanute. Towards the north, the Noxie interfingers with a silty shale unit capped by an underclay and the Thayer Coal. The Thayer Coal is a relatively thin but persistent unit that can be traced to the Kansas City area. The Cottage Grove sandstone composes the major part of the upper Chanute from Neosho county, Kansas, northward. At places the sandstone is replaced by a silty shale beneath the Iola Limestone. The Chanute as a whole thins from 27 ft (8.23m) to 6 ft (1.82 m), from the Kansas City area into Missouri, where most of the unit is composed of shale (Heckel, ms. in review).

The presence of a marine horizon above the Thayer Coal has been mentioned in the past, but has not been well documented. Reports by A. P. Bennison (pers. commun. to P. H. Heckel) of a limestone unit above the Thayer Coal near Bayard bridge (near ctr E line, NE, sec 2, T24S, R20E, Heckel, ms. in review) in Allen County has not been confirmed in the surface analysis of this study. The validity and possible correlation of this marine horizon will be addressed in the subsurface discussion below.

The Chanute Shale and the cyclothem concept

Early mention of cyclicity in Pennsylvanian deposits in Kansas

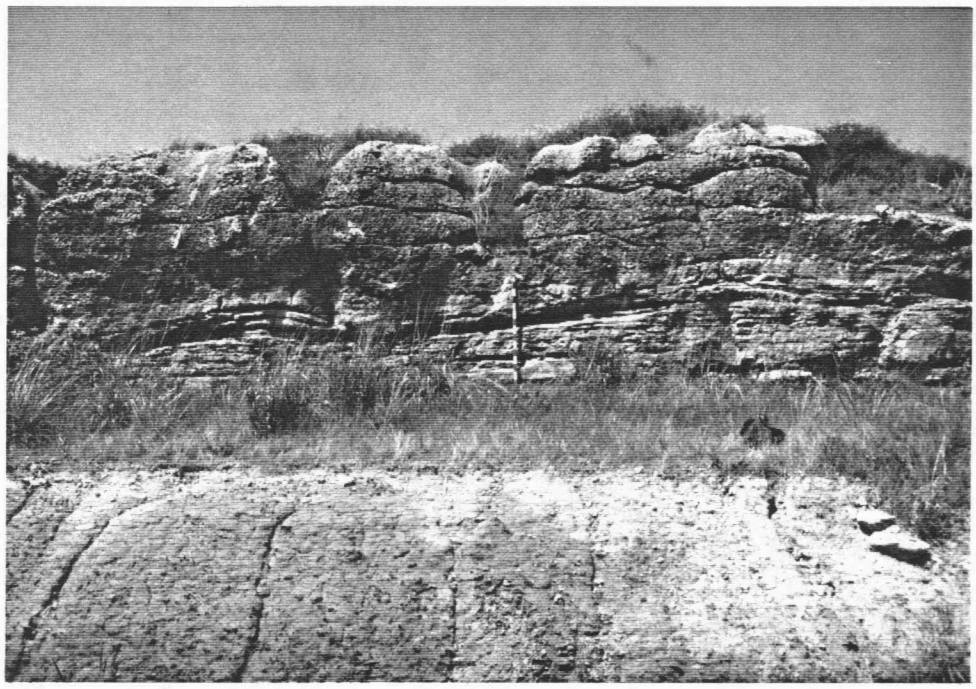


Figure 11. Contact between the Chanute Shale and the Iola Limestone exposed at the underpass of old US 169 and US 169. Here the Cottage Grove sandstone is laterally replaced by a shale facies beneath the Iola Limestone.

was by Moore (1936, 1949). Wanless and Shepard (1936) interpreted the cyclic deposits (termed cyclothems) as transgressive-regressive events resulting from eustatic sea level rise and fall from glaciation in Gondwana. Initially Moore defined two simple cyclothems, the Wabaunsee and Cherokee cyclothems, which comprised non-marine sandy shales and coals alternating with marine shales and limestones, the latter representing maximum marine inundation (Heckel, 1979). In order to explain more complex cyclothemic deposits, Moore (1936) developed the megacyclothem concept, which basically involved modified Wabaunsee cyclothems arranged in a hierarchical order. The thin phosphatic black shales present within the cyclothems, although very different from the other shales, were regarded as nearshore deposits in all of these earlier interpretations. Later work by Heckel (1977) suggested that the phosphatic, black fissile shale was deposited as an offshore marine deposit, therefore representing the maximum marine inundation within the cyclothem.

The idealized Kansas cyclothem (Figure 1), presented by Heckel (1977) is represented in ascending order by; 1) a sandy nearshore and non-marine shale locally with sandstone and coal (termed outside shale), which represents maximum regression at sea-level lowstand, 2) a thin basal transgressive limestone, 3) a phosphatic, black, fissile, offshore, marine shale (termed core shale), representing maximum transgression at sea-level highstand, and 4) a thick regressive limestone. The nearshore (outside) shales are variable in

thickness, with local siltstone and sandstone carrying plant fragments and locally containing sparse marine fauna of low diversity. It also contains definitely non-marine deposits such as coals and underclays locally with well preserved plant fossils, and channel sandstones devoid of marine fossils (Heckel, 1977). These shales are regarded as deltaic to terrestrial in origin, and they typically thicken toward the south (Kansas-Oklahoma border), where they are dominantly deltaic, and thin toward the north (Iowa and Nebraska), where they are dominantly blocky mudstones that include paleosols (Heckel, 1979). The Chanute Shale exhibits most of these general characteristics. The sandstone channels of the Noxie member are devoid of fossils. The main fossils known from the Chanute Shale are plant fragments and debris in sandstones and siltstones (Schoewe, 1944). The only invertebrates reported are some gastropods (*Worthenia tabulata*) found by Newell (1935), small pectanoid pelecypods found close to the Thayer Coal, and ostracodes and possible mollusks in dark shale and sandy shale above the Thayer Coal near Osawatomie (Heckel, et al., 1979, p. 42). There are non-marine units within the interval such as the Thayer Coal and the underclay beneath it. The Chanute overlies the regressive Cement City Limestone member of the Dewey Limestone, and is overlain by the transgressive Paola Limestone Member of the Iola Limestone (Figure 3). The Paola is overlain by the offshore phosphatic, locally black Muncie Creek Shale and the regressive Raytown Limestone Member, which complete the marine portion of the Iola cyclothem.

It can be clearly seen that the Chanute Shale is an "outside" shale representing maximum regression and sea level lowstand between the marine Dewey and marine Iola cyclothems (Figure 1). As sea level fell, Chanute siliciclastic deposits replaced marine limestone of the Dewey, and as sea level gradually rose, the marine limestone part of the Iola cyclothem developed.

Subsurface relationships

Characterization of the Chanute interval in geophysical well logs

Approximately 500 gamma ray-neutron density geophysical well logs were used to characterize the Chanute interval in the subsurface (Figure 12, Appendix 1), and this data was used to produce isopach, structural and isolith maps. In order to identify the unit, information from two cores was used, Gaddy # 1 (NE, SE, SE, sec 24, T31N, R16E, Appendix 3) and Joe Newland # 1 (SE, NE, NW, sec 06, T30N, R17E, Appendix 3) both provided by the Kansas Geological Survey. The geophysical logs from these two drillholes were used to correlate lithologies observed in their cores, with the well-log signatures of wells that were not cored. Figure 13 is an example of the well log signatures of units surrounding the Chanute. In each of the well logs studied, the Hushpuckney (not shown) and the higher Stark black shales were identified by their characteristic spiked, very-high gamma-ray signatures. Above the Stark Shale, the Winterset Limestone and the Fontana Shale-Block Limestone-Wea Shale interval were identified. The Block Limestone is seldom

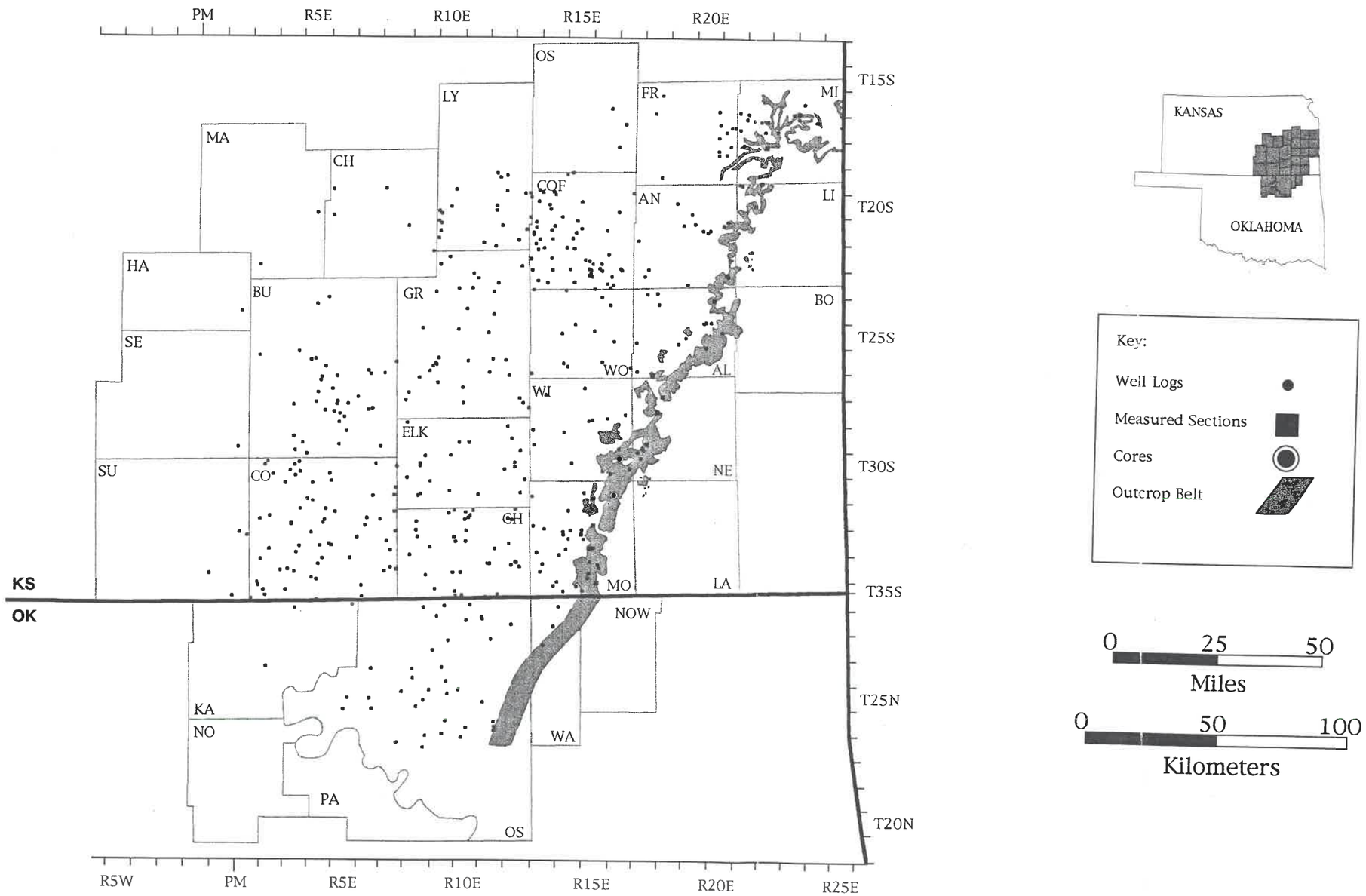


Figure 12. Location map of the geophysical well logs used in this study of the Chanute Shale. Approximately 500 wells were used to produce the isolith and isopach maps of the Chanute members.

Well Log: Gilcrest # 7
Location: SW, sec. 4, T18S, R21E

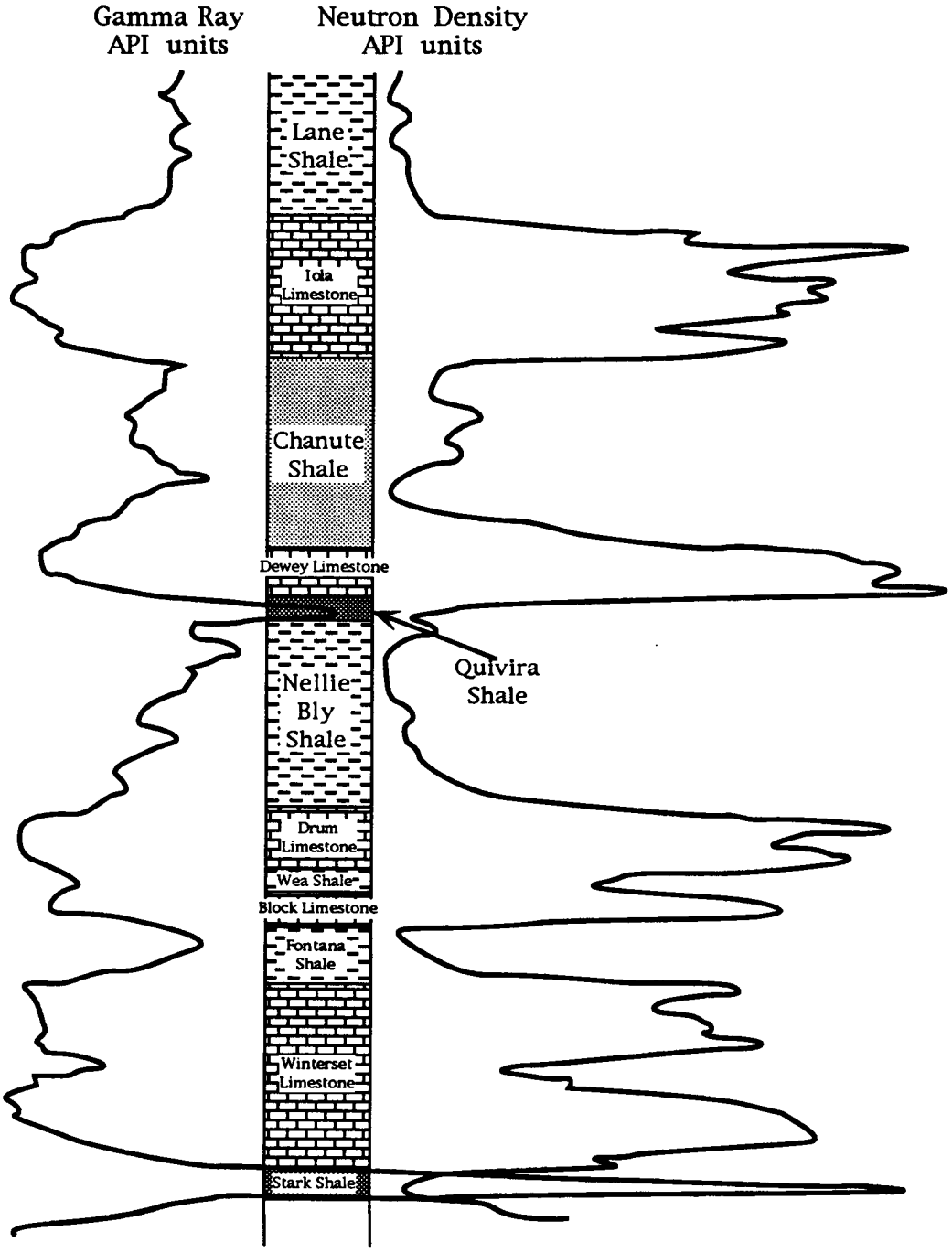


Figure 13. Example of well log signatures for the Chanute Shale and surrounding units.

observed, but even where it is, this entire interval usually appears as a thick shale unit characterized by a relatively high and "blocky" gamma-ray count. Above the Fontana-Block-Wea interval, well log signatures are variable. In a complete succesion, the Drum-Westerville Limestone (with "blocky" and very low gamma ray counts) is observed above the Wea, followed upward by the Nellie Bly Shale and the Quivira Black Shale with a relatively high gamma-ray spike. This interval is overlain by the Cement City Limestone (with extremely low, gamma ray counts, and usually doubled spiked, high neutron density counts), and this unit is capped by the Chanute Shale. The interval from the Fontana Shale through the Drum-Westerville Limestones are members of the Cherryvale Formation, is undifferentiated in places where the Block, and the Drum-Westerville limestones are absent. The Drum Limestone of southern Kansas correlates with the Westerville Limestone of northern Kansas, Iowa, and Nebraska (Heckel, ms. in review), and the black Quivira Shale and the Cement City Limestone are members of the Dewey Limestone. This is shown in Figure 14, which is a revised stratigraphic column of Missourian strata by Heckel (ms. in review). The Chanute Shale appears to lie directly above the Fontana-Block-Wea interval in places where lower Chanute Noxie channels have cut out the Dewey Limestone and parts of the underlying Nellie Bly-Quivira interval. Since the Nellie Bly and the Wea shales have similar well log signatures, they are undifferentiated where they occur together without the intervening Drum or Westerville

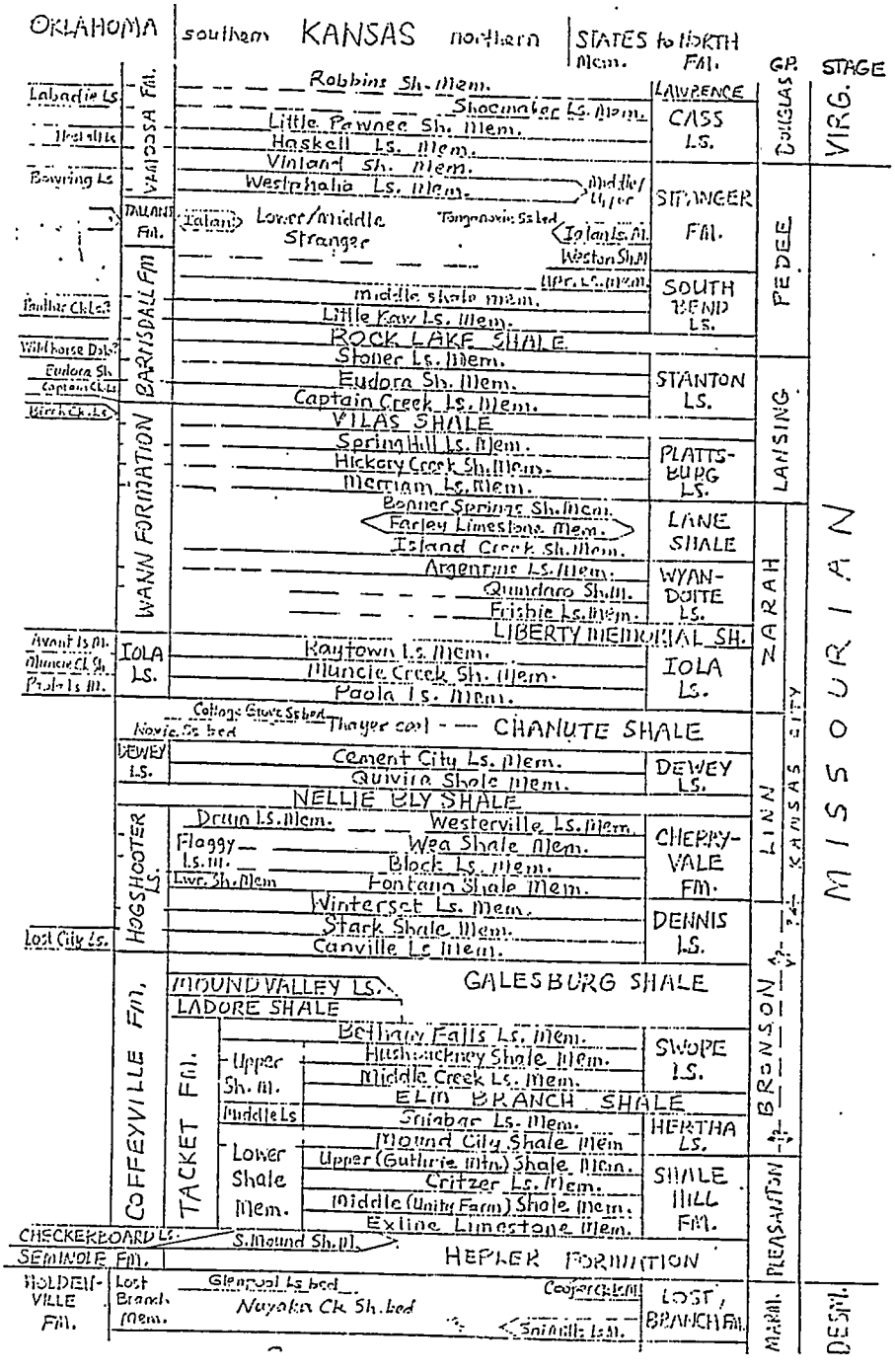


Figure 14. Proposed revision of Pennsylvanian (Missourian) stratigraphic nomenclature Kansas and Oklahoma, Heckel, ms. in review.

Limestone, thus making the Chanute appear to lie on top of the Wea Shale while in fact it is lying above the Nellie Bly Shale.

The Chanute Shale well log signature changes dramatically northward, in a trend parallel to the outcrop belt, and westward, deep into the subsurface as shown on cross sections A-A', B-B' and C-C' (Figures 15, 16, 17, 18). An example of the Chanute's signature can be observed in Figure 19. The bottom of the unit is picked at the top of the Cement City Limestone member of the Dewey Limestone. Where the Cement City is cut out, the top of the Quivira-Nellie Bly interval was used as the base of the Chanute Shale. The base of the Chanute Shale is characterized by an increase in the gamma ray count due to the increased radioactivity of the Chanute's Shale lithologic components (sandstone-siltstones-shales). Towards the south into northeastern Oklahoma, the Noxie sandstone channels are present, yielding different well-log signatures depending on the position of the well in the channel or interchannel area. Where the Cement City Limestone is present (interchannel), the gamma count increase is quite sharp but where the Cement City is absent (channel), the contrast against the Nellie Bly Shale (another sandy shale) is gradational.

The Thayer Coal and its associated underclay are observed in about half of the well logs analyzed within the Chanute's signature, possibly because of the thickness of the coal is less than the resolution of the geophysical tool. Where they are observed, the underclay signature is characterized by a high gamma and low

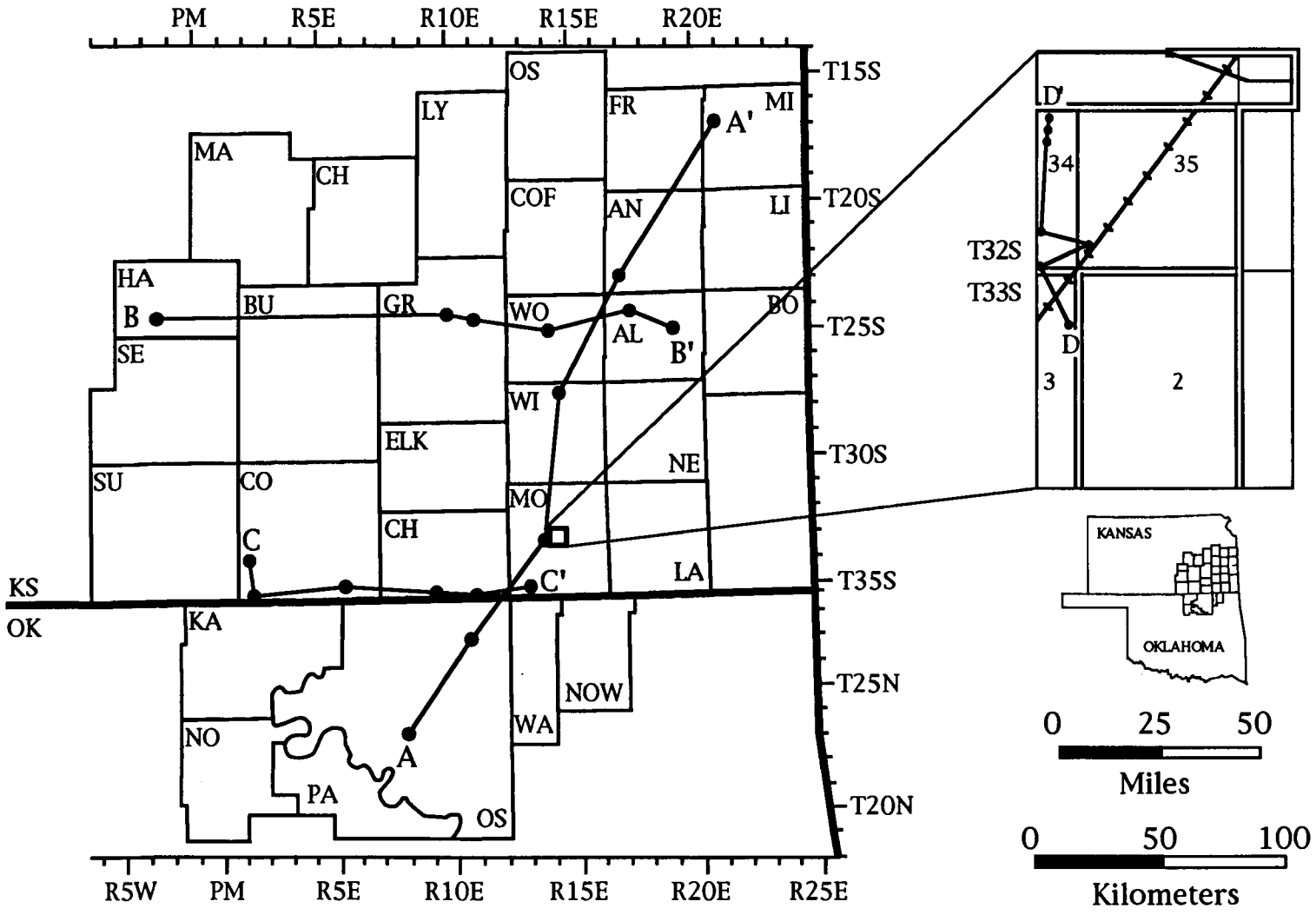


Figure 15. Location map for cross sections through the study area.

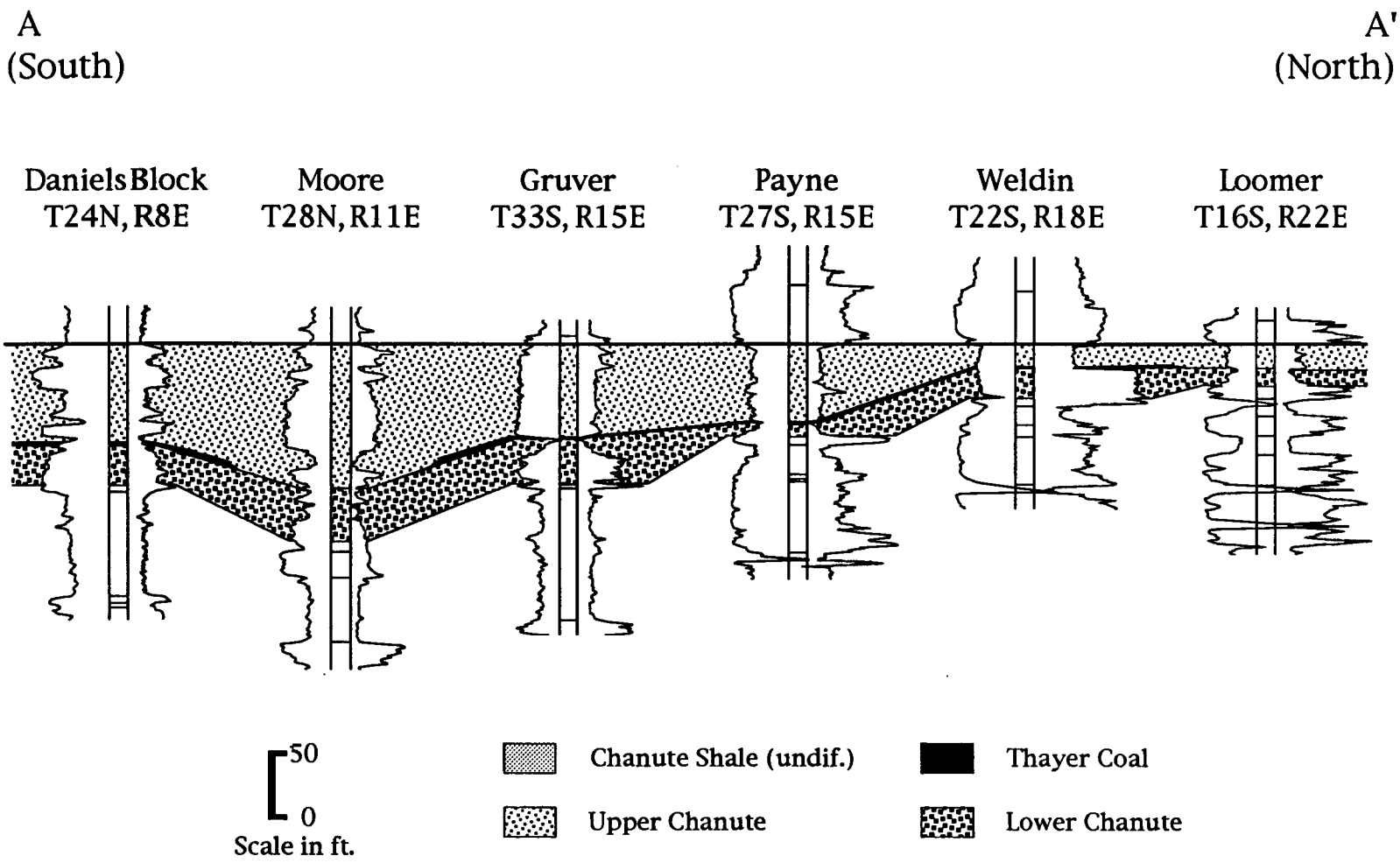


Figure 16. Cross section through the Chanute Shale from Oklahoma (south) to Kansas (north).

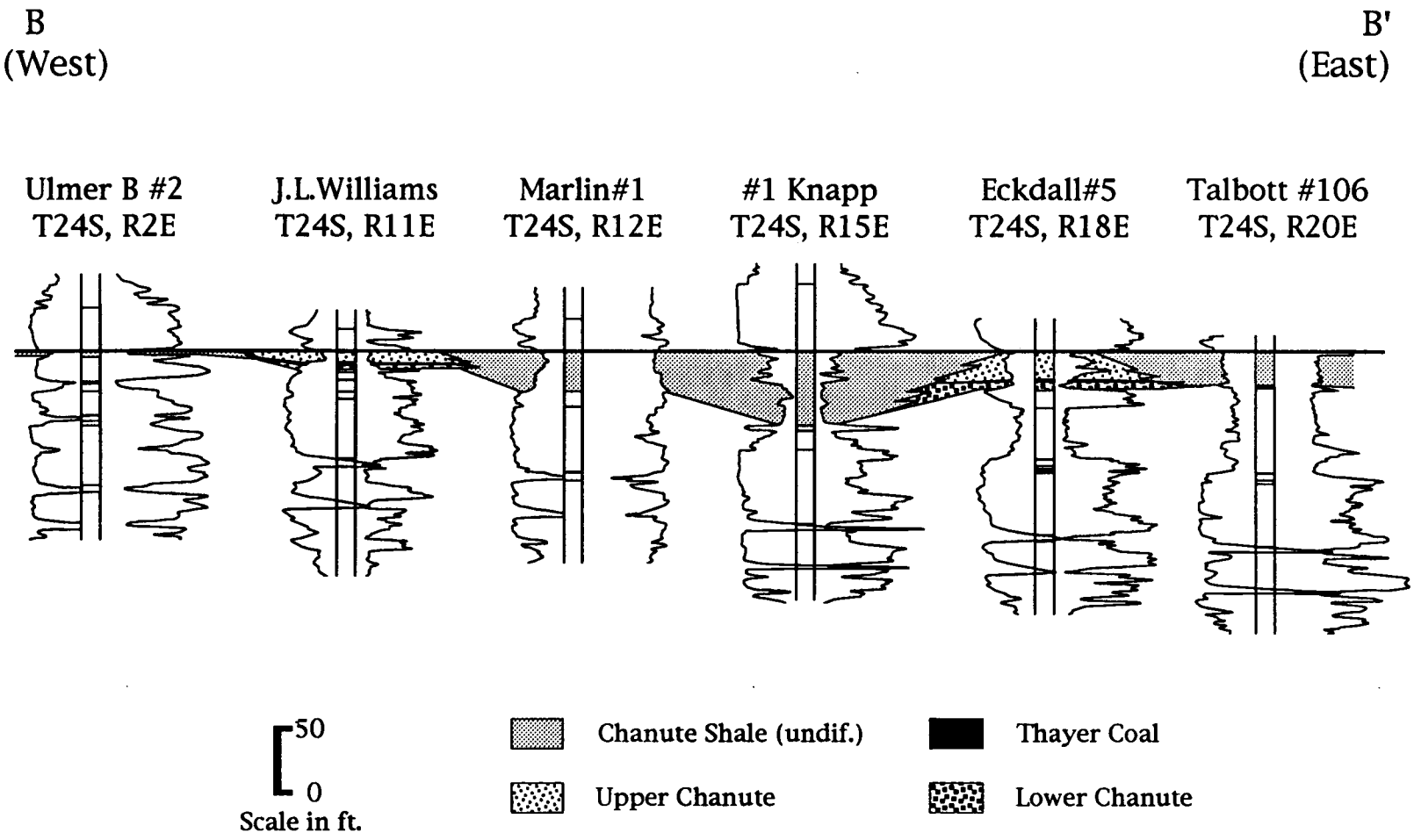


Figure 17. Cross section through the Chanute Shale from east to west, across the northern part of the study area.

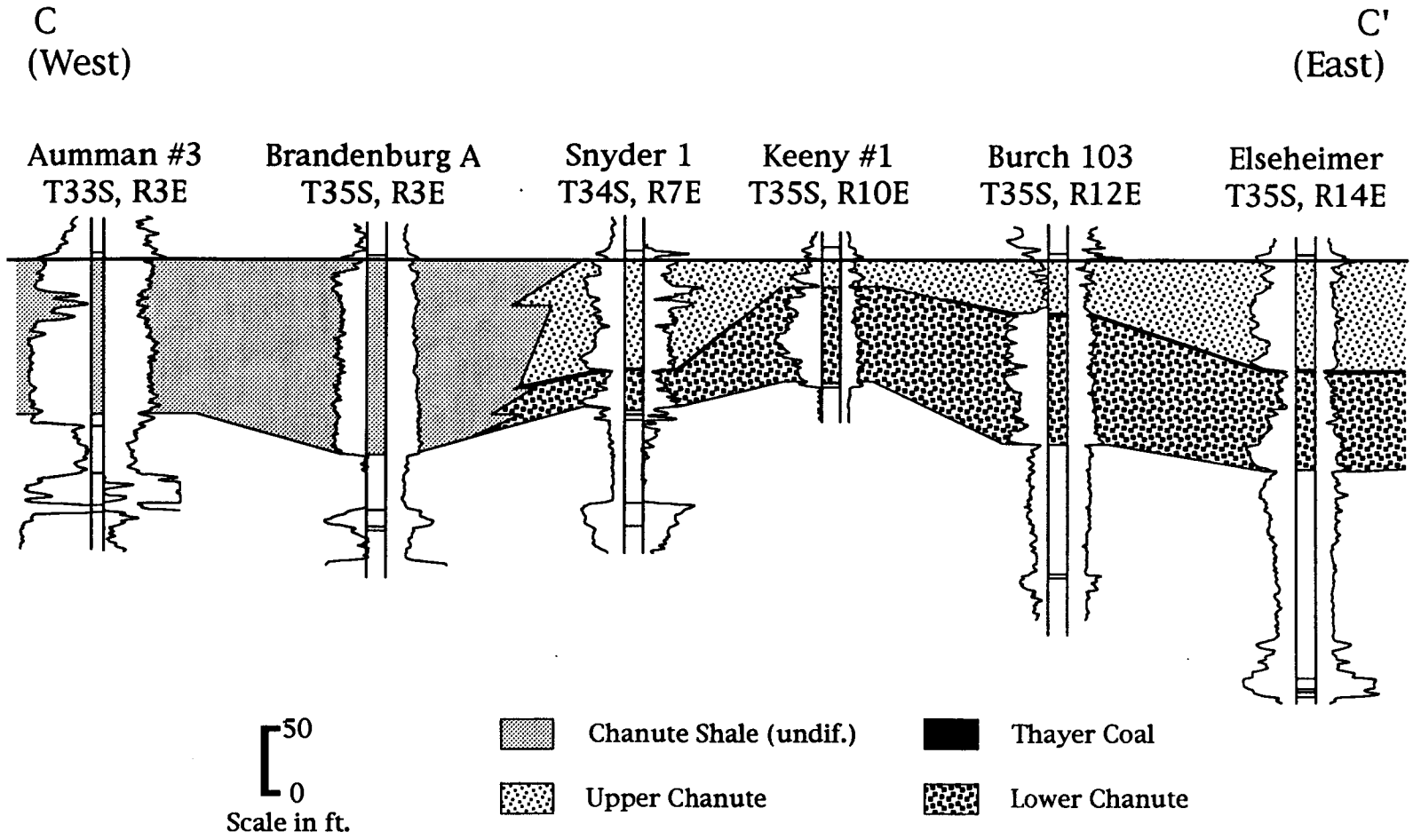


Figure 18. Cross section through the Chanute Shale from east to west, across the southern part of the study area.

Well log: Gruver # 20
Location: NE, NE, NE, sec.6, T33S, R15E

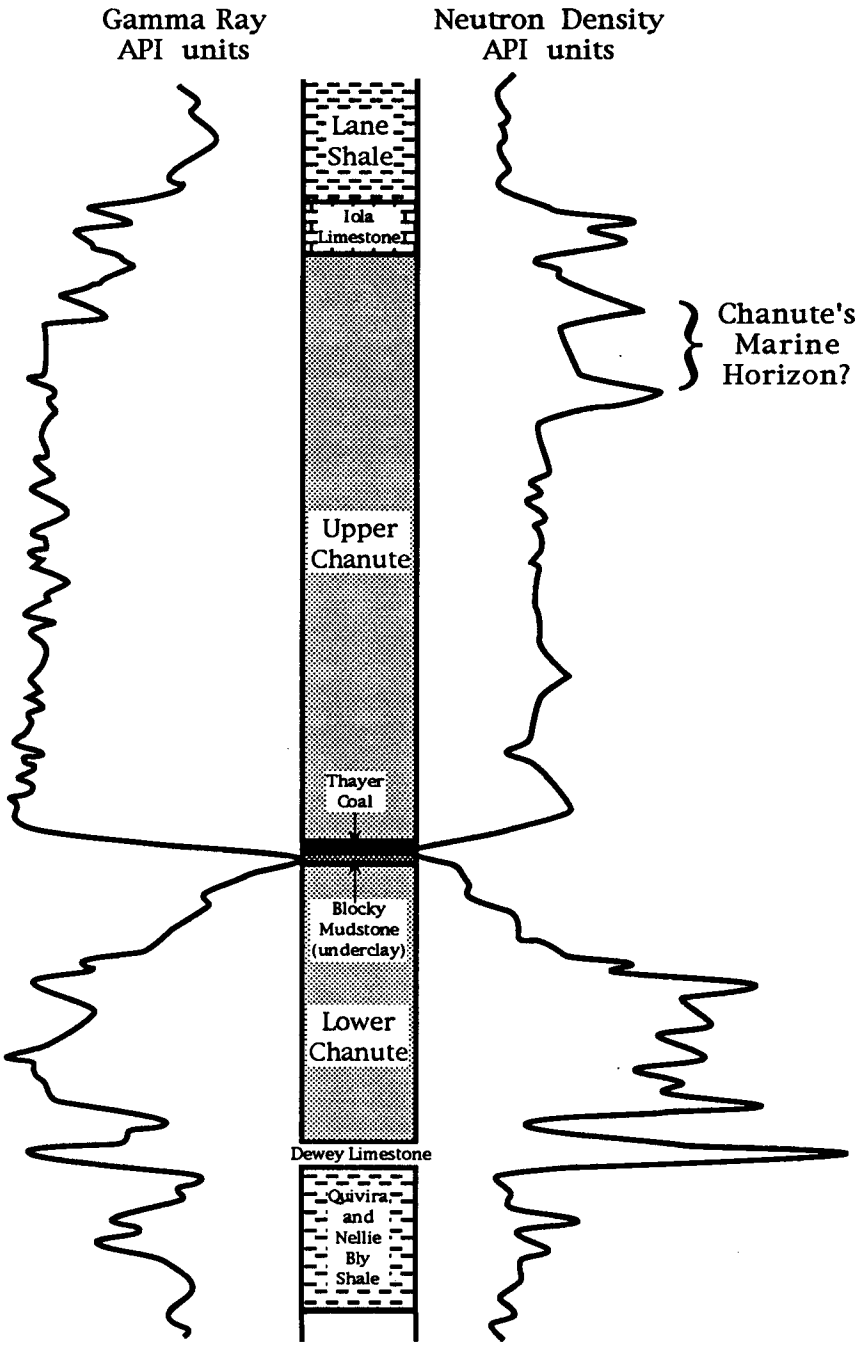


Figure 19. Example of Chanute Shale well log signature.

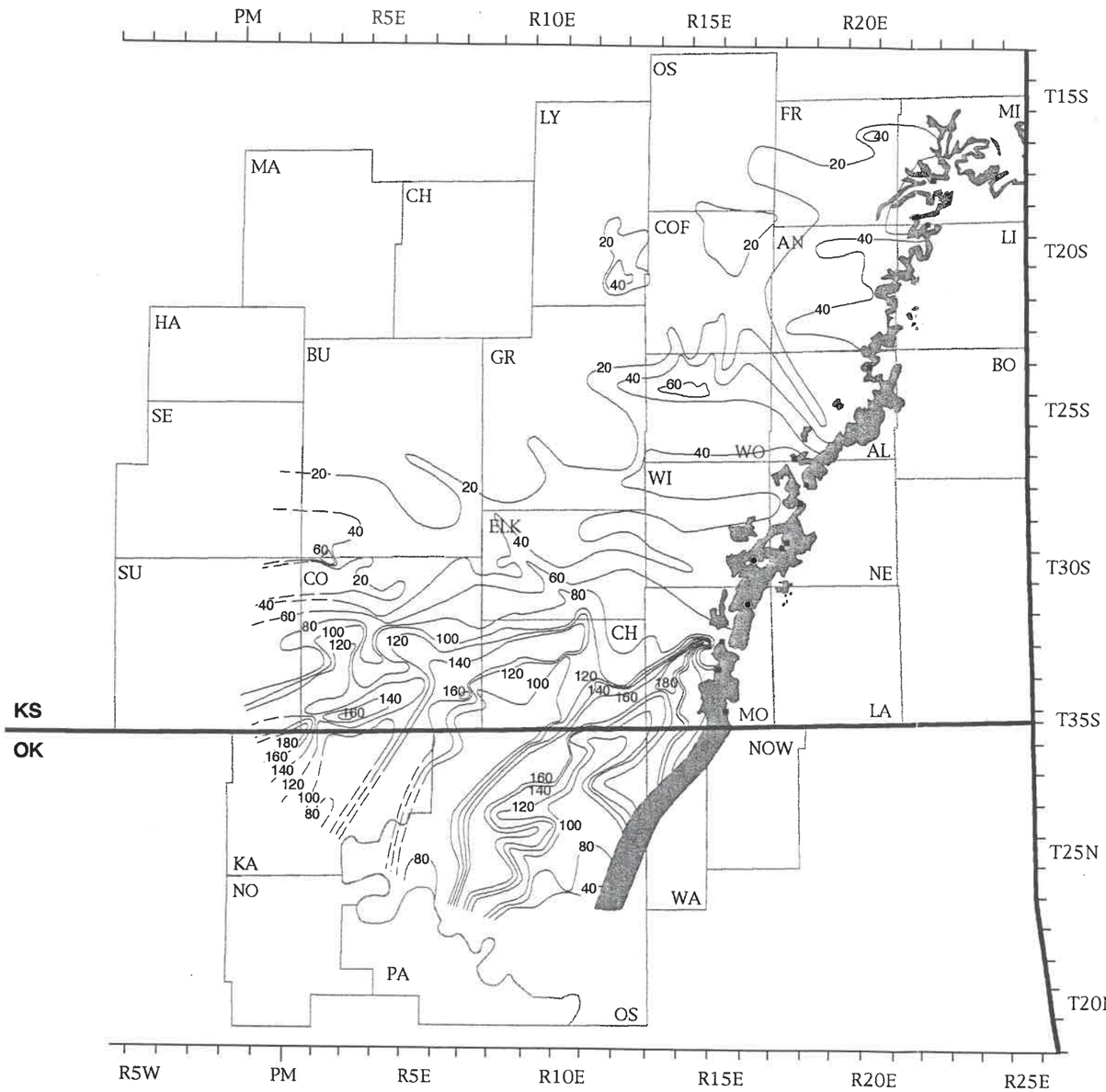
neutron density count. The Thayer Coal signature has an intermediate gamma count and an extremely low neutron density count (Figure 19). The combination of the underclay and the coal well log signature characteristically shows a displaced high gamma ray-low neutron density peaks (Figure 19).

The top of the Chanute Shale is picked at the base of the Iola Formation which shows a low gamma ray count and very high doubled spiked neutron density count where it is thin (Figure 19). The lower spike is the Paola limestone member of the Iola and the upper spike is the Raytown Limestone member of the Iola. Raytown Limestone member varies from thick to thin across the study area (Figure 16). This well log signature usually shows only a low neutron density count between the spikes because the intervening Muncie Creek Shale is typically gray rather than black in this area. The Iola Limestone, in most of the study area is capped by the thin Wyandotte Limestone, which is usually not differentiable. Therefore the base of the Lane Shale, with a signature that indicates a very thick shale (high gamma, low neutron density counts) is used to mark the top of the Iola (Figures 13, 19). The Lane Shale stands in contrast with the signature of the top of the Chanute, where the Cottage Grove sandstone shows intermediate gamma counts and intermediate neutron density counts. Where the Iola Limestone is absent, the base of the Lane was used to define the top of the Chanute.

The degree of cementation of the sandstones within the Chanute Shale has profound effects on well log signatures. The neutron density response of a carbonate-cemented sandstone (like those at the top of the Cottage Grove in Figure 19), looks very similar to that of a "normal" limestone signature. In the same way, the neutron density response of a porous limestone looks like that of a "normal" sandstone. This was taken into consideration when correlating the well logs throughout the study area by visual inspection of the signatures of true limestones within that particular well log and comparing these with the signature in question, and by comparison with surrounding well logs already correlated.

Thickness variations in the Chanute Shale interval

The isopach map of the entire Chanute Shale interval (Figure 20) shows that the thickest portion of the unit lies in Kay and Osage counties in Oklahoma, and southern Montgomery, Chautauqua, and Cowley counties in Kansas. The unit as a whole thins toward the north and the west throughout the study area. In the south, where the unit is thickest, two major "thicks", interpreted as channels are delineated, striking approximately N45°E, separated by a "thinner" area (western Osage, southwestern Chautauqua), possibly a high between the channels. These channels show a strong NE-SW directional component roughly parallel to the outcrop belt. These channels terminate northward, and the same thickness relationship as well as the presence of the channels is also observed in some cross sections whose locations are shown in Figure 15. A N-S cross section





Key:

Measured Sections

Cores

Outcrop Belt

0 25 50
Miles

0 50 100
Kilometers

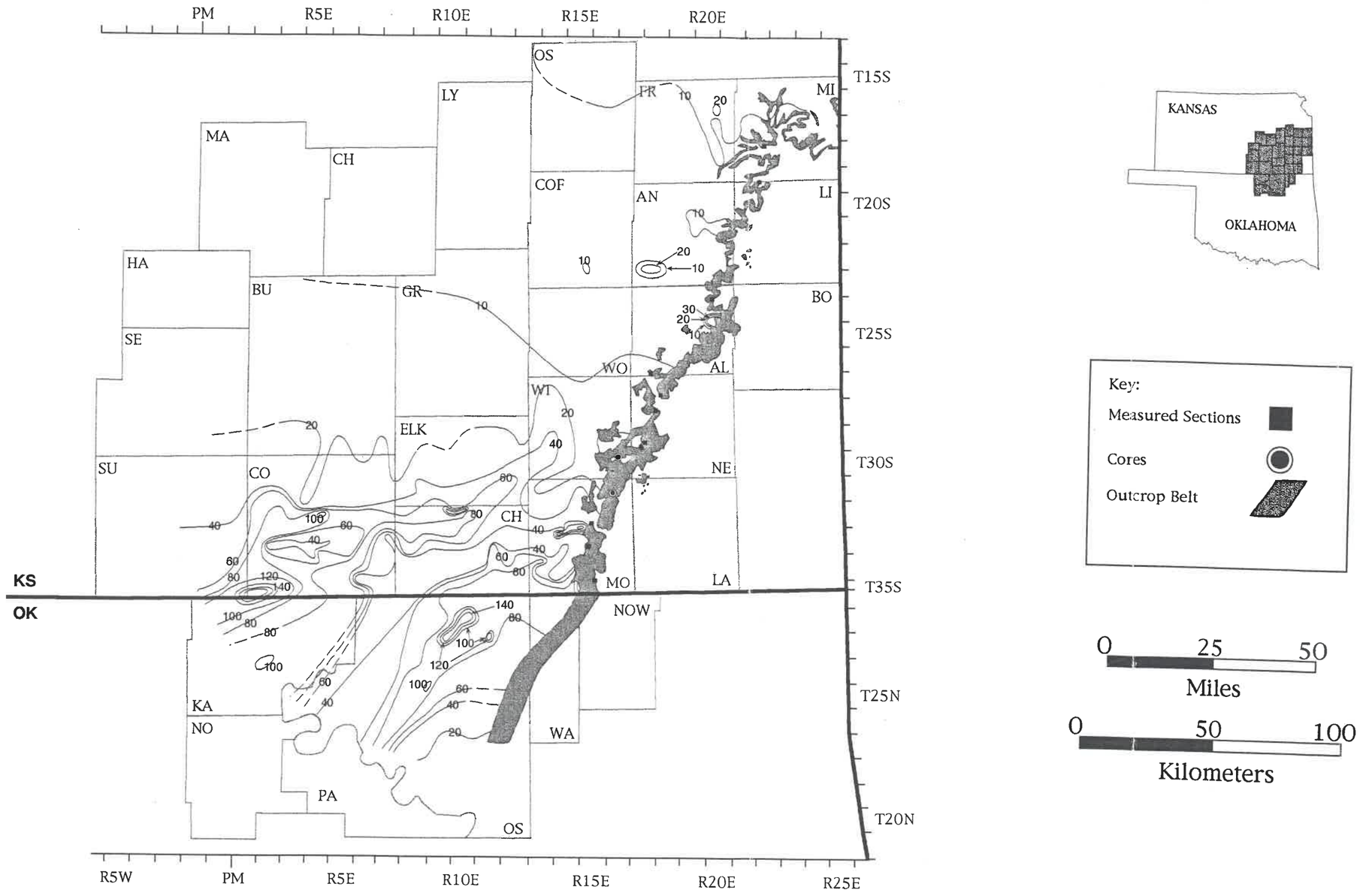
Figure 20. Isopach map of the entire Chanute Shale interval. Contour interval is 20 feet.

of the unit (A-A') from Oklahoma (Daniels Block and Moore wells) to Kansas (Figure 16) shows a Noxie channel sandstone (at the base of the lower Chanute) cutting out the Cement City limestone (member of the Dewey Limestone) in the Moore well log. This well (Moore) is located in one of the Noxie channel areas in Oklahoma where the Dewey Limestone is absent underlying the Chanute Shale. The rest of the wells of the cross section lie in interchannel areas and northern parts of the study area where the limestone is present as the Chanute thins towards the north. The channel and interchannel areas (channels and intervening high) can also be observed in an E-W cross section through the south (C-C', Figure 18) where the Cement City is absent or very thin (Aumann # 3, and Keeny # 1 well logs). Across the thinner area beyond the channels in the Chanute isopach (Figure 20), several poorly defined lobes of thicker sediment accumulation are present. These lobes strike roughly E-W, suggesting a different drainage pattern or perhaps different sediment sources north and south of approximately T33S. In cross section B-B' (Figure 17) well log # 1 Knapp is located in one of these lobes, and is the thickest portion of the cross section and the thickness of the unit is mostly composed of silty shales and shales but little sandstone. The Chanute can be seen clearly thinning out towards the west.

Following the premise developed from outcrop data that the Noxie sandstones are filling the channels while the Cottage Grove sandstones were deposited as a sheet sand on top, separate isopachs

of the lower and upper Chanute were made. In the isopach of the lower Chanute (Figure 21), the channels and the "high" area in between them can be easily identified, therefore supporting the outcrop interpretation made concerning the Noxie channels. North of about T33S the channels are lost and the unit thins to about 10 ft (3.04 m) in T26S in contrast to the 140 ft (42.7 m) recorded in the southern part of the study area. This is also observed in the cross section A-A' (Figure 16) where the lower Chanute begins to thin north of T33S and becomes really thin north of T27S. In the upper Chanute isopach map (Figure 22), the channels and their intervening "high" are still present but less well defined. North of about T30S, two well defined E-W trending lobes can be observed in Wilson and Woodson counties. In the same cross section (A-A', Figure 16) the upper Chanute also thins towards the north confirming the general trend of the Chanute thickness as a whole in outcrop with both its members in the subsurface.

The data from the isopach maps and cross sections clearly show that there was a pronounced channelization event prior to lower Chanute deposition. The sediment accumulations north of T33S might be either erosional remnants, sediments deposited in low lying areas during floods, or a combination of both. During upper Chanute deposition the pronounced topography left from the lower Chanute (Noxie channels) might have influenced the poorly defined channels in the southern part of the study area. Therefore, although the upper Chanute sediments were probably derived from the east, they



Key:

Measured Sections

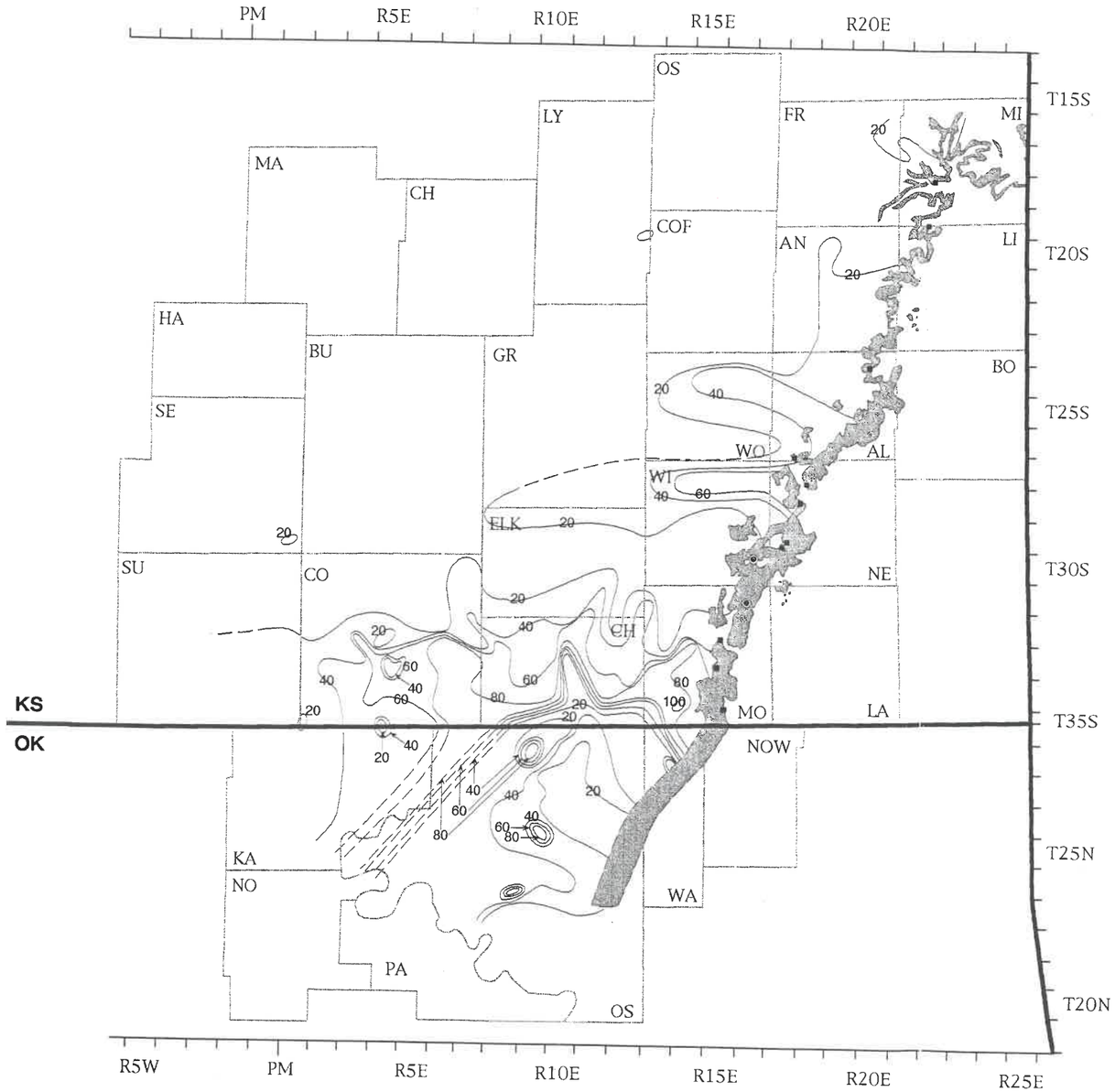
Cores

Outcrop Belt

0 25 50
Miles

0 50 100
Kilometers

Figure 21. Isopach of the lower Chanute. Contour interval is 20 feet south of Woodson and Allen counties, 10 feet from them towards the north.





Key:

Measured Sections

Cores

Outcrop Belt

0 25 50
Miles

0 50 100
Kilometers

Figure 22. Isopach map of the upper Chanute. Contour interval is 20 feet.

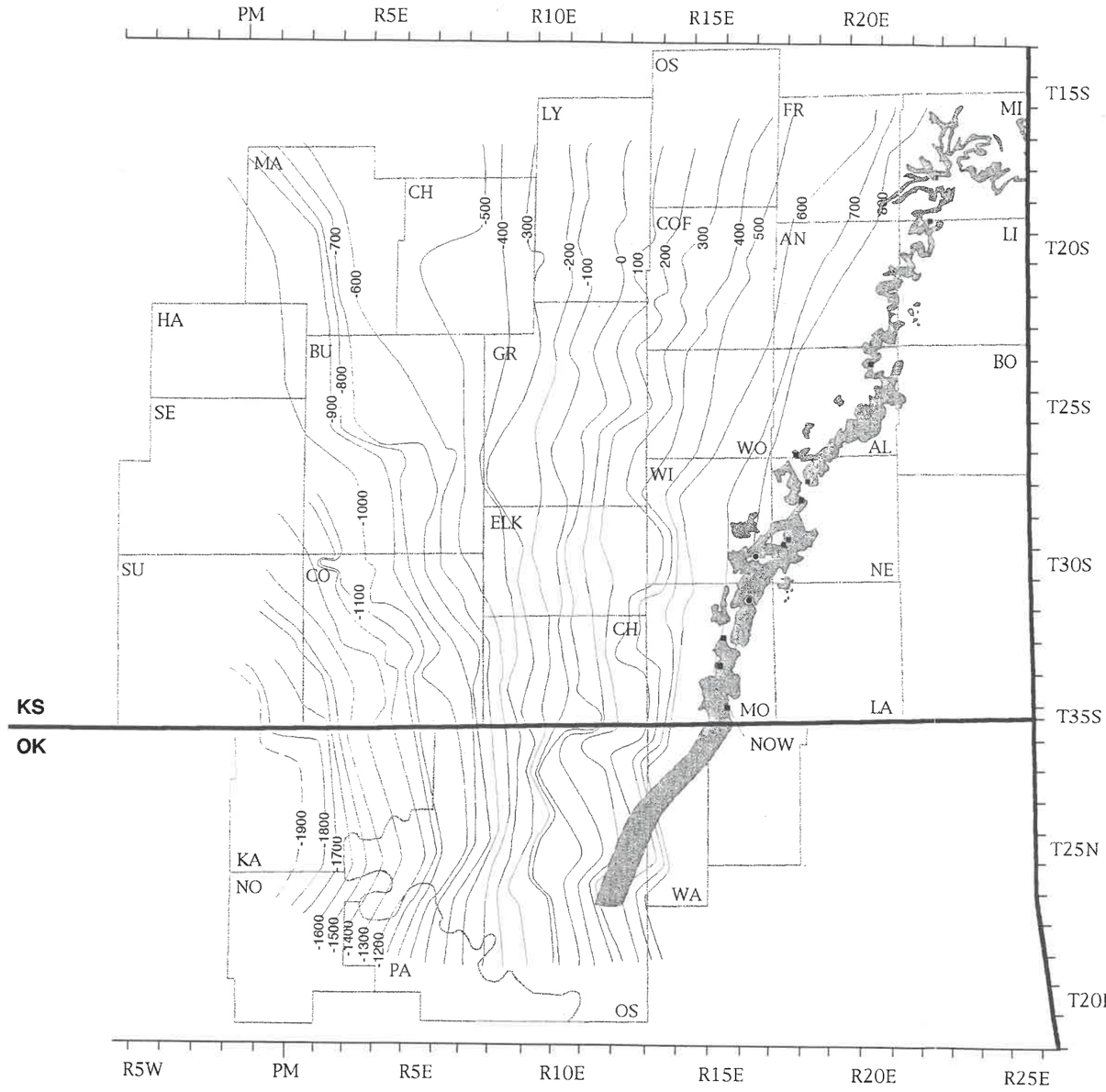
filled the lowest topographical areas first, and the interchannel areas afterwards. Since there was little or no topographical effect of the lower Chanute towards the north, the true E-W trend of the upper Chanute was preserved.

One question concerning the Noxie channels and their related "high" is whether they were topographically or structurally controlled. A structural map of the base of the Noxie sandstone was made in order to address this question by showing the topography prior to Noxie deposition. The map (Figure 23) shows a general westward slope with an inclination of about 0.33° suggesting that no obvious structural or topographical control was acting upon Noxie channels prior to deposition.

Another idea that was explored was what effect, if any, did the Bourbon Arch have upon Chanute Shale sediments. The isopachs and the isoliths maps both show similar sedimentary characteristics: thick deposits in the south and very thin deposits from about T33S northward. This suggests that the Bourbon Arch, which strikes roughly E-W across Bourbon Co. (T24-26S), Kansas had some minimal effects on the major thickness variation in Chanute deposition. More data is needed to unequivocally resolve this matter.

Sandstone distribution in the Chanute Shale

Isolith maps of the Chanute were constructed to determine sandstone distribution and overall geometries. The Noxie isolith map (Figure 24) shows the same channels and intervening "high" that were observed in the isopach maps described earlier (Figures 20,





Key:

Measured Sections

Cores

Outcrop Belt

0 25 50
Miles

0 50 100
Kilometers

Figure 23. Structural map of the base of the Chanute Shale. Contour interval is 100 feet.

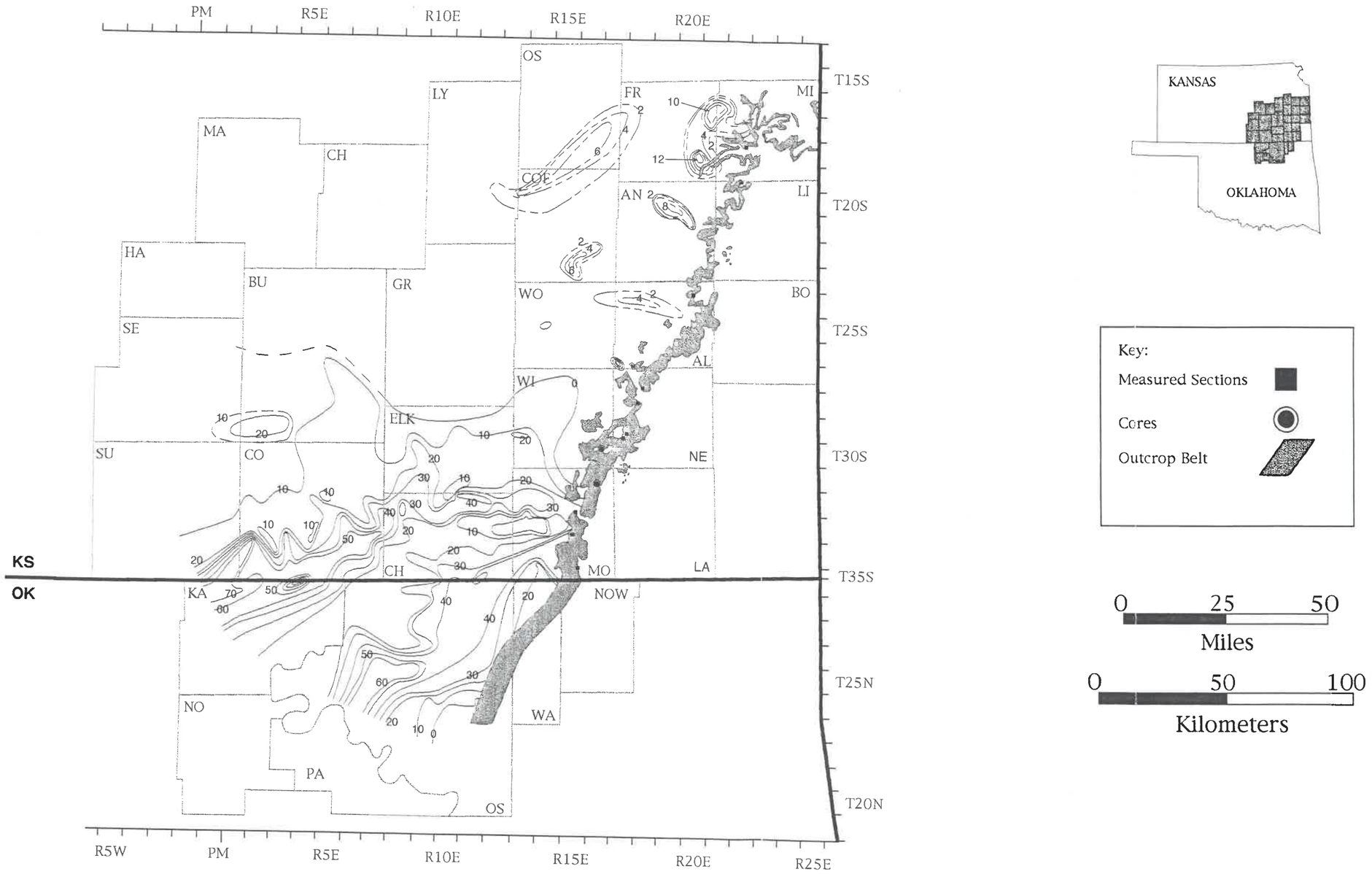
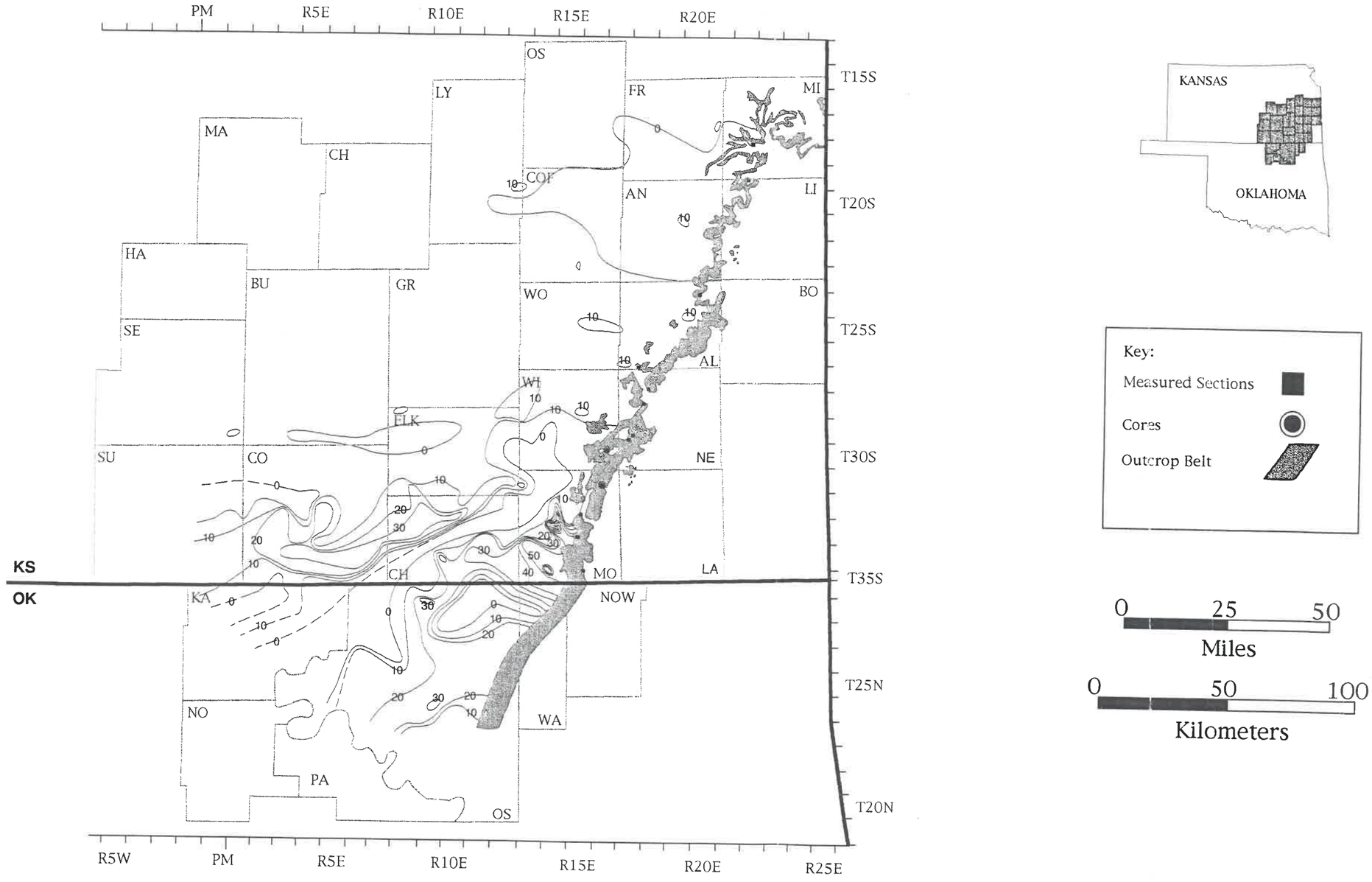


Figure 24. Isolith map of the Noxie sandstone, lower Chanute. Contour interval is 20 feet south of Woodson and Allen counties, 2 feet from them north (dashed contours).

21). The sandstone deposits compose from about 15 to 65 % of the total lower Chanute thickness. The main difference found is that the thickest sandstones are located slightly displaced to the south in the isolith map compared to the isopach map of the lower Chanute. This fact is attributable to amounts of other types of sediments (silty shale, and shales) that occur within the topographic lows in the study area. Towards the north, the maximum sandstone thickness is only about 12 ft (3.6 m), and this sandstone could represent erosional remnants, sediments deposited in low lying areas during floods, or a combination of both. Cross section C-C' (Figure 18) shows that the majority of the lower Chanute deposits are basal channeled sandstones (Noxie) with minor amounts of silty shales and shales except where the Chanute members can not be differentiated. Thicknesses vary between channel and interchannel areas.

Cottage Grove sandstones compose about 80% of the total upper Chanute thickness in the thickest areas and about 15 to 50% throughout the rest of the study area. This relationship can also be observed in cross section A-A' (Figure 16) where thickest deposits are located in the southern areas and thinner deposits in the north. In the Cottage Grove isolith map (Figure 25) the topographical influence of the Noxie channels is somewhat obscured. Some hint of channelization can be observed at both sides of the "high" between the channels, which still shows up rather poorly defined in the southern part of the study area. Well defined E-W directional components can be seen across Chautauqua and Cowley counties and



Key:

Measured Sections

Cores

Outcrop Belt

0 25 50

Miles

0 50 100

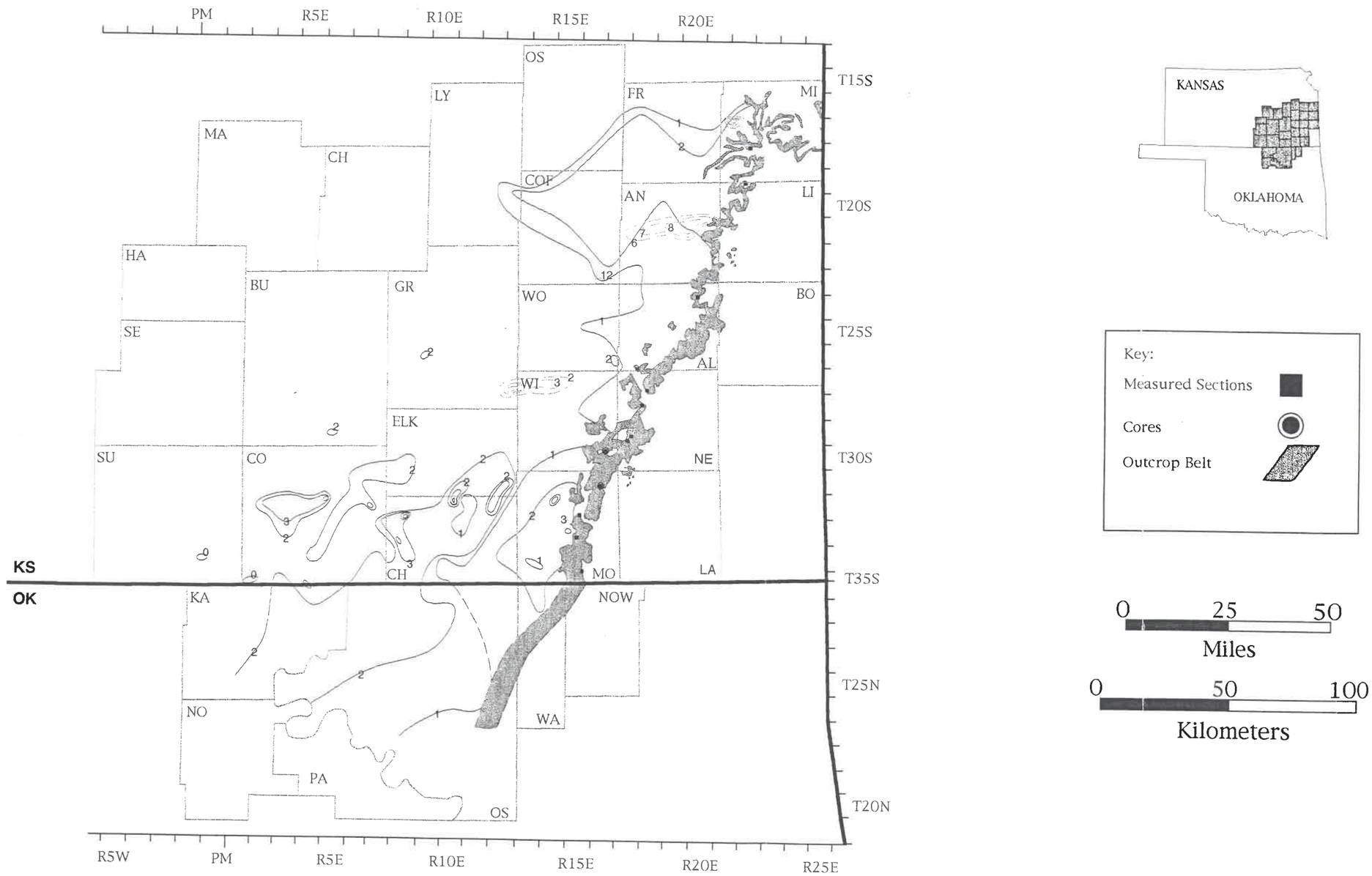
Kilometers

Figure 25. Isolith of the Cottage Grove sandstone, upper Chanute. Contour interval is 10 feet throughout the area.

in southern Montgomery Co., Kansas where the Cottage Grove is thickest (up to 90 ft -27.4 m). This is no surprise since the Cottage Grove is at the very top of the Chanute Shale and the topographical influence of the Noxie channels should not be as great at the time of Cottage Grove sand deposition. The stronger influence shown in the upper Chanute's isopach is enhanced by the silty shales and shales deposited prior to the sandstone. These older deposits were more influenced by the topography left from the Noxie channels than the younger Cottage Grove sandstones on top. This situation allowed the Cottage Grove sands to be deposited mostly as sheet deposits rather than as channel sands. The B-B' cross section (Figure 17) across the north, shows the Chanute deposits again thinner with only minor amounts of sandstones in both members.

The Thayer Coal and associated (possible) marine horizon

Figure 26 shows the isolith of the Thayer Coal and associated marine horizon. The Thayer Coal is a thin but persistent unit throughout the study area as shown by the isopach and the cross sections. Maximum thickness of the coal and underclay interval is about 4 ft (1.22 m) in western Chautauqua county, Kansas, but is more consistently 1 or 2 ft (0.3 or 0.61 m) thick elsewhere. A possible explanation for this is that some kind of paleodepression from pre-existing topography developed towards this southern part of the study area, which was filled with decaying plant material, therefore leaving thicker coal deposits or a higher rate of accumulation due to greater rate of subsidence.



Key:

Measured Sections

Cores

Outcrop Belt

0 25 50

Miles

0 50 100

Kilometers

Figure 26. Isolith of the Thayer Coal and the Chanute's marine horizon. Contour interval is 1 foot throughout, solid lines represent the Thayer Coal, dashed lines represent the marine horizon.

The main reason that the isolith of the marine horizon was included with the Thayer Coal involves data extracted from new cores taken by the Kansas Geological Survey during the summer of 1991 (after field and core sampling for this study). The well logs taken from these boreholes were used in the subsurface part of this study. Figure 27 is a cross-section through these well logs that helps to resolve several stratigraphic problems. First, the black shale on the top of the Bredenhoft 1 and 2, Clarkson 1 and 2, and Ferrel 3 logs is the Muncie Creek Shale member of the Iola Limestone and not the older Quivira Shale member of the Dewey Limestone as previously thought. This identifies the Chanute as being present in the subsurface at these locations. The other problem was the appearance of a limestone within the Cottage Grove sandstone in wells Bredenhoft 1 and 2, and Clarkson 1 and 2. The true identity of this limestone was confirmed by sampling and visual inspection of the cores by R. L. Brenner during the summer of 1992. He reported an agrillaceous, crinoidal limestone in the Clarkson and the Bredenhoft cores at the same depth where the limestone signature showed up on the well logs. This limestone seems to correlate with the Thayer Coal in nearby logs (Ferrel 1 to 3) as shown in the cross-section D-D' (Figure 27). This observation raised the question if the limestone could be the marine equivalent of the Thayer Coal, with the coal developing on high topographical areas while the limestone formed in marine water in adjacent low-lying areas. If this were the case,

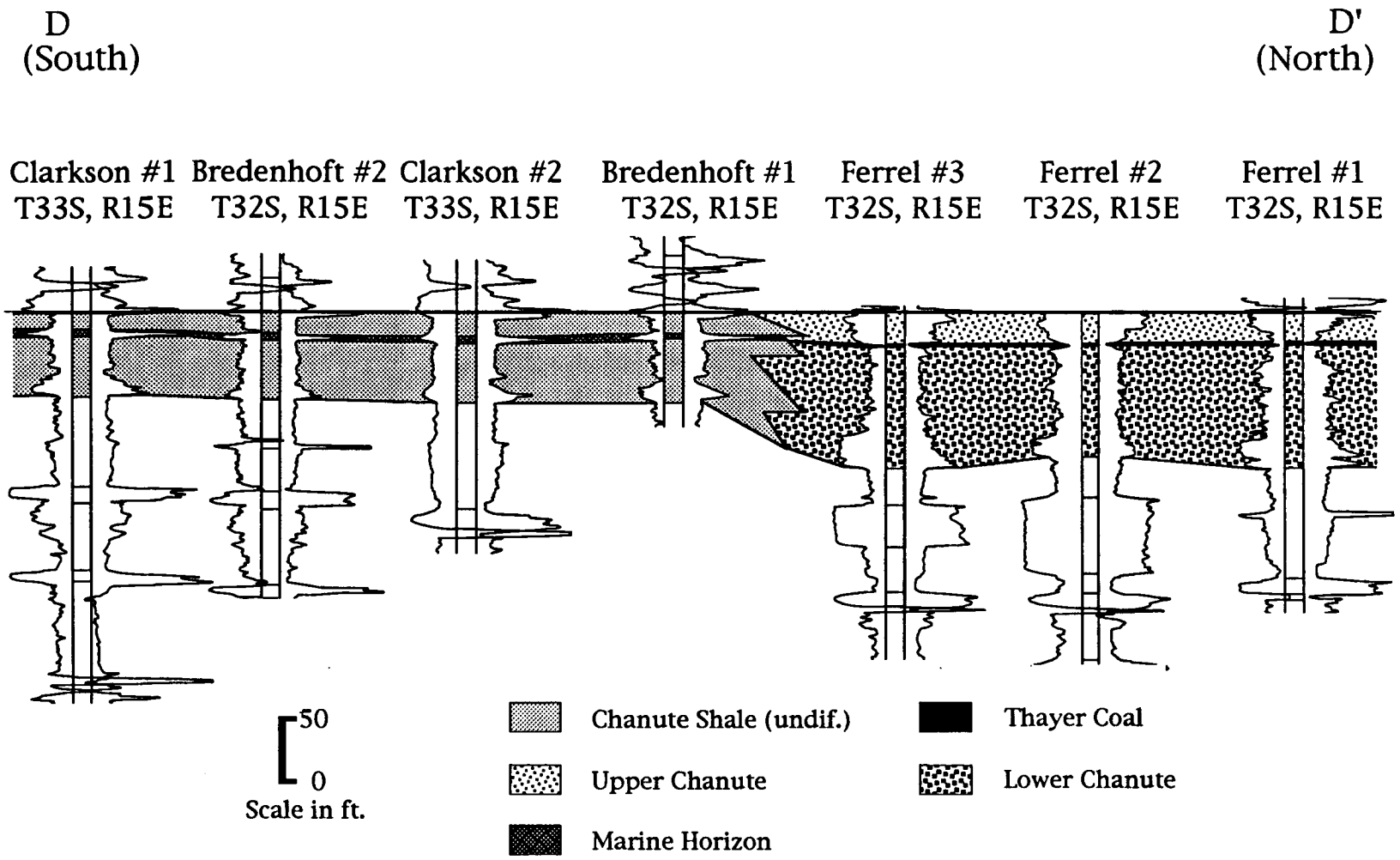


Figure 27. Cross section through the Chanute Shale from south to north, across the southern part of the study area. Relationship between the coal and the marine horizon is local.

one would expect the marine horizon to be present only in the low lying channel areas towards the south and only where the coal was absent. This turned out to be true in only one place in Montgomery county, very close to the outcrop belt (Figures 15, 27). Towards the north, both the Thayer Coal and the marine horizon (within the Cottage Grove sandstones) were identified in some well logs, in areas where no apparent channels were present. These cores and their well logs help to confirm the existence of the marine horizon, at least locally, in the Chanute as reported by Bennison (near Bayard bridge, pers. comm. to Heckel) but they do not explain their relation to each other or to the depositional environment of the Chanute deposits.

The Chanute Shale is known to extend into western Oklahoma where Cottage Grove sandstone in the upper Chanute was identified in the subsurface in northwestern Oklahoma with thicknesses up to a maximum of 100 ft. (30.5 m), and containing a producing oil and gas field (Fruit and Elmore, 1988). The Chanute Shale is also recognized in Iowa and Nebraska, where it previously had been misidentified as the Lane Shale (Heckel, ms. in review).

CHAPTER III
LITHOFACIES

Definition of lithofacies

Nine lithofacies are recognized in the Chanute Shale from outcrops and cores studied (Figure 28). These are: 1) Interbedded fine sandstone and silty clay shale, 2) Massive channeled sandstones, 3) Gray, fissile clayey shale, 4) Silty shale, 5) Mottled blocky mudstone, 6) Coal, 7) Thinly-bedded, thinly-laminated micaceous sandstone, 8) Carbonate cemented, contorted fine micaceous sandstone, and 9) Interlaminated siltstone and shale.

Interbedded fine sandstone and silty clay shale

This lithofacies is characterized by gray, fissile, micaceous (concentrated in laminae), clayey shale, with silt concentration increasing towards the top. These shales are interbedded with massive, micaceous (mostly concentrated in laminae), oxidized (by weathering upon exposure), organic-rich, fine-grained sandstones which have gradational contacts with the shales. The sandstones are thinly-laminated and thinly-bedded towards the top of each particular interbed. In gamma ray-neutron density well logs this lithofacies is characterized by a serrated signature that fluctuates from the shale baseline to past the 60% sandstone line (Figure 28).

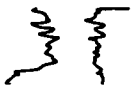
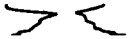
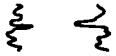
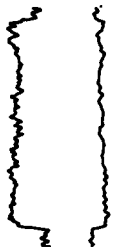
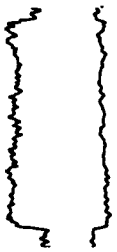
Chanute Shale Lithofacies									
Lithofacies	Interbedded fine sanstone and silty clay shale	Massive channelled sandstones	Gray, fissile clayey shale	Silty shale	Mottled blocky mudstone	Coal	Thinly-bedded thinly-laminated micaceous sandstone	Carbonate-cemented contorted sandstone	Interlaminated siltstone and shale
Description	Gray, fissile, micaceous, clay shale interbedded with massive, micaceous, oxidized, organic-rich, fine-grained sandstone.	Massive, fine-grained, oxidized, well-cemented, organic-rich, micaceous sandstone.	Gray, Fe-stained, heavily weathered clay shale.	Heavily weathered, poorly exposed, Fe-stained silty shale.	Light gray to dark brown, blocky mudstone.	Blocky, crumbly, sulfurous, oxidized, coal.	Very fine-grained, micaceous, well-cemented, and Fe-stained.	Carbonate cemented, micaceous, Fe-stained, very fine to fine-grained sandstones.	Interlaminated siltsone and shale. Silt/Sh= 4/1. Thickness of siltstone increases upwards.
Sedimentary Structures	Thin, micaceous, laminations in sandstones and shales.	Homogeneous, nested, channelized, sandstones with weak laminations towards the top.	Fissile, and organic-rich (plant remains). Contains concretions at the base.	Organic-rich	Mottled, with scattered plant remains.	Thin, but continuous. Plant structures preserved.	Localized ripple laminations, sub-parallel bedding, organic-rich. Shale chips	Thinly-bedded, contorted, and organic-rich. Ripple laminations.	Uniformly spaced interlaminations. Contorted, rippled and mottled laminae, silt lenses, and flaser beds. Reactivation surfaces.
Typical Gamma-Ray Neuton Signatures				Signature not observed					Signature not observed
Depositional Environment	Interdistributary Bay and Crevasse Splay Deposits	Major Distributary Channels at Lower Delta Plain	Channel Abandonment Fill	Channel Abandonment Fill	Marsh-Swamp in interdistributary bay	Marsh-Swamp in interdistributary bay	Distributary mouth bar (deltaic system) or sand shoal in (estuarine system).	Distributary mouth bar (deltaic system) or sand shoal in (estuarine system).	Funnel shaped (drowned stream) estuary.

Figure 28. Relationships between sandstone characteristics, log signature, and depositional environment.

Massive channeled sandstones

This lithofacies consists of massive fine-grained, oxidized, well-cemented, organic-rich, micaceous sandstone occurring in nested channels in outcrop. These sandstone bodies are mostly homogeneous, but are commonly laminated towards the top, and usually appear above sharp contacts with underlying beds. In gamma ray-neutron density well logs these units show a sharp deflection to the left (low gamma) past the 60% sandstone line (Figure 28). There is a marked contrast between this signature and the Nellie Bly Shale signature as discussed in the stratigraphy chapter.

Gray, fissile, clayey shale

The clayey shale consists of a gray, fissile, iron-stained, clayey shale, which is commonly heavily weathered in outcrop and contains some concretions at its base. This facies occurs in outcrop locations where the Noxie and the Cottage Grove sandstones are absent. The shale lacks marine fossils, but contains organic fragments including plant remains. In gamma ray-neutron density well logs, this facies is represented by a sharp deflection to the right (high gamma, low neutron) commonly referred to as "shale-out" by loggers or by a thick high gamma signature (Figure 28).

Silty shale

This facies consists of a silty, iron-stained, unfossiliferous, organic-rich shale. It occurs in gradational contact with units

underlying and overlying it, and it is usually heavily weathered (recent) in outcrop. A characteristic well-log signature for this facies was not observed; an explanation for this could be that this facies thicknesses were not resolved by the logging tool, or that no major radioactivity differences with surrounding mud-dominated facies were detected by the logging tools.

Mottled blocky mudstone

This lithofacies consisted of light gray to dark brown, mottled blocky mudstone, with scattered organic matter (roots and other plant remains) in gradational contact with the underlying unit. Thicknesses of this facies differed locally, in cores, generally from 3 to 5 ft (0.7- 1.5 m), and thinner in the outcrops; 4 in to 5 ft.(10 to 30 cm). The thickness of this facies is beyond the resolution of logging tools, but when combined with the signature of the overlying Thayer Coal, it produces a signature similar to that of a black shale (high gamma, low density neutron) with displaced peaks, as was explained in the stratigraphy chapter (see Figures 19, 28).

Coal

This lithofacies applies strictly to the Thayer Coal. In outcrop, the coal occurs as a blocky, crumbly, sulfurous, oxidized, thin but persistent coal bed in sharp contact with the underlying blocky mudstone. The coal is shiny on fresh broken surfaces but dull elsewhere. The original wood fabric or appearance can be observed easily in both outcrop and core. In core, some carbonate veins can be

observed in the coal. The well-log signature of the coal is characterized by it's low gamma-ray, and low neutron-density counts (Figure 28). Since this facies is thin, generally beyond resolution of logging tool, it becomes difficult to trace in the subsurface although it is very continuous in outcrop.

Thinly-bedded, thinly-laminated, micaceous sandstone

This lithofacies consists of thin beds of fine to very fine-grained sandstone that is micaceous, organic-rich (roots and plant fragments), well-cemented, and iron-stained. Although uncommon, some ripple laminations are observed in portions of this facies. In cores, organic matter is concentrated in lamellae parallel-subparallel to bedding. Shale chips are also observed in the cores. In outcrop, this type of sandstone is underlain by silty shale, rooted towards the base. The well-log signature of this facies is blocky in nature with low gamma-ray counts that pass beyond the 60% sandstone line (Figure 28).

Carbonate cemented, contorted, fine micaceous sandstone

This lithofacies consists of thinly bedded, carbonate-cemented, micaceous, organic-rich, iron-stained, contorted, very fine-to-fine-grained sandstones in abruptly gradational contact with underlying beds. Ripple laminations are commonly observed in outcrop and cores. The well-log signature of this facies is indistinguishable from that of the thinly-bedded sandstone described above.

Interlaminated siltstone and shale

This lithofacies consists of uniformly spaced interlaminations of siltstone and shale that are in sharp contact with underlying beds. The silt to shale ratio is 4:1, with siltstone laminae approximately 5 mm thick and shale laminae 1 mm thick. Distance between the silt/shale laminations increases in groups towards the top of the facies. Contorted laminae are observed throughout, while pyritized root fragments and mottling are common only at the base. In one core Gaddy # 1 (Figure 29), this lithofacies underlies the sandstone with mottled texture and roots towards the bases. The well-log signature of this lithofacies can not be resolved from other mud-dominated lithofacies by the geophysical tool.

Lithofacies distribution

The occurrence of the lithofacies is related for the most part to the different members of the Chanute Shale and to their occurrence in outcrops and in the subsurface. The interbedded sandstone and silty shale lithofacies and the massive channeled sandstones are for the most part restricted to the Noxie sandstone in the lower Chanute, therefore to the southern part of the study area. The signature of the massive channeled sandstones lithofacies is commonly observed within the Noxie channel areas that were discussed in the stratigraphy section. In outcrop, this lithofacies occurs in the areas of southern Montgomery county, Kansas, and parts of Nowata county, in adjacent Oklahoma. The interbedded sandstone and silty shale is not often present on the well logs, but when it does occur is mostly

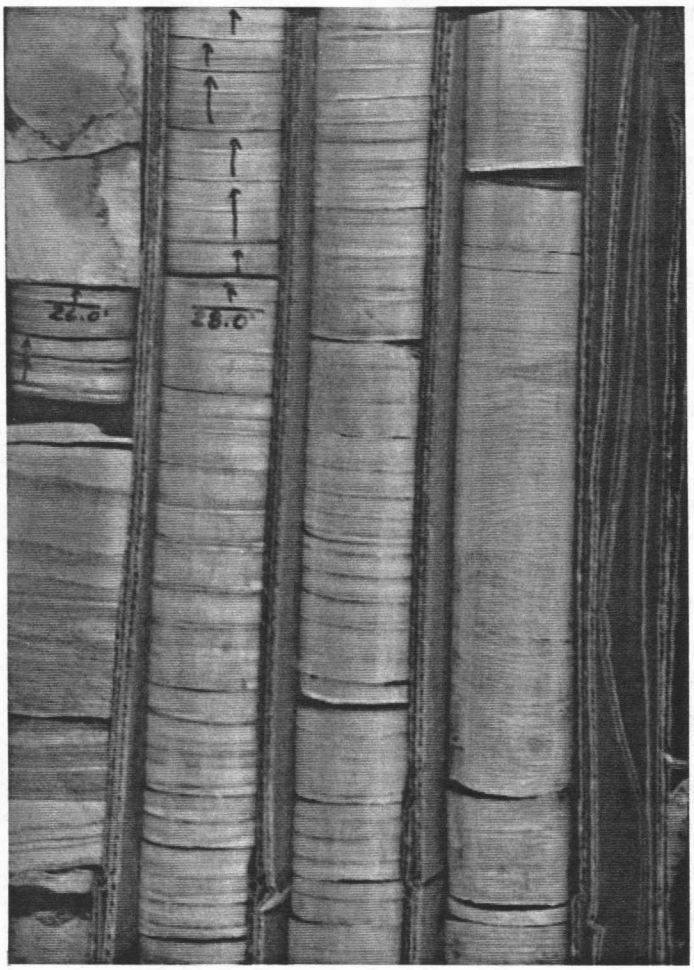


Figure 29. Rhythmically spaced interlaminations in core Gaddy #1. These correspond to the interlaminated siltstone and shale lithofacies of the upper Chanute. These interlaminations may be interpreted as "tidal bundles" or "tidalites."

restricted to the interchannel areas (Figures 20, 21, 22). The gray silty shale is more common to the north and the west where the Chanute loses its sandstone bodies. In outcrop this lithofacies occurs in areas where the Noxie sandstone and the Cottage Grove are not present. An example is the North Chanute outcrop, where the Cottage Grove is absent and a shale takes its place beneath the Iola Limestone (Figure 11, Appendix 3). The signature of the silty shale was not resolved in the well logs, but in outcrop this shale is quite common. This lithofacies, for the most part, is a transitional facies between the sandstones and their surrounding lithologies, such as underneath the blocky mudstone, or above the Thayer Coal and beneath the Cottage Grove sandstone. The main problem with this lithofacies is that it is usually thin, so its thickness is beyond the resolution of the well logs. The blocky mudstone (underclay) and the coal thickness are both well illustrated in the Thayer Coal isolith map. These two lithofacies can be seen pinching out in this map towards the north and west of the outcrop belt. The thinly-bedded, thinly-laminated sandstone and the contorted sandstone lithofacies apply mostly to the Cottage Grove sandstone, and their distribution is illustrated by the Cottage Grove isolith. This map shows that these lithofacies are concentrated in the southern and eastern portions of the study area, and are better defined close to the outcrop belt. The interlaminated siltstone and shale lithofacies was observed only in the Gaddy core, where it occurs between the coal and the thinly-laminated and thinly-bedded sandstone (Appendix 3).

CHAPTER IV
DEPOSITIONAL ENVIRONMENTS

Introduction

The sediments of the Chanute Shale record the effects of sea level changes in terrestrial to transitional marine environments. In the following discussion, the lithofacies present in the Chanute Shale and their interpreted depositional environments will be discussed. The depositional environments of the members of the Chanute Shale will be presented with their corresponding supporting evidence collected from outcrop, cores, and subsurface well logs. At the end of the chapter, these interpretations will be presented within the context of the Pennsylvanian paleogeography of the area.

Lithofacies depositional environments

Interbedded fine sandstone and silty shale

This lithofacies represents interdistributary bay deposits and crevasse splays common between distributary channels in the lower deltaic plain of a delta system (Figure 28). Interdistributary bays are shallow open or closed bays between major distributaries that extend seaward through a system of "radial" bifurcating channels (Coleman, and Pryor, 1982). These bays may be closed to the sea but are commonly open, or connected to it by small tidal channels, and

are commonly surrounded by marshes, and distributary channels (Coleman, and Pryor, 1982). Rapid distributary progradation, coupled with rapid subsidence and low nearshore wave energy, frequently results in the occupation of interdistributary areas by these shallow open or closed bays (Davis, 1985). Interdistributary bay deposits in the lower Chanute are represented by silty clay shales, interbedded with fine-grained sandstones that represent crevasse splay deposits. Crevasse splays form when a major channel levee breaks, and coarser sediments from the channel are deposited on top of bay deposits. The fine-grained, massive sandstones at the base of the sandstone interbeds (in this lithofacies of the lower Chanute), records the results of the initial break of the levee. These massive sandstones represent rapid deposition from turbulent water, similar to the depositional conditions of a Bouma A interval from a turbidite. The massive sandstones grade upward into plane laminations towards the top of each sandstone interbed representing less turbulent unidirectional flow, similar to Bouma B depositional conditions. The absence of marine fossils in these deposits suggests deposition on a more fluvial environment like the interdistributary fresh water lakes in the upper delta plain, or a floodplain in a fluvial system. Lakes associated with delta plains are also subjected to crevassing, and/or channel diversion (Coleman and Pryor, 1982) producing the same type of deposits as interdistributary bay crevassing in the lower deltaic plain. These deposits usually contain abundant lacustrine microfaunal remains, ostracodes, and intense

bioturbation by soft bodied organisms (i. e. polychaete worms) which are also absent in this lithofacies of the Chanute. Overbank splays in a floodplain of a fluvial-alluvial system may also explain this lithofacies but the lack of common fluvial sedimentary structures in this and other lithofacies of the Chanute deposits also poses a problem. These three depositional environments may all be possible scenarios that would leave the same type of deposits found in this lithofacies, but the lack of fossils and distinctive sedimentary structures preclude more definite interpretation.

Massive channeled sandstones

This lithofacies is interpreted to represent the infillings of major distributary channels in the lower delta plain of the Chanute deltaic system (Figure 28). According to Coleman and Pryor (1982), distributary channels tend to be stable in their position, although migration can occur. This stability is due to the initial deep scouring of the channel into underlying deposits restricting channel migration. In the lower Chanute, this lithofacies is characterized by massive, fine-grained sandstone, with organic matter and shale chips above the scoured base, and weakly defined planar laminations towards the top. A conglomerate composed of reworked underlying Dewey Limestone deposits is present in some localities above the scoured-erosional surface representing the initial channel scouring of underlying units. This conglomerate could also represent alluvial channels in the upper deltaic plain, or a fluvial system. Although other common fluvial sedimentary structures like cross-beds, ripples,

contorted bedding, and slump structures were not observed in this lower Chanute lithofacies the conglomerate and overlying sandstones could be the product of any of the above systems.

Silty shale

When channels are abandoned, progressively finer-grained sediments are deposited (Coleman, and Pryor, 1982; Boggs, 1987; Davis, 1985). Deprived of a an active influx of sediment and water, the channel will undergo an infilling process with local upstream and downstream sediments (Coleman, and Pryor, 1982). These infilling clays generally contain little or no fauna and virtually no marine fauna (Coleman, and Pryor, 1982). In the lower Chanute these deposits are represented by the silty shale lithofacies and are underlain by a clayey shale with siltstone lenses (Figure 28). The silty shales occur with high organic content towards the top. This lithofacies represent the continued infilling of the distributary channels in the lower delta plain which began with the deposition of the sands described above, and continued with the mud deposition towards the top. This infilling event may also represent channel avulsion in the upper delta plain or in a fluvial system.

Blocky mudstone and coal

The mudstone at the top of the lower Chanute that occurs underlying the Thayer Coal is blocky, mottled, and has significant amounts of plant remains. The coal commonly displays sulfur, carbonate and iron-oxide concentrations, and preserved plant

structures along fractures and "cleavage" planes of outcrop samples. Pyrite is present in cores. The depositional environment of these two lithofacies is interpreted as a marsh-swamp type environment common in interdistributary bays of the lower delta plain (Figure 28). In a deltaic setting, marshes tend to occur in the marginal areas of the interdistributary bays. If subsidence is slow, these bays may become completely infilled with marsh or mangrove swamp (Davis 1985). These are the areas where water is very shallow and vegetation is abundant, therefore marsh deposits are characterized by abundant bioturbation and rooting. In a well drained swamp, oxidizing conditions are dominant and formation of Fe-oxide and carbonate nodules are common; in a poorly drained swamp, reducing conditions dominate and carbonate, vivianite and pyrite nodules are common (Davis, 1985). The presence of both oxidizing and reducing products (carbonate, and pyrite) within the coal samples from outcrops and cores, indicates a change in the drainage of the depositional environment, or in the composition of the diagenetic waters, while the iron-oxide might be a weathering product. Although the time of formation of these products was not determined, they may reflect the change between a poorly drained swamp and a well drained swamp and vice-versa, or a change in the diagenetic environment. These lower Chanute lithofacies may be related to the interdistributary bays marsh-swamp environments as well as to the top of a channel fill sequence in either upper delta plain or a fluvial system. The latter may involve subaerial exposure

developing a paleosol under oxidizing conditions before formation of the coal. Further studies of the blocky mudstone may help to determine if such subaerial exposure did took place. Although coals deposited on fluvial systems tend to be localized and very thick (Horne et al., 1978), in contrast to the thin and continuous Thayer Coal, a fluvial depositional environment is also possible.

Interlaminated siltstone and shale

The rhythmically spaced interlaminations of this lithofacies suggest an estuarine environment in which tides affected the deposition of the available sediments (Figure 28). In an estuarine setting, the sediments are mostly provided by the rivers (Davis, 1985, Boggs, 1987, Coleman, and Pryor, 1982). Parallel laminations, consisting of alternating coarse-grained and fine-grained material, are apparent in many low-energy estuarine deposits. These interlaminations may be caused by seasonal variations, or by normal periodic tidal processes in higher-energy environments (Davis, 1985). In the case of the upper Chanute, these interlaminations show an upward increase in both the amount of coarser material, and the thickness of the siltstone interbeds towards the top of the lithofacies (Figure 29). This may reflect a change in the general depositional environment of the area from a tide-influenced to a more stream-influenced environment.

Thinly-bedded, thinly-laminated, micaceous sandstone, and carbonate cemented, contorted sandstone

This upper Chanute lithofacies, characterized by rippled, cross-laminated sandstones, with high organic matter, shale chips, flame structures, reactivation surfaces, and flaser bedding is carbonate-cemented towards the top. The characteristics of this lithofacies suggest deposition in either a distributary mouth bar in a deltaic system, or a sand shoal in an estuarine system (Figure 28). Distributary mouth bars occur in the subaqueous delta plain; they contain the coarsest sand deposits in the deltaic system, and are located directly at the mouths of active distributaries (Coleman and Pryor, 1982). Mouth-bar deposits in general are characterized by rippled cross laminations, with occasional cut-and-fill and scour structures, organic debris, and sometimes thin clay beds and flaser bedding; specially where currents are moderate (Davis, 1985). In a funnel-shaped estuarine setting, sand shoals are located near the estuary's mouth and are characterized by cross bedded or rippled sand, with clay lenses or pebbles, overlain by megaripples. In both interpretations the presence of the carbonate cement only at the top of the sandstones can be explained by an increase in marine influence on the system by sea level rise.

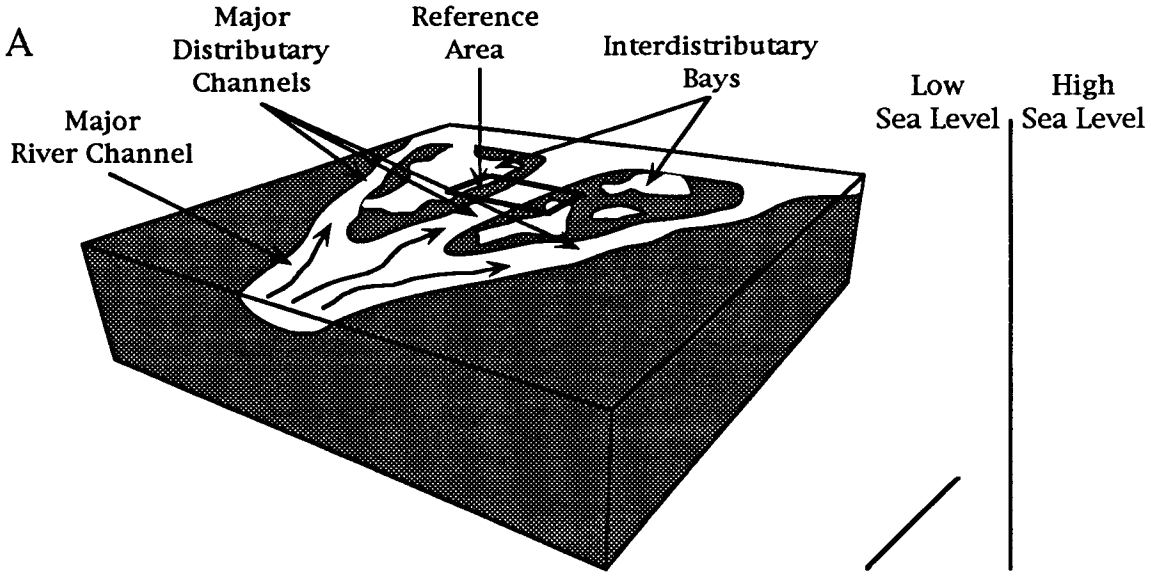
The lower Chanute

The depositional environment of nearshore shales has been interpreted in the past as fluvially dominated deltas in which coals and underlying deposits were usually considered the shallowest

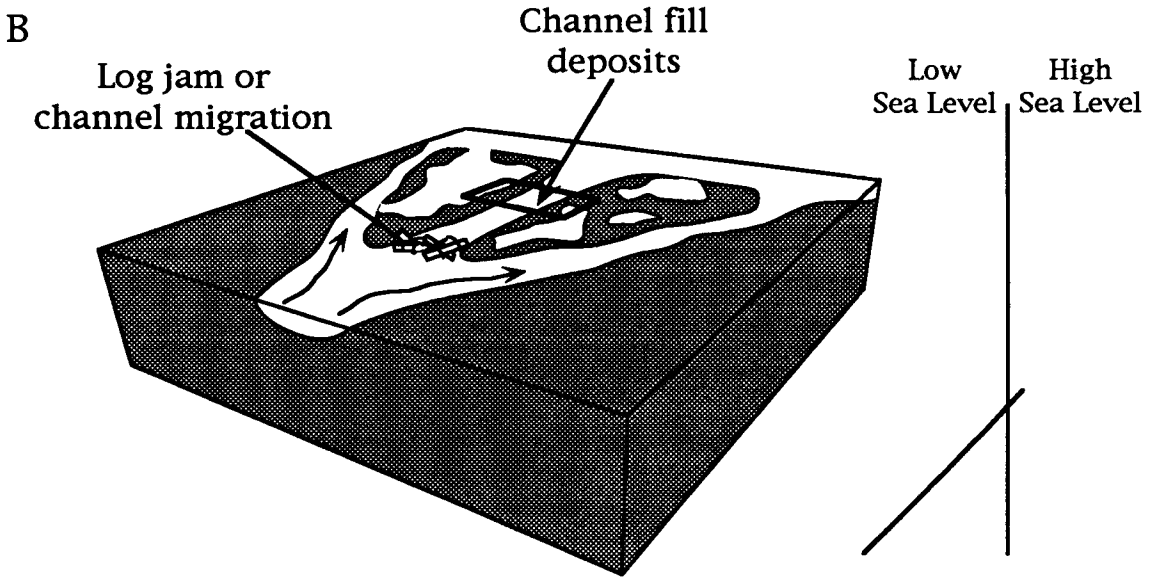
deposit, therefore representing maximum regression (Figure 1). The above interpretation would make the seatearth of the Thayer Coal representative of maximum regression. During the early part of such regression, the regressive member of the Dewey Limestone would have been deposited, and as sea level continued falling the Noxie channels would have eroded parts of the Dewey. Later the channels were abandoned (possibly due to main channel migration, or upstream blockage) and the silty shale, blocky mudstone and the Thayer Coal would have been deposited on top as part of channel fill and interdistributary bay deposits in the lower delta plain. In such a setting, channel lag and cross-bedded sands would normally occur at the base of the channels, and fining upwards sediments like the silty shale lithofacies would follow, representing channel abandonment; shallow water deposits (marsh type in interdistributary bay) would follow, represented by the underclay and eventually the coal. The lower Chanute stratigraphic configuration (Figure 3) supports the interpretation above, but the tendency of the Noxie sandstones to occur as nested channels without sedimentary structures poses a conflict. Channels are considered to be high energy environments with clear indications of directional flow (like cross-bedding and ripple laminations) but the Noxie channel sandstones show no such evidence of flow. In the studied outcrops where the Noxie is exposed (Allin Hill, Noxie road and South Independence, Appendix 3) the absence of cross bedding and ripple laminations in the Noxie channel sandstones suggests a channel with flow velocities under the onset of

ripple lamination formation. Bioturbation or fossil fauna was not observed in the channeled sandstones studied, which may eliminate the possibility of structure obliteration by burrowing, and therefore supports the idea that the sandstones were deposited as massive deposits in a low-flow distributary or alluvial channel after the sea had withdrawn some distance southward.

An interpretation that could explain the relatively low-energy environment suggested by the massive channel sandstones, is that the erosional surface of the channels themselves and the reworked Dewey conglomerate at the base of the lower Chanute represent maximum regression and the coals were deposited under "ever wet" conditions during a marine transgression like has been proposed for the Appalachian coals (Heckel, 1980). When the Noxie channels were active, erosional processes were dominant removing parts of the underlying Dewey Limestone and leaving the conglomeratic Dewey sediments from this depositional stage. As sea level began to rise (not necessarily reaching the study area, but altering drainage), reduced flow within the lower Chanute distributary channels resulted in less available sediments and deposition of very fine-grained sands with the shale chips and plant remains at the base of the channels from local sources upstream and downstream (Figure 30 A). These are the only sedimentary structures present in the massive channel sands of the outcrops studied and represent the distributary's "channel lag". As the transgression proceeded, some channels were abandoned (possibly because of channel migration,



During this time, the distributary channels of the delta were active, depositing the Noxie channeled sandstones. A major transgression had already begun.



A log jam or a channel migration stopped the flow on a distributary producing the channel fill sequence from the lower Chanute (shale, silty shale). The transgression continued beginning to push the shoreline landward.

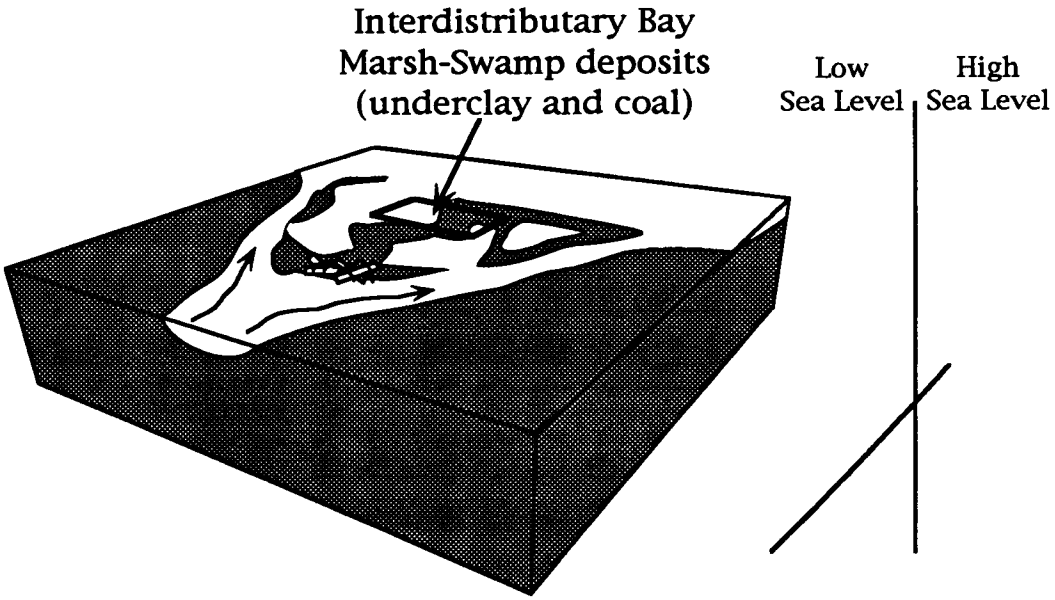
Figure 30. Proposed depositional model for the Chanute Shale; A, B, C, D, E, F.

upstream blockages, or sand source was cut out by moving the main channel further inland, due to transgression). The channels filled up with muds and silty muds as a result of less coarse sediment input (Figure 30 B). As sea level kept rising (not necessarily reaching the area yet) the underclay developed, and later the area was eventually flooded, forming a marsh-like environment at the margins of interdistributary bays represented by the coal capping the sequence (Figure 30 C). Marine fossils, which are common in interdistributary bay deposits, are absent in the lower Chanute deposits suggesting a more fluvial depositional environment, either upper deltaic plain or a fluvial system. Although these are possible scenarios, the lack of fresh water fauna within the shales and silty shales also poses problems for an upper deltaic plain environment, which normally have these in abundance. The lack of obvious sedimentary structures in the sandstones also poses problems for a totally fluvial model for the whole lower Chanute. Even if the stream were very turbulent, depositing only massive sandstones and no other structures, its flow would definitely be reduced by the events that eventually produced the coal, either through regression (old model) or through channel abandonment and fill (this study). This would have produced lower flow regime sedimentary structures like cross bedding and ripples to be deposited on top of the massive channel sands. This was not the case, leaving open the possibility of any of the models described above.

In the Allin Hill outcrop (Appendix 3), the channels were underlain by interbedded shale and sandstone. These deposits might represent distributary channel migration into a interdistributary bay into which the interbedded muds and sands were deposited in the form of crevasse splays from the nearby channels, which eventually migrated above the deposits forming the nested channels seen in outcrop. The same type of deposits may result from crevassing into interdistributary lakes in the upper delta plain or by overbank splays in a fluvial environment. This lithofacies in Allin Hill is about 13.1 ft (4 m) thick and if present in well logs, it is thick enough to be resolved by the logging tool, but was not found underlying the channels in the subsurface. This may have been a result of signature similarities with the underlying Nellie Bly Shale, making these deposits indistinguishable from one another.

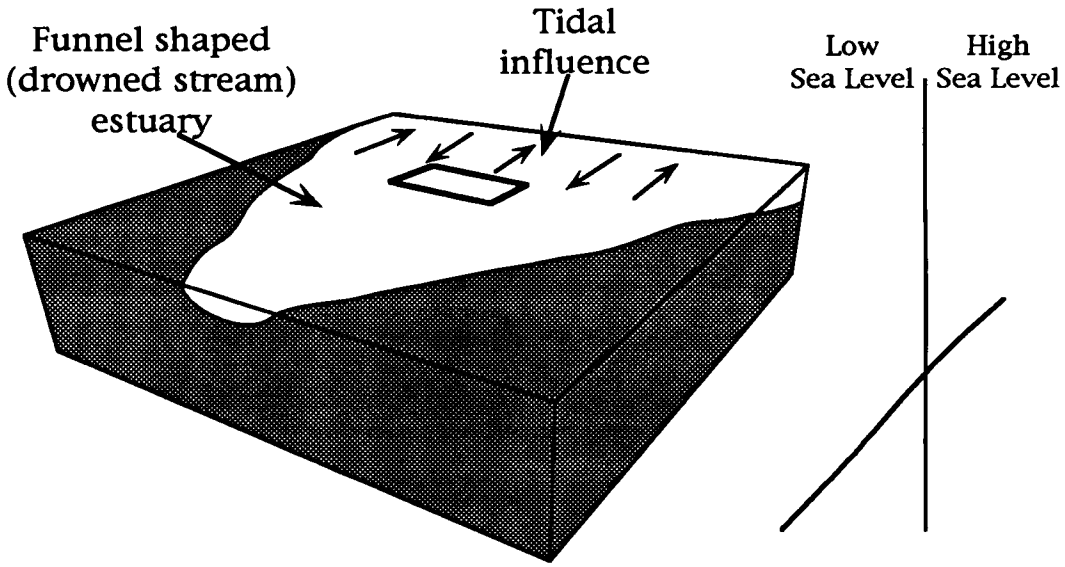
The lower Chanute's well-log signatures in general show a fining upward sequence up to the Thayer Coal's signature (Figures 16, 17, 18, 19). This supports both the regressive-transgressive and the transgressive-channel-fill interpretations above. The morphology of the channels, as shown on the isopach of the lower Chanute (Figure 21) and the isolith of the Noxie (Figure 24) also supports both the regressional-transgressional, and the transgressional-channel-fill scenarios, since the intervening "high" between the channels, in both cases, represents the environments that characteristically have lower sediment input and slower depositional rates (interdistributary bays). Both models also fit with

C



Continued transgression pushes the shoreline farther inland, and begins to flood the area resulting in the deposition of the underclay and coal in the marsh-swamp areas of the interdistributary bays.

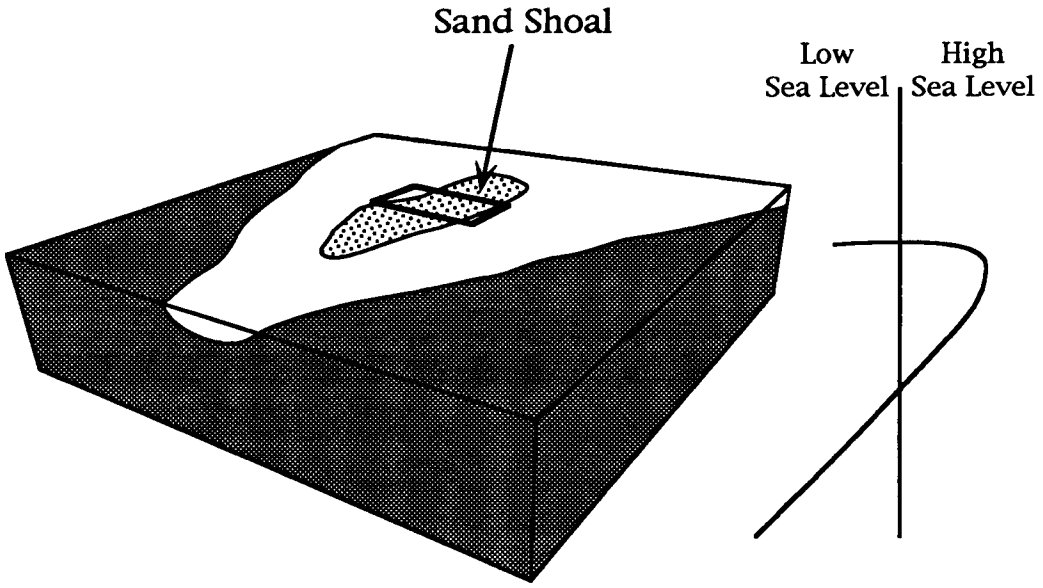
D



The transgression eventually floods the whole delta producing a funnel shaped estuary under tidal influence. This results in the deposition of the interlaminated siltstone and shale of the upper Chanute.

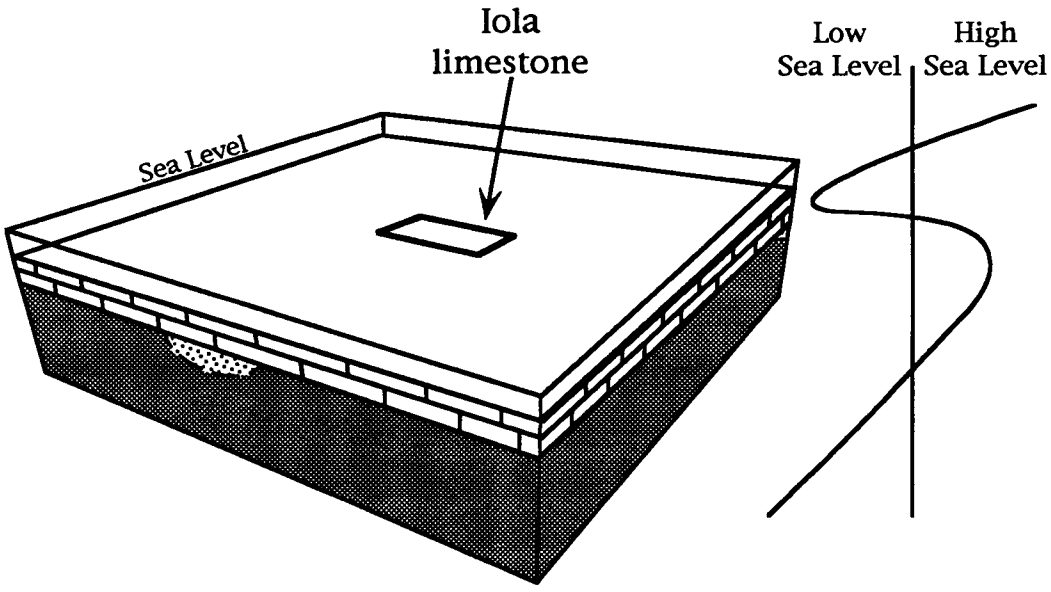
Figure 30. continued.

E



During a minor regression, shoreline is pushed seaward diminishing tidal influence. Sand shoals are formed in the estuary's mouth as a result of increased riverine influence upon the area.

F



Renewed transgression drowned the whole area and eventually deposited the Iola limestone on top of the Chanute Shale.

Figure 30. continued.

the position of the nearshore shale in the Kansas cyclothem as the onset of a marine transgression. The main differences between these two models is the onset of the marine transgression within the nearshore shale, the position of the coal in relation to sea level, and the implications of the lack of sedimentary structures and fossils in the lower Chanute deposits. Although there is evidence pointing into the old model of a more fluvial lower Chanute (seatearth=maximum regression) I believe that the unit represents a transition from an initially fluvial system (erosional surface and conglomerate representing maximum regression) to a lobate, fluvially-dominated delta in which channel fill and interdistributary bays initially dominated the depositional environments. During or after the blocky mudstone was formed the marine transgression began to affect the study area flooding the area and forming the coal. This same transgression would be responsible of the upper Chanute deposits.

The upper Chanute

The upper Chanute sediments consist of silty shale and shales, capped by the Cottage Grove sandstone. The Cottage Grove is primarily represented by thinly-bedded, thinly and gently inclined laminated (some are wavy or contorted), fine-grained sandstones which have ripple laminations, possible flaser bedding, and flame structures.

After deposition of the lower Chanute and the Thayer Coal, the depositional environment had to change in order to account for the differences between the Cottage Grove sandstone and the older Noxie

sandstone. In the isolith map, the Cottage Grove behaves more like a sheet sand filling topographical lows and draping highs within the study area (Figure 25). There are no well defined channels and the sand seems to have come from the east. Sandstone characteristics observed along the outcrop belt are consistent with a sheet sand morphology. Following the interpretation of the marine transgression in a deltaic system, as sea level continued rising, silty shale would have been deposited in a now shallow but flooded interdistributary bay in the lower delta plain. The rooting and mottling at the base of the silty shale would have represented this initial flooding event in a marsh-like environment. The delta retreated landward as a result of the marine transgression moving the delta front sandstone facies in that direction and increasing the sand and silt supply in the area, possibly because of the proximity of the river's mouth. The same effect can also be attained by an increase in accommodation space. Eventually the Cottage Grove sands were deposited as distributary mouth bars in the subaqueous delta plain. As sea level continued to rise, the Iola limestone was deposited on top.

The only problem with this interpretation is that it does not explain the absence of cross beds (which are common in mouth bar deposits), the presence of inclined laminations, the rhythmically spaced, silt and shale deposits, the reactivation surfaces, and the flaser bedding. A possible explanation to this arises if we change

from a deltaic to a funnel shaped (drowned river valley) estuarine setting.

During the same marine transgression that deposited the upper part of the lower Chanute, the still shallow interdistributary bay was connected to the rest of the deltaic system creating a funnel-shaped estuary (Figure 30 D). The transgression would have also "moved" the estuary's mouth closer to the area previously occupied by interdistributary bays. In this system, the deposits would be affected by the tides. Sand and silt availability was increased by the proximity of the estuary's mouth, and with each tide, silt and mud layers accumulated rapidly, explaining the rhythmically-spaced interbedded silt and shale above the Thayer Coal. As sea level continued rising, the amount of accumulated silt would have increased as the estuary's mouth got closer to the area, or by an increase in accommodation space. This silt increase was observed in the cores (Figure 29). This stage may also be represented by the silty shale commonly found underlying the Cottage Grove sandstone in outcrop, since weathering could have obliterated the structures. The roots and the mottled sediments and the fossils found at the bottom of this lithofacies represent the early flooding of the shallow bays in which circulation was increased due to marine processes, therefore allowing for marine fauna to move in, and increasing the silt content. This event marks the beginning of the later estuarine setting. The presence of oxidizing and reducing products within the Thayer Coal also suggest a transition between a poorly-drained to a

well-drained swamp. The increase in circulation by marine processes could produce aerobic conditions thus changing the conditions from a restricted swamp (reducing conditions) to an open, well drained swamp (oxidizing conditions) producing the change in deposits within the coal and supporting the flooding event. The Cottage Grove sandstones could represent sand shoals deposited near the estuary's mouth parallel to the estuary's shore during a minor regression (Figure 30 E). This would explain the increase in sand supply, the ripples, and the flaser bedding found in the Cottage Grove sandstones. Even though the sand shoals are located within a stream-influenced area, it was close enough to the estuary's mouth to have some marine influence. This idea might explain the occurrence of the carbonate cements, observed in the petrographic analysis, towards the top of the Cottage Grove sandstone beds. The east-west trending lobes in the northern part of the upper Chanute isopach (Figure 22) supports this idea since the paleoshoreline would be roughly parallel to the outcrop belt and the ridges could represent the drowned, funnel-shaped estuary, with sand shoals within the thicker deposits. This situation was complicated towards the south where the irregular topography left from the Noxie channels was still affecting the area. Although the Cottage Grove isolith is more chaotic, an east-west trend can be observed even in the south, close to the outcrop belt, where the thickest sands are located (Figure 25).

The sedimentary structures in the Cottage Grove sandstones suggests that the estuary idea is plausible, but the apparent lack of

marine fossils in the sand shoals, and brackish fossils in the shallow drowned bay is puzzling. The evidence for the interpretation above is ambiguous, and certainly more cores would help resolve the problem. However, with the available data, the concept of a funnel-shaped estuarine development during a marine transgression best explains the depositional environment of the upper Chanute.

Paleogeography

The Chanute Shale, as previously discussed, was deposited during the Missourian Stage of the Late Pennsylvanian. According to Heckel (1980) nearshore shales typically represent maximum regression. Heckel also stated that the some nearshore shales seem to be almost entirely prodeltaic, suggesting that sea level did not withdraw past the mid-continent outcrop belt. The evidence gathered during this study seems to agree with this interpretation. The Chanute is a nearshore shale representing maximum regression in its depositional area, and this regression may not have extended farther south than northern Oklahoma (Heckel, 1986).

Upper Desmoinesian sediments with a Ouachita source terrane were identified by Krumme in 1981. These sediments marked a change in source area from a northerly to a southerly source. The Ouachita foldbelt became the source area for upper Desmoinesian and succeeding Pennsylvanian siliciclastics in the Arkoma and Anadarko basins (Rascoe and Adler, 1983). A general increase in the extent of marine transgressions occurred during the late Desmoinesian, eventually inundated the area, bypassing the Nemaha

and the Central Kansas uplifts and continued onto the Kansas shelf area. Rascoe and Adler (1983) noted a west to east increase in general sandstone content and progression from a marine to marginal marine environment. They also noted the disconformable contact between the regressive limestones and the nearshore shales of the succeeding cyclothem. They interpreted this as a hiatus representing the time of maximum regression therefore adding support to the interpretation of the Noxie channels as having been scoured during maximum regression.

The sedimentologic and stratigraphic evidence collected during this study places the Chanute into a fluvial to marginal marine setting environment during a marine transgression (with a minor regression) on the Cherokee shelf. The onset of this transgression is represented by the infilling of the Noxie channels (Figure 30 A), from which time sea level proceeded to rise steadily until the deposition of the Cottage Grove sandstone during a minor regression (Figure 30 E), and continued rising until the deposition of the Muncie Creek black shale member of the Iola Limestone (Figure 30 F). Fluvial channels at the base of the Noxie sandstone cut and reworked underlying sediments depositing the reworked Dewey conglomerate. Distributary channels of the Noxie, a lobate, fluvially dominated, deltaic system, were abandoned and filled with finer-grained sediments from nearby sources in the lower delta plain (Figure 30 B). The area was flooded by continued sea level rise producing a shallow marsh-type interdistributary bay (Figure 30 C). This bay was

eventually connected to the rest of the delta and the sea as the rising waters flooded the delta plain forming a funnel-shaped estuary and also producing migration of the system's mouth closer to the study area (Figure 30 D). This increased the amount of sediments reaching the area, depositing the tidal-influenced interlaminated siltstones and shales, followed by the Cottage Grove sandstone as a sand shoal within the estuary's mouth during a minor regression (Figure 30 E). After deposition of the Cottage Grove, sea level rose again to deposit the Iola limestone on top of the Chanute siliciclastics (Figure 30 F).

CHAPTER V

SANDSTONE PETROGRAPHY

Introduction

This chapter focuses on the petrographic characteristics of the sandstone samples taken from the Chanute Shale outcrops and cores. Sandstone components will be described in general first, and a discussion of the characteristics from the Noxie and the Cottage Grove sandstones will follow. Appendix 2 contains point counts of the petrographic data taken from these samples and can be used as reference during the following discussion.

Detrital constituents

Monocrystalline quartz

Monocrystalline quartz composes 20 to 47% of the bulk rock and it is the major detrital constituent present in the thin sections analyzed (Figure 31). These grains are angular to sub-angular, and have minor amounts of inclusions and some fracturing (mostly along the edges possibly a result of the grinding process). Approximately 5 to 10% of the monocrystalline quartz grains in each thin section show undulose extinction, but the majority of the grains have normal parallel extinction. The average grain size is between coarse silt (0.05 mm) and medium sand (0.46 mm).

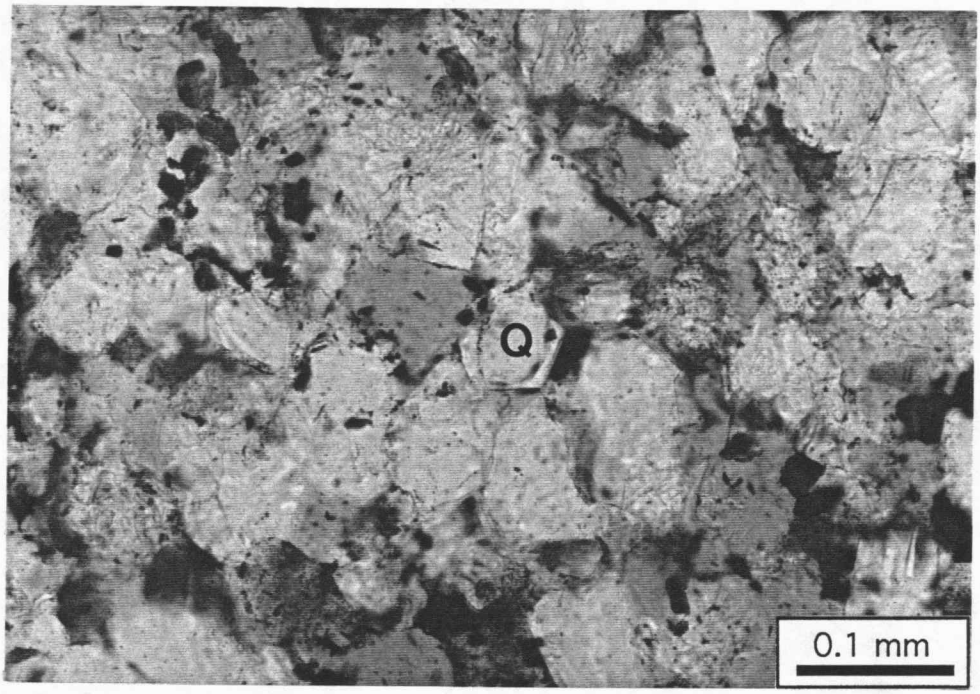


Figure 31. Monocrystalline quartz (Q) in the Chanute sandstones. Partly dissolved quartz overgrowths and secondary porosity are also observed; PPL. Photomicrograph taken from outcrop sample GC 2.8 of the Noxie sandstone.

Thin and discontinuous overgrowths (Figure 31) are present in 55% of the samples. Chemical alteration of quartz grains was primarily observed in carbonate cemented samples, although partial dissolution of overgrowths was commonly observed (Figure 31).

Polycrystalline quartz

Polycrystalline quartz composes 0 to 10% of the bulk rock in the thin sections analyzed. These grains consist of irregularly-sutured, anhedral crystals showing both undulose and normal parallel extinction. Some fracturing occurs along the edges of crystals, but there were no visible overgrowths. Roundness ranges from sub-angular to sub-rounded, and grain size ranges from coarse silt (0.05 mm) to medium sand (0.46 mm).

Feldspars

Plagioclase

Plagioclase, identified by its albite twinning, composes 1 to 11% of the bulk rock in the thin sections and represents, along with orthoclase, about 80% of the feldspars present. Grains are mostly sub-angular, usually showing some degree of chemical alteration. Grain size ranges from coarse silt (0.05 mm) to medium sand (0.46 mm), and no visible overgrowths were observed. The types of plagioclase represented were mostly albite (60%) and oligoclase (50%), with minor amounts of andesine (11%) found in some thin sections. This was determined by using the Michel-Levy method for identifying plagioclase feldspars. Albite and oligoclase coexist in

about 50% of the thin sections analyzed. The degree of chemical alteration of oligoclase was usually slightly higher than that of albite.

Orthoclase

Orthoclase composes 1 to 8% of the bulk rock in the thin sections analyzed. Orthoclase grains are mostly angular to sub-rounded, with grain sizes ranging from fine silt (0.05 mm) to medium sand (0.46 mm), and with Carlsbad twins present in 16% of the samples analyzed. Most of the orthoclase grains show some degree of chemical alteration or partial dissolution, although some of the samples appear intact.

Microcline

Microcline composes trace to 1% of bulk rock in the thin sections analyzed. Grains are mostly angular to sub-angular, with grain size ranging from coarse silt (0.05 mm) to medium sand (0.46 mm). Minor degrees of alteration and partial dissolution was observed in the grains (Figure 32 a, b). Microcline seems to be restricted to the Noxie sandstone except for one core sample from the Cottage Grove sandstone.

Perthite

Perthite is another minor component of the Chanute sandstones representing trace to 1% of the bulk rock in the analyzed thin sections. Chemical alterations of grains, and partial dissolution are minor but present (Figure 33), and grains are angular to sub-rounded. Grain size ranges from coarse silt (0.05 mm) to

a

b

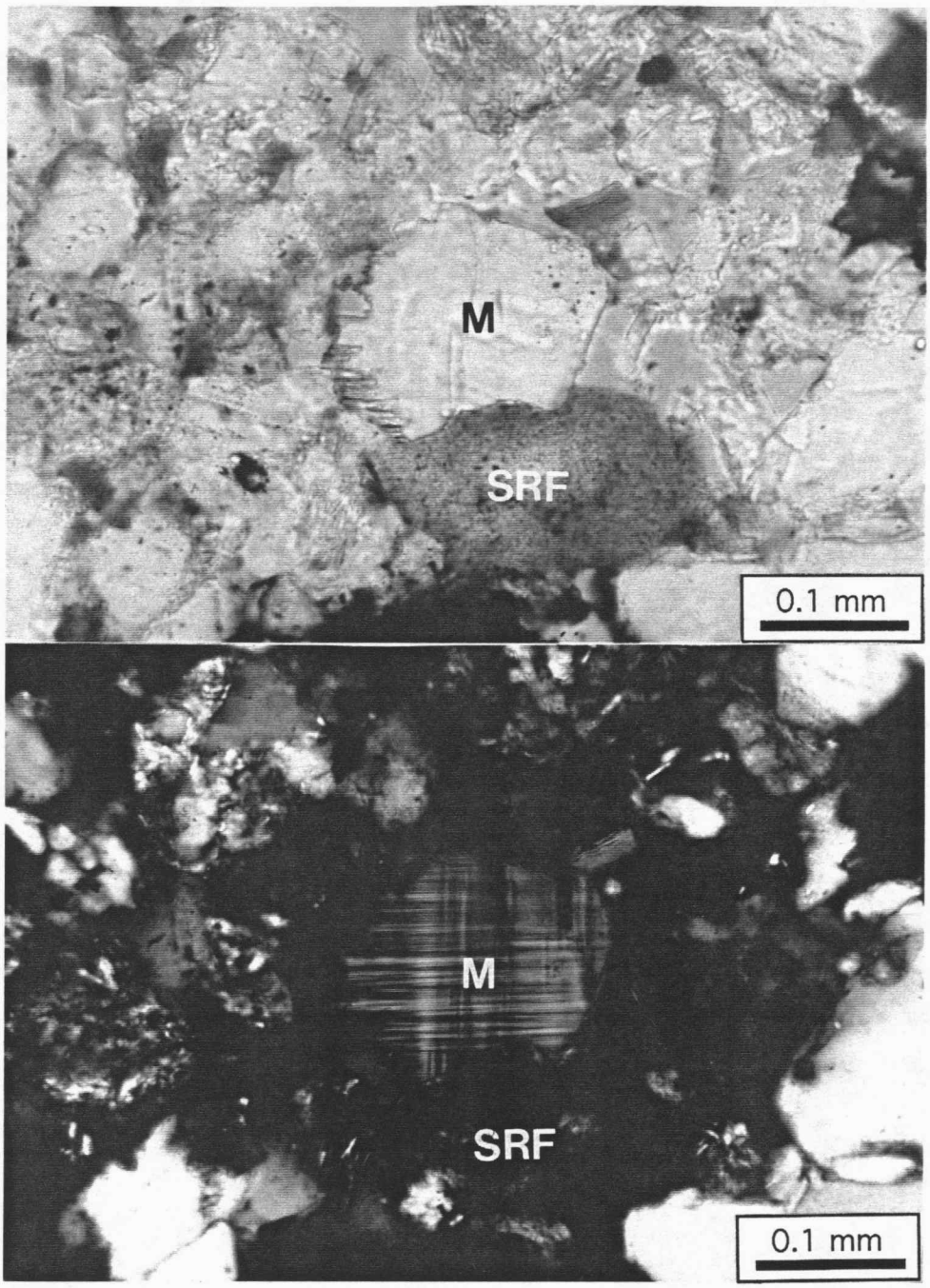


Figure 32. Microcline feldspar (M) showing partial dissolution along preferred twins. Secondary porosity and an SRF also present; a: PPL, b: XN. Photomicrographs taken from outcrop sample AH 8.3 of the Noxie sandstone.

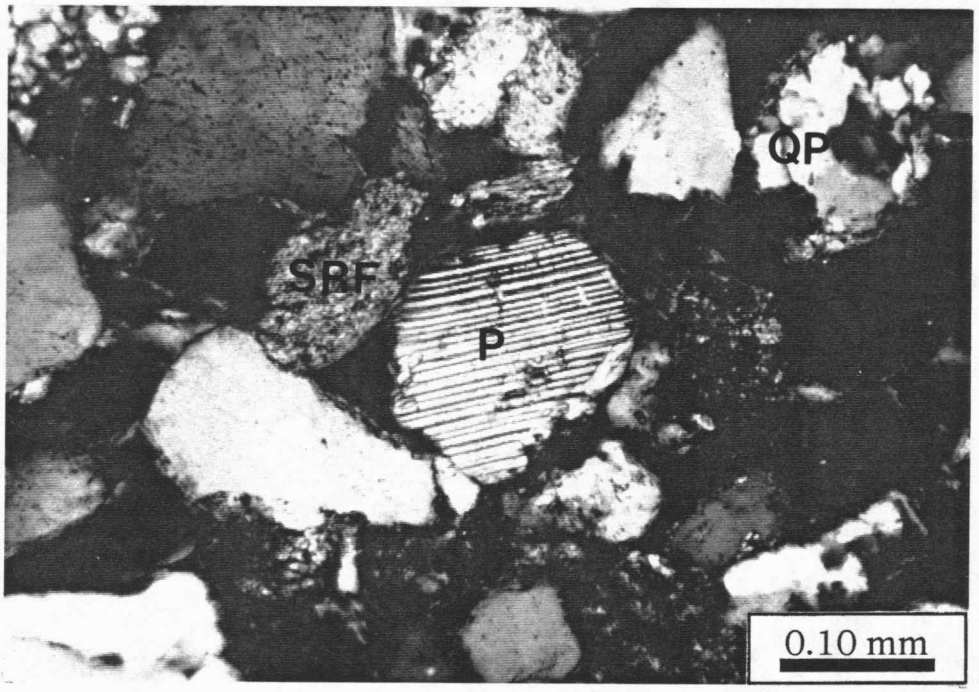


Figure 33. Perthite (P), SRF, and polycrystalline quartz (QP) grains in the Noxie sandstone. Some alteration can be observed in the right side of the perthite grain (bright spots); XN. Photomicrograph taken from outcrop sample NPC of the Noxie sandstone.

medium sand (0.46 mm). Although a minor component, perthite is present in both the Noxie and Cottage Grove sandstones.

Micas

Muscovite, biotite and chlorite are the three types of micas present in the Chanute sandstones. The most abundant is muscovite composing trace to 7% of bulk rock, followed by biotite from trace to 6%, and chlorite from trace to 2% of bulk rock. The mica grains in general were angular-prismatic, with grain sizes ranging from coarse silt (0.05 mm) to medium sand (0.46 mm). Muscovite is commonly unaltered and highly birefringent, although some grains show partial alteration to clay. Biotite (Figure 34 a, b) and chlorite (Figure 35 a, b) show extensive chemical alteration, mostly to clay, but biotite appears to be altered to chlorite in some grains. Partial dissolution and deformation of micas (squeezed between grains) was common within the samples analyzed (Figure 34 a, b).

Chert

Chert grains compose trace to 2% of the bulk rock and are present in about 50% of the thin sections. Chert grains are composed of microcrystalline quartz with a clearly defined grain boundary surrounding the clusters of small quartz crystals (Figure 36). Chert grains are sub-angular to sub-rounded with grain sizes ranging from coarse silt (0.05 mm) to fine sand (0.46 mm). Grain chemical alterations (replacement by carbonate) were rare but present, mostly in carbonate cemented samples.

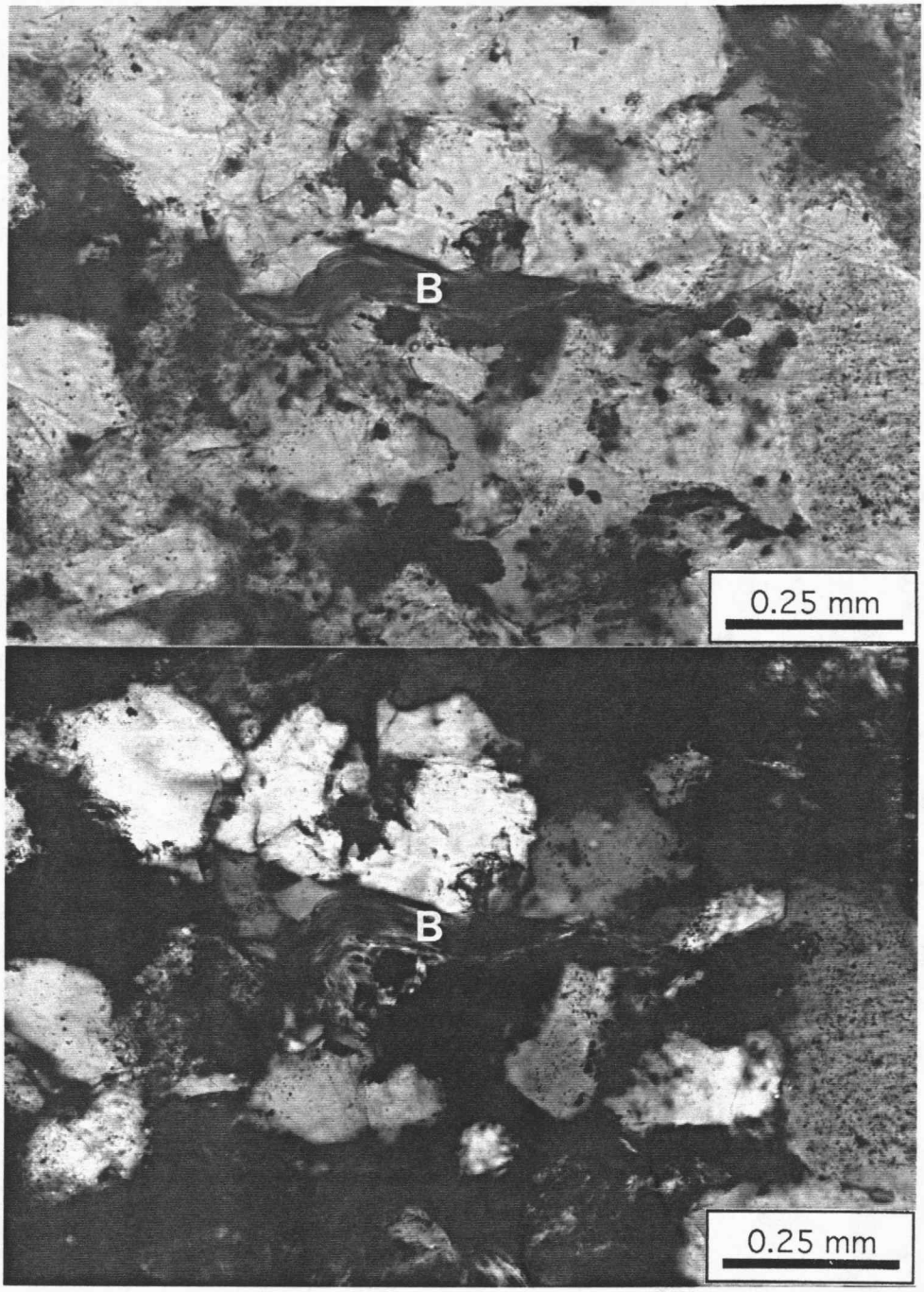


Figure 34. Biotite grain (B) in the Chanute sandstone showing partial chemical alteration to chlorite and clay; a: PPL, b: XN. Photomicrographs taken from outcrop sample AH 11.6 of the Noxie sandstone.

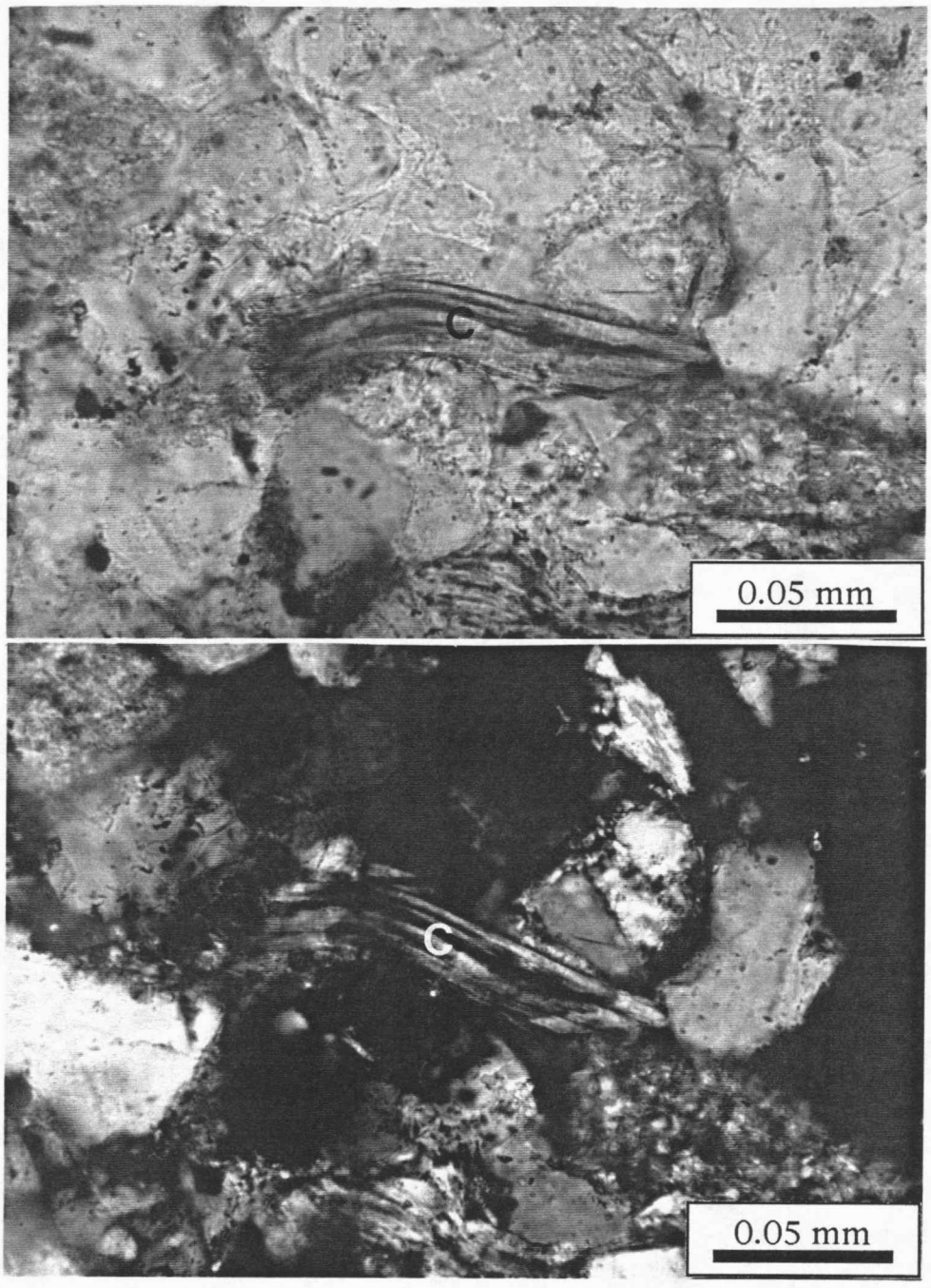


Figure 35. Detrital chlorite fragment (C) in the Chanute Shale. Chlorite is often observed showing partial dissolution and alteration to clay; a: PPL, b: XN. Photomicrographs taken from outcrop sample BE 3.75 of the Cottage Grove sandstone.

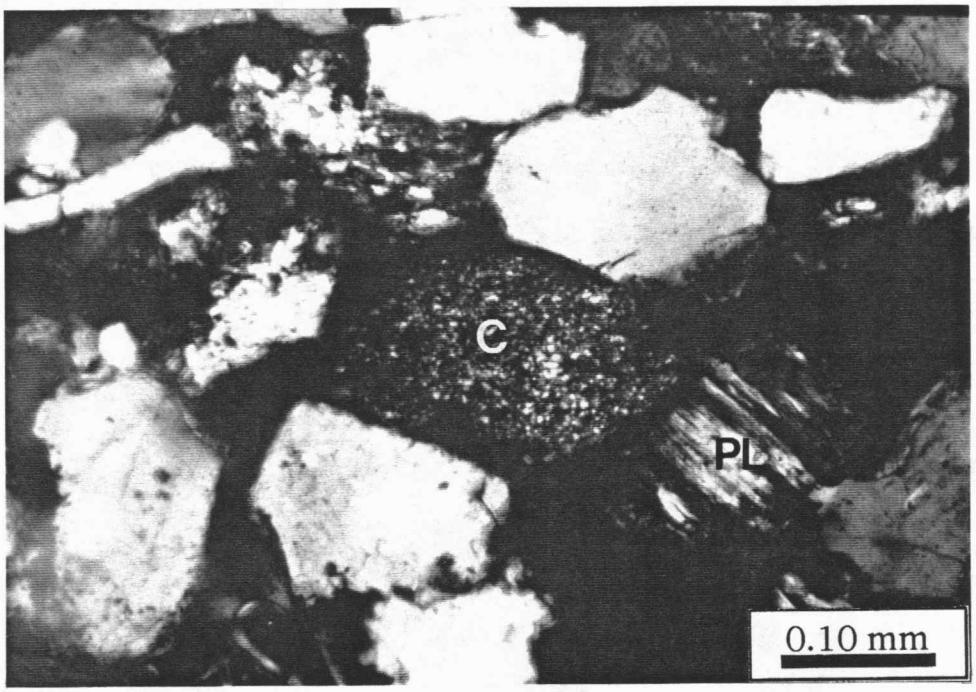


Figure 36. Chert fragment (C) showing a clear grain boundary around the interlocking quartz crystals; XN. A partially dissolved plagioclase (PL) is also present. Photomicrograph taken from outcrop sample NPC of the Noxie sandstone.

Rock fragments

Igneous, sedimentary and metamorphic rock fragments were all observed in the thin sections. Metamorphic rock fragments (MRF-Figure 37) were the most abundant (trace to 12%), followed by sedimentary (SRF) with trace to 9%, and lastly igneous rock fragments (IRF-Figure 38) with trace to 1%. MRF and SRF occur in both the Noxie and the Cottage Grove sandstones but IRF are only found near the top of the Noxie sandstone. MRF consist of micaceous, silicate-rich aggregates and highly birefringent foliated clay chips (Figures 37). SRF consist of highly birefringent, non-foliated clay chips and highly altered clay grains that look like intensely altered feldspars. These grains have feldspar-like shape, and in some places would look as if they had albite twinning, but are too degraded to positively be identified as plagioclase. IRF consist of silica-rich aggregates (granitic, Figure 38). IRF show no apparent chemical alteration, but the micaceous MRF, and the SRF show different degrees of chemical alteration. Chemical alteration was observed in MRF within carbonate cemented samples, mainly in the silica-rich areas of the grains, while the micaceous portions were more affected in the rest of the samples. Some SRF are chemically altered to clay and partially dissolved. Deformation of SRF was also observed in the samples. All rock fragments are sub-angular to sub-rounded with grain sizes ranging from coarse silt (0.05 mm) to fine sand (0.1 mm).

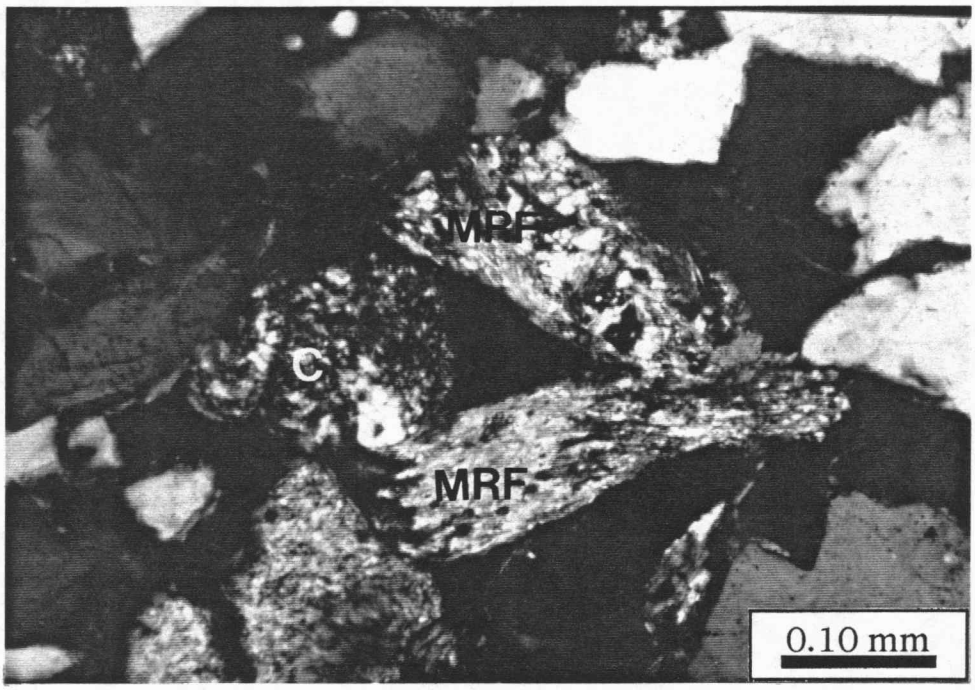


Figure 37. Metamorphic rock fragment (MRF), chert (C) and a foliated clay chip (schistose MRF). in the Chanute sandstones. MRF consist of micaceous rich, silicate aggregates and foliated clay chips; XN. Photomicrograph taken from outcrop sample NPC of the Noxie sandstone.

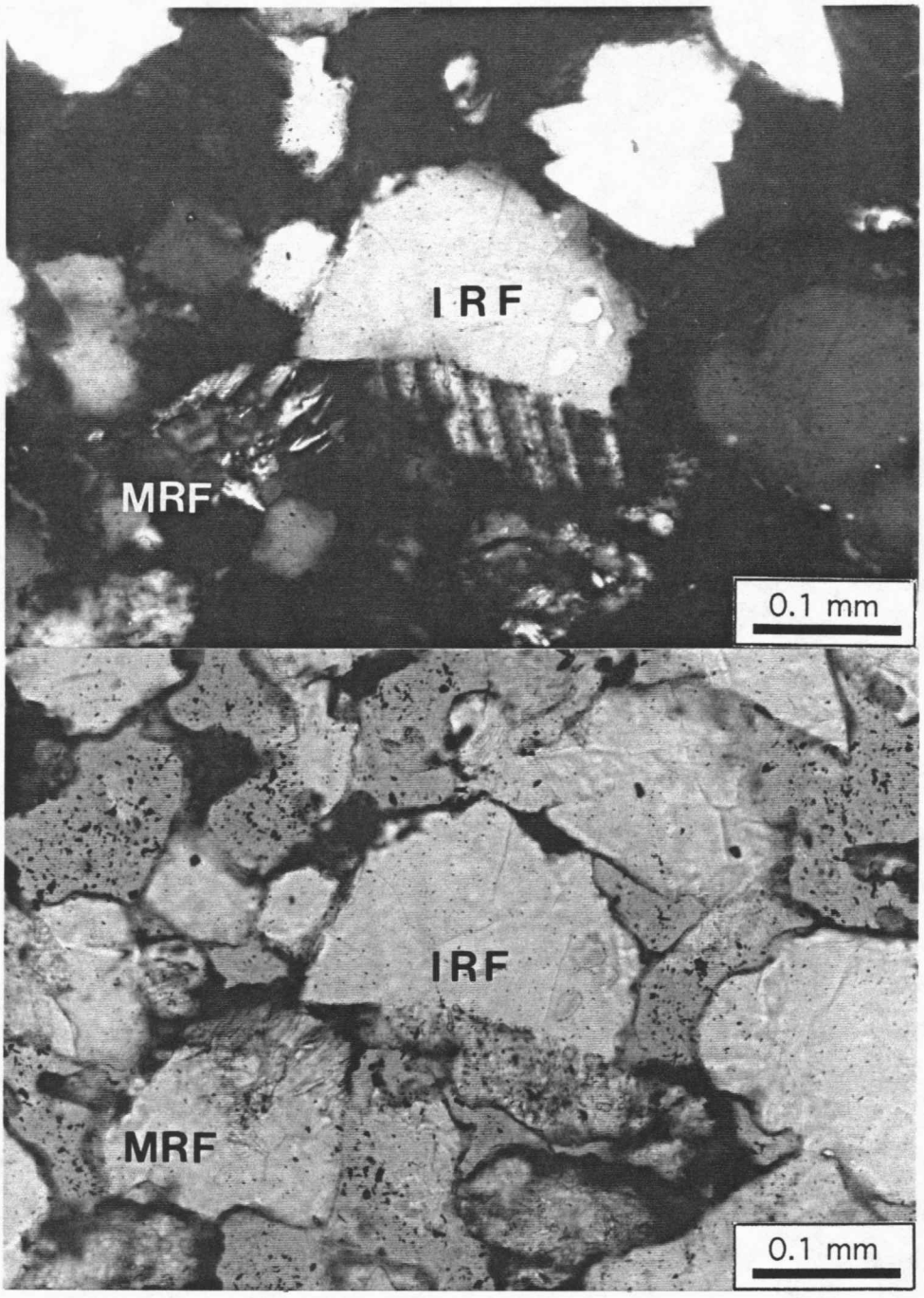


Figure 38. Igneous rock fragments (IRF) in the Chanute consists of polymineralic (granitic) grains; a: XN. b: PPL. Photomicrographs taken from outcrop sample NPC of the Noxie sandstone.

Carbonate skeletal fragments

Carbonate skeletal fragments were only present in samples taken at the Allin Hill section, a sample from the Iola Limestone called BB, and two other sandy limestones (one in the Noxie sandstone, AH 14.0, and one in the Iola limestone, SC 2.5). The samples at the bottom of the Allin Hill outcrop were described and included in Appendix 2, but are part of the units underlying the Chanute, same with the Iola sample. The Noxie sample, being truly part of the Chanute Shale was studied. Skeletal grains found were disarticulated brachiopod shells (1%), bryozoan fragments (11 and 41%), echinoderm (mostly crinoid) fragments(trace and 1%), bivalves (1 and 4%) and algae (1 and 2%).

Glauconite, pyrite, and heavy minerals

Glauconite was also present in trace amounts, with sub-rounded grains and no alteration. Pyrite is present (using light reflection over the thin section), but because of the difficulty of separating it from the iron oxides, it was point counted with them. The light reflection technique suggest only trace amounts of the mineral present. Heavy minerals observed in the thin sections are, zircon, tourmaline, and rutile, all in trace amounts when present.

Organic matter

Organic matter composes up to 13% of the bulk rock in the thin sections analyzed. It commonly occurs within pore spaces and in laminae parallel to bedding, but it also occurs cutting across bedding

in some core samples (possibly rhizomes). Partial dissolution of the organic matter was commonly observed in the thin sections analyzed.

Authigenic minerals

Quartz overgrowths

Quartz overgrowths are thin and discontinuous, and identified mainly where "dust rims" coating detrital quartz cores are present. The overgrowths are syntaxial to the detrital cores, and are commonly embayed and partly filled by iron oxides, carbonates, or clay coatings (Figure 31). Overgrowths are common in both the Noxie and the Cottage Grove sandstones and are more readily abundant in portions of thin sectioned samples where iron oxides and clays are less abundant.

Iron-oxide

Iron-oxide represents 1 to 52% of the bulk rock in the samples analyzed. The oxide is commonly found as pore fillings, pore linings, concentrated in bands parallel to bedding, or as boxwork structures commonly found in core samples and in a few outcrop samples (Figure 39). In many of the samples, iron-oxide coatings are commonly found covering every grain surface present. Partial dissolution of the coatings, and pore-filling, pore-lining oxides were also commonly observed. The boxwork structures appear to be restricted in outcrop samples to the lower and upper contacts of the Noxie sandstone. In cores, they appear randomly in the Cottage Grove sandstone samples, and are usually associated with the

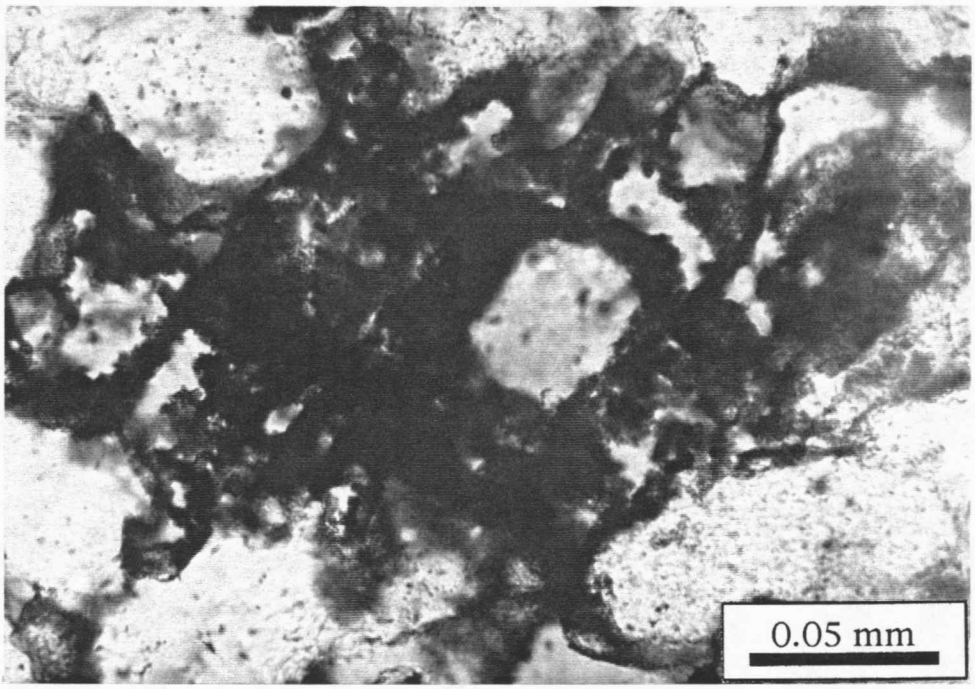


Figure 39. Boxwork structures of iron-oxide are common in outcrop and core samples, with secondary porosity very often observed; PPL. Photomicrograph taken from outcrop sample BE 3.75 of the Cottage Grove sandstone.

carbonate cements such as ankerite (Figure 40). This relation is not observed in the outcrop samples.

Carbonate cements

Calcite cement

Apart from the carbonate samples from the Nellie Bly and the Iola, calcite cement is present in 7 of the outcrop samples studied. Three of these samples are from near the top of the Noxie sandstone, one is a sandy carbonate concretion with 46% calcite cement, one is a silty limestone with 40% calcite cement, and the last is a carbonate-cemented sandstone with 6% calcite cement. The rest of the carbonate cemented samples are: a sandstone with a calcite cemented band (2%), and three calcite-cemented sandstones (3%, 42%, and 45%). These samples are from the Cottage Grove near the contact with the Iola Limestone. The poikilotopic calcite cement is always patchy, and "clean" (no opaques related to it), and is usually found replacing parts of detrital grains, mostly quartz and feldspars (Figure 41). This cement is readily found in core samples, where it sometimes is partially obscured by iron-oxide. Percentages in the cores are of total carbonate cement (including ankerite) so actual percentages of only the calcite cement are not available.

Ankerite

The presence of ankerite was detected after the petrographic analysis was performed, so the percentage of ankerite in the thin sections is not available. Ankerite is present only in core samples. It

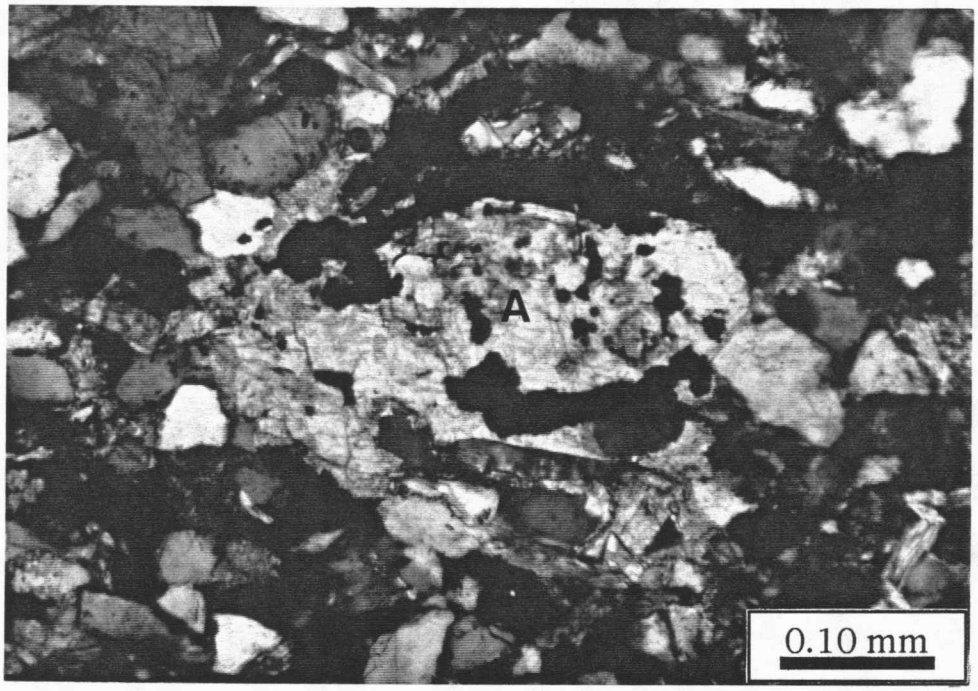


Figure 40. The iron-oxide boxwork structures are observed in association with carbonates (ankerite: A) only in core samples; XN. Photomicrograph taken from core sample G1 22', 2.5" of the Cottage Grove sandstone.

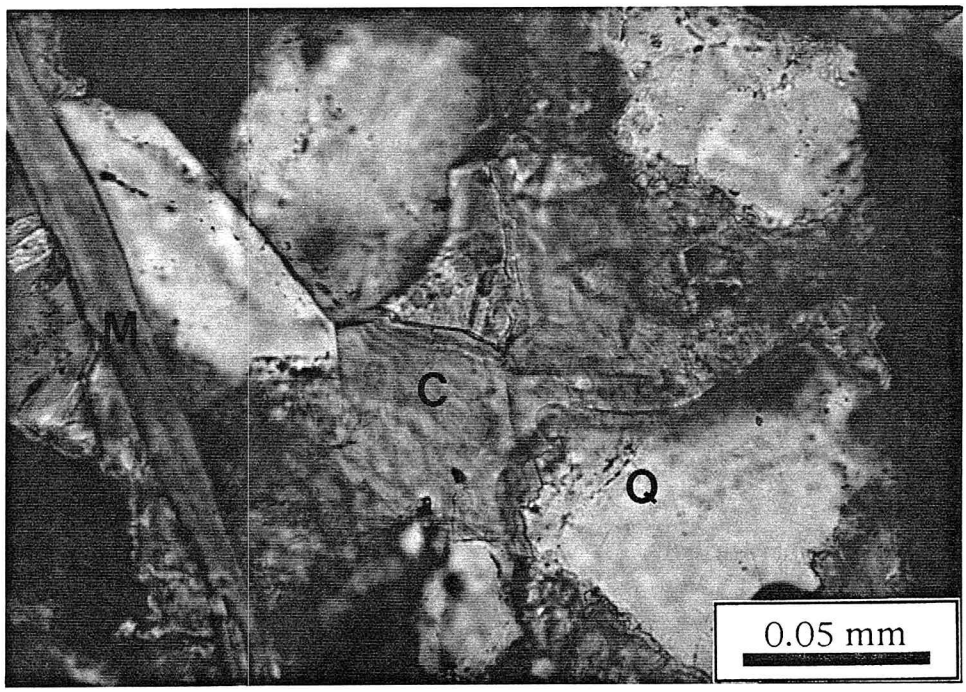


Figure 41. Poikilotopic calcite cement (C) is usually found in very small patches in the Chanute sandstones both in outcrop and in cores; XN. Calcite (C) can be seen here filling embayments in quartz (Q); XN. Photomicrograph taken from outcrop sample SI 4.9 of the Cottage Grove sandstone.

is patchy in nature, and is always related to the boxwork structures of iron-oxide. This cement displays the typical rhombohedral crystalline shape of dolomite and exhibits a deep navy blue color when stained with a mix of Potassium Ferricyanide and Alizarin Red (Figure 42).

Dolomite

The presence of dolomite in the Chanute samples is not certain. Dolomite occurs in the unstained centers of ankerite rhombs shown by a deep navy blue along the rims (ankerite) and no stain in the center (dolomite, Figure 42; the absence of color in stained samples suggests the presence of dolomite). This has not been confirmed in either microprobe or X-Ray diffraction, so further study is needed to verify the presence of dolomite in Chanute sandstones.

Clays

Clays are a major authigenic constituent representing 1 to 30% of the bulk rock in the thin sections analyzed. Most of the clays present are either pore filling, pore lining, or appear as clay coatings on the detrital grains. Kaolinite "books" were commonly observed in thin section (Figure 43) and its presence was confirmed by petrographic and X-ray diffraction techniques. Clays were commonly observed filling embayments on etched grains, and enveloping detrital quartz grains without overgrowths.

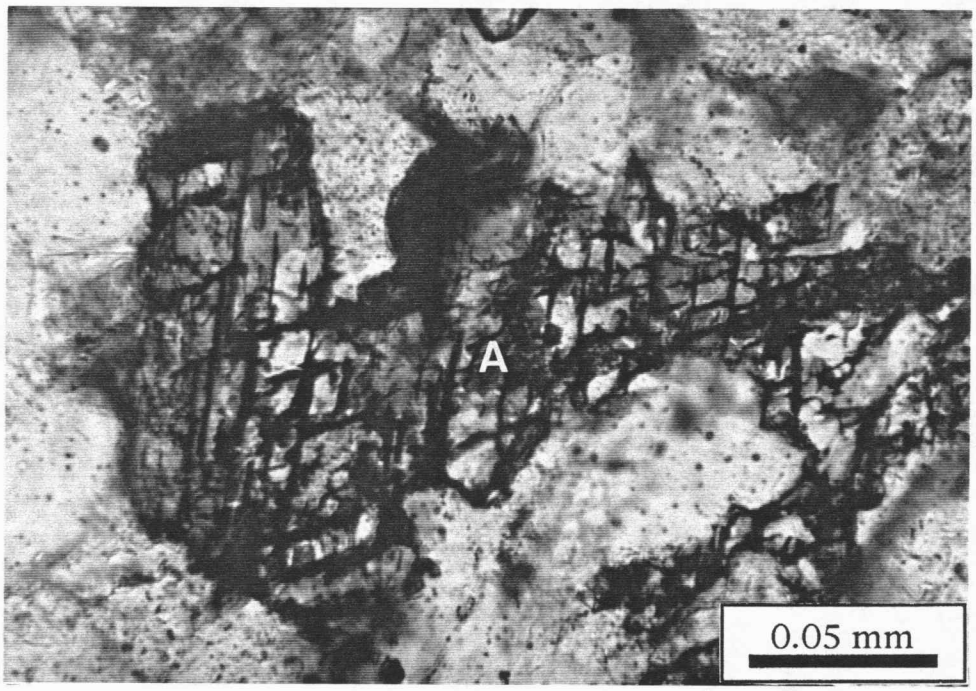


Figure 42. Stained ankerite (A). The typical rhombohedral shape and the navy blue color are clearly identify the ankerite in the Chanute sandstones (cores only); PPL. The absence of stain in the cores of some rhombs suggest the presence of dolomite in the Chanute core samples. Photomicrograph taken from core sample G1 22', 2.5" of the Cottage Grove sandstone.

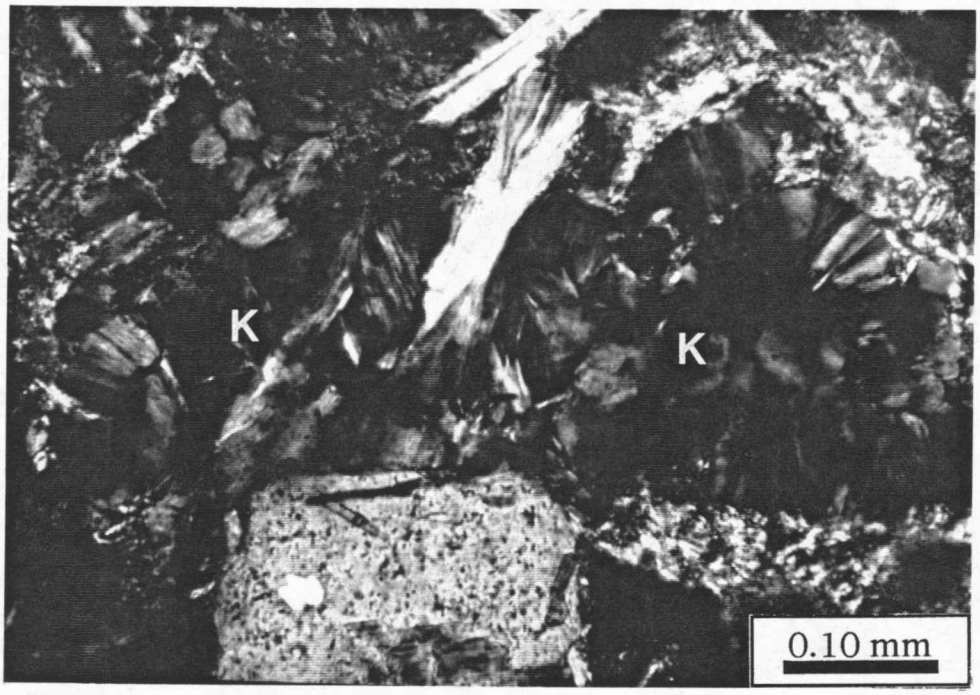


Figure 43. Kaolinite "books" (K) filling available pore space in the Chanute samples. Kaolinite is common both in outcrop and core samples; XN. Photomicrograph taken from outcrop sample NPC of the Noxie sandstone.

Porosity

Secondary porosity represents 1% to 44% of the bulk rock, although the average ranges from 20% to 30%. It consists mostly of partial dissolution of detrital grains and authigenic constituents (Figures 31, 39). Porosity is clearly distinguished from "plucked out grains" by impregnation with a blue dyed epoxy resin used in all the samples. The possibility of artifact porosity was also eliminated by impregnating the samples with this resin prior to grinding. Primary porosity was not observed in any of the samples analyzed. The high secondary porosity observed suggests strong diagenetic effects upon the Chanute sandstones. The amount of porosity does not appear to be related to lithologic contacts, sandstone bodies, or outcrop vs. core samples.

Petrographic characteristics of the Noxie sandstone

The Noxie sandstones, are a combination of quartz arenites, sublitharenites, subarkoses, litharenites, feldspathic litharenites, quartz wackes, and lithic wackes (Figure 44). Average grain size of the Noxie sandstones ranges from very fine (0.10 mm) to medium sand (0.47 mm). Samples of the Noxie were taken from the Allin Hill, Noxie Road, Water Works, and the base of Greenwood Cemetery sections (Appendix 3).

Polycrystalline quartz is absent in the finer-grained samples. All types of feldspars and mica are represented in the Noxie. The types of plagioclases present include albite, oligoclase, and andesine, and microcline feldspar appears to be present only in the Noxie

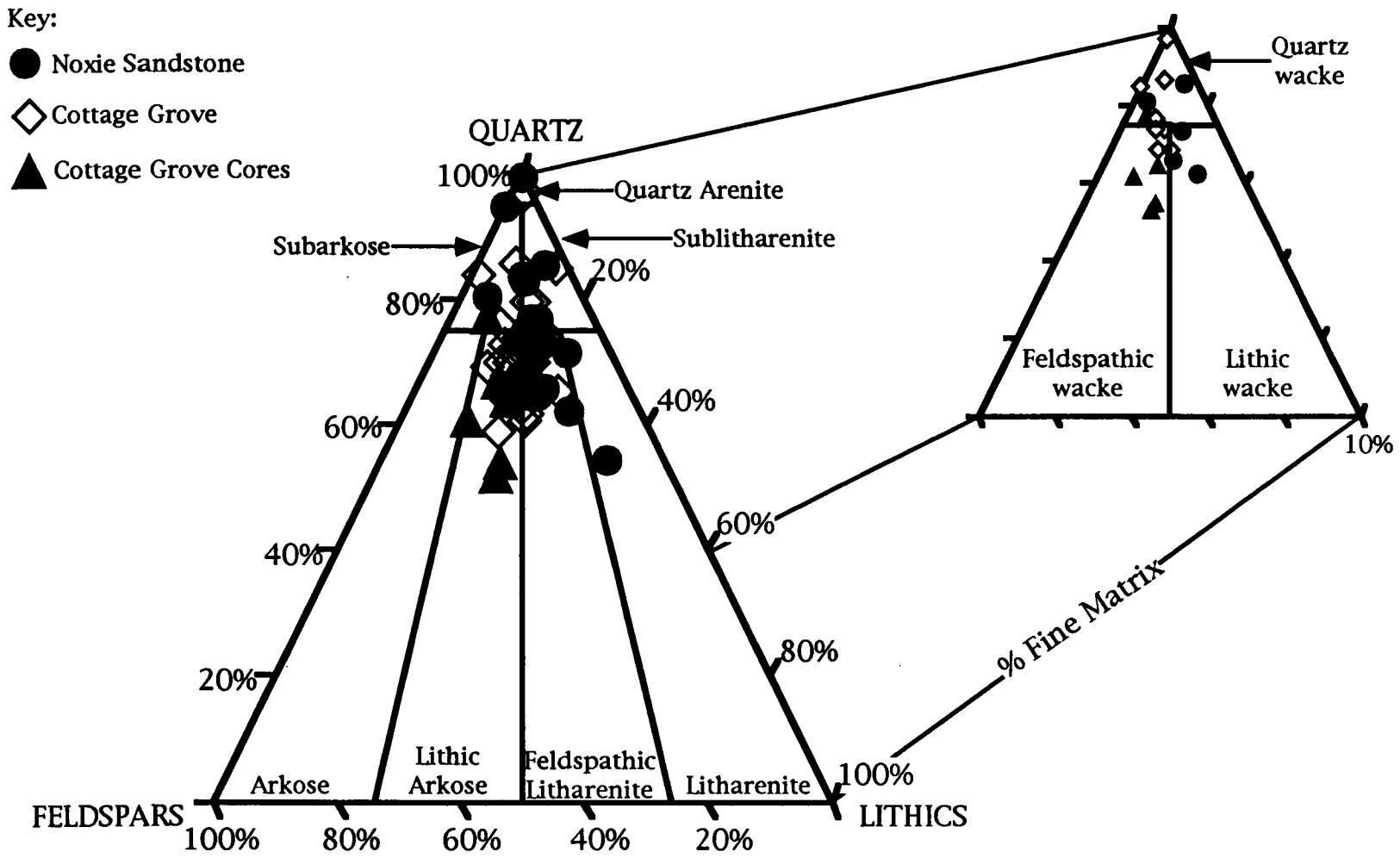


Figure 44. Compositions of the Chanute Shale sandstones and wackes; classification after Folk, 1968.

sandstones. All rock fragment types are represented in these sandstones with metamorphic rock fragments (MRF, Figure 37) being the most abundant (trace to 12%), followed by sedimentary rock fragments (SRF, trace to 9%), and igneous rock fragments (IRF, Figure 38) which are present only in the top of the Chanute interval (trace to 1%). MRF are micaceous silicate aggregates and highly birefringent foliated clay chips. SRF are highly birefringent non-foliated clay chips, and the chemically altered clay grains mentioned previously. IRF are polymineralic (granitic) grains.

Matrix is represented mostly by authigenic constituents like organic matter (trace to 4%), iron-oxide and pyrite (trace to 29%), calcite cement (40 to 46%, in two samples, a carbonate concretion and a sandy limestone), and clay (10 to 25%). Five samples, with more than 10% clays, were classified as wackes. All porosity is secondary, with oversized pores and dissolution of constituents, mainly overgrowths, feldspars, micas, organic matter, iron-oxide, and clays.

Evidence for compaction is scarce. The most common compactional feature is deformed and squeezed micas and clay chips, followed by concave-convex contacts between grains (Figure 45), some sutured contacts, and some fractures.

Petrographic characteristics of the Cottage Grove sandstone

Like the Noxie, the Cottage Grove sandstones also show a combination of compositions including quartz arenites, subarkoses, sublitharenites, feldspathic-litharenites, lithic arkoses, quartz wackes, and feldspathic wackes (Figure 44). The average grain size

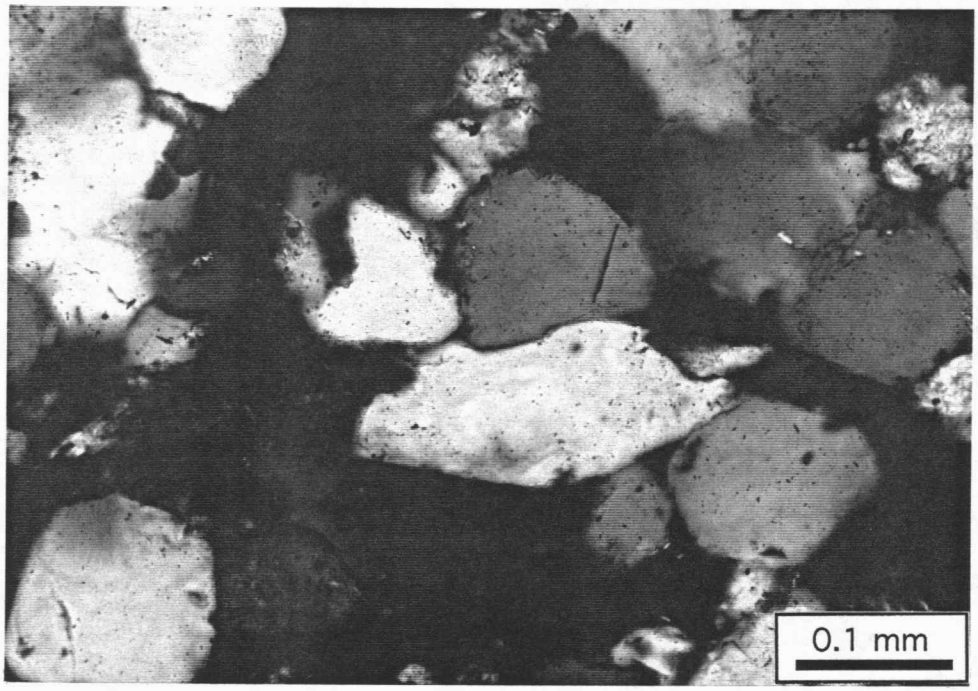


Figure 45. Concave convex contacts between quartz grains in the Chanute sandstones are common but not pervasive; XN. Photomicrograph taken from outcrop sample AH 8.45 of the Noxie sandstone.

of these sandstones ranges from coarse silt (0.05 mm), to fine sand (0.32 mm). Samples from the Cottage Grove were taken from the sections at South Independence, East Thayer, Thayer Dam, South Chanute, Greenwood Cemetery, Beagle, and from the Gaddy # 1, and Joe Newland cores.

Both types of quartz are represented in the Cottage Grove samples, with monocrystalline quartz being the most abundant type (Figure 31) followed by polycrystalline quartz (Figure 33). The latter are found only in the coarsest samples because in finer grained samples the interlocking quartz crystals in polycrystalline quartz are dissagregated by normal breakdown of the grains during transportation. Feldspars present are plagioclase (albite, oligoclase and andesine), orthoclase, and perthite. All the mica types are represented along with two of the three rock fragment types: MRF (Figure 37) and SRF. MRF are the most abundant with trace to 9% of the bulk rock, closely followed by SRF, with trace to 8% of the bulk rock. MRF are schistose grains (quartz-mica) and highly birefringent foliated clay chips. SRF are highly birefringent non-foliated clay chips, and the chemically altered clay grains previously discussed.

Matrix materials consist mostly of organic matter (trace to 13%), iron-oxide (trace to 52%), carbonate cement (trace to 45%), and clay (10 to 30%). Four outcrop samples (40 to 45%) found close to the contact with the Iola Limestone and core samples (only trace to 19%) in the Cottage Grove are carbonate cemented sandstones. Samples of the Cottage Grove with more than 10% clays (13 samples)

were classified as wackes. All porosity was secondary (trace to 44%), consisting mainly of oversized pores, and partial dissolution of constituents, mainly quartz overgrowths, feldspars, micas, organic matter, iron-oxide, and clays (Figures 31, 39). Evidence for compaction was mainly deformed and squeezed micas and clay chips, concave-convex grain contacts (Figure 45), some sutured grain contacts and some fractures.

Cathodoluminescence

Cathodoluminescence studies were performed in the Chanute samples in an attempt first, to distinguish between detrital quartz grains and non-visible quartz overgrowths, and second, to determine if there was more than one carbonate cementation event. Quartz was non-luminescent in all samples, therefore I was unable to discern if there were additional overgrowths to the ones with the visible "dust rims". The calcite cement was brightly luminescent but no banding was observed. The ankerite was non-luminescent because of the high amount of iron present in the mineral.

CHAPTER VI
DIAGENESIS

Diagenetic characteristics of sandstones in the Chanute Shale

The Noxie and the Cottage Grove sandstones display similar diagenetic characteristics. The most striking diagenetic feature is the high amount of secondary porosity produced by intensive dissolution of detrital grains and authigenic constituents. Practically every type of grain shows some degree of dissolution and this characteristic is common in all the samples both from outcrop and cores of the Chanute. Other diagenetic characteristics of the Chanute sandstones are quartz overgrowths, local early calcite cement, concave-convex contacts, alteration of biotite to chlorite, chloritization of clays, precipitation of late calcite, dolomite and ankerite cements, precipitation of late kaolinite, dissolution of late cements, formation of iron-oxide boxwork structures, and of clay and iron-oxide grain coatings. In this chapter, I will present all the diagenetic characteristics observed in the Chanute sandstones and their possible mechanisms of formation. The chapter will conclude with the paragenesis of diagenetic events in the Chanute Shale.

Secondary porosity

When pore waters move through sediments, the ionic concentrations of the waters play an important role in diagenesis and

in the creation of secondary porosity. Pore waters undersaturated with respect to a particular mineral, given proper conditions, can dissolve materials rich in ions of that mineral, therefore creating secondary porosity (Schwartz and Longstaffe, 1988, Bjørlykke, 1984). For example, silica-undersaturated waters, under certain conditions of temperature, pressure, and pH, will dissolve silica overgrowths and detrital quartz grains (Blatt, 1979). If the space left from the dissolution event is not filled with other materials, then that space remains as secondary porosity.

Secondary porosity in the Chanute sandstones occurs as oversized pores, and partial dissolution of: quartz overgrowths and detrital quartz, feldspars (plagioclase, orthoclase microcline, and perthite), micas (muscovite, biotite, chlorite), rock fragments (MRF, and SRF), organic matter, iron-oxide, carbonate cements (calcite, ankerite and dolomite), and clays. The chemistry involved in the dissolution of the minerals listed above will be discussed with other related diagenetic features.

Early silica cementation

Early silica cementation in the Chanute sandstones occurs in the form of thin and discontinuous quartz overgrowths around detrital quartz grains (Figure 46). As observed in the micrograph, these overgrowths are commonly partly dissolved, having embayments filled with other authigenic materials, such as iron-oxide, carbonates, and clay coatings. Overgrowths are more common in portions of thin sections that have less amounts of iron-oxides and clays.

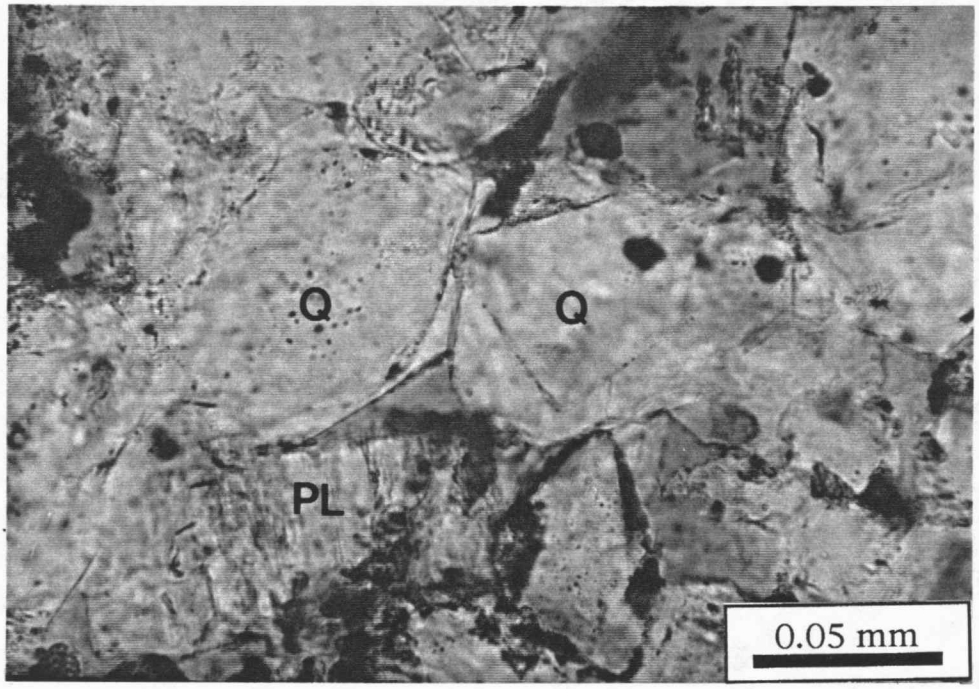


Figure 46. Thin and discontinuous quartz overgrowths on detrital quartz grains (Q). Note also a partially dissolved feldspar (plagioclase: PL), secondary porosity, and iron-oxide coatings; PPL. Photomicrograph taken from outcrop sample GC 2.8 of the Noxie sandstone.

Solubility of silica depends on pH, presence of other ions, pressure, and temperature (Krauskopf, 1959). High pH of 9 or above will dramatically increase the solubility of silica, and lower pH will actually accelerate the rate of precipitation. Increased temperatures also increase solubility slightly and increase the rate of reaction (Krauskopf, 1959). Possible sources of silica include pressure solution, diagenetic alteration of feldspars and clays, and dissolution of fine grained quartz in interstratified shales (Schwartz and Longstaffe, 1988).

Precipitation of silica mobilized by pressure solution has become one of the most generally accepted mechanisms for increasing the amount of dissolved silica in pore fluids and stimulating the growth of secondary quartz (Blatt, 1979). Since pressure solution requires significant amounts of compaction to take place, and the Chanute sandstones show little evidence of compaction, pressure solution alone may not be an adequate mechanism to explain secondary quartz in the Chanute sandstones.

Dissolution of plagioclase occurs by the following reactions:

$$\underset{\text{(albite)}}{NaAlSi_3O_8} + 4H^+(aq) \Rightarrow Na^+(aq) + Al^{+3}(aq) + \underset{\text{(quartz)}}{3SiO_2(s)} + 2H_2O \qquad (1)$$

$$\underset{\text{(albite)}}{NaAlSi_3O_8} + 2H_2O \Rightarrow Na^+(aq) + Al(OH)_4^-(aq) + \underset{\text{(quartz)}}{3SiO_2(s)} \qquad (2)$$

which are mechanisms that produce silica at low pH (1) and high pH (2) (Siebert, et al., 1984). A significant volume of feldspars is present in the Chanute sandstones. Even though the reaction products tend to be removed from the site of the reactants (Siebert,

et al., 1984), it is likely that feldspar dissolution in the Chanute sandstones provided the silica for overlying or underlying sediments and not for the Chanute Shale. Diagenesis of clays (smectite-illite transformation) and dissolution of fine grained quartz from adjacent shales are other potential sources of silica (Hayes, 1979, Moncure, et al., 1984). These diagenetic products from adjacent clays also have a tendency to be removed from the source, so acidified cross-formational connate waters from adjacent shales could have provided silica to the Chanute sandstones.

The solubility of quartz is in the range from 6 to 14 ppm at ordinary temperatures (Krauskopf, 1959). Amounts of dissolved silica in most river and ground waters averages 13 ppm, sufficient to cause cementation (Blatt, 1979). The main problem with this mechanism is how to move sufficient amounts of silica saturated waters through the formation to precipitate quartz overgrowths. This can be attained by vertically moving surface and ground waters relatively close to the surface (Blatt, 1979). Although the precipitation of silica is a slow process, the acidic nature (by organic acids) of most groundwaters, and their position close to the surface could serve as a catalyst for this process. This is a possible mechanism to precipitate quartz overgrowths early after deposition in the units that are at shallow depths. Silica ions from the surface and ground waters nucleate on the detrital quartz grain surfaces, precipitating syntaxial quartz overgrowths on the detrital grain

(Blatt, 1979). This mechanism may best explain the origin of the early quartz overgrowths in the Chanute sandstones.

Dissolution and chemical alteration of labile grains

The Chanute sandstones underwent extensive dissolution of labile grains during their diagenetic history. Feldspars, especially plagioclases, show intensive dissolution and chemical alteration (Figures 47 a, b, 32 a). Some of these grains have dissolved completely leaving grain size pores within the thin sections. Most often, traces of the grain outline, or partially dissolved remains of the grains make it possible to identify the original framework grain. Plagioclases usually show preferential dissolution along preferred twins (Figure 47 a). Rarely observed but present, are clay rims showing the original outline of a grain even when it has been completely dissolved. Chemical alteration of feldspars was mostly in the form of sericitization (Figure 47 b) and montmorillonitization. A hierarchy in feldspar chemical alteration and dissolution was observed as plagioclases showed higher degrees of dissolution and chemical alteration than orthoclase, microcline, and perthite. MRF and SRF also show partial dissolution of grains and chemical alteration of mica-rich portions of the grains into clays (Figure 48).

Silicate and aluminosilicate dissolution occurs in saline, alkaline non-marine waters (Hay, 1966). Increases in temperature and pH, as mentioned above, will enhance silica solubility and rates of reaction. Connate or compactional waters, with their saline, and alkaline nature (Tucker, 1981), combined with higher temperature and

a

b

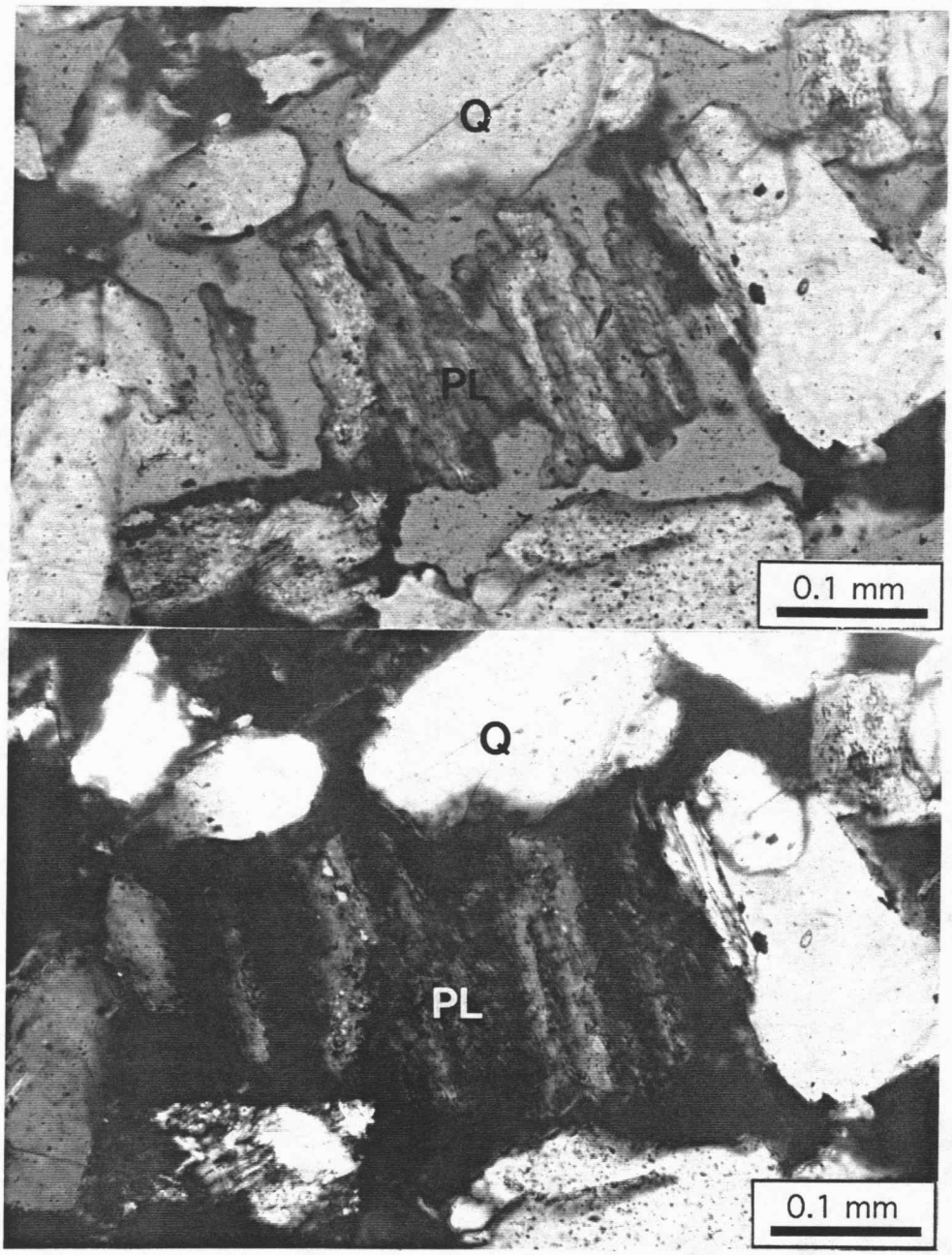


Figure 47. Plagioclase (PL) showing partial dissolution of preferred twins, and chemical alteration to sericite. Also observed are a detrital quartz grain (Q) and overgrowth partially dissolved, secondary porosity, iron-oxide and clay coatings; a: PPL, b: XN. Photomicrographs taken from outcrop sample NPC of the Noxie sandstone.

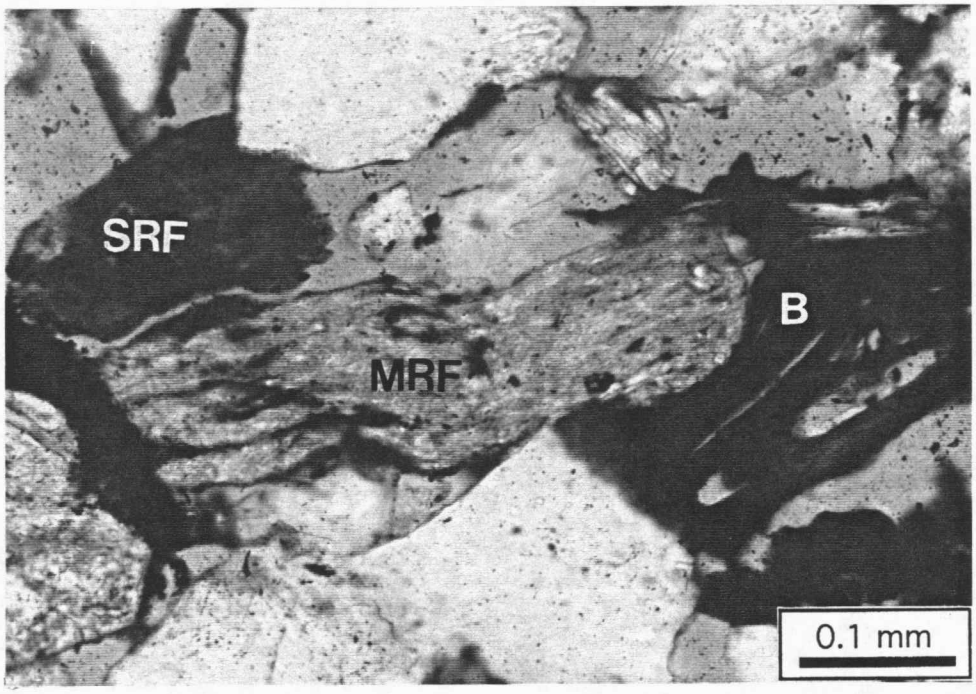


Figure 48. Schistose MRF, SRF, and biotite (B) showing partial dissolution and chemical alteration of the detrital grains into clays. Secondary porosity also observed; PPL. Photomicrograph taken from outcrop sample NPC of the Noxie sandstone.

pressures (common with increased burial), increase the solubility of silica, thereby providing a suitable environment for silicate dissolution. As mentioned above, the ions released are usually transported out of the formation by circulating waters (Siebert, et al., 1984). Another mechanism for the dissolution of aluminosilicates is by the interaction of organic acids from organic matter. This mechanism concentrates on the Ca and K ions in the mineral and promotes the mobility of Al, Fe, and carbonates. This increases dissolution in calcium-rich feldspars. Although most of the partial dissolution and chemical alteration of MRF's concentrates on the micaceous portions of the grains, the mechanisms discussed above also apply to the silica-rich portions of these grains (MRF's).

Chemical alteration of the feldspars to sericite (illite family), montmorillonite (smectite family), and kaolinite is commonly observed. Sericite and montmorillonite are micas very close in composition to muscovite, and have straw-yellow birefringence under the microscope (Blatt, 1982). These clay minerals are fibrous and silky and are a common diagenetic product of feldspar alteration (Figure 47 b).

Apparent replacement of minerals by phyllosilicates or clay minerals, (physils of Weaver, 1989) occurs in at least two ways: by dissolution of the mineral and crystallization in the space created by the dissolution (e.g., kaolinite replacing calcite), or by alteration (hydration) of the surface of a silicate mineral (e.g., kaolinite and illite replacing feldspar, Weaver, 1989). Studies of weathered

feldspars show that during early stages of weathering, physils will form in vacuoles within the feldspar crystal, such as in crystal lattices (Eggleton and Buseck, 1980). This is very similar to the sericite and montmorillonite alteration that is observed in thin sections. Other studies show that highly weathered K-feldspar was altered to halloysite and gibbsite (from the kaolin family) with primitive clay precursors in the surface of the mineral (Tazaki and Fyfe, 1986). These mechanisms might explain the initial chemical alteration of the feldspars in the Chanute sandstones.

Micas (muscovite, biotite and chlorite) also are as partially dissolved and chemically altered to clays. Muscovite is more resistant to alteration than biotite and chlorite. Biotite can be observed either chemically altered to clay or to diagenetic chlorite (Figure 34 a). Chlorite also occurs as detrital grains partly dissolved or chemically altered to clay (Figure 35 a). Very often grains that were initially a mica are completely replaced by clay, and the fibrous structure left is the only indication that the grain was previously a mica.

The alteration of muscovite and biotite to clay (kaolinite) during weathering occurs in the following sequence:

muscovite⇒M/S (or M/V)⇒smectite⇒kaolinite (3)

biotite⇒Fe dioctahedral mica⇒illite⇒kaolinite (4)

These reactions tend to occur where the K^+ and Al^{+3} concentrations are high such as near dissolving K-feldspars (Weaver, 1989). At initial stages of weathering illite was found forming at the

boundaries between muscovite and orthoclase, the muscovite and orthoclase; grains were altered to vermiculite (chloritic physil) and beidellite (smectite physil). With time all the physils were altered to kaolinite (Meunier and Velde, 1979). Although these mechanisms occur during weathering, they might explain mica alteration in the diagenetic environment. Organic acids might also play a role in the alteration of micas and formation of physils (Weaver, 1989). Kaolinite commonly forms in fresh acidic waters while illite, smectite, and chlorite form in modified sea water or concentrated (with respect to K) meteoric waters (Weaver, 1989). These conditions, in addition to the ions dissolved in the water, and temperature might determine the type of clay to be formed from the alteration of micas.

Precipitation of late kaolinite

Kaolinite books are a common diagenetic product in the Chanute sandstones filling pores in portions of some thin sections (Figures 43, 48) and replacing plagioclase.

Precipitation of kaolinite is mostly related to the dissolution of plagioclase, Al mobilization, and precipitation of silica. This can be driven by different reactions:

$$(2NaAlSi_3O_8 \cdot CaAl_2Si_2O_8) + 4H^+(aq) + 2H_2O \Rightarrow$$
(andesine plagioclase)

$$2Al_2Si_2O_5(OH)_4 + 4SiO_2 + 2Na^+(aq) + Ca^{+2}(aq) \qquad (5)$$
(authigenic kaolinite) (quartz o.)

$$2KAlSi_3O_8 + 2H^+ H_2O \Rightarrow Al_2Si_2O_5(OH)_4 + 4SiO_2 + 2K^+ \qquad (6)$$
feldspar kaolinite quartz

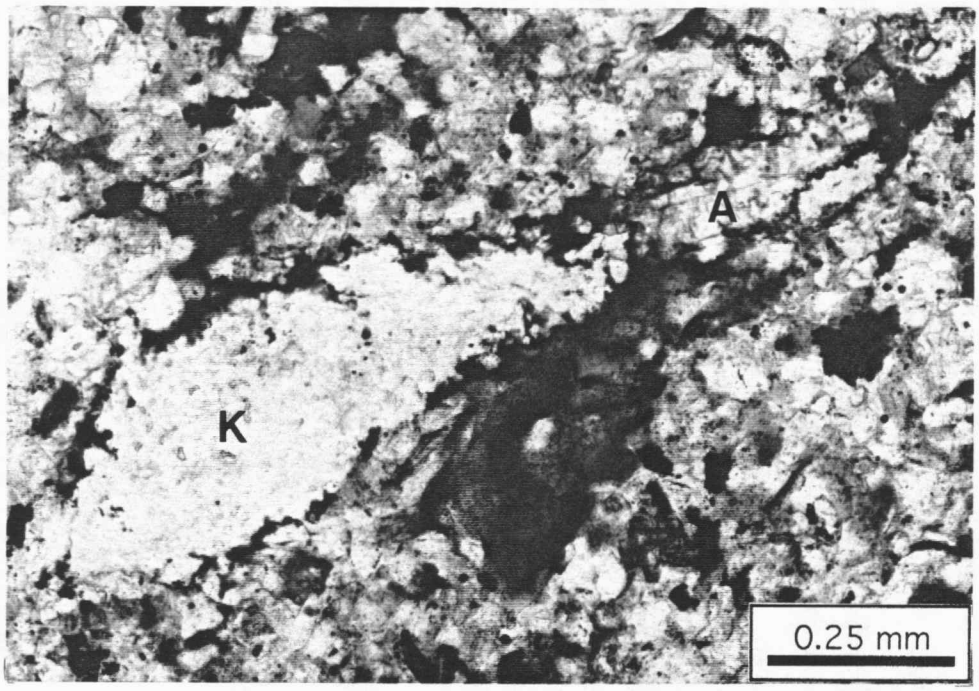


Figure 49. Kaolinite (K) and ankerite (A) filling a rhizome in a core sample of the Cottage Grove sandstone; PPL. Timing between the occurrence of the kaolinite and the ankerite can not be determined by petrographic analysis. Some chloritized clays are also observed in the upper left corner of the photomicrograph. Photomicrograph taken from core sample NL 20', 4.5" of the Cottage Grove sandstone.

If Al and Si are not removed, the dissolution of the feldspars will precipitate as pore-filling kaolinite, therefore no major net change in effective porosity will be observed. Pore fluid volumes required for these reactions to occur become a problem at increased burial. The nature of the porewater is also a problem since moving compactional porewater is likely to be in equilibrium with feldspar and mica (Bjørlykke, 1988). Precipitation of kaolinite at depth requires a sink for Na^+ or K^+ and this can be provided by the smectite-illite transformation driven by the following equation (Boles and Franks, 1979):

smectite + $K^+ \Rightarrow$ illite +H_4SiO_4 + cations (Ca^{+2}, Mg^{+2}, Na^+, Fe^{+2}) (7)

These conditions require coprecipitation of illite and kaolinite (Bjørlykke, 1988). Since kaolinite commonly forms in fresh acidic waters, its precipitation at depth is made possible by several coexisting factors: low pH maintained by organic acids; K-feldspars providing a source of Al and Si; a sink for K^+ by transformation of smectite to illite; and porosity and permeability, allowing migration of interstitial pore water and growth space (Bucke and Mankin, 1971). This last mechanism does not explain the precipitation of kaolinite from plagioclase at depth, but using equation 5, plus acidified connate waters from underlying shales (to provide the H^+ ion) provides a suitable mechanism (Siebert et al., 1984). Since both types of feldspars (K and plagioclase) are found in the Chanute sandstones, and the sandstones may have very well gone through

such a diagenetic environment, these mechanisms might explain the precipitation of late kaolinite in the Chanute sandstones.

Compaction

Evidence of compaction in a sediment can be observed petrographically by the nature of grain contacts and the relationships between the grains. Mechanical compaction of sediments is dependent on overburden and pore pressures as well as the composition of the sediments. Clay-rich sandstones, particularly if matrix supported, will loose primary porosity rapidly upon loading. Well-sorted sandstones with low mechanical grain strength will also deform under moderate overburden (Bjørlykke, 1988). Cementation also plays an important role in the compaction process by preventing it. Pressure solution is another consequence of increased burial when pressure at grain contacts force ions into solution that can reprecipitate later.

In the Chanute sandstones, evidence for light to moderate compaction was found. Features related to compaction include deformation of clay chips, micas, and other "soft" materials, undulatory extinction of primarily quartz grains, concave-convex grain contacts (Figure 45), and a few sutured contacts. The limited evidence for compaction in the Chanute sandstones suggests that Chanute sediments did not subside into the deep burial or deep compactional regime but remained at relatively shallow depths within the depositional basin.

Chloritization of biotite and clays

The presence of detrital mica as part biotite and part chlorite may suggest alteration of biotite to chlorite. Also, the apparent chloritization of clays is a common diagenetic feature in the Chanute sandstones.

Chlorite precipitates from alkaline pore fluids containing little K^+ but sufficient Mg^{2+} (Tucker, 1981). Chlorite might also precipitate from (1) pre-existing clay minerals like the transformation of smectite to illite when K^+ is added (Boles and Franks, 1979),

$$\text{smectite} + K^+ \Rightarrow \text{illite} + \text{chlorite} + \text{quartz} + H^+ \quad (8)$$

(2) from chemical alteration of biotite, which is commonly observed and involves the loss of Si, Fe, and K, or (3) by the alteration of kaolinite when Fe, and Mg are supplied from adjacent shales (Weaver, 1989) shown in equation 9:

$$3Al_2Si_2O_5(OH)_4 + 3.5Fe^{2+} + 3.5Mg + 17H_2O \Rightarrow$$
$$\text{(kaolinite)}$$
$$Fe_{3.5}Mg_{3.5}Al_6Si_6O_{20}(OH)_{16} + 30H^+ \quad (9)$$
$$\text{(chlorite)}$$

Chlorite precipitation, like kaolinite, can occur early or late (Weaver, 1989) as shown by Kaiser (1984), where two generations of authigenic chlorite formed: one early at the expense of smectite (montmorillonite) grain coats at conditions of less than 75°C, and one late at the expense of kaolinite at conditions of 100°C or greater. Chlorite precipitation seems to be independent of temperature and its occurrence can be related to kerogen maturation during late diagenesis, and to clay replacement on earlier stages.

Early Calcite Cement

Early calcite cement occurs in the Chanute sandstones as a patchy poikilotopic cement (Figure 41). The occurrence of the calcite is mostly restricted to the upper part of the Cottage Grove sandstone. The cement is patchy but widespread through the few thin sections where its observed, and commonly replace quartz and other labile grains (Figure 41). Ghosts of completely replaced grains are commonly observed within the calcite cement. No other type of diagenetic features are present in the samples with the early calcite cement.

Precipitation of calcite, as with quartz, also depends on pH, and temperature. Calcite solubility also involves a gas phase, CO_2 in solution, making the precipitation of calcite more complex than that of quartz. Calcite is also more soluble than quartz, therefore complicating the conditions for equilibrium. At atmospheric pCO_2, sea water is saturated to slightly supersaturated with respect to either calcite or aragonite (Blatt, 1979). These waters are commonly saline and slightly alkaline, and the source of Ca is mostly provided by dissolution of carbonate skeletal grains (Tucker, 1981). These conditions provide a good mechanism for early calcite precipitation by marine phreatic waters.

Since the samples containing this early calcite cement do not show any of the diagenetic features common in the rest of the samples (i.e. quartz overgrowths, extensive dissolution, evidence for

compaction, late cements, etc.), this cement is interpreted as having been precipitated very early, possibly soon after deposition.

Late calcite, dolomite and ankerite

The late carbonate cements present in the Chanute sandstones appear to be all related to a single event. The late calcite cement is patchy in nature, and is commonly found partially obscured by iron-oxide. Ankerite occurs only in cores as a patchy cement with characteristic rhombic structures that are commonly partly altered to iron-oxide along the edges of the patches and along some of the cleavage traces (Figure 40). The presence of dolomite is confirmed only by the absence of stain in the cores of the ankerite rhombs (Figures 42, 50).

The presence of ankerite was detected after preliminary petrographic analysis was completed by staining the carbonate-cemented samples. Microprobe analysis later confirmed the presence of ankerite in the Cottage Grove samples (Appendix 4). Problems with "compromised" grain boundaries due to the width of the microprobe beam and the small grain size of the Cottage Grove samples provided only a few reliable data points. Further analytical data is needed to confirm the presence of the ankerite.

The solubility of calcite, contrary to that of quartz, decreases with depth, while increases in temperature and pressure also decrease calcite solubility. As mentioned above, calcite precipitation is very sensitive to pH and pCO_2, being favored by high pH and low pCO_2. Calcite also dissolves to the charged chemical species: HCO_3^-,

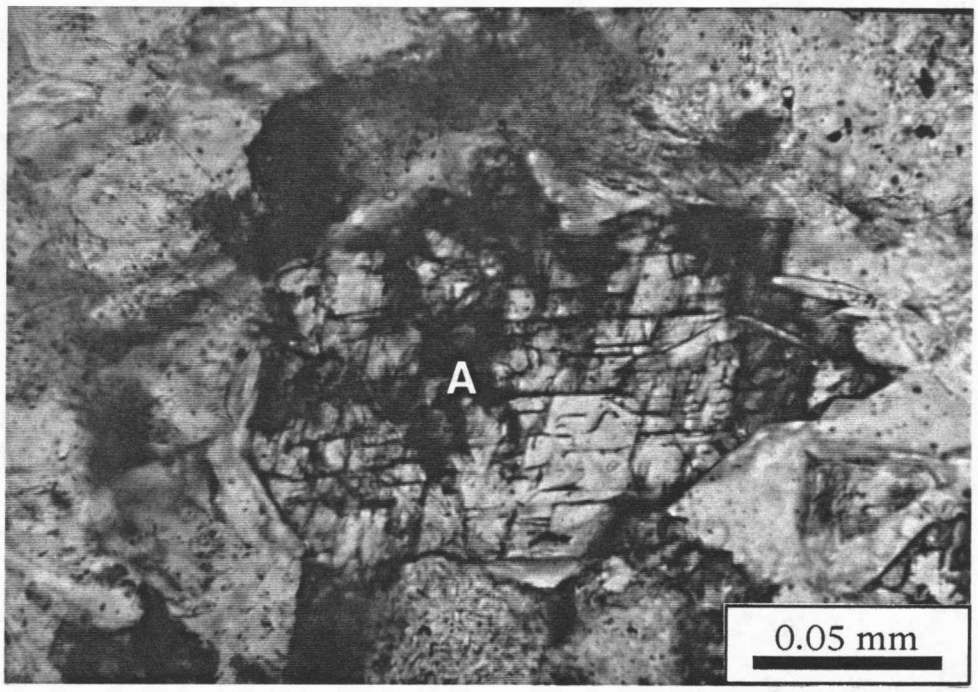


Figure 50. When stained with a mix of potassium ferricyanide and alizarin red, ankerite (A) stains deep navy blue. The absence of stain in the ankerite rhomb cores suggests the presence of dolomite. Iron-oxide can also be observed in this micrograph; PPL. Photomicrograph taken from core sample G1 22',2.5" of the Cottage Grove sandstone.

CO_3^{-2}, and Ca^{+2}, that tend to form ionic pairs from which the magnesium carbonate pair is the most common in subsurface waters. Since dissolved Ca and carbonate are charged ions, they are affected by changes in concentrations, and activities, they will be affected by salt sieving, a process by which clay flakes in mudrocks act as semipermeable membranes trapping the salt behind the membrane and allowing fresh and saline waters through (Blatt, 1979). When these conditions are met, they increase the chances of late carbonate precipitation. Possible sources of carbonate are connate pore waters that migrated from adjacent limestones and shales. At depth, compaction of a limestone by increased burial may have induced pressure solution in the limestone, forcing part of the Ca into solution. These Ca-saturated waters can produce cements in an adjacent sandstone (Mimran, 1977, from Blatt, 1979). Also at depth, kerogen maturation reactions in adjacent shales increase the amount of CO_2 into solution. This increase in CO_2 will produce leaching of carbonates and calcium bearing silicates (feldspars and some clay minerals) present in the shales or surrounding sandstones (Siebert et al., 1984).

$$\underset{\text{(albite)}}{NaAlSi_3O_8} + 2Ca^{+2}(aq) + 4HCO_3^-(aq) \Rightarrow Na^+(aq) +$$

$$Al(OH)_2^+(aq) + 2HCO_3^-(aq) + \underset{\text{(quartz)}}{3SiO_2(s)} + \underset{\text{(calcite)}}{2CaCO_3(s)} \quad (10)$$

Reactions with the silicates may neutralize the waters (Bjørlykke, 1988) releasing the Ca to nearby sandstones and thus promoting carbonate cementation.

Precipitation of ankerite and dolomite is also governed by the relationships discussed above. Boles (1978) and Boles and Franks (1979) stated that a source of Fe^{+2} and Mg^{+2} is needed to precipitate ankerite from preexisting calcite, and that such ions could be provided by the smectite to illite transformation from adjacent shales, which is also related to kerogen maturation. This reaction is shown below (Siebert et al., 1984):

$$\underset{\text{(calcite)}}{4CaCO_3} + Fe^{+2} + Mg^{+2} \Rightarrow \underset{\text{(ankerite)}}{2CaFe_{0.5}Mg_{0.5}(CO_3)_2} + 2Ca^{+2} \qquad (11)$$

and is a possible mechanism for the precipitation of late ankerite cement in the Cottage Grove sandstones. The presence of dolomite as cores in the ankerite rhombs is not definitively proven yet, but a possible mechanism for the formation is the precipitation of dolomite from existing calcite (Bath et al., 1987):

$$\underset{\text{(calcite)}}{2CaCO_3} + Mg^{2+} \Rightarrow \underset{\text{(dolomite)}}{CaMg(CO_3)_2} + Ca^{2+} \qquad (12)$$

and later altered to ankerite by addition of Fe^{+2} from solution. This might explain the dolomite cores and the ankerite around them.

Late diagenetic events

During the late stage of Chanute sediment diagenesis (possibly prior to exposure), partial dissolution of the late cements, and mobilization of clays and iron-oxide (from the ankerite) occurred. Formation of boxwork iron-oxide structures (Figures 39, 51) occurred after the dissolution of the late ankerite cements. The mechanisms that produced this late dissolution and mobilization stage are

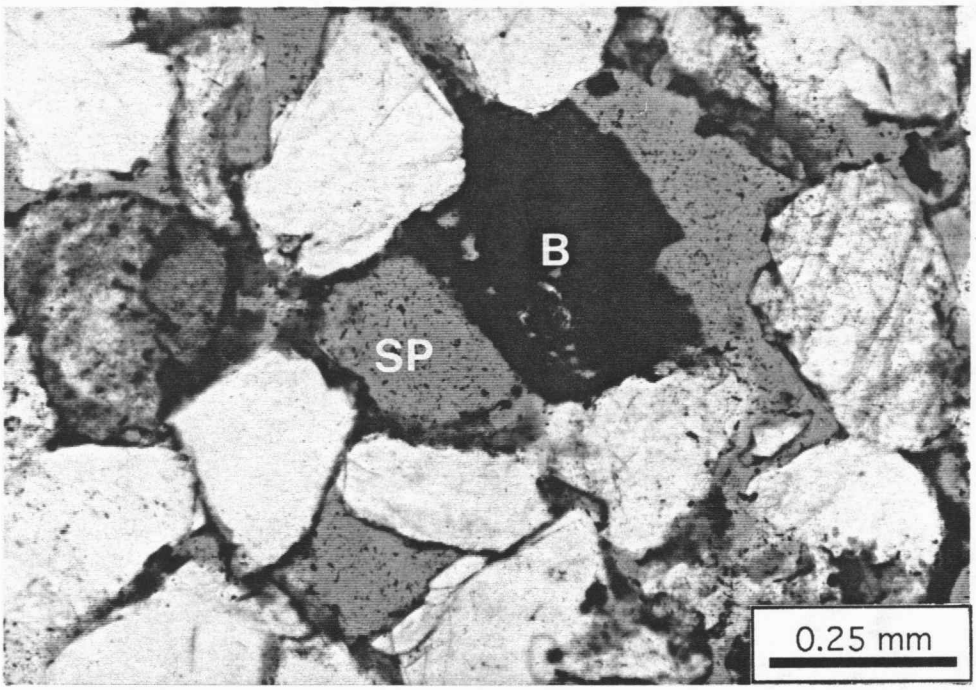


Figure 51. Boxwork iron-oxide structures (B) in the Chanute sandstones. An SRF, secondary porosity (SP), and iron-oxide coatings can also be observed in this photomicrograph; PPL. Photomicrograph taken from outcrop sample NR 0.55 of the Noxie sandstone.

produced by the same conditions of mineral stabilities described above.

Paragenesis of the diagenetic events in the Chanute sandstones

The sequence of diagenetic events that the Chanute sandstones went through are illustrated in Figure 52. Precipitation of quartz overgrowths and calcite cements were the initial diagenetic events in the Chanute sands. Quartz overgrowth precipitation was possibly syndepositional, precipitated by silica supersaturated meteoric waters in Chanute sand facies with greater terrestrial influence (Figures 52, 53 A) like the Noxie sandstone and the lower parts of the Cottage Grove sandstone. Early calcite cement was precipitated by marine derived phreatic waters in marine influenced facies (Figures 52, 53 B). This calcite cementation event might be related to the sea level high stand that led to the deposition of the overlying Iola Limestone. This idea is supported by the observation that only Cottage Grove samples close to the contact with the Iola show the early, poikilotopic calcite cement. Subsequent smaller-scale marine transgressions and regressions deposited younger thick clastic and carbonate units on top of the Chanute (Figures 52, 53 C) causing the Chanute to subside into the compactional regime. The post-Iola pre-Wyandotte regressions did not reach the study area (Heckel, 1988) and later regressions exposed only the tops of much thicker, younger detrital units in this region (Lane, Vilas shales) therefore the Chanute Shale remained in the compactional regime until prior to recent subaerial exposure. The carbonate-cemented facies remained mainly

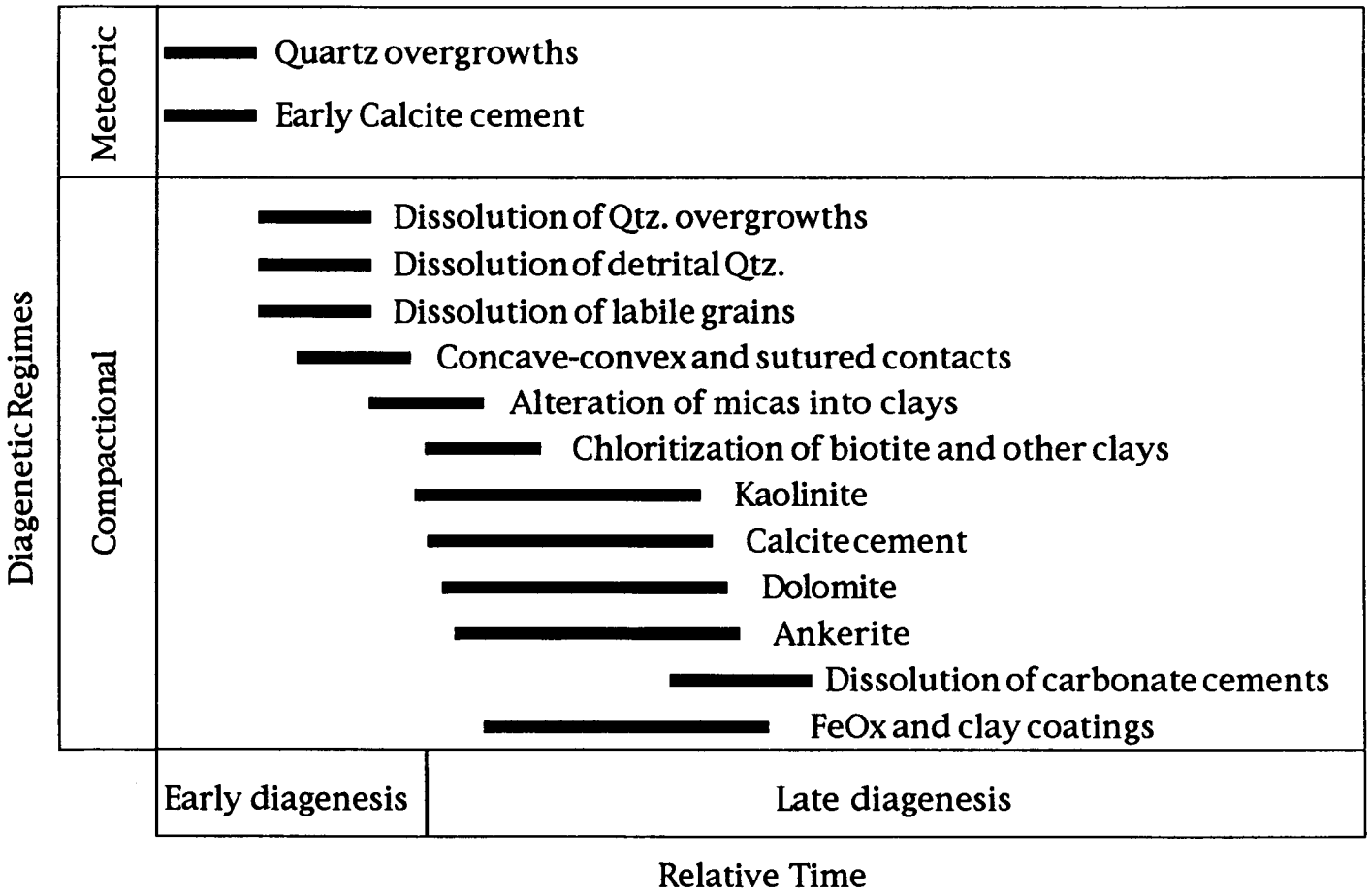


Figure 52. Paragenetic diagram for the Chanute Shale sandstones.

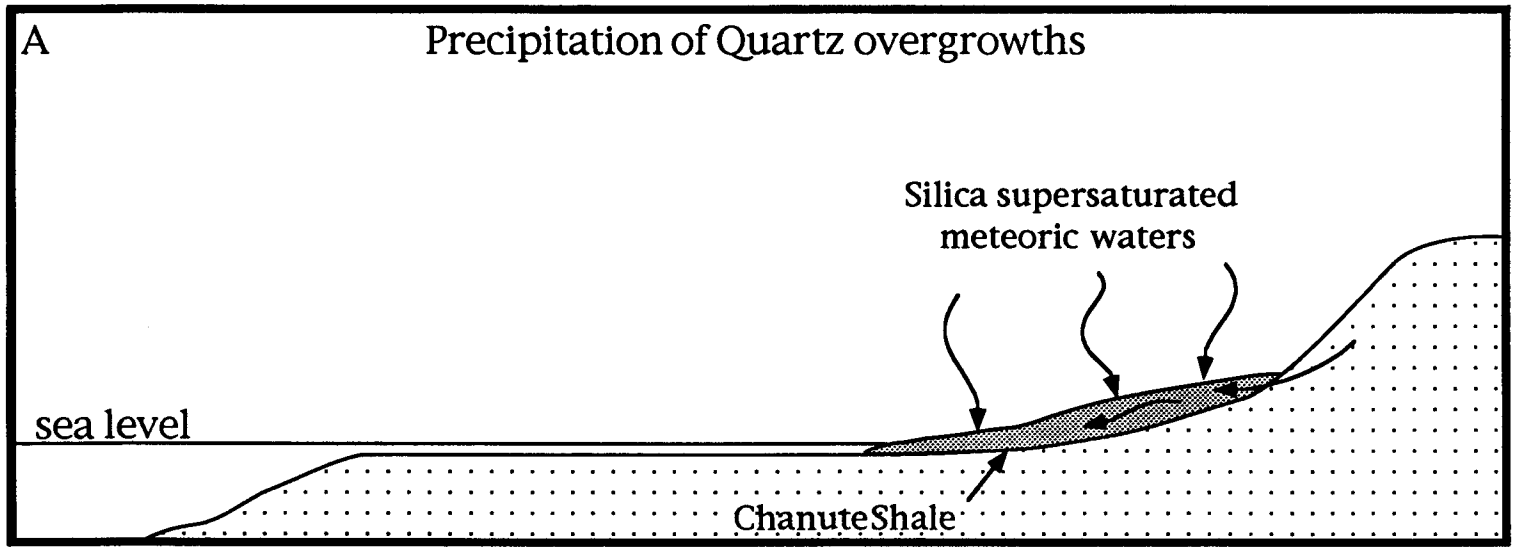


Figure 53 . Diagenetic model for the Chanute Shale sandstones; A, B, C, D.

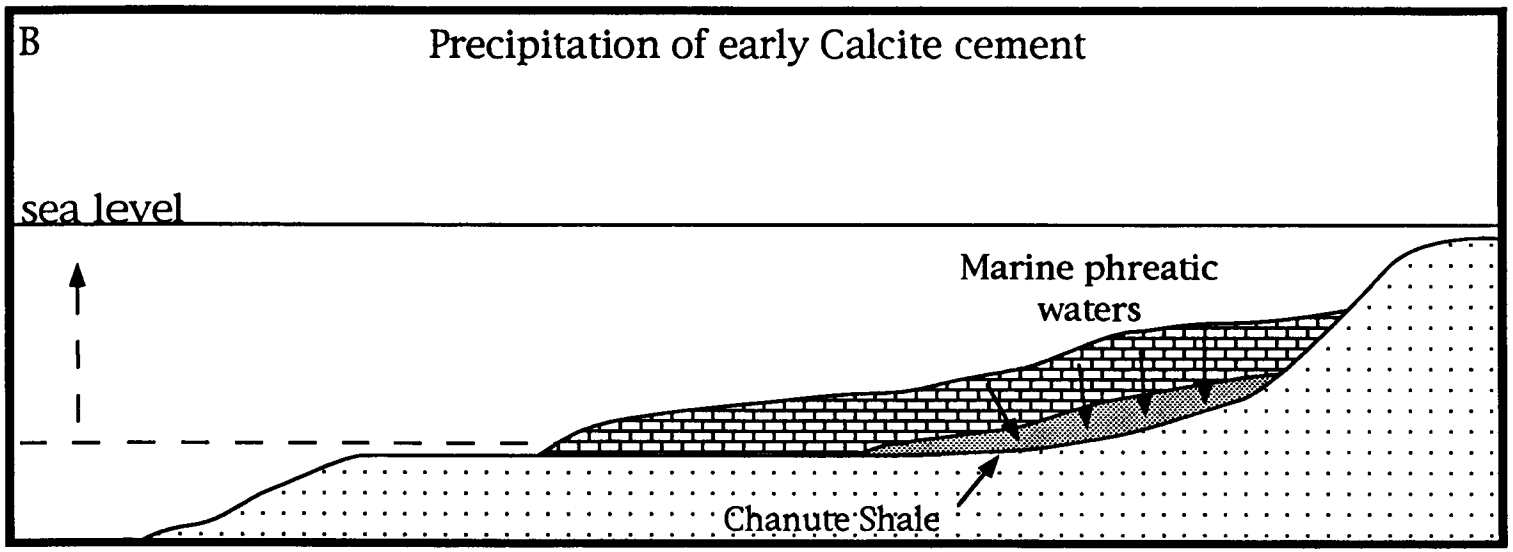


Figure 53. continued.

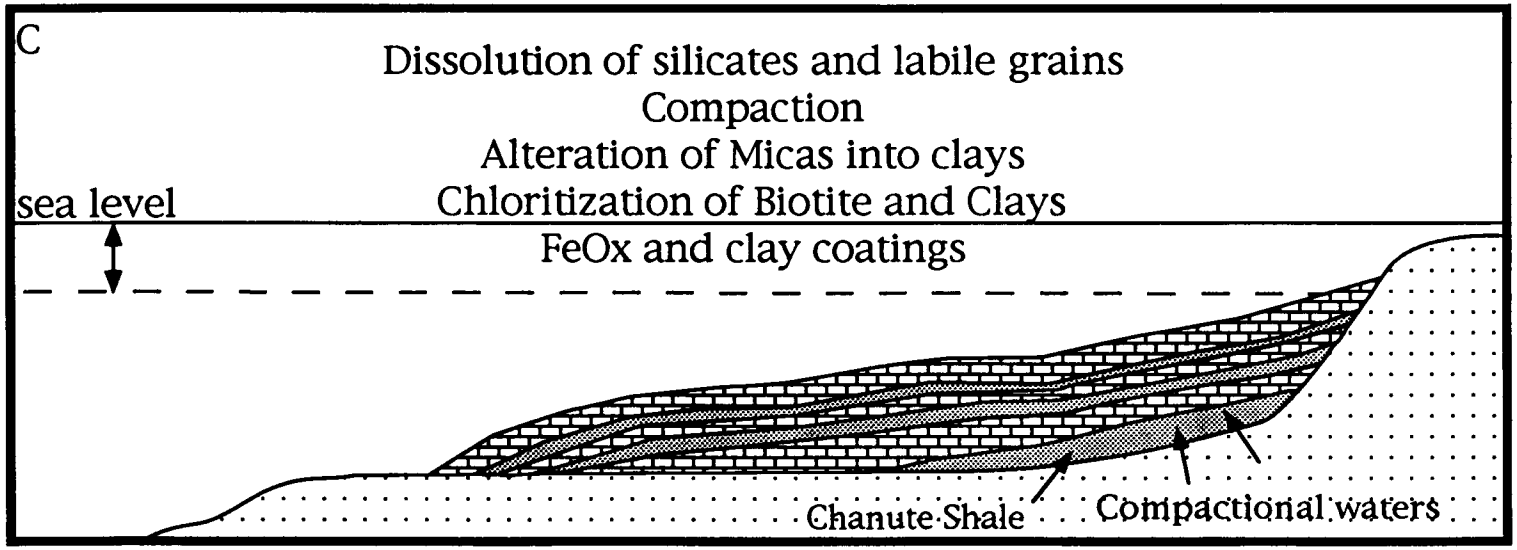


Figure 53. continued.

unchanged while the silica cemented facies underwent a strong dissolution phase. This is supported by the absence of dissolution and other diagenetic features in the early carbonate cemented samples while the silica cemented samples suffered a strong dissolution event. Silica cement, detrital quartz, rock fragments and feldspars were intensely altered and dissolved by saline and alkaline compactional waters. The dissolution allowed some compaction to take place producing concave-convex contacts between grains (Figure 52).

Compactional waters from underlying shales and coals within the oil maturation window had a major role in the late diagenesis of the Chanute sandstones. Acidified waters released from underlying shales, and coals provided the necessary ions for the late precipitation of kaolinite and the late carbonate cements (Figures 52, 53 D). Kaolinite was possibly deposited first since it's major ion source comes from the dissolution of feldspars and rock fragments and is usually not precipitated far from them. Partial dissolution, alteration and chloritization of biotite and clay minerals, also took place in the compactional regime (Figures 52, 53 C). Alteration of clay minerals was the primary source for the late chloritization event. The order in which the late carbonate cements precipitated is not clear from petrographic observations, but a possible scenario might be calcite precipitation followed by calcite alteration to dolomite by Mg-bearing waters coming from underlying units (see equation 12), and then alteration of dolomite to ankerite when Fe

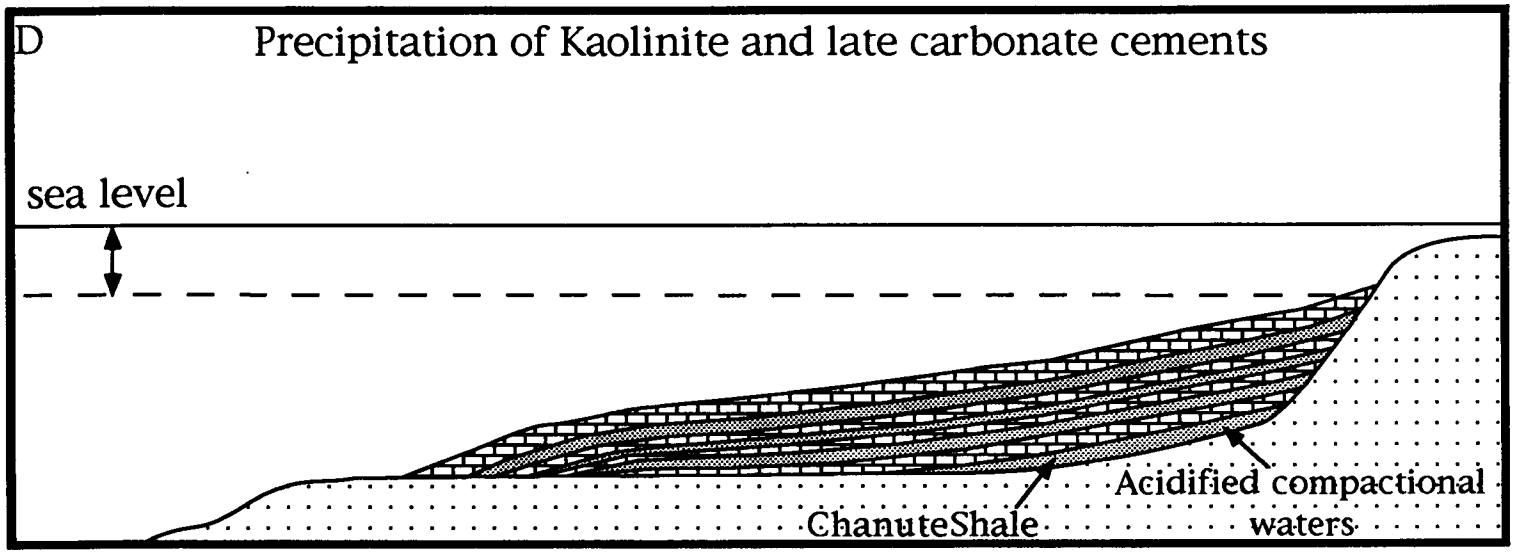


Figure 53. continued.

was added to the system from underlying shales (see equation 11). Another possibility is to have ankerite cores depleted of Fe,. This would diminish the reaction of the stain mix with the iron thus leaving the unstained rhomb cores.

Dissolution of the late carbonate cements and mobilization of iron-oxides and clays possibly occurred later when the rocks were exposed again to the meteoric regime, where fresh meteoric waters moved through the Chanute Shale sandstones prior to exposure to the surface (Figure 52).

CHAPTER VII

SUMMARY AND CONCLUSIONS

The Upper Pennsylvanian (Missourian) Chanute Shale is recognized as the nearshore shale component of the idealized Kansas cyclothem. This formation consists of the lower Chanute, the Thayer Coal and the upper Chanute members. Twelve exposures of the Chanute interval, as well as 2 cores, and approximately 500 well logs were used to interpret the stratigraphy, petrology, depositional environments, and diagenesis of the Chanute Shale in northeastern Oklahoma and southeastern Kansas.

The lower Chanute consists of the Noxie sandstones (which occur as channel sands), shales and silty shales capped by a blocky mudstone (underclay). This interval is capped by the thin but continuous Thayer Coal. Overlying the coal, the upper Chanute consists of silty shales and shales capped by the Cottage Grove sandstone, which occurs as a sheet sand.

The Chanute Shale represents a terrestrial to transitional marine environment of which the upper part was deposited during the early stages of a marine transgression. The lower Chanute was initially deposited in a fluvial system gradually changing to a fluvially-dominated deltaic system while the upper Chanute represents a funnel-shaped estuarine environment. Nine lithofacies

were identified using outcrop, cores, and well log data. These are: 1) Interbedded fine sandstone and silty clay shale, 2) Massive channeled sandstones, 3) Gray, fissile clayey shale, 4) Silty shale, 5) Mottled blocky mudstone, 6) Coal, 7) Thinly-bedded, thinly-laminated micaceous sandstone, 8) Carbonate cemented, contorted fine micaceous sandstone, and 9) Interlaminated siltstone and shale.

Isoliths and isopach maps for the whole interval and from the different members of the Chanute were constructed using the subsurface data. The Chanute Shale isopach reflects well defined NE-SW striking channels in the southern part of the study area, while more lobate and thinner E-W striking sediments were deposited towards the north. The thickest deposits are located in the south, within the Noxie channels area. Overall, the Chanute Shale thins northward and westward from the outcrop belt. The source of sediments for both members are the Ouachita Mountains, south to southeast of the study area.

Petrographically the Chanute sandstones consist of coarse silt to medium-grained sand, displaying significant compositional variability, ranging from quartz arenites, sublitharenite, subarkoses, litharenites, feldspathic litharenites, to quartz, lithic and feldspathic wackes. The Chanute sandstones, although they remained relatively in shallow burial, were exposed to strong diagenetic alterations in the meteoric and compactional regimes. Precipitation of early silica, and calcite cements occurred early after deposition with calcite related to the proximity of the overlying Iola Limestone. Secondary porosity

(avg. 20 to 35%), formed by dissolution of framework grains and early cements. This occurred early in the compactional regime, and was one of the major diagenetic features observed in the Chanute sandstones. Considerable chemical alteration of framework grains, and precipitation of authigenic clays and cements was also intensive, probably late within the compactional regime. Many of the diagenetic changes observed in the late diagenesis of the Chanute sandstones are related to acidic compactional waters from adjacent shales and coals underneath the formation, and possibly to kerogen maturation within them. Mobilization of clays and Fe-oxides occurred prior to exposure when the Chanute sands entered the meteoric environment once more.

APPENDIX I

WELL-LOG DATA

This appendix is composed by two tables with the information obtained from approximately 500 well logs from Kansas and Oklahoma. Table 1 contains the information of tops and bottoms (in feet) of the Chanute as a whole and of its members (Lower Chanute, Thayer Coal, and Upper Chanute). Table 2 contains the thicknesses and sand counts (in feet) used for the construction of the maps used in the study.

Both tables contain a well code and the name of each particular well log used. The well code indicates the location of the well in the study area. The first two letters represent the state; KS-Kansas, ON-Oklahoma. The three following numbers represent the quarters; 1-NW, 2-NE, 3-SW, 4-SE. These are followed by the section number, the township, and the range numbers due E-east.

KS123123406E

Abbreviations are widely used in the tables. The following list will help you to understand their meaning.

TOP: top of the unit

BOT: bottom of the unit

CHAN: Chanute Shale

U CHAN.: Upper Chanute

L CHAN: Lower Chanute

MH: marine horizon

GL ELEV: ground level elevation

KB ELEV: kelly bushing elevation

THK: thickness of the unit

SAND: sand counts

CG: Cottage Grove sandstone

Table 1. Tops and bottoms of the Chanute Shale members.

WELL CODE	WELL NAME	GL ELEV.	KB ELEV.	TOP CHAN	BOT. CHAN	BOT. UCHAN	TOP LCHAN	TOP IOLA	TOP MH	BOTT MH
KS002201624E	SUNLEY #S-2	-	NA	108	120	116	116	94	-	-
KS000311624E	A-2	-	NA	no top	22	-	-	-	-	-
KS000361623E	#1	-	NA	70	78	76	76	55	-	-
KS224311622E	#16	-	NA	224	260	-	-	202	233	246
KS042311622E	LOOMER #A-13	-	NA	216	250	236	236	197	-	-
KS042261621E	CUMMINGS #S-20	1012.0	NA	208	239	224	224	187	-	-
KS442251620E	W. G. BROERS	980.0	NA	332	377	355	355	308	-	-
KS001021618E	MERLIN BARTON #1	1003.0	NA	470	478	474	474	441	-	-
KS004281618E	PARKS #3	961.0	NA	405	423	415	417	376	-	-
KS421231616E	WOODWARD #1	1103.0	1108.0	723	737	727	727	681	-	-
KS000061724E	# 8	-	NA	103	110	-	-	87	-	-
KS000061724E	# 7	-	NA	95	107	-	-	81	-	-
KS002111724E	MILLS #S-6	-	NA	483	500	494	494	464	-	-
KS214121724E	RIGNEY #12	-	NA	115	130	124	124	87	-	-
KS000061724E	#9	-	NA	80	90	86	86	65	-	-
KS211201723E	SCHUKNECHT #2	845.0	846.5	41	48	44	44	21	-	-
KS042061722E	HARBISON A-4	-	NA	202	230	220	222	182	212	220
KS001061722E	HARBINSON #A-5	-	NA	193	228	210	212	173	204	210
KS113041722E	PURDUE #40	-	NA	207	231	226	226	188	-	-
KS044031722E	SHOFNER #A-1	-	NA	72	103	96	96	54	87	90
KS021231722E	ROHRER # A-1	-	NA	34	46	44	44	-	-	-
KS333011722E	PRICE #17	-	NA	30	66	56	56	13	-	-
KS002161721E	CAYLOR #101-31A	870.0	874.0	40	69	58	58	-	-	-
KS001201721E	HOBBS #4	-	NA	148	171	158	158	123	-	-
KS121151721E	SPRINGER #L-20	930.0	NA	96	124	112	112	76	-	-
KS044141721E	BULLOU #1	-	NA	no top	26	-	-	-	-	-
KS012151721E	# 079	-	NA	149	182	169	170	130	-	-
KS000251720E	ANDERSON # 4-A	-	NA	203	227	217	217	183	-	-
KS342121720E	RAY EVANS NORTH #9	-	NA	130	150	146	146	109	-	-
KS034051717E	BRIGGS ALTEX #1	934.0	939.0	479	500	491	492	447	-	-
KS002011821E	RITCH #6	-	NA	24	47	-	-	-	-	-
KS003041821E	GILCREST #7	-	NA	144	172	-	-	123	-	-
KS000171821E	# 24A-17	-	-	73	94	-	-	54	-	-
KS114131820E	J. E. BURKDOLL #2	-	NA	210	242	226	228	190	-	-
KS000121820E	BURKDOLL #24	-	NA	no top	224	-	207	-	-	-
KS011061817E	GREER #1	954.0	NA	499	519	514	514	468	-	-
KS444321812E	T. ANDERSON #1	1158	NA	1196	1208	-	-	1158	-	-
KS013241921E	F.B. HUETTENMUELLER #1	1112.0	NA	210	218	-	-	179	-	-
KS032231921E	MILLER #1	-	NA	203	220	214	215	177	208	214

Table 1- continued.

WELL CODE	WELL NAME	GL ELEV.	KB ELEV.	TOP CHAN	BOT. CHAN	BOT. UCHAN	TOP LCHAN	TOP IOLA	TOP MH	BOTT MH
KS031111918E	PIERSOL #1	1000.0	1006.0	372	386	-	-	336	-	-
KS112341917E	JAMES #1	1139.0	NA	592	605	-	-	555	-	-
KS221051915E	#1 P. GEORGE	1159.0	1163.0	862	888	881	882	818	-	-
KS331061915E	W. JONES #1	1154.0	NA	856	874	-	-	810	-	-
KS112341914E	JEFFERS #1	1143.0	NA	887	900	-	-	854	-	-
KS331271914E	DOTSON #1	-	-	910	918	-	-	877	-	-
KS114301914E	H. SMITH #1	1108.0	1113.0	936	942	-	-	902	-	-
KS334241913E	SLEAD #1	1151.0	1155.0	1005	1018	1015	1016	-	-	-
KS024341913E	OWENS #1	1091.0	NA	974	994	986	988	958	-	-
KS114271913E	DOTY #1	1130.0	NA	1006	1037	1035	1035	966	-	-
KS423281913E	ST. BONNETT #1	1073.0	1077.0	960	993	987	989	930	-	-
KS212261912E	CARPENTER #1	1080.0	NA	1048	1068	1064	1065	1004	-	-
KS232021912E	VAN GUNDY #1	1124.0	NA	1109	1128	-	-	1075	-	-
KS314041912E	DAVIS #1	1182.0	NA	1188	1207	-	-	1149	-	-
KS114231910E	PENNY #1	1120.0	1124.0	1361	1373	1372	1372	1318	-	-
KS111201908E	RETTINGER #1	1180.0	1185.0	1690	1705	-	-	1662	-	-
KS311201906E	#1 OPEL MILLER	1396.0	1401.0	1716	1723	-	-	1681	-	-
KS000162022E	FEVERBORN #1	-	NA	no top	22	-	-	-	-	-
KS000162022E	FEVERBORN #2	-	NA	no top	32	-	-	-	-	-
KS001252019E	WHITE #4	-	NA	233	262	250	250	204	-	-
KS144082019E	GATES # 22D-A	965.0	975.0	229	275	267	269	223	-	-
KS442192017E	KITCHENS #1	1181.0	NA	630	649	646	646	588	-	-
KS334032015E	NUSZ #1	1146.0	1150.0	782	806	-	-	702	-	-
KS114332015E	PHILLIPS #1	1098.0	NA	728	744	-	-	670	-	-
KS031252014E	WARREN #3	1072.0	1078.0	752	769	765	767	719	-	-
KS441162014E	BUSBOOM #1	1092.0	NA	832	844	-	-	796	-	-
KS331092014E	HODGES #1	1087.0	NA	839	852	-	-	813	-	-
KS323362013E	MCGREW #1	1108.0	NA	904	917	-	-	860	-	-
KS224012013E	WOODS #1	1102.0	1106.0	923	925	-	-	889	-	-
KS132272013E	GILLIGAN #1	1107.0	NA	925	938	-	-	889	-	-
KS024172012E	VAN SICKLE #1	1166.0	NA	1209	1221	1217	1218	1162	-	-
KS224082012E	R. CIBSON #1	1149.0	1153.0	1169	1177	1172	1174	1128	-	-
KS014102010E	REES A-1	1217.0	NA	1436	1450	1446	1446	1394	-	-
KS331322010E	REES #4	1390.0	1395.0	1660	1665	-	-	1605	-	-
KS111202010E	MILLER #2	1348.0	1352.0	1633	1650	-	-	-	-	-
KS014182010E	COUGHLEN B #1	1328.0	1332.0	1606	1624	-	-	1570	-	-
KS443302010E	DAVIS #1	1381.0	1385.0	1680	1690	-	-	1640	-	-
KS032172006E	L. M. WANER #1	1388.0	1393.0	1890	1894	-	-	1861	-	-
KS334362008E	NORTON #1	-	1339.7	1746	1759	-	-	-	-	-

Table 1- continued.

WELL CODE	WELL NAME	GL ELEV.	KB ELEV.	TOP CHAN	BOT. CHAN	BOT. UCHAN	TOP LCHAN	TOP IOLA	TOP MH	BOTT MH
KS023152005E	KAUFMAN #1	1380.0	1385.0	1881	1888	-	-	1851	-	-
KS001042121E	SCHEMERHORN # S-11	-	NA	26	75	64	64	-	-	-
KS100042121E	SCHEMERHORN # S-8	-	NA	26	75	64	64	-	47	54
KS021082121E	GALDEMAN # 0-11	-	NA	77	129	114	114	49	98	104
KS311142120E	ODAFFER # N-5	-	NA	231	277	260	260	202	252	260
KS000152120E	WEIS #12	-	NA	250	280	277	279	215	-	-
KS000062120E	MELCHER A # 2	-	NA	246	277	266	266	208	-	-
KS221162120E	WEST HUNLEY #18 (R-30)	1135.0	NA	227	265	248	248	194	-	-
KS003032119E		1013.0	1016.0	216	250	-	-	180	226	234
KS221242117E	DRUM #1	-	1059.0	426	448	-	-	383	434	440
KS113112116E	DALBY #1	1090.0	NA	578	596	-	-	528	-	-
KS111112115E	REINKER #1	1069.0	NA	674	683	680	681	624	-	-
KS334332115E	GRIFFIN #1	1079.0	NA	696	712	-	-	620	-	-
KS331212115E	NOEL #1	1042.0	NA	696	702	-	-	636	-	-
KS122162115E	NEWKIRK #1	1026.0	1030.0	636	649	-	-	584	-	-
KS331292115E	WARD #1	1059.0	1063.0	730	736	-	-	667	-	-
KS314312115E	ALLEN #1	1088.0	NA	758	765	-	-	712	-	-
KS134112114E	HOSS-GUPTON #3	1085.0	NA	758	767	-	-	708	-	-
KS131342114E	PAXSON #1	1099.0	NA	890	902	-	-	839	-	-
KS441222114E	HARRINGTON # 1-B	1092.0	1096.0	838	849	-	-	791	-	-
KS231102114E	KRAUSE #1	1141.0	1147.0	837	845	-	-	793	-	-
KS331032114E	THEOBALD #1	1125.0	1131.0	815	830	-	-	798	-	-
KS444162114E	BOWMAN #1	1149.0	NA	909	919	-	-	859	-	-
KS423312114E	KAUFMAN #1	1164.0	NA	922	932	-	-	878	-	-
KS441312114E	MERRITT #1	1153.0	NA	949	955	-	-	908	-	-
KS142312114E	TRUELOVE #1	-	NA	932	948	942	942	884	-	-
KS123192114E	BEYER #4	1129.0	NA	926	940	936	936	868	-	-
KS444362113E	BEYER #1	1183.0	1184.0	965	972	-	-	910	-	-
KS441252113E	KNAPP #1	1137.0	NA	952	963	-	-	900	-	-
KS333242113E	KNAPP #1	1154.0	NA	948	955	-	-	898	-	-
KS332012113E	#1 WILSON A	1117.0	1122.0	924	936	-	-	878	-	-
KS132352113E	BASHAW BIRK #2	1177.0	1182.0	992	999	-	-	936	-	-
KS122262113E	JAMIESON #1	1155.0	1160.0	949	959	-	-	928	-	-
KS422232113E	GASCHE #1	1135.0	NA	934	941	-	-	883	-	-
KS142142113E	O'MARRA #2	1184.0	1189.0	1003	1022	-	-	950	-	-
KS144112113E	WILSON #1	1157.0	NA	971	980	-	-	924	-	-
KS111102113E	JONES #1	1109.0	1113.0	938	960	-	-	890	-	-
KS224202113E	GARDNER #1	1169	1174.0	1086	1100	-	-	1031	-	-
KS221032112E	GRIEDER #1	1174.0	1178.0	1148	1190	-	-	1101	-	-

Table 1- continued.

WELL CODE	WELL NAME	GL ELEV.	KB ELEV.	TOP CHAN	BOT. CHAN	BOT. UCHAN	TOP LCHAN	TOP IOLA	TOP MH	BOTT MH
KS022322112E	NUESSEN A-2	1189.0	1194.0	1193	1202	-	-	1175	-	-
KS211252111E	MATILE #1	-	-	1268	1279	-	-	1232	-	-
KS111082110E	RALPH & DARREL JONES #1-A	-	-	1551	1558	-	-	1506	-	-
KS034182110E	KAPP #2	-	-	1582	1591	-	-	1532	-	-
KS443362109E	ATYEO #2-G	-	-	1607	1614	-	-	1587	-	-
KS442292218E	WELDIN #2	-	NA	287	331	305	306	244	-	-
KS343292217E	PARMELLY #5	-	NA	417	436	428	430	360	-	-
KS013292217E	PARMELLY #6	1040.0	NA	430	448	-	-	377	-	-
KS221112216E	FISCHER #1	1040.0	1044.0	490	506	499	499	430	-	-
KS013222216E	EDWARDS/HEIRS #5	-	NA	472	483	480	480	430	-	-
KS004282226E	REMER #5	1004.0	NA	451	464	461	461	405	-	-
KS442282216E	FLAKE #6	1005.0	NA	456	472	466	467	402	-	-
KS124212216E	GLEUE #8	1016.0	NA	474	486	482	483	424	-	-
KS242212216E	J. WRIGHT #5	1015.0	NA	480	492	488	488	430	-	-
KS113312216E	SUTHERLAND #3	-	-	556	583	572	573	509	-	-
KS003302216E	MINNIE GRAY #2	-	NA	529	556	538	539	484	-	-
KS142192216E	BIRBECK #2	-	NA	507	528	519	520	462	-	-
KS444362216E	MURRAY #1	-	NA	541	568	558	558	494	-	-
KS442252215E	SMITH #1	-	NA	538	560	543	543	484	-	-
KS224132215E	WUEFERLE #1	1090.0	NA	624	642	635	636	575	-	-
KS242142215E	GOULDIE-RICH #1	1107.0	NA	663	674	-	-	612	-	-
KS441292215E	BORN #1	1115.0	1120.0	737	750	-	-	685	-	-
KS123272214E	KNAPP #1	1127.0	1132.0	827	847	-	-	765	-	-
KS133102214E	MERRITT #1	1117.0	1121.0	856	862	-	-	802	-	-
KS114262213E	BANWART #1	1175.0	NA	968	981	-	-	911	-	-
KS233112213E	ISCH #1	1175.0	NA	992	1000	-	-	930	-	-
KS113212213E	ELMER OTT #1	1193.0	NA	1029	1042	-	-	979	-	-
KS002322211E	SCHANKIE #1	-	NA	1271	1278	-	-	1256	-	-
KS021102210E	PIXLEE # 7	1375.0	1380.0	1612	1616	-	-	1581	-	-
KS333172210E	BROWNNING # 1	-	-	1714	1716	-	-	1670	-	-
KS441162203E	LITTON # 1	123.0	1428.0	2206	2219	-	-	2173	-	-
KS434032321E	MCGEE # 1	1080.0	1080.0	no top	28	-	-	-	-	-
KS233042321E	GADDIS #7	-	NA	no top	34	-	-	-	-	-
KS331042321E	MCCASLIN-V.B #116	-	NA	23	58	-	-	-	-	-
KS311042321E	GADDIS #24	-	NA	20	-	-	-	-	-	-
KS242052321E	MCCASLIN-V.B. #105	-	NA	no top	38	-	-	-	-	-
KS232142319E	BRIGGS TRACT 1 #3	1111.9	NA	180	214	-	-	140	-	-
KS142272318E	CARPENTER #1	1060.0	NA	226	250	-	-	180	-	-
KS141292318E	MCGHEE #1	-	NA	220	225	-	-	158	-	-

Table 1- continued.

WELL CODE	WELL NAME	GL ELEV.	KB ELEV.	TOP CHAN	BOT. CHAN	BOT. UCHAN	TOP LCHAN	TOP IOLA	TOP MH	BOTT MH
KS141062318E	KELLY #5	1013.6	NA	284	320	-	-	236	-	-
KS044122316E	NELSON WEBB # B-4	NA	NA	363	385	382	382	307	-	-
KS132132316E	MARTZ #4	980.0	NA	377	390	386	386	328	-	-
KS332132316E	MARTZ #3	-	NA	376	394	389	391	330	-	-
KS002132316E	JERRY MURRAY #8	980.0	NA	383	408	400	401	328	388	400
KS343122316E	MEATS #7	980.0	NA	375	395	391	392	352	-	-
KS003122316E	S. MEATS #6	980.0	NA	377	398	392	393	365	-	-
KS001012316E	SUNBEAM #6	-	NA	403	444	-	-	-	-	-
KS144142316E	CHARLES JONES #4	973.0	NA	388	419	-	-	354	-	-
KS131142316E	FREEMAN #1	980.0	NA	399	418	414	415	346	-	-
KS413112316E	ROBERT BADER #1	-	NA	410	424	-	-	358	-	-
KS434102316E	JOAN FREEMAN #2	-	NA	403	416	412	412	367	-	-
KS002332316E	FULLER #15	-	-	498	501	-	-	-	-	-
KS033112316E	ALICE CROTTS #2	-	NA	410	422	-	-	349	-	-
KS001202316E	DEARINGER#1	-	NA	526	553	-	-	500	-	-
KS121062316E	WRIGHT #2	-	NA	518	547	-	-	460	-	-
KS441092315E	EVANS A #2	1065.0	NA	640	658	655	655	586	-	-
KS001192315E	TEBBINS #1	-	-	658	670	-	-	600	-	-
KS331092314E	BAHR C #1	1096.0	NA	804	810	-	-	762	-	-
KS044012313E	CROTTY #1	1140.0	1146.0	910	921	-	-	846	-	-
KS122232313E	CHRIS BAHR #21	1185.0	1190.0	908	913	-	-	850	-	-
KS000092312E	LOCKHARD #1	1102.0	1106.0	1020	1026	-	-	773	-	-
KS000202312E	STAUFFER #1	1132.0	1136.0	1078	1084	-	-	1030	-	-
KS002032311E	CURRY #2	-	NA	1249	1252	-	-	1228	-	-
KS314162311E	REDDING #1	1206.0	1210.0	1300	1305	-	-	1280	-	-
KS113132310E	BURKETT # B-30	-	NA	1400	1405	-	-	1389	-	-
KS131192310E	ZIMMERMAN #6	1351.0	1356.0	1658	1674	-	-	1625	-	-
KS131302306E	BUSENITZ #3	1522.0	1527.0	1864	1870	-	-	1859	-	-
KS443342305E	WYSS A #1	1404.0	1411.0	2017	2022	-	-	2003	-	-
KS241352420E	APT. #116	-	NA	no top	35	-	-	-	-	-
KS132342420E	WINSLOW # 128	-	NA	no top	40	-	-	-	-	-
KS114332420E	TALBOTT #106	-	NA	13	42	36	36	-	-	-
KS313022418E	ECKDALL #5	-	NA	176	208	199	200	-	-	-
KS004022416E	ALEXANDER # 0-35	-	NA	437	492	488	489	384	-	-
KS332332415E	#1 KNAPP	1093.0	NA	570	630	-	-	516	-	-
KS134172412E	MARLIN #1	-	NA	1012	1045	-	-	986	-	-
KS231082411E	J.L. WILLIAMS #1	1216.0	NA	1354	1370	1354	1356	1337	-	-
KS313342409E	MARSHALL #3	1320.0	1325.0	1658	1663	-	-	1649	-	-
KS001112402E	ULMER B # 2	1412.0	1417.0	2396	2402	-	-	2360	-	-

Table 1- continued.

WELL CODE	WELL NAME	GL ELEV.	KB ELEV.	TOP CHAN	BOT. CHAN	BOT. UCHAN	TOP LCHAN	TOP IOLA	TOP MH	BOTT MH
KS111072521E	BARNETT #10	-	NA	no top	34	-	-	-	-	-
KS442332520E	SAGER #103	-	NA	no top	31	-	-	-	-	-
KS343142519E	SCOTT # B-1	-	NA	no top	70	-	-	-	-	-
KS332282519E	FRONK #2	-	NA	47	65	-	-	-	-	-
KS324232517E	WILLIS #12	-	NA	164	196	193	193	122	-	-
KS132242516E	DRAIN #1	-	NA	256	294	289	290	200	-	-
KS444062516E	EARL DAVIDSON #1	996.0	1002.0	367	406	406	406	321	-	-
KS231122514E	J TAYLOR #2	1106.0	NA	658	696	691	691	597	-	-
KS121072512E	HUBER #1	1077.0	1079.0	1145	1158	-	-	1134	-	-
KS423252504E	MITCHELL #5	1383.0	1389.0	2074	2076	-	-	2050	-	-
KS423332503E	CLEARWATER # 6	1294.0	1299.0	2266	2270	-	-	2242	-	-
KS221012510E	HAWTHORNE #1	-	-	1261	1276	-	-	1237	-	-
KS331252617E	OSBORN #1	971.0	NA	106	158	141	142	62	-	-
KS000222617E	DIETRICH D #14	-	NA	37	72	52	54	-	-	-
KS223162616E	YOUNG A #15	-	NA	362	399	-	-	305	-	-
KS142192615E	LAUBER B #7	1056.0	NA	525	563	-	-	470	-	-
KS242132614E	SAUBERS #6	-	NA	423	456	-	-	-	-	-
KS142262613E	KERNS #1	974.0	NA	616	668	-	-	566	-	-
KS021362612E	SHOBE #21-36	1050.0	NA	811	828	-	-	754	-	-
KS441112612E	HODGSON #1	1008.0	NA	794	805	-	-	773	-	-
KS321082612E	BOONE #1	1111.0	1116.0	987	1000	-	-	976	-	-
KS332302612E	DORA RUSSEL #1	1129.0	1134.0	1014	1024	-	-	999	-	-
KS214082611E	EASTMAN #1	1063.0	1069.0	1070	1085	-	-	1061	-	-
KS411182610E	SHINKLE #2	1093.0	1098.0	1279	1301	-	-	1273	-	-
KS333072610E	MONHART #10	1163.0	1168.0	1339	1347	1344	1346	1328	-	-
KS144062610E	DOUGHERTY #4	-	-	1326	1330	-	-	1315	-	-
KS114132609E	LIFE # H	-	-	1297	1308	-	-	1286	-	-
KS144232609E	MOON #4	-	NA	1363	1378	-	-	1354	-	-
KS001332609E	KTW FEE E #1	1336.5	1342.0	1548	1560	-	-	1540	-	-
KS341102608E	RICE #7	-	-	1834	1842	-	-	1823	-	-
KS411292608E	DRUMM #19	1553.0	1558.0	2025	2029	-	-	2018	-	-
KS111262607E	MOORE "A"	1450.0	1457.0	2048	2066	-	-	2014	-	-
KS432222607E	SIMON # 2-A	1493.0	1498.0	2082	2091	-	-	2077	-	-
KS003282606E	MCALLISTER # 1	1398.0	1403.0	2144	2164	2149	2150	2139	-	-
KS142132605E	TAGUE #4	-	-	2023	2035	-	-	2018	-	-
KS414352605E	BISAGNO #4	1304.0	1308.0	2103	2119	-	-	2098	-	-
KS244262605E	SLUSS B-1	1339.0	1344.0	2136	2153	-	-	2129	-	-
KS341032605E	WILKINSON #1	1339.0	1344.0	2015	2032	-	-	2009	-	-
KS323042605E	FINNEY (2) # 4	1325.0	1331.0	1972	1985	-	-	1966	-	-

Table 1- continued.

WELL CODE	WELL NAME	GL ELEV.	KB ELEV.	TOP CHAN	BOT. CHAN	BOT. UCHAN	TOP LCHAN	TOP IOLA	TOP MH	BOTT MH
KS002142715E	PAYNE #9	-	NA	214	288	276	277	166	249	251
KS314202714E	MARR #S-2	-	NA	463	540	521	522	417	502	505
KS034292713E	ADAMS #1	-	NA	710	759	-	-	656	735	740
KS230332713E	FEE # 1-33	1038.0	1043.0	635	664	-	-	577	-	-
KS000312711E	CORA FRENCH #2	-	-	1126	1154	-	-	1113	-	-
KS013072711E	PETERSON #2	1060.0	1065.0	1065	1086	-	-	1055	-	-
KS043062710E	THOMAS #26 C	1182.0	1193.0	1396	1399	-	-	1383	-	-
KS341252708E	TEMPLE #4	1406.5	1409.0	1666	1674	-	-	1658	-	-
KS424132708E	WIEDEMANN TRUST A #1	1370.0	1375.0	1648	1649	-	-	1636	-	-
KS313202707E	HUMMEL #1	1456.0	1461.0	2088	2090	-	-	2082	-	-
KS022352706E	LEWIS A #16	1456.0	1458.0	1707	1718	-	-	1696	-	-
KS221332706E	SIMMONS # 3-B	1370.0	1375.0	2097	2110	-	-	2089	-	-
KS023282706E	SIMMONS # 2-A	1321.0	1325.0	2051	2055	-	-	2043	-	-
KS000272705E	HAVERHILL UNIT # 35	1346.0	1346.0	2187	2303	-	-	2182	-	-
KS242152705E	CHINN # 1	1335.0	1340.0	2184	2194	-	-	2178	-	-
KS213082706E	MAX MAIN #1	-	-	2133	2144	-	-	2125	-	-
KS241352704E	#1 HART	1289.0	1296.0	2050	2074	-	-	-	-	-
KS111162817E	UHREN # 4-A	-	NA	152	178	-	-	-	-	-
KS111232816E	STORDEVANT #1-23	940.0	NA	184	204	-	-	-	-	-
KS001192816E	CRITES #7	-	NA	191	219	206	207	180	-	-
KS114242825E	BOCO #3	-	NA	179	195	-	-	150	-	-
KS431342813E	OAKS #34-E-10-SE	-	NA	493	552	531	532	463	-	-
KS000032813E	FEE #2-3	1056.0	1061.0	620	652	652	652	598	-	-
KS444262812E	MCGINNIS #1	977.0	NA	724	770	758	759	671	-	-
KS314242808E	YOUNGMYER PALMER #B-2	1349.0	NA	1772	1812	1808	1808	1754	-	-
KS221022807E	BOLUNGER # 1	1469.0	1474.0	2018	-	-	-	2012	-	-
KS332032807E	MANKA # 1	1511.0	1516.0	2086	2096	-	-	2078	-	-
KS441352806E	KNOLLENBERG # 1	1434.0	1439.0	2158	2178	2166	2166	2152	-	-
KS222152806E	DUNN # 1	1132.0	1136.0	2012	2025	2013	2013	2005	-	-
KS232211806E	WALTERS # 1	1416.0	1421.0	2118	2130	-	-	2105	-	-
KS242092806E	LINDGREN # 4	1342.0	1347.0	2064	2077	-	-	2053	-	-
KS004052806E	TABBING #2	1379.0	1384.0	2122	2136	-	-	2113	-	-
KS000012805E	WEAVER TRUST #1	1357.0	1362.0	2161	2184	-	-	2154	-	-
KS311362917E	MCCOY #8	-	NA	18	74	40	41	15	-	-
KS341302917E	A. ERBE #2	-	NA	23	77	42	42	-	-	-
KS332012914E	DOCIA BATES #17	876.0	NA	238.0	271.0	248	248	215	-	-
KS022232913E	RUSSEL B-1	840.0	NA	498	554	516	516	482	-	-
KS000202913E	STOTS #2	1155.0	NA	878	912	890	890	859	-	-
KS314122912E	THOMAS #1	1056.0	NA	753	789	764	764	736	-	-

Table 1- continued.

WELL CODE	WELL NAME	GL ELEV.	KB ELEV.	TOP CHAN	BOT. CHAN	BOT. UCHAN	TOP LCHAN	TOP IOLA	TOP MH	BOTT MH
KS114173911E	KLING #1	1100.0	NA	1104	1143	1109	1109	1088	-	-
KS031132910E	LAND # 12-13	1096.0	NA	1240	1258	-	-	-	-	-
KS421342910E	DUNKELBORGER #1	1011.0	NA	1116	1149	1122	1122	1097	-	-
KS231342909E	PERKINS #3	1185.0	1190.0	1471	1512	1476	1476	1457	-	-
KS000192908E	SHINN #21	1545.0	1550.0	1963	1997	1970	1970	1960	-	-
KS214162906E	PRICE WATTS #2	1381.0	1386.0	2127	2162	2138	2140	2114	-	-
KS011182905E	PERISHO UNIT #2	-	-	2334	2357	2336	2336	2307	-	-
KS003292905E	POTTORF #3	-	-	2217	2254	2228	2228	2203	-	-
KS334232904E	BLOOD #3	1275.0	1280.0	2316	2349	2327	2327	2294	-	-
KS000022904E	BOULBY #1	1198.0	1203.0	2192	2234	2204	2205	2170	-	-
KS123152902E	# 1 OLSON	1331.0	1336.0	2611	2662	2637	2637	2588	-	-
KS243013017E	C. SMITH #6	-	NA	no top	88	-	-	-	-	-
KS311223017E	STEVE WHITE # 2	-	NA	no top	78	-	-	-	-	-
KS144303017E	LOFLIN # 1	-	NA	22	40	-	-	16	-	-
KS421063017E	JOE NEWLAND #1	-	NA	no top	56	20	23	-	-	-
KS332263016E	DICKENS #2 N	-	-	no top	54	-	-	-	-	-
KS000083015E	SHUGO #2	-	NA	384	427	402	403	377	-	-
KS421333013E	HARKEY #1	909.0	NA	538	613	570	572	535	-	-
KS131183013E	H. CANNON #1	908.0	NA	577	637	591	592	572	-	-
KS444153012E	BELL#1	945.0	NA	680	740	700	700	673	-	-
KS412353009E	BRADFORD SWD	1229.0	1234.0	1474	1524	1489	1490	1469	-	-
KS324093009E	HYDE #1	-	-	1733	1770	1742	1744	1708	-	-
KS112093009E	KYSER P #11	-	-	1614	1656	-	-	1597	-	-
KS033253008E	SLEEPER # 14-25	1330.0	NA	1729	1774	-	-	1725	-	-
KS443103008E	SLEEPER # 1-C	1567.0	NA	2013	2044	2032	2033	2009	-	-
KS321123007E	LA FEICHE #1	1443.0	1448.0	1946	1987	1966	1965	1943	-	-
KS342313006E	HENDERSON #1	1391.0	1400.0	2238	2255	-	-	2234	-	-
KS111193006E	WAKEFIELD A #1	1344.0	1349.0	2165	2191	-	-	2162	-	-
KS114333005E	STUBER # 1	-	-	2232	2259	2239	2240	-	-	-
KS332013004E	DRAKE 42 -628	1229.0	1233.0	2215	2229	-	-	2213	-	-
KS244133004E	FUSCH # 1	1287.0	1292.0	2274	2297	-	-	2271	-	-
KS312113004E	WILSON # 1	1200.0	1205.0	2203	2221	-	-	-	-	-
KS004233004E	MAGBY	1268.0	1273.0	2267	2280	-	-	-	-	-
KS000153004E	STELBAR # 1	-	-	2234	2251	-	-	-	-	-
KS423333004E	COBBLE #1	1205.0	1210.0	2272	2290	-	-	-	-	-
KS032243003E	MORTON #1	1209.0	1214.0	2476	2490	-	-	2472	-	-
KS312103003E	GOYER # 1-A	1191.0	1196.0	2253	2271	-	-	2251	-	-
KS441023003E	MUELLER #1	1242.0	1247.0	2500	2572	-	-	-	-	-
KS244243116E	GADDY#1	-	NA	no top	72	32	34	-	-	-

Table 1- continued.

WELL CODE	WELL NAME	GL ELEV.	KB ELEV.	TOP CHAN	BOT. CHAN	BOT. UCHAN	TOP LCHAN	TOP IOLA	TOP MH	BOTT MH
KS211303116E	MELVIN OLSON #1	-	NA	63	114	82	84	57	-	-
KS113143115E	GORTON #1-14	850.0	NA	104	156	110	112	95	-	-
KS000233113E	STATE #41	915.0	NA	414	482	455	456	-	-	-
KS412173113E	TROMBOLD 31-17	1008.0	NA	632	702	657	660	-	-	-
KS143153111E	OSBORN #1	1057.0	NA	948	1038	978	980	946	-	-
KS113103110E	KILL 1-A	1045.0	1050.0	1124	1194	1151	1152	1122	-	-
KS322163109E	REEVES #1	1178.0	NA	1444	1516	1461	1462	1441	-	-
KS314173109E	DEAN #1	1127.0	NA	1468	1546	1504	1506	1464	-	-
KS233033108E	DENTON #9	1457.0	NA	1841	1907	-	-	1835	-	-
KS124163108E	BANNON #1	1432.0	1437.0	1901	1962	1927	1928	1897	-	-
KS223143107E	SMITH #1	1420.0	1425.0	2017	2079	2042	2044	2014	-	-
KS113213105E	HAMMER # 4	1276.0	1281.0	2313	2335	-	-	2301	-	-
KS034363105E	LEWIS # 1-C	1354.0	1359.0	2330	2379	2346	2348	2324	-	-
KS113213105E	HAMMER #1	1276.0	1281.0	2313	2335	-	-	-	-	-
KS241203105E	SICKLES #1	1227.0	1232.0	2199	2224	2210	2210	2194	-	-
KS213363104E	HOLT #5	1230.0	1235.0	2290	2368	-	-	2278	-	-
KS344343215E	BREDENHOFT # 1	-	-	67	141	-	-	20	86	90
KS244343215E	BREDENHOFT # 2	-	-	63	133	-	-	-	79	84
KS142343215E	FERREL # 1	-	-	20	149	44	46	-	-	-
KS142343215E	FERREL # 2	-	-	no top	128	36	39	-	-	-
KS142343215E	FERREL # 3	-	-	13	140	39	41	-	-	-
KS331323215E	THOMPSON#1	-	NA	79	266	168	170	72	-	-
KS014063215E	CRANE-DAY #1	921.7	NA	240	306	262	266	-	-	-
KS004363214E	SULLIVAN#2	-	NA	222	332	291	293	215	-	-
KS211323214E	WILLIAM LINN #1	851.0	NA	338	400	350	352	325	-	-
KS322263213E	SHELLEY #1	940.0	NA	433	515	456	456.5	422	-	-
KS441063213E	WELCH #1	-	NA	567	633	590	592	550	-	-
KS114133212E	KHEB #1	-	NA	664	740	688	690	658	-	-
KS032143212E	OAK RIDGE RANCH #2	913.0	NA	576	649	591	594	572	-	-
KS233043211E	GARVIN #3	1097.0	NA	1007	1144	1070	1071	1001	-	-
KS232313211E	FLOYD B #2-A	1095.0	NA	975	1123	1057	1058	966	-	-
KS121173211E	MCNEE #1	-	NA	-	1136	-	-	-	-	-
KS124083211E	AIKEN #3	1066.0	NA	968	1125	1034	1036	964	-	-
KS312183211E	MCNEE #1	1071.0	NA	988	1136	1054	1056	983	-	-
KS214063211E	GLASSCOCK #2	1013.0	NA	1036	1119	1076	1080	1023	-	-
KS113023210E	MCNEE # 1-A	-	NA	1146	1233	1173	1173	1135	-	-
KS444043210E	WALKER #3	1095.0	1100.0	1220	1318	1277	1279	1215	-	-
KS243293209E	#1 BIRD	1125.0	1130.0	1450	1594	1500	1505	-	-	-
KS323173209E	KEMPTON # 2	1101.0	NA	1467	1572	1496	1497	1464	-	-

Table 1- continued.

WELL CODE	WELL NAME	GL ELEV.	KB ELEV.	TOP CHAN	BOT. CHAN	BOT. UCHAN	TOP LCHAN	TOP IOLA	TOP MH	BOTT MH
KS211343208E	HADEN A #1	1075.0	1080.0	1577	1694	1600	1603	1566	-	-
KS022043208E	THOMPSON #2	1420.0	NA	1926	2005	1962	1963	1920	-	-
KS411183208E	ELMORE # 10	-	NA	655	753	679	682	652	-	-
KS143103207E	#6 OVERMAN	1377.0	NA	2074	2160	2080	2082	2072	-	-
KS224213207E	GIROD # 1	1323.0	1328.0	2028	2112	2032	2033	2024	-	-
KS142053206E	LAWSON # 1	1338.0	1343.0	2275	2339	2294	2298	-	-	-
KS003133205E	# 2 SCHOFIELD	1293.0	1298.0	2308	2415	2325	2328	-	-	-
KS112133205E	PAUL A MILLER #1	1294.0	1299.5	2270	2389	2284	2284	-	-	-
KS321333205E	RADCLIFF-SNYDER #5	1252.0	1257.0	2360	2460	2378	2380	-	-	-
KS012223204E	J W DIEBENS #12	1195.0	1200.0	2296	2409	2339	2342	-	-	-
KS332153204E	STATE #1	1185.0	1190.0	2307	2417	2334	2337	2304	-	-
KS344023203E	IMA CRAIG #1	1185.0	1190.0	2453	2539	2456	2459	2440	-	-
KS314093203E	CURTIS-WILSON #1	1172.0	1177.0	2492	2578	2502	2503	2486	-	-
KS314363202E	#1 DONLEY A	1130.0	1140.0	2602	2678	2625	2626	-	-	-
KS344273202E	# 1 MILLER LIZIE	1175.0	1180.0	2706	2789	2744	2745	2704	-	-
KS000193316E	WALLACE # 1-19	-	NA	84	186	140	143	-	-	-
KS241113315E	WITT #2	-	NA	-	125	86	87	-	-	-
KS422033315E	CLARKSON #1	-	-	47	116	-	-	-	64	68
KS422033315E	CLARKSON #2	-	-	54	126	-	-	-	73	77
KS222063315E	GRUVER #20	-	NA	157	277	237	239	150	-	-
KS213193315E	BUTLER #1	837.0	NA	72	193	148	150	68	-	-
KS002013314E	DARBY # 3-A	-	NA	156	347	242	244	150	-	-
KS442353314E	WILEY SWD #1	-	NA	212	322	280	282	-	-	-
KS421253313E	HEY 1- 21- 25	847.0	863.0	310	460	404	407	305	-	-
KS002143301E	OAK RIDGE RA #3A	934.0	NA	507	590	559	560	504	-	-
KS432203312E	POWERS # 11	-	NA	563	655	589	591	560	-	-
KS214073311E	T- BONE # 9	-	NA	1120	1218	1154	1155	-	-	-
KS000113310E	YORKE #2	-	-	NT	1007	972	974	-	-	-
KS114023310E	EGGEN #17	1020.5	NA	1016	1166	1072	1074	1010	-	-
KS023143309E	KELLY #23-14	1106.0	1109.0	1341	1460	1400	1402	1322	-	-
KS004053309E	GOODE #3	1051.0	1056.0	1178	1333	1244	1246	1174	-	-
KS442253308E	HOLROYD #1	1014.0	1019.0	-	1560	1484	1488	-	-	-
KS331213308E	M D MILLS #1	1235.0	1240.0	1830	1984	1929	1930	1822	-	-
KS432083308E	JAAX #1	1033.0	1038.0	1635	1770	1728	1730	1626	-	-
KS332063307E	RADCLIFF #1	1304.0	1308.0	2099	2236	2184	2185	2094	-	-
KS421363306E	DAVID # 1	1179.0	1184.0	1927	2046	1995	1996	1918	-	-
KS322183306E	PRIEST # 2-B	1307.0	1312.0	2324	2422	2380	2382	-	-	-
KS023073306E	PRIEST #1	1284.0	1291.0	2310	2416	2374	2375	-	-	-
KS012353305E	BROWN #1	1257.0	1262.0	2350	2458	2383	2384	-	-	-

Table 1- continued.

WELL CODE	WELL NAME	GL ELEV.	KB ELEV.	TOP CHAN	BOT. CHAN	BOT. UCHAN	TOP LCHAN	TOP IOLA	TOP MH	BOTT MH
KS021143305E	JARVIS #3	1191.0	1196.0	2290	2380	2326	2327	-	-	-
KS221133304E	MC COLLUM #1	1117.0	1124.0	2359	2440	2398	2400	-	-	-
KS004233304E	#1 BIRDZELL	1095.0	1100.0	2360	2458	2412	2414	2357	-	-
KS234143303E	BERRIE #1	1163.0	1170.0	2620	2704	2670	2670	2616	-	-
KS112333303E	AUMANN #3	1114.0	NA	2628	2749	2664	2664	2623	-	-
KS421173416E	HALL #2	887.0	NA	-	65	-	-	-	-	-
KS000083416E	DUNCAN # 1-8	-	NA	-	117	-	-	-	-	-
KS003253415E	MUELLER # 1-B	747.0	NA	-	17	-	-	-	-	-
KS000243415E	GILLMAN DISPOSAL #1	-	NA	-	92	-	-	-	-	-
KS414013415E	BURROWS #8	-	NA	-	135	-	-	-	-	-
KS113353414E	RUSSELL #3	-	NA	184	326	287	288	178	-	-
KS112193414E	POWELL # P-1	-	NA	314	443	400	401	309	-	-
KS002073414E	DALBY #1-A	792.0	NA	196	378	292	294	190	-	-
KS003083413E	THORNE #3 DISPOSAL	-	NA	330	490	420	422	322	-	-
KS141063413E	W MOORE #25	848-98?	NA	568	685	622	624	-	-	-
KS211063413E	MOORE #1 SWD	1002.0	NA	687	782	725	727	683	-	-
KS141123412E	LEONARD-RISING #2	-	NA	410	554	474	476	-	-	-
KS333063412E	PADGETT #4	-	NA	591	734	668	669	587	-	-
KS441013411E	SMART # G-3	810.0	NA	609	735	702	704	606	-	-
KS334133410E	WHITWORTH #1	910.0	915.0	935	1051	1022	1024	932	-	-
KS004333410E	CHARLIE-KELLY # 1	1004.2	NA	1087	1179	1157	1159	1084	-	-
KS041223409E	LAYTON # 1	934.0	NA	1216	1318	1285	1288	1212	-	-
KS333103408E	LEEDY # 4	-	-	1502	1598	1557	1558	1496	-	-
KS331093408E	SEAMSTER #1 WASHDOWN	989.0	994.0	1574	1677	1632	1634	1568	-	-
KS242183408E	ECHOLS #1	1075.0	1080.0	1750	1915	1862	1864	-	-	-
KS244323407E	SNYDER #1	1234.0	1239.0	2085	2206	2172	2173	2078	-	-
KS032033405E	ALBRIGHT # 6	1135.0	1140.0	2254	2384	2324	2326	2248	-	-
KS121273405E	WILLIAMSON C-1	1200.0	1205.0	2298	2443	2353	2354	2294	-	-
KS013213405E	HICKMAN D #1	1244.0	1249.0	2407	2556	2478	2479	2404	-	-
KS121143404E	CRAIN #7	1216.0	1221.0	2474	2580	-	-	-	-	-
KS001093404E	FRANK BOSSI #12	1187.0	1192.0	2521	2640	2563	2564	2516	-	-
KS244073404E	GOFF #1	1143.0	1148.0	2489	2617	-	-	2482	-	-
KS422323403E	BAIRD-BRENNAN # 21	1140.0	1145.0	2660	2767	-	-	-	-	-
KS214293403E	BAIRD # 29-1	1129.0	1134.0	2644	2760	-	-	2640	-	-
KS231163401E	HUNT #3	1182.0	1188.0	3052	3134	3084	3084	3024	-	-
KS244103515E	FIELDES #4 SWD	840.0	NA	-	150	28	28	-	-	-
KS000043515E	COLLINS #2-C	840.0	840.5	-	198	-	87	-	-	-
KS024123514E	ROBINSON #1	-	NA	212	366	284	286	200	-	-
KS213033514E	ELSEHEIMER #15	-	NA	3169	3334	3254	3256	3164	-	-

Table 1- continued.

WELL CODE	WELL NAME	GL ELEV.	KB ELEV.	TOP CHAN	BOT. CHAN	BOT. UCHAN	TOP LCHAN	TOP IOLA	TOP MH	BOTT MH
KS224173512E	BURCH #103	793.0	NA	544	692	-	-	540	-	-
KS003133511E	CLINGAN #2	-	NA	770	900	812	812	764	-	-
KS412133510E	SWEENEY #1	810.0	NA	759	880	791	792	756	-	-
KS421143510E	LORENZ #1	-	NA	827	950	850	852	823	-	-
KS142113510E	KEENY #1	897.0	NA	925	1022	942	942	914	-	-
KS111013509E	WINEGER #2	804.0	809.5	-	1096	-	-	-	-	-
KS222173507E	DOROTHY #9	1204.0	1209.0	-	2146	2054	2056	-	-	-
KS331153505E	WARREN B #1	1227.0	1234.0	2365	2460	2382	2382	2365	-	-
KS341043504E	BOSSI #1	1066.0	1071.0	2382	2552	2436	2438	2376	-	-
KS011033503E	BRANDENBURG A #3	1147.0	1152.0	2613	2769	-	-	2610	-	-
KS241183503E	VICKERY #1	1183.0	1187.0	2726	2912	2744	2744	2720	-	-
KS332103503E	CAPITT #1 MCCLASKEY	1169.5	1175.0	2784	2903	2791	2791	2764	-	-
KS424083502E	KEMP #3	1135.0	1140.0	2712	2856	2737	2738	2704	-	-
OKLAHOMA		-	-	-	-	-	-	-	-	-
ON222242913E	LOWERY UNIT #6	790.0	NA	no top	103	-	-	-	-	-
ON344362910E	HUNTER #1-A	797.0	NA	480	583	-	-	-	-	-
ONOOO162910E	CARTER #1	-	-	583	653	-	-	-	-	-
ON432162909E	MOORE A #1	958.0	NA	1106	1216	1131	1132	1100	-	-
ON241312909E	HUTCHINSON A #1	1002.0	1008.0	1180	1338	1260	1262	1176	-	-
ON002222908E	OK LAND & CATTLE CO.	971.0	NA	1299	1393	1316	1317	1295	-	-
ON032142905E	STATE LINE #1-A	1226.0	NA	2034	2183	2088	2090	-	-	-
ON112212903E	LOVE #1	1136.0	1143.0	2418	2525	2466	2468	2393	-	-
ON444122813E	LUCAS #1	850.0	NA	56	165	65	67	50	-	-
ON001082812E	#2 FULLENDORE	713.0	NA	246	366	304	304	-	-	-
ON423282811E	MOORE #6	830.0	NA	494	650	524	524	-	-	-
ON421032810E	#1 MARY H	837.0	NA	522	701	544	546	-	-	-
ON222342809E	CONOCO G #1-A	1008.7	NA	1028	1200	1042	1042	1023	-	-
ON423052713E	GARRET NEIL	715.0	715.0	no top	38	-	-	-	-	-
ON321332709E	MANNING #1	977.0	982.0	1165	1273	1188	1190	1157	-	-
ON111072709E	BARNARD #10	1103.0	1108.0	1298	1426	1338	1338	-	-	-
ON434322708E	DRUMMOND # 1-C	1045.0	NA	1482	1597	1524	1524	-	-	-
ON334342706E	BIGHEART #16W	1040.0	NA	1914	2013	1962	1962	1910	-	-
ON034292702E	EDWARDS NCT 2 #1	1033.0	1034.5	2769	2842	2797	2799	2766	-	-
ON431312610E	LOOKOUT #6	894.2	899.2	870	962	-	-	-	-	-
ON231222609E	ELSIE #1	1009.0	1017.0	1080	1236	1160	1160	1064	-	-
ON001362608E	MULLENDORE #3	919.0	NA	1135	1290	1188	1188	-	-	-
ON422172608E	WHITEHORN #1-17	944.0	950.0	1347	1486	1399	1401	-	-	-
ON001352607E	AB I-35 AA DRUMMOND	1036.0	NA	1605	1768	1680	1682	-	-	-
ON011182511E	LATE # 8	929.0	934.0	848	921	-	-	-	-	-

Table 1- continued.

WELL CODE	WELL NAME	GL ELEV.	KB ELEV.	TOP CHAN	BOT. CHAN	BOT. UCHAN	TOP LCHAN	TOP IOLA	TOP MH	BOTT MH
ON112032509E	INDIAN VILLAGE	829.0	NA	793	914	-	-	-	-	-
ON442102508E	RODEO ANTICLINE #2-1	1013.5	1018.0	1216	1335	-	-	1204	-	-
ON333162508E	OXLEY 1-A	914.0	917.0	1200	1360	-	-	-	-	-
ON321222506E	FAIRFAX UNIT	1064.0	NA	1953	2048	-	-	1940	-	-
ON324042506E	FLETCHER #9	1005.5	1012.0	1883	1981	-	-	-	-	-
ON214032505E	MATHIS UNIT TRACT #3	990.0	1001.0	2125	2216	-	-	-	-	-
ON312212505E	MASHBURN #1	979.0	NA	2132	2218	2158	2160	2116	-	-
ON444162411E	#5	770.0	NA	358	417	-	-	-	-	-
ON004092411E	LOT 292- #3	821.0	NA	414	474	446	447	-	-	-
ON233042411E	BIGHEART #8-6	887.0	890.0	547	612	576	577	-	-	-
ON333092410E	MCCORMICK #1-9	820.0	NA	721	819	784	785	-	-	-
ON242312410E	GEORGIA #2	914.0	919.0	947	1003	983	983	-	-	-
ON113032409E	#B A COTTONMOUTH	931.0	NA	903	976	946	946	-	-	-
ON013212409E	FIELDS #7	950.0	989.2	1111	1180	-	-	-	-	-
ON333352408E	LEASE 3 WELL #1-A	846.0	NA	1122	1165	1136	1137	1055	-	-
ON023232408E	DANIELS BLOCK SW	944.0	951.0	1113	1230	1206	1208	-	-	-
ON001342407E	DRUMMOND B TRACT 30	1010.0	NA	1482	1598	-	-	-	-	-

Table 2. Thicknesses and sand counts of the Chanute Shale members.

WELL CODE	WELL NAME	THK. CHAN.	THK. T. COAL	THK. U. CHAN.	THK. L. CHAN.	SAND C. G.	SAND NOXIE	THK. IOLA	THK. M. H.
KS002201624E	SUNLEY #S-2	12	-	8	4	-	-	14	-
KS000311624E	A-2	-	-	-	-	-	-	-	-
KS000361623E	#1	8	-	6	2	-	-	15	-
KS224311622E	#16	36	-	-	-	-	-	22	15
KS042311622E	LOOMER #A-13	34	-	20	14	-	6B	19	-
KS042261621E	CUMMINGS #S-20	31	-	16	15	2	10	21	-
KS442251620E	W. G. BROERS	45	-	23	22	-	-	24	-
KS001021618E	MERLIN BARTON #1	8	-	4	4	-	-	29	-
KS004281618E	PARKS #3	18	2	10	6	5	3	29	-
KS421231616E	WOODWARD #1	14	-	4	10	-	-	42	-
KS000061724E	# 8	7	-	-	-	-	-	16	-
KS000061724E	# 7	12	-	-	-	-	-	14	-
KS002111724E	MILLS #S-6	17	-	11	6	1	0	19	-
KS214121724E	RIGNEY #12	15	-	9	6	6	0	28	-
KS000061724E	#9	10	-	6	4	-	-	15	-
KS211201723E	SCHUKNECHT #2	7	-	3	4	-	-	20	-
KS042061722E	HARBISON A-4	28	2	18	8	-	0	20	8
KS001061722E	HARBINSON #A-5	35	2	17	16	-	4	20	6
KS113041722E	PURDUE #40	24	-	19	5	-	-	19	-
KS044031722E	SHOFNER #A-1	31	-	24	7	4	0	18	3
KS021231722E	ROHRER # A-1	12	-	10	2	-	-	-	-
KS333011722E	PRICE #17	36	-	26	10	8	4	17	-
KS002161721E	CAYLOR #101-31A	29	-	18	11	11	9	-	-
KS001201721E	HOBBS #4	23	-	10	13	6	4	25	-
KS121151721E	SPRINGER #L-20	28	-	16	12	2	6	20	-
KS044141721E	BULLOU #1	-	-	-	-	-	-	-	-

Table 2- continued.

WELL CODE	WELL NAME	THK. CHAN.	THK. T. COAL	THK. U. CHAN.	THK. L. CHAN.	SAND C. G.	SAND NOXIE	THK. IOLA	THK. M. H.
KS012151721E	# 079	33	1	20	12	0	0	19	-
KS000251720E	ANDERSON # 4-A	24	-	14	10	2	5	20	-
KS342121720E	RAY EVANS NORTH #9	20	-	16	4	-	-	21	-
KS034051717E	BRIGGS ALTEX #1	21	1	12	8	0	6	32	-
KS002011821E	RITCH #6	23	-	-	-	-	-	-	-
KS003041821E	GILCREST #7	28	-	-	-	-	-	21	-
KS000171821E	# 24A-17	21	-	-	-	-	-	19	-
KS114131820E	J. E. BURKDOLL #2	32	2	16	14	0	12	20	-
KS000121820E	BURKDOLL #24	-	-	-	17	-	6	-	-
KS011061817E	GREER #1	20	-	15	5	3	5	31	-
KS444321812E	T. ANDERSON #1	12	-	-	-	-	-	38	-
KS013241921E	F.B. HUETTENMUELLER #1	8	-	-	-	-	-	31	-
KS032231921E	MILLER #1	17	1	11	5	-	0	26	6
KS031111918E	PIERSOL #1	14	-	-	-	-	-	36	-
KS112341917E	JAMES #1	13	-	-	-	-	-	37	-
KS221051915E	#1 P. GEORGE	26	1	19	6	0	6	44	-
KS331061915E	W. JONES #1	18	-	-	-	-	-	46	-
KS112341914E	JEFFERS #1	13	-	-	-	-	-	33	-
KS331271914E	DOTSON #1	8	-	-	-	-	-	33	-
KS114301914E	H. SMITH #1	6	-	-	-	-	-	34	-
KS334241913E	SLEAD #1	13	1	10	2	5	2	-	-
KS024341913E	OWENS #1	20	2	12	6	9	7	16	-
KS114271913E	DOTY #1	31	-	29	2	14	0	40	-
KS423281913E	ST. BONNETT #1	33	2	27	4	14	1	30	-
KS212261912E	CARPENTER #1	20	1	16	3	1	3	44	-
KS232021912E	VAN GUNDY #1	19	-	-	-	-	-	34	-

Table 2- continued.

WELL CODE	WELL NAME	THK. CHAN.	THK. T. COAL	THK. U. CHAN.	THK. L. CHAN.	SAND C. G.	SAND NOXIE	THK. IOLA	THK. M. H.
KS314041912E	DAVIS #1	19	-	-	-	-	-	39	-
KS114231910E	PENNY #1	12	-	11	1	3	0	43	-
KS111201908E	RETTINGER #1	15	-	-	-	-	-	28	-
KS311201906E	#1 OPEL MILLER	7	-	-	-	-	-	35	-
KS000162022E	FEVERBORN #1	-	-	-	-	-	-	-	-
KS000162022E	FEVERBORN #2	-	-	-	-	-	-	-	-
KS001252019E	WHITE #4	29	-	17	12	0	8	29	-
KS144082019E	GATES # 22D-A	46	2	38	6	0	7	6	-
KS442192017E	KITCHENS #1	19	-	16	3	-	-	42	-
KS334032015E	NUSZ #1	24	-	-	-	-	-	80	-
KS114332015E	PHILLIPS #1	16	-	-	-	-	-	58	-
KS031252014E	WARREN #3	17	2	13	2	0	2	33	-
KS441162014E	BUSBOOM #1	12	-	-	-	-	-	36	-
KS331092014E	HODGES #1	13	-	-	-	-	-	26	-
KS323362013E	MCGREW #1	13	-	-	-	-	-	44	-
KS224012013E	WOODS #1	2	-	-	-	-	-	34	-
KS132272013E	GILLIGAN #1	13	-	-	-	-	-	36	-
KS024172012E	VAN SICKLE #1	12	1	8	3	0	0	47	-
KS224082012E	R. CIBSON #1	8	2	3	3	0	0	41	-
KS014102010E	REES A-1	14	-	10	4	-	-	42	-
KS331322010E	REES #4	5	-	-	-	-	-	55	-
KS111202010E	MILLER #2	17	-	-	-	-	-	-	-
KS014182010E	COUGHLEN B #1	18	-	-	-	-	-	36	-
KS443302010E	DAVIS #1	10	-	-	-	-	-	40	-
KS032172006E	L. M. WANER #1	4	-	-	-	-	-	29	-
KS334362008E	NORTON #1	13	-	-	-	-	-	-	-

Table 2- continued.

WELL CODE	WELL NAME	THK. CHAN.	THK. T. COAL	THK. U. CHAN.	THK. L. CHAN.	SAND C. G.	SAND NOXIE	THK. IOLA	THK. M. H.
KS023152005E	KAUFMAN #1	7	-	-	-	-	-	30	-
KS001042121E	SCHEMERHORN # S-11	49	6	38	11	-	0	-	-
KS100042121E	SCHEMERHORN # S-8	49	6	38	11	-	0	-	7
KS021082121E	GALDEMAN # 0-11	52	-	37	15	-	0	28	6
KS311142120E	ODAFFER # N-5	46	-	29	17	-	0	29	8
KS000152120E	WEIS #12	30	2	27	1	0	6	35	-
KS000062120E	MELCHER A # 2	31	2	20	11	14	0	38	-
KS221162120E	WEST HUNLEY #18 (R-30)	38	2	21	17	10	0	33	-
KS003032119E		34	-	-	-	-	-	36	8
KS221242117E	DRUM #1	22	-	-	-	-	-	43	6
KS113112116E	DALBY #1	18	-	-	-	-	-	50	-
KS111112115E	REINKER #1	9	1	6	2	-	-	50	-
KS334332115E	GRIFFIN #1	16	-	-	-	-	-	76	-
KS331212115E	NOEL #1	6	-	-	-	-	-	60	-
KS122162115E	NEWKIRK #1	13	-	-	-	-	-	52	-
KS331292115E	WARD #1	6	-	-	-	-	-	63	-
KS314312115E	ALLEN #1	7	-	-	-	-	-	46	-
KS134112114E	HOSS-GUPTON #3	9	-	-	-	-	-	50	-
KS131342114E	PAXSON #1	12	-	-	-	-	-	51	-
KS441222114E	HARRINGTON # 1-B	11	-	-	-	-	-	47	-
KS231102114E	KRAUSE #1	-	-	-	-	-	-	44	-
KS331032114E	THEOBALD #1	15	-	-	-	-	-	17	-
KS444162114E	BOWMAN #1	10	-	-	-	-	-	50	-
KS423312114E	KAUFMAN #1	10	-	-	-	-	-	44	-
KS441312114E	MERRITT #1	6	-	-	-	-	-	41	-
KS142312114E	TRUELOVE #1	16	1	10	6	-	-	48	-

Table 2- continued.

WELL CODE	WELL NAME	THK. CHAN.	THK. T. COAL	THK. U. CHAN.	THK. L. CHAN.	SAND C. G.	SAND NOXIE	THK. IOLA	THK. M. H.
KS123192114E	BEYER #4	14	1	10	4	-	-	58	-
KS444362113E	BEYER #1	7	-	-	-	-	-	55	-
KS441252113E	KNAPP #1	11	-	-	-	-	-	52	-
KS333242113E	KNAPP #1	7	-	-	-	-	-	50	-
KS332012113E	#1 WILSON A	12	-	-	-	-	-	46	-
KS132352113E	BASHAW BIRK #2	7	-	-	-	-	-	56	-
KS122262113E	JAMIESON #1	10	-	-	-	-	-	21	-
KS422232113E	GASCHE #1	7	-	-	-	-	-	51	-
KS142142113E	O'MARRA #2	19	-	-	-	-	-	53	-
KS144112113E	WILSON #1	9	-	-	-	-	-	47	-
KS111102113E	JONES #1	22	-	-	-	-	-	48	-
KS224202113E	GARDNER #1	14	-	-	-	-	-	55	-
KS221032112E	GRIEDER #1	42	-	-	-	-	-	47	-
KS022322112E	NUESSEN A-2	9	-	-	-	-	-	18	-
KS211252111E	MATILE #1	11	-	-	-	-	-	36	-
KS111082110E	RALPH & DARREL JONES #1-A	7	-	-	-	-	-	45	-
KS034182110E	KAPP #2	9	-	-	-	-	-	50	-
KS443362109E	ATYEO #2-G	7	-	-	-	-	-	20	-
KS442292218E	WELDIN #2	44	1	18	25	19	22	43	-
KS343292217E	PARMELLY #5	19	2	11	6	0	3	57	-
KS013292217E	PARMELLY #6	18	-	-	-	-	-	53	-
KS221112216E	FISCHER #1	16	-	9	7	0	5	60	-
KS013222216E	EDWARDS/HEIRS #5	11	-	8	3	7	0	42	-
KS004282226E	REMER #5	13	-	10	3	7	1	46	-
KS442282216E	FLAKE #6	16	1	10	5	8	0	54	-
KS124212216E	GLEUE #8	12	1	8	3	7	0	50	-

Table 2- continued.

WELL CODE	WELL NAME	THK. CHAN.	THK. T. COAL	THK. U. CHAN.	THK. L. CHAN.	SAND C. G.	SAND NOXIE	THK. IOLA	THK. M. H.
KS242212216E	J. WRIGHT #5	12	-	8	4	8	0	50	-
KS113312216E	SUTHERLAND #3	27	1	16	10	4	6	47	-
KS003302216E	MINNIE GRAY #2	27	1	9	17	0	4	45	-
KS142192216E	BIRBECK #2	21	1	12	8	6	6	45	-
KS444362216E	MURRAY #1	27	-	17	10	0	9	47	-
KS442252215E	SMITH #1	22	-	5	17	0	6	54	-
KS224132215E	WUEFERLE #1	18	1	11	6	3	4	49	-
KS242142215E	GOULDIE-RICH #1	11	-	-	-	-	-	51	-
KS441292215E	BORN #1	13	-	-	-	-	-	52	-
KS123272214E	KNAPP #1	20	-	-	-	-	-	62	-
KS133102214E	MERRITT #1	6	-	-	-	-	-	54	-
KS114262213E	BANWART #1	13	-	-	-	-	-	57	-
KS233112213E	ISCH #1	8	-	-	-	-	-	62	-
KS113212213E	ELMER OTT #1	13	-	-	-	-	-	50	-
KS002322211E	SCHANKIE #1	7	-	-	-	-	-	15	-
KS021102210E	PIXLEE # 7	4	-	-	-	-	-	31	-
KS333172210E	BROWNNING # 1	2	-	-	-	-	-	44	-
KS441162203E	LITTON # 1	13	-	-	-	-	-	33	-
KS434032321E	MCGEE # 1	-	-	-	-	-	-	-	-
KS233042321E	GADDIS #7	-	-	-	-	-	-	-	-
KS331042321E	MCCASLIN-V.B #116	35	-	-	-	-	-	-	-
KS311042321E	GADDIS #24	-	-	-	-	-	-	-	-
KS242052321E	MCCASLIN-V.B. #105	-	-	-	-	-	-	-	-
KS232142319E	BRIGGS TRACT 1 #3	34	-	-	-	-	-	40	-
KS142272318E	CARPENTER #1	24	-	-	-	-	-	46	-
KS141292318E	MCGHEE #1	5	-	-	-	-	-	62	-

Table 2- continued.

WELL CODE	WELL NAME	THK. CHAN.	THK. T. COAL	THK. U. CHAN.	THK. L. CHAN.	SAND C. G.	SAND NOXIE	THK. IOLA	THK. M. H.
KS141062318E	KELLY #5	36	-	-	-	-	-	48	-
KS044122316E	NELSON WEBB # B-4	22	-	19	3	2	0	56	-
KS132132316E	MARTZ #4	13	-	9	4	-	-	49	-
KS332132316E	MARTZ #3	18	2	13	3	6	1	46	-
KS002132316E	JERRY MURRAY #8	25	1	17	7	7	0	55	12
KS343122316E	MEATS #7	20	1^	16	3	0	0	23	-
KS003122316E	S. MEATS #6	21	1	15	5	0	0	12	-
KS001012316E	SUNBEAM #6	41	-	-	-	-	-	-	-
KS144142316E	CHARLES JONES #4	31	-	-	-	-	-	34	-
KS131142316E	FREEMAN #1	19	1	15	3	0	0	53	-
KS413112316E	ROBERT BADER #1	14	-	-	-	0	0	52	-
KS434102316E	JOAN FREEMAN #2	13	-	9	4	-	-	36	-
KS002332316E	FULLER #15	3	-	-	-	-	-	-	-
KS033112316E	ALICE CROTTS #2	12	-	-	-	0	0	61	-
KS001202316E	DEARINGER#1	27	-	-	-	-	-	26	-
KS121062316E	WRIGHT #2	29	-	-	-	-	-	58	-
KS441092315E	EVANS A #2	18	-	15	3	3	0	54	-
KS001192315E	TEBBINS #1	12	-	-	-	-	-	58	-
KS331092314E	BAHR C #1	6	-	-	-	-	-	42	-
KS044012313E	CROTTY #1	11	-	-	-	-	-	64	-
KS122232313E	CHRIS BAHR #21	5	-	-	-	-	-	58	-
KS000092312E	LOCKHARD #1	6	-	-	-	-	-	247	-
KS000202312E	STAUFFER #1	6	-	-	-	-	-	48	-
KS002032311E	CURRY #2	3	-	-	-	-	-	21	-
KS314162311E	REDDING #1	5	-	-	-	-	-	20	-
KS113132310E	BURKETT # B-30	5	-	-	-	-	-	11	-

Table 2- continued.

WELL CODE	WELL NAME	THK. CHAN.	THK. T. COAL	THK. U. CHAN.	THK. L. CHAN.	SAND C. G.	SAND NOXIE	THK. IOLA	THK. M. H.
KS131192310E	ZIMMERMAN #6	16	-	-	-	-	-	33	-
KS131302306E	BUSENITZ #3	6	-	-	-	-	-	5	-
KS443342305E	WYSS A #1	5	-	-	-	-	-	14	-
KS241352420E	APT. #116	-	-	-	35	-	-	-	-
KS132342420E	WINSLOW # 128	-	-	-	-	-	-	-	-
KS114332420E	TALBOTT #106	29	-	23	6	17	2	-	-
KS313022418E	ECKDALL #5	32	1	23	8	2	4	-	-
KS004022416E	ALEXANDER # 0-35	55	1	51	3	5	2	53	-
KS332332415E	#1 KNAPP	60	-	-	-	-	-	54	-
KS134172412E	MARLIN #1	33	-	-	-	-	-	26	-
KS231082411E	J.L. WILLIAMS #1	16	2	0	14	5	0	17	-
KS313342409E	MARSHALL #3	5	-	-	-	-	-	9	-
KS001112402E	ULMER B # 2	6	-	-	-	-	-	36	-
KS111072521E	BARNETT #10	-	-	-	-	-	-	-	-
KS442332520E	SAGER #103	-	-	-	-	-	-	-	-
KS343142519E	SCOTT # B-1	-	-	-	-	-	-	-	-
KS332282519E	FRONK #2	18	-	-	-	-	-	-	-
KS324232517E	WILLIS #12	32	-	29	3	9	0	42	-
KS132242516E	DRAIN #1	38	1	33	4	9	0	56	-
KS444062516E	EARL DAVIDSON #1	39	1	39	0	14	0	46	-
KS231122514E	J TAYLOR #2	38	-	33	5	7	3	61	-
KS121072512E	HUBER #1	13	-	-	-	-	-	11	-
KS423252504E	MITCHELL #5	2	-	-	-	-	-	24	-
KS423332503E	CLEARWATER # 6	4	-	-	-	-	-	24	-
KS221012510E	HAWTHORNE #1	15	-	-	-	-	-	24	-
KS331252617E	OSBORN #1	52	1	35	16	17	6	44	-

Table 2- continued.

WELL CODE	WELL NAME	THK. CHAN.	THK. T. COAL	THK. U. CHAN.	THK. L. CHAN.	SAND C. G.	SAND NOXIE	THK. IOLA	THK. M. H.
KS000222617E	DIETRICH D #14	35	2	15	18	0	12	-	-
KS223162616E	YOUNG A #15	37	-	-	-	-	-	57	-
KS142192615E	LAUBER B #7	38	-	-	-	-	-	55	-
KS242132614E	SAUBERS #6	33	-	-	-	-	-	-	-
KS142262613E	KERNS #1	52	-	-	-	-	-	50	-
KS021362612E	SHOBE #21-36	17	-	-	-	-	-	57	-
KS441112612E	HODGSON #1	11	-	-	-	-	-	21	-
KS321082612E	BOONE #1	13	-	-	-	-	-	11	-
KS332302612E	DORA RUSSEL #1	10	-	-	-	-	-	15	-
KS214082611E	EASTMAN #1	15	-	-	-	-	-	9	-
KS411182610E	SHINKLE #2	22	-	-	-	-	-	6	-
KS333072610E	MONHART #10	8	2	5	1	4	0	11	-
KS144062610E	DOUGHERTY #4	4	-	-	-	-	-	11	-
KS114132609E	LIFE # H	11	-	-	-	-	-	11	-
KS144232609E	MOON #4	15	-	-	-	-	-	9	-
KS001332609E	KTW FEE E #1	12	-	-	-	-	-	8	-
KS341102608E	RICE #7	8	-	-	-	-	-	11	-
KS411292608E	DRUMM #19	4	-	-	-	-	-	7	-
KS111262607E	MOORE "A"	18	-	-	-	-	-	34	-
KS432222607E	SIMON # 2-A	9	-	-	-	-	-	5	-
KS003282606E	MCALLISTER # 1	20	1^	5	14	1	14	5	-
KS142132605E	TAGUE #4	12	-	-	-	-	-	5	-
KS414352605E	BISAGNO #4	16	-	-	-	-	-	5	-
KS244262605E	SLUSS B-1	17	-	-	-	-	-	7	-
KS341032605E	WILKINSON #1	17	-	-	-	-	-	6	-
KS323042605E	FINNEY (2) # 4	13	-	-	-	-	-	6	-

Table 2- continued.

WELL CODE	WELL NAME	THK. CHAN.	THK. T. COAL	THK. U. CHAN.	THK. L. CHAN.	SAND C. G.	SAND NOXIE	THK. IOLA	THK. M. H.
KS002142715E	PAYNE #9	74	1	62	11	4	4	48	2
KS314202714E	MARR #S-2	77	1	58	18	15	0	46	3
KS034292713E	ADAMS #1	49	-	-	-	-	-	54	5
KS230332713E	FEE # 1-33	29	-	-	-	-	-	58	-
KS000312711E	CORA FRENCH #2	28	-	-	-	-	-	13	-
KS013072711E	PETERSON #2	21	-	-	-	-	-	10	-
KS043062710E	THOMAS #26 C	3	-	-	-	-	-	13	-
KS341252708E	TEMPLE #4	8	-	-	-	-	-	8	-
KS424132708E	WIEDEMANN TRUST A #1	1	-	-	-	-	-	12	-
KS313202707E	HUMMEL #1	2	-	-	-	-	-	6	-
KS022352706E	LEWIS A #16	11	-	-	-	-	-	11	-
KS221332706E	SIMMONS # 3-B	13	-	-	-	-	-	8	-
KS023282706E	SIMMONS # 2-A	4	-	-	-	-	-	8	-
KS000272705E	HAVERHILL UNIT # 35	-	-	-	-	-	-	5	-
KS242152705E	CHINN # 1	-	-	-	-	-	-	6	-
KS213082706E	MAX MAIN #1	11	-	-	-	-	-	8	-
KS241352704E	#1 HART	24	-	-	-	-	-	-	-
KS111162817E	UHREN # 4-A	26	-	-	-	-	-	-	-
KS111232816E	STORDEVANT #1-23	20	-	-	-	-	-	-	-
KS001192816E	CRITES #7	28	1	15	12	13	0	11	-
KS114242825E	BOCO #3	16	-	-	-	-	-	29	-
KS431342813E	OAKS #34-E-10-SE	59	1	38	20	13	4	30	-
KS000032813E	FEE #2-3	32	-	32	0	14	0	22	-
KS444262812E	MCGINNIS #1	46	1	34	11	11	0	53	-
KS314242808E	YOUNGMYER PALMER #B-2	40	-	36	4	11	0	18	-
KS221022807E	BOLUNGER # 1	-	-	-	-	-	-	6	-

Table 2- continued.

WELL CODE	WELL NAME	THK. CHAN.	THK. T. COAL	THK. U. CHAN.	THK. L. CHAN.	SAND C. G.	SAND NOXIE	THK. IOLA	THK. M. H.
KS332032807E	MANKA # 1	10	-	-	-	-	-	8	-
KS441352806E	KNOLLENBERG # 1	20	-	8	12	2	11	6	-
KS222152806E	DUNN # 1	13	-	1	12	3	10	7	-
KS232211806E	WALTERS # 1	12	-	-	-	-	-	13	-
KS242092806E	LINDGREN # 4	13	-	-	-	-	-	11	-
KS004052806E	TABBING #2	14	-	-	-	-	-	9	-
KS000012805E	WEAVER TRUST #1	23	-	-	-	-	-	7	-
KS311362917E	MCCOY #8	56	1	22	33	9	0	3	-
KS341302917E	A. ERBE #2	54	-	19	35	7	0	-	-
KS332012914E	DOCIA BATES #17	33	-	10	23	0	5	23	-
KS022232913E	RUSSEL B-1	56	-	18	38	4	20	16	-
KS000202913E	STOTS #2	34	-	12	22	0	15	19	-
KS314122912E	THOMAS #1	36	-	11	25	2	1	17	-
KS114173911E	KLING #1	39	-	5	34	0	16	16	-
KS031132910E	LAND # 12-13	18	-	-	-	-	-	-	-
KS421342910E	DUNKELBORGER #1	33	-	6	27	0	4	19	-
KS231342909E	PERKINS #3	41	-	5	36	0	20	14	-
KS000192908E	SHINN #21	34	-	7	27	0	19	3	-
KS214162906E	PRICE WATTS #2	35	2	11	22	1	16	13	-
KS011182905E	PERISHO UNIT #2	23	-	2	21	0	8	27	-
KS003292905E	POTTORF #3	37	-	11	26	0	16	14	-
KS334232904E	BLOOD #3	33	-	11	22	0	11	22	-
KS000022904E	BOULBY #1	42	1	12	29	6	21	22	-
KS123152902E	# 1 OLSON	51	-	26	25	11	20	23	-
KS243013017E	C. SMITH #6	-	-	-	-	-	-	-	-
KS311223017E	STEVE WHITE # 2	-	-	-	-	-	-	-	-

Table 2- continued.

WELL CODE	WELL NAME	THK. CHAN.	THK. T. COAL	THK. U. CHAN.	THK. L. CHAN.	SAND C. G.	SAND NOXIE	THK. IOLA	THK. M. H.
KS144303017E	LOFLIN # 1	18	-	-	-	-	-	6	-
KS421063017E	JOE NEWLAND #1	-	3	-	33	-	0	-	-
KS332263016E	DICKENS #2 N	-	-	-	-	-	-	-	-
KS000083015E	SHUGO #2	43	1	18	24	3	0	7	-
KS421333013E	HARKEY #1	75	2	32	41	7	12	3	-
KS131183013E	H. CANNON #1	60	1	14	45	0	12	5	-
KS444153012E	BELL#1	60	-	20	40	4	14	7	-
KS412353009E	BRADFORD SWD	50	1	15	34	6	20	5	-
KS324093009E	HYDE #1	37	2	9	26	0	10	25	-
KS112093009E	KYSER P #11	42	-	-	-	-	-	17	-
KS033253008E	SLEEPER # 14-25	45	-	-	-	-	-	4	-
KS443103008E	SLEEPER # 1-C	31	1	19	11	0	6	4	-
KS321123007E	LA FEICHE #1	41	1	20	22	0	17	3	-
KS342313006E	HENDERSON #1	17	-	-	-	-	-	4	-
KS111193006E	WAKEFIELD A #1	26	-	-	-	-	-	3	-
KS114333005E	STUBER # 1	27	1	7	19	2	10	-	-
KS332013004E	DRAKE 42 -628	14	-	-	-	-	-	2	-
KS244133004E	FUSCH # 1	23	-	-	-	-	-	3	-
KS312113004E	WILSON # 1	18	-	-	-	-	-	-	-
KS004233004E	MAGBY	13	-	-	-	-	-	-	-
KS000153004E	STELBAR # 1	17	-	-	-	-	-	-	-
KS423333004E	COBBLE #1	18	-	-	-	-	-	-	-
KS032243003E	MORTON #1	14	-	-	-	-	-	4	-
KS312103003E	GOYER # 1-A	18	-	-	-	-	-	2	-
KS441023003E	MUELLER #1	72	-	-	-	-	-	-	-
KS244243116E	GADDY#1	-	2	-	38	17	0	-	-

Table 2- continued.

WELL CODE	WELL NAME	THK. CHAN.	THK. T. COAL	THK. U. CHAN.	THK. L. CHAN.	SAND C. G.	SAND NOXIE	THK. IOLA	THK. M. H.
KS211303116E	MELVIN OLSON #1	51	2	19	30	6	0	6	-
KS113143115E	GORTON #1-14	52	2	6	44	0	0	9	-
KS000233113E	STATE #41	68	1	41	26	27	25	-	-
KS412173113E	TROMBOLD 31-17	70	3	25	42	12	19	-	-
KS143153111E	OSBORN #1	90	2	30	58	2	6	2	-
KS113103110E	KILL 1-A	70	1	27	42	9	25	2	-
KS322163109E	REEVES #1	72	1	17	54	0	22	3	-
KS314173109E	DEAN #1	78	2	36	40	22	26	4	-
KS233033108E	DENTON #9	66	-	-	-	-	-	6	-
KS124163108E	BANNON #1	61	1	26	34	7	12	4	-
KS223143107E	SMITH #1	62	2	25	35	6	15	3	-
KS113213105E	HAMMER # 4	22	-	-	-	-	-	12	-
KS034363105E	LEWIS # 1-C	49	2	16	31	0	13	6	-
KS113213105E	HAMMER #1	22	-	-	-	-	-	-	-
KS241203105E	SICKLES #1	25	-	11	14	5	8	5	-
KS213363104E	HOLT #5	78	-	-	-	-	-	12	-
KS344343215E	BREDENHOFT # 1	74	-	-	-	8	9	47	4
KS244343215E	BREDENHOFT # 2	70	-	-	-	0	5	63	5
KS142343215E	FERREL # 1	129	2	24	103	3	21	-	-
KS142343215E	FERREL # 2	-	3	-	89	-	13	-	-
KS142343215E	FERREL # 3	127	2	26	99	8	26	-	-
KS331323215E	THOMPSON#1	187	2	89	96	66	40	7	-
KS014063215E	CRANE-DAY #1	66	4	22	40	14	32	-	-
KS004363214E	SULLIVAN#2	110	2	69	39	11	23	7	-
KS211323214E	WILLIAM LINN #1	62	2	12	48	0	8	13	-
KS322263213E	SHELLEY #1	82	0.5	23	58.5	0	32	11	-

Table 2- continued.

WELL CODE	WELL NAME	THK. CHAN.	THK. T. COAL	THK. U. CHAN.	THK. L. CHAN.	SAND C. G.	SAND NOXIE	THK. IOLA	THK. M. H.
KS441063213E	WELCH #1	66	2	23	41	0	28	17	-
KS114133212E	KHEB #1	76	2	24	50	0.5	29	6	-
KS032143212E	OAK RIDGE RANCH #2	73	3	15	55	6	40	4	-
KS233043211E	GARVIN #3	137	1	63	73	8	47	6	-
KS232313211E	FLOYD B #2-A	148	1	82	65	36	37	9	-
KS121173211E	MCNEE #1	-	-	-	-	-	-	-	-
KS124083211E	AIKEN #3	157	2	66	89	4	30	4	-
KS312183211E	MCNEE #1	148	2	66	80	14	36	5	-
KS214063211E	GLASSCOCK #2	83	4	40	39	44	0	13	-
KS113023210E	MCNEE # 1-A	87	-	27	60	13	19	11	-
KS444043210E	WALKER #3	98	2	57	39	50	-	5	-
KS243293209E	#1 BIRD	144	5	50	89	28	2	-	-
KS323173209E	KEMPTON # 2	105	1	29	75	0	17	3	-
KS211343208E	HADEN A #1	117	3	23	91	20	46	11	-
KS022043208E	THOMPSON #2	79	1	36	42	14	15	6	-
KS411183208E	ELMORE # 10	98	3	24	71	0	28	3	-
KS143103207E	#6 OVERMAN	86	2	6	78	4	12	2	-
KS224213207E	GIROD # 1	84	1	4	79	5	38	4	-
KS142053206E	LAWSON # 1	64	4	19	41	17	6	-	-
KS003133205E	# 2 SCHOFIELD	107	3	17	87	20	13	-	-
KS112133205E	PAUL A MILLER #1	119	-	14	105	11	40	-	-
KS321333205E	RADCLIFF-SNYDER #5	100	2	18	80	7	17	-	-
KS012223204E	J W DIEBENS #12	113	3	43	67	26	18	-	-
KS332153204E	STATE #1	110	3	27	80	0	34	3	-
KS344023203E	IMA CRAIG #1	86	3	3	80	0	4	13	-
KS314093203E	CURTIS-WILSON #1	86	1	10	75	0	15	6	-

Table 2- continued.

WELL CODE	WELL NAME	THK. CHAN.	THK. T. COAL	THK. U. CHAN.	THK. L. CHAN.	SAND C. G.	SAND NOXIE	THK. IOLA	THK. M. H.
KS314363202E	#1 DONLEY A	76	1	23	52	0	11	-	-
KS344273202E	# 1 MILLER LIZIE	83	1	38	44	5	1	2	-
KS000193316E	WALLACE # 1-19	102	3	56	43	56	43	84	-
KS241113315E	WITT #2	-	1	-	38	-	18	-	-
KS422033315E	CLARKSON #1	69	-	-	-	-	-	-	4
KS422033315E	CLARKSON #2	72	-	-	-	-	-	-	4
KS222063315E	GRUVER #20	120	2	80	38	90	14	7	-
KS213193315E	BUTLER #1	121	2	76	43	20	2	4	-
KS002013314E	DARBY # 3-A	191	2	86	103	74	0	6	-
KS442353314E	WILEY SWD #1	110	2	68	40	24	23	-	-
KS421253313E	HEY 1- 21- 25	150	3	94	53	50	14	5	-
KS002143301E	OAK RIDGE RA #3A	83	1	52	30	0	0	3	-
KS432203312E	POWERS # 11	92	2	26	64	25	10	3	-
KS214073311E	T- BONE # 9	98	1	34	63	0	19	-	-
KS000113310E	YORKE #2	-	2	-	33	2	17	-	-
KS114023310E	EGGEN #17	150	2	56	92	23	34	6	-
KS023143309E	KELLY #23-14	119	2	59	58	31	18	19	-
KS004053309E	GOODE #3	155	2	66	87	4	20	4	-
KS442253308E	HOLROYD #1	-	4	-	72	-	22	-	-
KS331213308E	M D MILLS #1	154	1	99	54	28	56	8	-
KS432083308E	JAAX #1	135	2	93	40	26	27	9	-
KS332063307E	RADCLIFF #1	137	1	85	51	6	44	5	-
KS421363306E	DAVID # 1	119	1	68	50	16	38	9	-
KS322183306E	PRIEST # 2-B	98	2	56	40	20	23	-	-
KS023073306E	PRIEST #1	106	1	64	41	24	7	-	-
KS012353305E	BROWN #1	108	1	33	74	10	6	-	-

Table 2- continued.

WELL CODE	WELL NAME	THK. CHAN.	THK. T. COAL	THK. U. CHAN.	THK. L. CHAN.	SAND C. G.	SAND NOXIE	THK. IOLA	THK. M. H.
KS021143305E	JARVIS #3	90	1	36	53	14	14	-	-
KS221133304E	MC COLLUM #1	81	2	39	40	12	16	-	-
KS004233304E	#1 BIRDZELL	98	2	52	44	20	40	3	-
KS234143303E	BERRIE #1	84	?	50	34	22	0	4	-
KS112333303E	AUMANN #3	121	?	36	85	20	74	5	-
KS421173416E	HALL #2	-	-	-	-	-	-	-	-
KS000083416E	DUNCAN # 1-8	-	-	-	-	-	-	-	-
KS003253415E	MUELLER # 1-B	-	-	-	-	-	-	-	-
KS000243415E	GILLMAN DISPOSAL #1	-	-	-	-	-	-	-	-
KS414013415E	BURROWS #8	-	-	-	135	-	-	-	-
KS113353414E	RUSSELL #3	142	1	103	38	80	4	6	-
KS112193414E	POWELL # P-1	129	1	86	42	41	46	5	-
KS002073414E	DALBY #1-A	182	2	96	84	54	29	6	-
KS003083413E	THORNE #3 DISPOSAL	160	2	90	68	38	21	8	-
KS141063413E	W MOORE #25	117	2	54	61	32	22	-	-
KS211063413E	MOORE #1 SWD	95	2	38	55	6	14	4	-
KS141123412E	LEONARD-RISING #2	144	2	64	78	26	12	-	-
KS333063412E	PADGETT #4	143	1	77	65	0	9	4	-
KS441013411E	SMART # G-3	126	2	93	31	58	20	3	-
KS334133410E	WHITWORTH #1	116	2	87	27	14	21	3	-
KS004333410E	CHARLIE-KELLY # 1	92	1	70	20	36	14	3	-
KS041223409E	LAYTON # 1	102	3	69	30	0	25	4	-
KS333103408E	LEEDY # 4	96	1	55	40	10	14	6	-
KS331093408E	SEAMSTER #1 WASHDOWN	103	2	58	43	18	23	6	-
KS242183408E	ECHOLS #1	165	2	112	51	43	47	-	-
KS244323407E	SNYDER #1	121	1	87	33	32	6	7	-

Table 2- continued.

WELL CODE	WELL NAME	THK. CHAN.	THK. T. COAL	THK. U. CHAN.	THK. L. CHAN.	SAND C. G.	SAND NOXIE	THK. IOLA	THK. M. H.
KS032033405E	ALBRIGHT # 6	130	2	70	58	34	13	6	-
KS121273405E	WILLIAMSON C-1	145	1	55	89	27	54	4	-
KS013213405E	HICKMAN D #1	149	1	71	77	25	38	3	-
KS121143404E	CRAIN #7	106	-	-	-	-	-	-	-
KS001093404E	FRANK BOSSI #12	119	1	42	76	30	9	5	-
KS244073404E	GOFF #1	128	-	-	-	-	-	7	-
KS422323403E	BAIRD-BRENNAN # 21	107	-	-	-	-	-	-	-
KS214293403E	BAIRD # 29-1	116	-	-	-	-	-	-	-
KS231163401E	HUNT #3	82	0	32	50	12	15	28	-
KS244103515E	FIELDES #4 SWD	-	0	-	122	-	60	-	-
KS000043515E	COLLINS #2-C	-	-	-	-	-	46	-	-
KS024123514E	ROBINSON #1	154	2	72	80	50	16	12	-
KS213033514E	ELSEHEIMER #15	165	2	85	78	44	22	5	-
KS224173512E	BURCH #103	148	-	-	-	0	69	4	-
KS003133511E	CLINGAN #2	130	0	42	88	0	38	6	-
KS412133510E	SWEENEY #1	121	1	32	88	26	38	3	-
KS421143510E	LORENZ #1	123	2	23	98	16	20	4	-
KS142113510E	KEENY #1	97	0	17	80	0	35	11	-
KS111013509E	WINEGER #2	-	-	-	-	-	-	-	-
KS222173507E	DOROTHY #9	-	2	-	90	-	27	-	-
KS331153505E	WARREN B #1	95	0	17	78	12	10	0	-
KS341043504E	BOSSI #1	170	2	54	114	0	44	6	-
KS011033503E	BRANDENBURG A #3	156	0	-	-	-	-	3	-
KS241183503E	VICKERY #1	186	0	18	168	6	52	6	-
KS332103503E	CAPITT #1 MCCLASKEY	119	0	-	-	3	60	-	-
KS424083502E	KEMP #3	144	1	25	118	11	76	8	-

Table 2- continued.

WELL CODE	WELL NAME	THK. CHAN.	THK. T. COAL	THK. U. CHAN.	THK. L. CHAN.	SAND C. G.	SAND NOXIE	THK. IOLA	THK. M. H.
OKLAHOMA		-	-	0	0	-	-	0	-
ON222242913E	LOWERY UNIT #6	-	-	-	-	-	-	-	-
ON344362910E	HUNTER #1-A	103	-	-	-	-	-	-	-
ONOOO162910E	CARTER #1	70	-	-	-	-	-	-	-
ON432162909E	MOORE A #1	110	1	25	84	11	28	6	-
ON241312909E	HUTCHINSON A #1	158	2	80	76	36	10	4	-
ON002222908E	OK LAND & CATTLE CO.	94	1	17	76	14	28	4	-
ON032142905E	STATE LINE #1-A	149	2	54	93	6	38	-	-
ON112212903E	LOVE #1	107	2	48	57	0	37	25	-
ON444122813E	LUCAS #1	109	2	9	98	0	12	6	-
ON001082812E	#2 FULLENDORE	120	-	58	62	9	40	-	-
ON423282811E	MOORE #6	156	-	30	126	8	48	-	-
ON421032810E	#1 MARY H	179	2^	22	155	7	48	-	-
ON222342809E	CONOCO G #1-A	172	-	14	158	0	32	5	-
ON423052713E	GARRET NEIL	-	-	-	-	-	-	-	-
ON321332709E	MANNING #1	108	2	23	83	25	25	8	-
ON111072709E	BARNARD #10	128	-	40	88	20	36	-	-
ON434322708E	DRUMMOND # 1-C	115	-	42	73	4	11	-	-
ON334342706E	BIGHEART #16W	99	-	48	51	15	36	4	-
ON034292702E	EDWARDS NCT 2 #1	73	2	28	43	0	25	3	-
ON431312610E	LOOKOUT #6	92	-	-	-	-	-	-	-
ON231222609E	ELSIE #1	156	-	80	76	20	46	16	-
ON001362608E	MULLENDORE #3	155	-	53	102	12	69	-	-
ON422172608E	WHITEHORN #1-17	139	2	52	85	0	49	-	-
ON001352607E	AB I-35 AA DRUMMOND	163	2	75	86	16	68	-	-
ON011182511E	LATE # 8	73	-	-	-	-	29	-	-

Table 2- continued.

WELL CODE	WELL NAME	THK. CHAN.	THK. T. COAL	THK. U. CHAN.	THK. L. CHAN.	SAND C. G.	SAND NOXIE	THK. IOLA	THK. M. H.
ON112032509E	INDIAN VILLAGE	121	-	-	-	-	-	-	-
ON442102508E	RODEO ANTICLINE #2-1	119	-	-	-	-	-	12	-
ON333162508E	OXLEY 1-A	160	-	-	-	-	-	-	-
ON321222506E	FAIRFAX UNIT	95	-	-	-	-	-	13	-
ON324042506E	FLETCHER #9	98	-	-	-	-	-	-	-
ON214032505E	MATHIS UNIT TRACT #3	91	-	-	-	-	-	-	-
ON312212505E	MASHBURN #1	86	2	26	58	0	17	16	-
ON444162411E	#5	59	-	-	-	-	-	-	-
ON004092411E	LOT 292- #3	60	1	32	27	15	0	-	-
ON233042411E	BIGHEART #8-6	65	1	29	35	18	0	-	-
ON333092410E	MCCORMICK #1-9	98	1	63	34	6	0	-	-
ON242312410E	GEORGIA #2	56	-	36	20	6?	?	-	-
ON113032409E	#B A COTTONMOUTH	73	-	43	30	32	9	-	-
ON013212409E	FIELDS #7	69	-	-	-	-	-	-	-
ON333352408E	LEASE 3 WELL #1-A	43	1^?	14	28	2	11	67	-
ON023232408E	DANIELS BLOCK SW	117	2^	93	22	23	12	-	-
ON001342407E	DRUMMOND B TRACT 30	116	-	-	-	-	-	-	-

APPENDIX II

POINT COUNTS

Table 3. Point counts of Chanute Shale core and outcrop samples.

COMPOSITION	AH 1.55			AH 2.75			AH 8.3		
	# GRAINS	TOTAL %	DETRITAL %	# GRAINS	TOTAL %	DETRITAL %	# GRAINS	TOTAL %	DETRITAL %
QUARTZ MONO	41	14%	46%	22	7%	20%	127	42%	62%
QUARTZ POLY	0	0%	0%	0	0%	0%	8	3%	4%
FELDSPARS		0%	0%		0%	0%		0%	0%
PLAGIOCLASE	0	0%	0%	0	0%	0%	12	4%	6%
ORTHOCLASE	0	0%	0%	0	0%	0%	18	6%	9%
MICROCLINE		0%	0%	0	0%	0%	2	1%	1%
PERTHITE	0	0%	0%		0%	0%	0	0%	0%
MICAS		0%	0%		0%	0%		0%	0%
MUSCOVITE	0	0%	0%	2	1%	1%	3	1%	2%
BIOTITE		0%	0%		0%	0%	0	0%	0%
CHLORITE		0%	0%	0	0%	0%	3	1%	2%
CHERT	0	0%	0%		0%	0%	0	0%	0%
SKELETALS UNK.	5	2%	6%		0%	0%		0%	0%
BRACHIOPODS	3	1%	3%	6	2%	3%		0%	0%
BRYOZOANS		0%	0%	6	2%	3%		0%	0%
ALGAE	10	3%	11%	11	4%	5%		0%	0%
ECHINODERM PLATES		0%	0%	60	20%	25%		0%	0%
ECHINODERM SPINES		0%	0%		0%	0%		0%	0%
BIVALVES	10	3%	11%	2	1%	1%		0%	0%
OSTRACODS	18	6%	20%	0	0%	0%		0%	0%
ROCK FRAGMENTS		0%	0%		0%	0%		0%	0%
SED. RX. FRAG.		0%	0%		0%	0%	4	1%	2%
IGN. RX. FRAG.		0%	0%		0%	0%	0	0%	0%
MET. RX. FRAG.		0%	0%		0%	0%	28	9%	13%
GLAUCONITE	3	1%	3%	0	0%	0%		0%	0%
ACCESORY		0%	0%		0%	0%	0	0%	0%
		0%			0%			0%	
OPAQUES		0%			0%		1	0%	
ORG.MATTER	54	18%		6	2%		0	0%	
FE OXIDE	3	1%		0	0%		11	4%	
MICRITE	3	1%			0%			0%	
CA CEMENT	146	49%		183	61%			0%	
SI CEMENT		0%			0%			0%	
CLAY		0%		0	0%		27	9%	
PYRITE		0%			0%			0%	
PRIMARY POROSITY		0%			0%		0	0%	
SECONDARY POROSITY	5	2%			0%		55	18%	
TOTALS=	300	100%	89.7	300	100%	110.1	300	100%	205.9

Table 3- continued.

COMPOSITION	AH 8.45			AH 11.1			AH 11.2		
	# GRAINS	TOTAL %	DETRITAL %	# GRAINS	TOTAL %	DETRITAL %	# GRAINS	TOTAL %	DETRITAL %
QUARTZ MONO	102	34%	56%	80	27%	65%	74	25%	59%
QUARTZ POLY	14	5%	7%	10	3%	8%	6	2%	5%
FELDSPARS		0%	0%		0%	0%		0%	0%
PLAGIOCLASE	2	1%	1%	5	2%	4%	4	1%	4%
ORTHOCLASE	24	8%	13%	3	1%	3%	10	3%	8%
MICROCLINE		0%	0%	0	0%	0%		0%	0%
PERTHITE	1	0%	1%	0	0%	0%	1	0%	1%
MICAS		0%	0%		0%	0%		0%	0%
MUSCOVITE	1	0%	1%	10	3%	8%	1	0%	1%
BIOTITE	0	0%	0%	4	1%	3%	0	0%	0%
CHLORITE	0	0%	0%	1	0%	1%		0%	0%
CHERT	3	1%	2%	2	1%	2%	3	1%	3%
SKELETALS UNK.		0%	0%		0%	0%		0%	0%
BRACHIOPODS		0%	0%		0%	0%		0%	0%
BRYOZOANS		0%	0%		0%	0%		0%	0%
ALGAE		0%	0%		0%	0%		0%	0%
ECHINODERM PLATES		0%	0%		0%	0%		0%	0%
ECHINODERM SPINES		0%	0%		0%	0%		0%	0%
BIVALVES		0%	0%		0%	0%		0%	0%
OSTRACODS		0%	0%		0%	0%		0%	0%
ROCK FRAGMENTS		0%	0%		0%	0%		0%	0%
SED. RX. FRAG.	5	2%	2%		0%	0%	9	3%	7%
IGN. RX. FRAG.		0%	0%		0%	0%		0%	0%
MET. RX. FRAG.	31	10%	17%	9	3%	7%	16	5%	13%
GLAUCONITE	0	0%	0%		0%	0%		0%	0%
ACCESORY	0	0%	0%	0	0%	0%		0%	0%
		0%			0%			0%	
OPAQUES	0	0%		1	0%			0%	
ORG.MATTER	0	0%		6	2%			0%	
FE OXIDE	53	18%		5	2%		2	1%	
MICRITE		0%			0%			0%	
CA CEMENT		0%		138	46%			0%	
SI CEMENT		0%			0%			0%	
CLAY	7	2%		10	3%		0	0%	
PYRITE		0%			0%		164	55%	
PRIMARY POROSITY	0	0%			0%			0%	
SECONDARY POROSITY	57	19%		15	5%		10	3%	
TOTALS=	300	100%	183.0	300	100%	124.3	300	100%	123.8

Table 3- continued.

COMPOSITION	AH 11.6			AH 12.5			AH 14.0		
	# GRAINS	TOTAL %	DETRITAL %	# GRAINS	TOTAL %	DETRITAL %	# GRAINS	TOTAL %	DETRITAL %
QUARTZ MONO	109	36%	65%	149	50%	71%	73	24%	56%
QUARTZ POLY	23	8%	14%	7	2%	3%	4	1%	3%
FELDSPARS		0%	0%		0%	0%		0%	0%
PLAGIOCLASE	4	1%	2%	4	1%	2%	0	0%	0%
ORTHOCLASE	20	7%	12%	18	6%	8%	2	1%	2%
MICROCLINE	0	0%	0%		0%	0%	2	1%	2%
PERTHITE	0	0%	0%	0	0%	0%	0	0%	0%
MICAS		0%	0%		0%	0%		0%	0%
MUSCOVITE	2	1%	1%	2	1%	1%	0	0%	0%
BIOTITE	2	1%	1%	5	2%	2%		0%	0%
CHLORITE	0	0%	0%		0%	0%	0	0%	0%
CHERT	1	0%	1%	0	0%	0%	0	0%	0%
SKELETALS UNK.		0%	0%		0%	0%		0%	0%
BRACHIOPODS		0%	0%		0%	0%	2	1%	2%
BRYOZOANS		0%	0%		0%	0%	34	11%	26%
ALGAE		0%	0%		0%	0%	2	1%	2%
ECHINODERM PLATES		0%	0%		0%	0%	4	1%	3%
ECHINODERM SPINES		0%	0%		0%	0%	2	1%	2%
BIVALVES		0%	0%		0%	0%	4	1%	3%
OSTRACODS		0%	0%		0%	0%		0%	0%
ROCK FRAGMENTS		0%	0%		0%	0%		0%	0%
SED. RX. FRAG.	0	0%	0%	9	3%	4%		0%	0%
IGN. RX. FRAG.		0%	0%		0%	0%		0%	0%
MET. RX. FRAG.	7	2%	4%	16	5%	8%	0	0%	0%
GLAUCONITE		0%	0%	1	0%	1%	0	0%	0%
ACCESORY		0%	0%		0%	0%	0	0%	0%
		0%			0%			0%	
OPAQUES	0	0%		0	0%			0%	
ORG.MATTER	2	1%		0	0%		6	2%	
FE OXIDE	20	7%		14	5%		0	0%	
MICRITE		0%			0%		44	15%	
CA CEMENT		0%			0%		120	40%	
SI CEMENT		0%			0%			0%	
CLAY	39	13%		21	7%			0%	
PYRITE		0%			0%			0%	
PRIMARY POROSITY		0%			0%			0%	
SECONDARY POROSITY	69	23%		54	18%		0	0%	
TOTALS=	300	100%	169.5	300	100%	210.9	300	100%	130.1

Table 3- continued.

COMPOSITION	AH 15.45			AH 15.55			AH 15.95		
	# GRAINS	TOTAL %	DETRITAL %	# GRAINS	TOTAL %	DETRITAL %	# GRAINS	TOTAL %	DETRITAL %
QUARTZ MONO	104	35%	60%	86	29%	48%	61	20%	57%
QUARTZ POLY	21	7%	12%	11	4%	6%	12	4%	11%
FELDSPARS		0%	0%		0%	0%		0%	0%
PLAGIOCLASE	12	4%	7%	4	1%	2%	1	0%	1%
ORTHOCLASE	8	3%	4%	9	3%	5%	5	2%	5%
MICROCLINE		0%	0%	0	0%	0%	0	0%	0%
PERTHITE	3	1%	2%	3	1%	2%	1	0%	1%
MICAS		0%	0%		0%	0%		0%	0%
MUSCOVITE	7	2%	4%	12	4%	7%	0	0%	0%
BIOTITE	1	0%	1%	10	3%	5%	0	0%	0%
CHLORITE	0	0%	0%	2	1%	1%	0	0%	0%
CHERT	4	1%	3%	2	1%	1%	5	2%	5%
SKELETALS UNK.		0%	0%		0%	0%		0%	0%
BRACHIOPODS		0%	0%		0%	0%		0%	0%
BRYOZOANS		0%	0%		0%	0%		0%	0%
ALGAE		0%	0%		0%	0%		0%	0%
ECHINODERM PLATES		0%	0%		0%	0%		0%	0%
ECHINODERM SPINES		0%	0%		0%	0%		0%	0%
BIVALVES		0%	0%		0%	0%		0%	0%
OSTRACODS		0%	0%		0%	0%		0%	0%
ROCK FRAGMENTS		0%	0%		0%	0%		0%	0%
SED. RX. FRAG.	3	1%	2%	4	1%	2%	2	1%	2%
IGN. RX. FRAG.		0%	0%		0%	0%	2	1%	2%
MET. RX. FRAG.	25	8%	14%	35	12%	20%	17	6%	16%
GLAUCONITE		0%	0%	1	0%	1%		0%	0%
ACCESORY	0	0%	0%		0%	0%		0%	0%
		0%			0%			0%	
OPAQUES		0%		0	0%			0%	
ORG.MATTER		0%		0	0%			0%	
FE OXIDE	30	10%		3	1%		156	52%	
MICRITE		0%			0%			0%	
CA CEMENT		0%			0%			0%	
SI CEMENT		0%			0%			0%	
CLAY	26	9%		75	25%		5	2%	
PYRITE		0%			0%			0%	
PRIMARY POROSITY		0%			0%			0%	
SECONDARY POROSITY	55	18%		41	14%		32	11%	
TOTALS=	300	100%	173.0	300	100%	180.9	300	100%	107.5

Table 3- continued.

COMPOSITION	AH 17.5			NPC			NR 0.55		
	# GRAINS	TOTAL %	DETRITAL %	# GRAINS	TOTAL %	DETRITAL %	# GRAINS	TOTAL %	DETRITAL %
QUARTZ MONO	76	25%	47%	79	26%	43%	140	47%	72%
QUARTZ POLY	15	5%	9%	19	6%	10%	25	8%	13%
FELDSPARS		0%	0%		0%	0%		0%	0%
PLAGIOCLASE	14	5%	8%	5	2%	3%	2	1%	1%
ORTHOCLASE	5	2%	3%	10	3%	5%	3	1%	2%
MICROCLINE		0%	0%	1	0%	1%		0%	0%
PERTHITE	3	1%	2%	1	0%	1%	1	0%	1%
MICAS		0%	0%		0%	0%		0%	0%
MUSCOVITE	15	5%	9%	2	1%	1%	0	0%	0%
BIOTITE	1	0%	1%	1	0%	1%	0	0%	0%
CHLORITE	3	1%	2%		0%	0%		0%	0%
CHERT	2	1%	1%	3	1%	2%	2	1%	1%
SKELETALS UNK.		0%	0%		0%	0%		0%	0%
BRACHIOPODS		0%	0%		0%	0%		0%	0%
BRYOZOANS		0%	0%		0%	0%		0%	0%
ALGAE		0%	0%		0%	0%		0%	0%
ECHINODERM PLATES		0%	0%		0%	0%		0%	0%
ECHINODERM SPINES		0%	0%		0%	0%		0%	0%
BIVALVES		0%	0%		0%	0%		0%	0%
OSTRACODS		0%	0%		0%	0%		0%	0%
ROCK FRAGMENTS		0%	0%		0%	0%		0%	0%
SED. RX. FRAG.	4	1%	3%	26	9%	14%	5	2%	3%
IGN. RX. FRAG.		0%	0%	3	1%	2%	4	1%	2%
MET, RX. FRAG.	21	7%	13%	35	12%	19%	12	4%	6%
GLAUCONITE	1	0%	1%		0%	0%		0%	0%
ACCESORY	1	0%	1%	0	0%	0%	1	0%	1%
		0%			0%			0%	
OPAQUES		0%		1	0%			0%	
ORG.MATTER	1	0%		1	0%		2	1%	
FE OXIDE	19	6%		24	8%		12	4%	
MICRITE		0%			0%			0%	
CA CEMENT	6	2%			0%			0%	
SI CEMENT		0%			0%			0%	
CLAY	71	24%		9	3%		32	11%	
PYRITE		0%			0%			0%	
PRIMARY POROSITY		0%			0%			0%	
SECONDARY POROSITY	42	14%		80	27%		60	20%	
TOTALS=	300	100%	160.5	300	100%	184.8	300	100%	194.5

Table 3- continued.

COMPOSITION	NR 860			NR 902			NR 910		
	# GRAINS	TOTAL %	DETRITAL %	# GRAINS	TOTAL %	DETRITAL %	# GRAINS	TOTAL %	DETRITAL %
QUARTZ MONO	128	43%	62%	109	36%	70%	105	35%	60%
QUARTZ POLY	19	6%	9%		0%	0%	30	10%	17%
FELDSPARS		0%	0%		0%	0%		0%	0%
PLAGIOCLASE	7	2%	4%	7	2%	5%	6	2%	4%
ORTHOCLASE	12	4%	6%	5	2%	3%	4	1%	2%
MICROCLINE		0%	0%		0%	0%	0	0%	0%
PERTHITE	0	0%	0%		0%	0%	2	1%	1%
MICAS		0%	0%		0%	0%		0%	0%
MUSCOVITE	3	1%	2%	5	2%	3%	2	1%	1%
BIOTITE	0	0%	0%	10	3%	6%	1	0%	1%
CHLORITE	1	0%	1%		0%	0%	1	0%	1%
CHERT	3	1%	2%		0%	0%	6	2%	4%
SKELETALS UNK.		0%	0%		0%	0%		0%	0%
BRACHIOPODS		0%	0%		0%	0%		0%	0%
BRYOZOANS		0%	0%		0%	0%		0%	0%
ALGAE		0%	0%		0%	0%		0%	0%
ECHINODERM PLATES		0%	0%		0%	0%		0%	0%
ECHINODERM SPINES		0%	0%		0%	0%		0%	0%
BIVALVES		0%	0%		0%	0%		0%	0%
OSTRACODS		0%	0%		0%	0%		0%	0%
ROCK FRAGMENTS		0%	0%		0%	0%		0%	0%
SED. RX. FRAG.	10	3%	5%	7	2%	5%	3	1%	2%
IGN. RX. FRAG.		0%	0%		0%	0%	1	0%	1%
MET. RX. FRAG.	23	8%	11%	12	4%	8%	11	4%	6%
GLAUCONITE	0	0%	0%	0	0%	0%		0%	0%
ACCESORY	0	0%	0%		0%	0%	0	0%	0%
		0%			0%			0%	
OPAQUES	1	0%		0	0%			0%	
ORG.MATTER		0%		12	4%		0	0%	
FE OXIDE	6	2%			0%		87	29%	
MICRITE		0%			0%			0%	
CA CEMENT		0%			0%			0%	
SI CEMENT		0%			0%			0%	
CLAY	30	10%		12	4%		3	1%	
PYRITE		0%			0%			0%	
PRIMARY POROSITY		0%			0%			0%	
SECONDARY POROSITY	57	19%		119	40%		35	12%	
TOTALS=	300	100%	206.2	300	100%	156.2	300	100%	174.19

Table 3- continued.

COMPOSITION	SI 3.95			SI 4.9			SIA 1.3		
	# GRAINS	TOTAL %	DETRITAL %	# GRAINS	TOTAL %	DETRITAL %	# GRAINS	TOTAL %	DETRITAL %
QUARTZ MONO	97	32%	57%	114	38%	70%	107	36%	68%
QUARTZ POLY	11	4%	7%	6	2%	3%	15	5%	10%
FELDSPARS		0%	0%		0%	0%		0%	0%
PLAGIOCLASE	11	4%	7%	9	3%	6%	1	0%	1%
ORTHOCLASE	8	3%	5%	5	2%	3%	10	3%	6%
MICROCLINE		0%	0%		0%	0%		0%	0%
PERTHITE		0%	0%		0%	0%	0	0%	0%
MICAS		0%	0%		0%	0%		0%	0%
MUSCOVITE	22	7%	13%	5	2%	3%	9	3%	6%
BIOTITE	19	6%	11%	1	0%	1%	3	1%	2%
CHLORITE	0	0%	0%		0%	0%	1	0%	1%
CHERT		0%	0%	1	0%	1%	2	1%	1%
SKELETALS UNK.		0%	0%		0%	0%		0%	0%
BRACHIOPODS		0%	0%		0%	0%		0%	0%
BRYOZOANS		0%	0%		0%	0%		0%	0%
ALGAE		0%	0%		0%	0%		0%	0%
ECHINODERM PLATES		0%	0%		0%	0%		0%	0%
ECHINODERM SPINES		0%	0%		0%	0%		0%	0%
BIVALVES		0%	0%		0%	0%		0%	0%
OSTRACODS		0%	0%		0%	0%		0%	0%
ROCK FRAGMENTS		0%	0%		0%	0%		0%	0%
SED. RX. FRAG.		0%	0%	6	2%	3%	2	1%	1%
IGN. RX. FRAG.		0%	0%		0%	0%		0%	0%
MET. RX. FRAG.	0	0%	0%	18	6%	11%	5	2%	3%
GLAUCONITE		0%	0%	0	0%	0%	0	0%	0%
ACCESORY		0%	0%	0	0%	0%	1	0%	1%
		0%			0%			0%	
OPAQUES	0	0%			0%		0	0%	
ORG.MATTER	0	0%		0	0%		0	0%	
FE OXIDE	36	12%		92	31%		28	9%	
MICRITE		0%			0%			0%	
CA CEMENT		0%		5	2%			0%	
SI CEMENT		0%			0%			0%	
CLAY	61	20%		14	5%		89	30%	
PYRITE		0%			0%			0%	
PRIMARY POROSITY		0%			0%			0%	
SECONDARY POROSITY	33	11%		26	9%		26	9%	
TOTALS=	300	100%	169.4	300	100%	164.2	300	100%	157.0

Table 3- continued.

COMPOSITION	ET 0.0			ET 0.4			ET 0.6		
	# GRAINS	TOTAL %	DETRITAL %	# GRAINS	TOTAL %	DETRITAL %	# GRAINS	TOTAL %	DETRITAL %
QUARTZ MONO	129	43%	63%	100	33%	59%	115	38%	63%
QUARTZ POLY	10	3%	5%	2	1%	1%	11	4%	6%
FELDSPARS		0%	0%		0%	0%		0%	0%
PLAGIOCLASE	9	3%	4%	16	5%	9%	10	3%	5%
ORTHOCLASE	17	6%	8%	13	4%	8%	21	7%	11%
MICROCLINE		0%	0%		0%	0%		0%	0%
PERTHITE		0%	0%		0%	0%		0%	0%
MICAS		0%	0%		0%	0%		0%	0%
MUSCOVITE	4	1%	2%	2	1%	1%	2	1%	1%
BIOTITE	4	1%	2%	7	2%	4%	0	0%	0%
CHLORITE	0	0%	0%	0	0%	0%		0%	0%
CHERT		0%	0%	0	0%	0%	1	0%	1%
SKELETALS UNK.		0%	0%		0%	0%		0%	0%
BRACHIOPODS		0%	0%		0%	0%		0%	0%
BRYOZOANS		0%	0%		0%	0%		0%	0%
ALGAE		0%	0%		0%	0%		0%	0%
ECHINODERM PLATES		0%	0%		0%	0%		0%	0%
ECHINODERM SPINES		0%	0%		0%	0%		0%	0%
BIVALVES		0%	0%		0%	0%		0%	0%
OSTRACODS		0%	0%		0%	0%		0%	0%
ROCK FRAGMENTS		0%	0%		0%	0%		0%	0%
SED. RX. FRAG.	15	5%	7%	13	4%	8%	7	2%	4%
IGN. RX. FRAG.		0%	0%		0%	0%		0%	0%
MET. RX. FRAG.	17	6%	8%	15	5%	9%	16	5%	9%
GLAUCONITE	1	0%	1%	0	0%	0%		0%	0%
ACCESORY	1	0%	1%	0	0%	0%	1	0%	1%
		0%			0%			0%	
OPAQUES	0	0%		1	0%		2	1%	
ORG.MATTER	1	0%			0%			0%	
FE OXIDE	15	5%		16	5%		16	5%	
MICRITE		0%			0%			0%	
CA CEMENT		0%			0%			0%	
SI CEMENT		0%			0%			0%	
CLAY		0%		27	9%		21	7%	
PYRITE		0%			0%			0%	
PRIMARY POROSITY		0%			0%		1	0%	
SECONDARY POROSITY	77	26%		88	29%		76	25%	
TOTALS=	300	100%	206.56	300	100%	168.5	300	100%	183.9

Table 3- continued.

COMPOSITION	ET 0.85			ET 1.3			TD 0.6		
	# GRAINS	TOTAL %	DETRITAL %	# GRAINS	TOTAL %	DETRITAL %	# GRAINS	TOTAL %	DETRITAL %
QUARTZ MONO	114	38%	65%	100	33%	54%	97	32%	67%
QUARTZ POLY	5	2%	3%	3	1%	2%	4	1%	3%
FELDSPARS		0%	0%		0%	0%		0%	0%
PLAGIOCLASE	17	6%	10%	25	8%	13%	4	1%	3%
ORTHOCLASE	10	3%	6%	18	6%	10%	15	5%	11%
MICROCLINE		0%	0%		0%	0%		0%	0%
PERTHITE		0%	0%		0%	0%		0%	0%
MICAS		0%	0%		0%	0%		0%	0%
MUSCOVITE	2	1%	1%	2	1%	1%	10	3%	7%
BIOTITE	2	1%	1%	4	1%	2%	2	1%	2%
CHLORITE		0%	0%		0%	0%		0%	0%
CHERT	3	1%	2%	1	0%	1%		0%	0%
SKELETALS UNK.		0%	0%		0%	0%		0%	0%
BRACHIOPODS		0%	0%		0%	0%		0%	0%
BRYOZOANS		0%	0%		0%	0%		0%	0%
ALGAE		0%	0%		0%	0%		0%	0%
ECHINODERM PLATES		0%	0%		0%	0%		0%	0%
ECHINODERM SPINES		0%	0%		0%	0%		0%	0%
BIVALVES		0%	0%		0%	0%		0%	0%
OSTRACODS		0%	0%		0%	0%		0%	0%
ROCK FRAGMENTS		0%	0%		0%	0%		0%	0%
SED. RX. FRAG.	9	3%	5%	7	2%	4%	4	1%	3%
IGN. RX. FRAG.		0%	0%		0%	0%		0%	0%
MET. RX. FRAG.	10	3%	6%	21	7%	11%	7	2%	5%
GLAUCONITE		0%	0%		0%	0%		0%	0%
ACCESORY	1	0%	1%	6	2%	3%	1	0%	1%
		0%			0%			0%	
OPAQUES	1	0%		1	0%		0	0%	
ORG.MATTER	2	1%		3	1%		4	1%	
FE OXIDE	44	15%		10	3%		34	11%	
MICRITE		0%			0%			0%	
CA CEMENT		0%			0%			0%	
SI CEMENT		0%			0%			0%	
CLAY	16	5%		19	6%		44	15%	
PYRITE		0%			0%			0%	
PRIMARY POROSITY		0%			0%			0%	
SECONDARY POROSITY	62	21%		79	26%		72	24%	
TOTALS=	300	100%	174.52	300	100%	187.4	300	100%	145.6

Table 3- continued.

COMPOSITION	TD 8.9			TD 10.0			TD 10.65		
	# GRAINS	TOTAL %	DETRITAL %	# GRAINS	TOTAL %	DETRITAL %	# GRAINS	TOTAL %	DETRITAL %
QUARTZ MONO	90	30%	79%	128	43%	65%	87	29%	63%
QUARTZ POLY	5	2%	4%		0%	0%	4	1%	3%
FELDSPARS		0%	0%		0%	0%		0%	0%
PLAGIOCLASE	1	0%	1%	20	7%	10%	7	2%	5%
ORTHOCLASE	1	0%	1%	2	1%	1%	16	5%	12%
MICROCLINE		0%	0%		0%	0%		0%	0%
PERTHITE		0%	0%		0%	0%		0%	0%
MICAS		0%	0%		0%	0%		0%	0%
MUSCOVITE	4	1%	3%	4	1%	2%	1	0%	1%
BIOTITE	0	0%	0%	0	0%	0%	4	1%	3%
CHLORITE		0%	0%	0	0%	0%	0	0%	0%
CHERT	0	0%	0%	0	0%	0%		0%	0%
SKELETALS UNK.		0%	0%		0%	0%		0%	0%
BRACHIOPODS		0%	0%		0%	0%		0%	0%
BRYOZOANS		0%	0%		0%	0%		0%	0%
ALGAE		0%	0%		0%	0%		0%	0%
ECHINODERM PLATES		0%	0%		0%	0%		0%	0%
ECHINODERM SPINES		0%	0%		0%	0%		0%	0%
BIVALVES		0%	0%		0%	0%		0%	0%
OSTRACODS		0%	0%		0%	0%		0%	0%
ROCK FRAGMENTS		0%	0%		0%	0%		0%	0%
SED. RX. FRAG.	2	1%	2%	16	5%	8%	6	2%	4%
IGN. RX. FRAG.		0%	0%		0%	0%		0%	0%
MET. RX. FRAG.	11	4%	10%	28	9%	14%	12	4%	8%
GLAUCONITE		0%	0%	0	0%	0%		0%	0%
ACCESORY	0	0%	0%	0	0%	0%		0%	0%
		0%			0%			0%	
OPAQUES		0%		0	0%		0	0%	
ORG.MATTER	1	0%		2	1%		6	2%	
FE OXIDE	155	52%		6	2%		30	10%	
MICRITE		0%			0%			0%	
CA CEMENT		0%			0%			0%	
SI CEMENT		0%			0%			0%	
CLAY	2	1%		22	7%		45	15%	
PYRITE		0%			0%			0%	
PRIMARY POROSITY		0%			0%			0%	
SECONDARY POROSITY	27	9%		73	24%		81	27%	
TOTALS=	300	100%	114.6	300	100%	197.4	300	100%	137.7

Table 3- continued.

COMPOSITION	TD 11.2			TD 11.9			SC 0.2		
	# GRAINS	TOTAL %	DETRITAL %	# GRAINS	TOTAL %	DETRITAL %	# GRAINS	TOTAL %	DETRITAL %
QUARTZ MONO	83	28%	62%	101	34%	66%	74	25%	62%
QUARTZ POLY	1	0%	1%	2	1%	1%	3	1%	3%
FELDSPARS		0%	0%		0%	0%		0%	0%
PLAGIOCLASE	11	4%	8%	13	4%	8%	7	2%	5%
ORTHOCLASE	13	4%	10%	9	3%	5%	11	4%	9%
MICROCLINE		0%	0%		0%	0%		0%	0%
PERTHITE		0%	0%		0%	0%		0%	0%
MICAS		0%	0%		0%	0%		0%	0%
MUSCOVITE	8	3%	6%	0	0%	0%	12	4%	10%
BIOTITE	2	1%	2%	1	0%	1%	2	1%	2%
CHLORITE	1	0%	1%	0	0%	0%	0	0%	0%
CHERT		0%	0%	0	0%	0%		0%	0%
SKELETALS UNK.		0%	0%		0%	0%		0%	0%
BRACHIOPODS		0%	0%		0%	0%		0%	0%
BRYOZOANS		0%	0%		0%	0%		0%	0%
ALGAE		0%	0%		0%	0%		0%	0%
ECHINODERM PLATES		0%	0%		0%	0%		0%	0%
ECHINODERM SPINES		0%	0%		0%	0%		0%	0%
BIVALVES		0%	0%		0%	0%		0%	0%
OSTRACODS		0%	0%		0%	0%		0%	0%
ROCK FRAGMENTS		0%	0%		0%	0%		0%	0%
SED. RX. FRAG.	4	1%	3%	11	4%	7%	4	1%	4%
IGN. RX. FRAG.		0%	0%		0%	0%		0%	0%
MET. RX. FRAG.	7	2%	5%	13	4%	8%	7	2%	5%
GLAUCONITE		0%	0%	1	0%	1%	0	0%	0%
ACCESORY	2	1%	2%	0	0%	0%		0%	0%
		0%			0%			0%	
OPAQUES	8	3%		1	0%		0	0%	
ORG.MATTER	0	0%		6	2%		3	1%	
FE OXIDE	53	18%		35	12%		83	28%	
MICRITE		0%			0%			0%	
CA CEMENT		0%			0%		9	3%	
SI CEMENT		0%			0%			0%	
CLAY	28	9%		45	15%		61	20%	
PYRITE		0%			0%			0%	
PRIMARY POROSITY		0%			0%			0%	
SECONDARY POROSITY	78	26%		61	20%		25	8%	
TOTALS=	300	100%	133.2	300	100%	152.8	300	100%	119.6

Table 3- continued.

COMPOSITION	SC 0.65			SC 1.1			SC 2.5		
	# GRAINS	TOTAL %	DETRITAL %	# GRAINS	TOTAL %	DETRITAL %	# GRAINS	TOTAL %	DETRITAL %
QUARTZ MONO	106	35%	79%	111	37%	88%		0%	0%
QUARTZ POLY		0%	0%		0%	0%		0%	0%
FELDSPARS		0%	0%		0%	0%		0%	0%
PLAGIOCLASE	3	1%	2%	1	0%	1%		0%	0%
ORTHOCLASE	0	0%	0%		0%	0%		0%	0%
MICROCLINE		0%	0%		0%	0%		0%	0%
PERTHITE		0%	0%		0%	0%		0%	0%
MICAS		0%	0%		0%	0%		0%	0%
MUSCOVITE	13	4%	10%	9	3%	7%		0%	0%
BIOTITE	4	1%	3%	1	0%	1%		0%	0%
CHLORITE	7	2%	5%	1	0%	1%		0%	0%
CHERT		0%	0%		0%	0%		0%	0%
SKELETALS UNK.		0%	0%		0%	0%		0%	0%
BRACHIOPODS		0%	0%		0%	0%	3	1%	2%
BRYOZOANS		0%	0%		0%	0%	122	41%	86%
ALGAE		0%	0%		0%	0%	5	2%	4%
ECHINODERM PLATES		0%	0%		0%	0%	0	0%	0%
ECHINODERM SPINES		0%	0%		0%	0%		0%	0%
BIVALVES		0%	0%		0%	0%	13	4%	9%
OSTRACODS		0%	0%		0%	0%		0%	0%
ROCK FRAGMENTS		0%	0%		0%	0%		0%	0%
SED. RX. FRAG.	1	0%	1%	1	0%	1%		0%	0%
IGN. RX. FRAG.		0%	0%		0%	0%		0%	0%
MET. RX. FRAG.		0%	0%		0%	0%		0%	0%
GLAUCONITE	0	0%	0%	1	0%	1%		0%	0%
ACCESORY		0%	0%		0%	0%		0%	0%
		0%			0%			0%	
OPAQUES	0	0%		0	0%			0%	
ORG.MATTER	1	0%		4	1%		13	4%	
FE OXIDE	4	1%		9	3%		0	0%	
MICRITE		0%			0%		33	11%	
CA CEMENT	126	42%		136	45%		109	36%	
SI CEMENT		0%			0%			0%	
CLAY	35	12%		24	8%			0%	
PYRITE		0%			0%			0%	
PRIMARY POROSITY		0%			0%			0%	
SECONDARY POROSITY		0%			0%		3	1%	
TOTALS=	300	100%	133.9	300	100%	126.2	300	100%	142.37

Table 3- continued.

COMPOSITION	GC 1.1			GC 2.8			GC 4.0		
	# GRAINS	TOTAL %	DETRITAL %	# GRAINS	TOTAL %	DETRITAL %	# GRAINS	TOTAL %	DETRITAL %
QUARTZ MONO	101	34%	67%	140	47%	72%	112	37%	64%
QUARTZ POLY	6	2%	4%	13	4%	6%	7	2%	4%
FELDSPARS		0%	0%		0%	0%		0%	0%
PLAGIOCLASE	11	4%	8%	8	3%	4%	20	7%	12%
ORTHOCLASE	8	3%	6%	7	2%	4%	3	1%	2%
MICROCLINE		0%	0%		0%	0%		0%	0%
PERTHITE	0	0%	0%		0%	0%		0%	0%
MICAS		0%	0%		0%	0%		0%	0%
MUSCOVITE	1	0%	1%	1	0%	1%	6	2%	3%
BIOTITE	3	1%	2%	3	1%	2%	2	1%	1%
CHLORITE	0	0%	0%		0%	0%	5	2%	3%
CHERT	3	1%	2%	0	0%	0%	0	0%	0%
SKELETALS UNK.		0%	0%		0%	0%		0%	0%
BRACHIOPODS		0%	0%		0%	0%		0%	0%
BRYOZOANS		0%	0%		0%	0%		0%	0%
ALGAE		0%	0%		0%	0%		0%	0%
ECHINODERM PLATES		0%	0%		0%	0%		0%	0%
ECHINODERM SPINES		0%	0%		0%	0%		0%	0%
BIVALVES		0%	0%		0%	0%		0%	0%
OSTRACODS		0%	0%		0%	0%		0%	0%
ROCK FRAGMENTS		0%	0%		0%	0%		0%	0%
SED. RX. FRAG.	7	2%	5%	10	3%	5%	0	0%	0%
IGN. RX. FRAG.	1	0%	1%		0%	0%		0%	0%
MET. RX. FRAG.	8	3%	6%	10	3%	5%	20	7%	12%
GLAUCONITE	0	0%	0%	0	0%	0%		0%	0%
ACCESORY	0	0%	0%	2	1%	1%	0	0%	0%
		0%			0%			0%	
OPAQUES	0	0%		2	1%		0	0%	
ORG.MATTER	7	2%		3	1%		2	1%	
FE OXIDE	11	4%		39	13%		1	0%	
MICRITE		0%			0%			0%	
CA CEMENT		0%			0%			0%	
SI CEMENT		0%			0%			0%	
CLAY	53	18%		15	5%		17	6%	
PYRITE		0%			0%			0%	
PRIMARY POROSITY	1	0%		1	0%		0	0%	
SECONDARY POROSITY	77	26%		45	15%		104	35%	
TOTALS=	300	100%	150.5	300	100%	195.5	300	100%	175.5

Table 3- continued.

COMPOSITION	GC 6.7			GC 11.4			GC12.5		
	# GRAINS	TOTAL %	DETRITAL %	# GRAINS	TOTAL %	DETRITAL %	# GRAINS	TOTAL %	DETRITAL %
QUARTZ MONO	133	44%	59%	107	36%	60%	124	41%	77%
QUARTZ POLY	4	1%	2%	8	3%	4%	1	0%	1%
FELDSPARS		0%	0%		0%	0%		0%	0%
PLAGIOCLASE	30	10%	13%	26	9%	14%	6	2%	3%
ORTHOCLASE	12	4%	5%	7	2%	4%	9	3%	6%
MICROCLINE		0%	0%		0%	0%		0%	0%
PERTHITE		0%	0%		0%	0%		0%	0%
MICAS		0%	0%		0%	0%		0%	0%
MUSCOVITE	8	3%	3%	1	0%	1%	2	1%	1%
BIOTITE	3	1%	1%	1	0%	1%	3	1%	2%
CHLORITE	1	0%	0%		0%	0%		0%	0%
CHERT	1	0%	0%	1	0%	1%	0	0%	0%
SKELETALS UNK.		0%	0%		0%	0%		0%	0%
BRACHIOPODS		0%	0%		0%	0%		0%	0%
BRYOZOANS		0%	0%		0%	0%		0%	0%
ALGAE		0%	0%		0%	0%		0%	0%
ECHINODERM PLATES		0%	0%		0%	0%		0%	0%
ECHINODERM SPINES		0%	0%		0%	0%		0%	0%
BIVALVES		0%	0%		0%	0%		0%	0%
OSTRACODS		0%	0%		0%	0%		0%	0%
ROCK FRAGMENTS		0%	0%		0%	0%		0%	0%
SED. RX. FRAG.	10	3%	4%	14	5%	8%	10	3%	6%
IGN. RX. FRAG.		0%	0%		0%	0%		0%	0%
MET. RX. FRAG.	21	7%	9%	13	4%	8%	6	2%	3%
GLAUCONITE		0%	0%		0%	0%	0	0%	0%
ACCESORY	1	0%	0%	0	0%	0%	0	0%	0%
		0%			0%			0%	
OPAQUES	0	0%		0	0%		1	0%	
ORG.MATTER	0	0%		2	1%		1	0%	
FE OXIDE	5	2%		36	12%		75	25%	
MICRITE		0%			0%			0%	
CA CEMENT		0%			0%			0%	
SI CEMENT		0%			0%			0%	
CLAY	18	6%		23	8%		10	3%	
PYRITE		0%			0%			0%	
PRIMARY POROSITY	2	1%			0%			0%	
SECONDARY POROSITY	51	17%		61	20%		52	17%	
TOTALS=	300	100%	224.2	300	100%	177.8	300	100%	160.5

Table 3- continued.

COMPOSITION	BB Iola			B 1.43			B 2.9		
	# GRAINS	TOTAL %	DETRITAL %	# GRAINS	TOTAL %	DETRITAL %	# GRAINS	TOTAL %	DETRITAL %
QUARTZ MONO		0%	0%	121	40%	59%	116	39%	67%
QUARTZ POLY		0%	0%	6	2%	3%	6	2%	3%
FELDSPARS		0%	0%		0%	0%		0%	0%
PLAGIOCLASE		0%	0%	23	8%	11%	20	7%	12%
ORTHOCLASE		0%	0%	15	5%	7%	11	4%	6%
MICROCLINE		0%	0%		0%	0%		0%	0%
PERTHITE		0%	0%		0%	0%	0	0%	0%
MICAS		0%	0%		0%	0%		0%	0%
MUSCOVITE		0%	0%	0	0%	0%	0	0%	0%
BIOTITE		0%	0%	0	0%	0%	0	0%	0%
CHLORITE		0%	0%	0	0%	0%		0%	0%
CHERT		0%	0%		0%	0%		0%	0%
SKELETALS UNK.	3	1%	3%		0%	0%		0%	0%
BRACHIOPODS	13	4%	13%		0%	0%		0%	0%
BRYOZOANS	64	21%	64%		0%	0%		0%	0%
ALGAE	0	0%	0%		0%	0%		0%	0%
ECHINODERM PLATES	18	6%	18%		0%	0%		0%	0%
ECHINODERM SPINES	3	1%	3%		0%	0%		0%	0%
BIVALVES		0%	0%		0%	0%		0%	0%
OSTRACODS		0%	0%		0%	0%		0%	0%
ROCK FRAGMENTS		0%	0%		0%	0%		0%	0%
SED. RX. FRAG.		0%	0%	13	4%	6%	10	3%	6%
IGN. RX. FRAG.		0%	0%		0%	0%		0%	0%
MET. RX. FRAG.		0%	0%	26	9%	13%	9	3%	5%
GLAUCONITE		0%	0%	0	0%	0%	0	0%	0%
ACCESORY		0%	0%	0	0%	0%	2	1%	1%
		0%			0%			0%	
OPAQUES		0%		0	0%		1	0%	
ORG.MATTER		0%		2	1%		3	1%	
FE OXIDE		0%		16	5%		48	16%	
MICRITE	175	58%			0%			0%	
CA CEMENT	25	8%			0%			0%	
SI CEMENT		0%			0%			0%	
CLAY		0%		9	3%		15	5%	
PYRITE		0%			0%			0%	
PRIMARY POROSITY		0%			0%			0%	
SECONDARY POROSITY		0%		68	23%		58	19%	
TOTALS=	300	100%	99.2	300	100%	204.7	300	100%	174.6

Table 3- continued.

COMPOSITION	BE 3.75			G1 16,3.5			G1 22,2.5		
	# GRAINS	TOTAL %	DETRITAL %	# GRAINS	TOTAL %	DETRITAL %	# GRAINS	TOTAL %	DETRITAL %
QUARTZ MONO	105	35%	61%	86	29%	48%	115	38%	66%
QUARTZ POLY	1	0%	1%	4	1%	2%	8	3%	4%
FELDSPARS		0%	0%		0%	0%		0%	0%
PLAGIOCLASE	28	9%	16%	32	11%	18%	14	5%	8%
ORTHOCLASE	2	1%	1%	10	3%	6%	9	3%	5%
MICROCLINE		0%	0%	0	0%	0%		0%	0%
PERTHITE		0%	0%		0%	0%		0%	0%
MICAS		0%	0%		0%	0%		0%	0%
MUSCOVITE	3	1%	2%	25	8%	14%	10	3%	6%
BIOTITE	0	0%	0%	3	1%	2%	0	0%	0%
CHLORITE		0%	0%	3	1%	2%	1	0%	1%
CHERT		0%	0%	0	0%	0%	1	0%	1%
SKELETALS UNK.		0%	0%		0%	0%		0%	0%
BRACHIOPODS		0%	0%		0%	0%		0%	0%
BRYOZOANS		0%	0%		0%	0%		0%	0%
ALGAE		0%	0%		0%	0%		0%	0%
ECHINODERM PLATES		0%	0%		0%	0%		0%	0%
ECHINODERM SPINES		0%	0%		0%	0%		0%	0%
BIVALVES		0%	0%		0%	0%		0%	0%
OSTRACODS		0%	0%		0%	0%		0%	0%
ROCK FRAGMENTS		0%	0%		0%	0%		0%	0%
SED. RX. FRAG.	22	7%	13%	7	2%	4%	10	3%	6%
IGN. RX. FRAG.		0%	0%		0%	0%		0%	0%
MET. RX. FRAG.	10	3%	6%	8	3%	4%	8	3%	4%
GLAUCONITE		0%	0%	0	0%	0%		0%	0%
ACCESORY	0	0%	0%	0	0%	0%	0	0%	0%
		0%			0%			0%	
OPAQUES	1	0%		0	0%			0%	
ORG.MATTER	2	1%		7	2%		3	1%	
FE OXIDE	18	6%		10	3%		6	2%	
MICRITE		0%			0%			0%	
CA CEMENT		0%		0	0%		56	19%	
SI CEMENT		0%			0%			0%	
CLAY	25	8%		31	10%		14	5%	
PYRITE		0%			0%			0%	
PRIMARY POROSITY		0%			0%			0%	
SECONDARY POROSITY	81	27%		75	25%		46	15%	
TOTALS=	300	100%	171.9	300	100%	177.8	300	100%	174.2

Table 3- continued.

COMPOSITION	G1 25,7.5			G1 26,6.0			G1 27,5.0		
	# GRAINS	TOTAL %	DETRITAL %	# GRAINS	TOTAL %	DETRITAL %	# GRAINS	TOTAL %	DETRITAL %
QUARTZ MONO	98	33%	48%	116	39%	58%	133	44%	69%
QUARTZ POLY	8	3%	4%	3	1%	2%	5	2%	3%
FELDSPARS		0%	0%		0%	0%		0%	0%
PLAGIOCLASE	34	11%	16%	26	9%	13%	17	6%	9%
ORTHOCLASE	12	4%	6%	9	3%	5%	6	2%	3%
MICROCLINE		0%	0%		0%	0%		0%	0%
PERTHITE	3	1%	2%		0%	0%	0	0%	0%
MICAS		0%	0%		0%	0%		0%	0%
MUSCOVITE	9	3%	4%	14	5%	7%	7	2%	4%
BIOTITE	1	0%	1%	5	2%	2%	1	0%	1%
CHLORITE	3	1%	2%	5	2%	2%	1	0%	1%
CHERT	0	0%	0%	1	0%	1%		0%	0%
SKELETALS UNK.		0%	0%		0%	0%		0%	0%
BRACHIOPODS		0%	0%		0%	0%		0%	0%
BRYOZOANS		0%	0%		0%	0%		0%	0%
ALGAE		0%	0%		0%	0%		0%	0%
ECHINODERM PLATES		0%	0%		0%	0%		0%	0%
ECHINODERM SPINES		0%	0%		0%	0%		0%	0%
BIVALVES		0%	0%		0%	0%		0%	0%
OSTRACODS		0%	0%		0%	0%		0%	0%
ROCK FRAGMENTS		0%	0%		0%	0%		0%	0%
SED. RX. FRAG.	17	6%	8%	10	3%	5%	11	4%	6%
IGN. RX. FRAG.		0%	0%		0%	0%		0%	0%
MET. RX. FRAG.	20	7%	10%	10	3%	5%	10	3%	5%
GLAUCONITE		0%	0%	0	0%	0%	0	0%	0%
ACCESORY	0	0%	0%	0	0%	0%	0	0%	0%
		0%			0%			0%	
OPAQUES	0	0%		0	0%		0	0%	
ORG.MATTER	5	2%		39	13%		5	2%	
FE OXIDE	15	5%		5	2%		14	5%	
MICRITE		0%			0%			0%	
CA CEMENT	7	2%			0%		3	1%	
SI CEMENT		0%			0%			0%	
CLAY	32	11%		20	7%		20	7%	
PYRITE		0%			0%			0%	
PRIMARY POROSITY		0%			0%			0%	
SECONDARY POROSITY	35	12%		37	12%		65	22%	
TOTALS=	300	100%	207.2	300	100%	200.0	300	100%	192.4

Table 3- continued.

COMPOSITION	NL 15,10.0			NL 17,1.5			NL 19,4.5		
	# GRAINS	TOTAL %	DETRITAL %	# GRAINS	TOTAL %	DETRITAL %	# GRAINS	TOTAL %	DETRITAL %
QUARTZ MONO	80	27%	55%	83	28%	58%	72	24%	48%
QUARTZ POLY		0%	0%	2	1%	2%		0%	0%
FELDSPARS		0%	0%		0%	0%		0%	0%
PLAGIOCLASE	21	7%	14%	20	7%	14%	23	8%	15%
ORTHOCLASE	3	1%	2%	4	1%	3%	15	5%	10%
MICROCLINE		0%	0%		0%	0%		0%	0%
PERTHITE		0%	0%		0%	0%		0%	0%
MICAS		0%	0%		0%	0%		0%	0%
MUSCOVITE	18	6%	12%	10	3%	7%	13	4%	9%
BIOTITE	1	0%	1%	2	1%	2%	1	0%	1%
CHLORITE	3	1%	2%	2	1%	2%	0	0%	0%
CHERT		0%	0%		0%	0%		0%	0%
SKELETALS UNK.		0%	0%		0%	0%		0%	0%
BRACHIOPODS		0%	0%		0%	0%		0%	0%
BRYOZOANS		0%	0%		0%	0%		0%	0%
ALGAE		0%	0%		0%	0%		0%	0%
ECHINODERM PLATES		0%	0%		0%	0%		0%	0%
ECHINODERM SPINES		0%	0%		0%	0%		0%	0%
BIVALVES		0%	0%		0%	0%		0%	0%
OSTRACODS		0%	0%		0%	0%		0%	0%
ROCK FRAGMENTS		0%	0%		0%	0%		0%	0%
SED. RX. FRAG.	17	6%	11%	10	3%	7%	23	8%	15%
IGN. RX. FRAG.		0%	0%		0%	0%		0%	0%
MET. RX. FRAG.	1	0%	1%	10	3%	7%	3	1%	2%
GLAUCONITE	0	0%	0%		0%	0%	0	0%	0%
ACCESORY	2	1%	2%		0%	0%	0	0%	0%
		0%			0%			0%	
OPAQUES	0	0%		0	0%			0%	
ORG.MATTER	10	3%		8	3%		23	8%	
FE OXIDE	4	1%		0	0%		11	4%	
MICRITE		0%			0%			0%	
CA CEMENT	11	4%		8	3%		9	3%	
SI CEMENT		0%			0%			0%	
CLAY	40	13%		9	3%		39	13%	
PYRITE		0%			0%			0%	
PRIMARY POROSITY		0%			0%			0%	
SECONDARY POROSITY	89	30%		132	44%		67	22%	
TOTALS=	300	100%	146.1	300	100%	143.4	300	100%	151.1

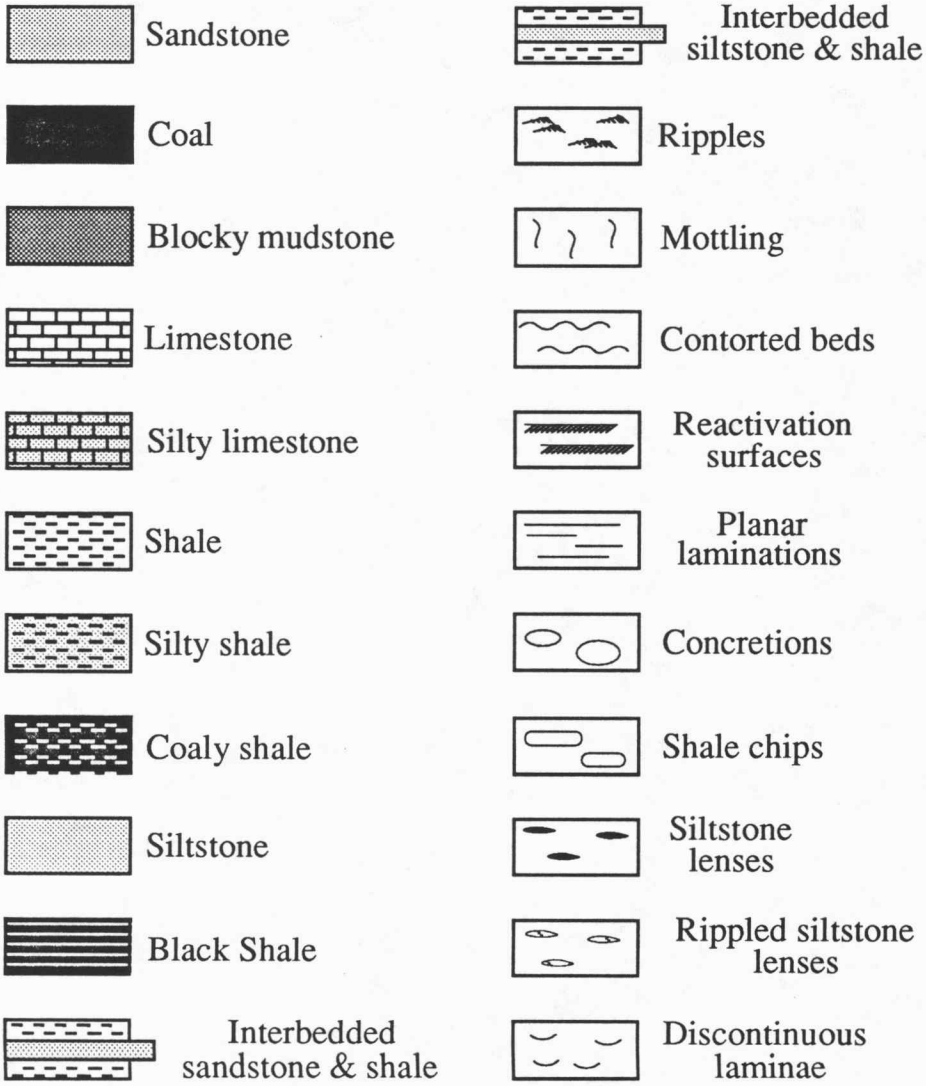
Table 3- continued.

COMPOSITION	NL 19,6.5			NL 20,4.5			
	# GRAINS	TOTAL %	DETRITAL %	# GRAINS	TOTAL %	DETRITAL %	
QUARTZ MONO	87	29%	72%	114	38%	60%	
QUARTZ POLY	1	0%	1%	5	2%	2%	
FELDSPARS		0%	0%		0%	0%	
PLAGIOCLASE	11	4%	9%	27	9%	14%	
ORTHOCLASE	8	3%	6%	6	2%	3%	
MICROCLINE		0%	0%		0%	0%	
PERTHITE		0%	0%		0%	0%	
MICAS		0%	0%		0%	0%	
MUSCOVITE	3	1%	3%	11	4%	6%	
BIOTITE	3	1%	3%	1	0%	1%	
CHLORITE	1	0%	1%	1	0%	1%	
CHERT		0%	0%	0	0%	0%	
SKELETALS UNK.		0%	0%		0%	0%	
BRACHIOPODS		0%	0%		0%	0%	
BRYOZOANS		0%	0%		0%	0%	
ALGAE		0%	0%		0%	0%	
ECHINODERM PLATES		0%	0%		0%	0%	
ECHINODERM SPINES		0%	0%		0%	0%	
BIVALVES		0%	0%		0%	0%	
OSTRACODS		0%	0%		0%	0%	
ROCK FRAGMENTS		0%	0%		0%	0%	
SED. RX. FRAG.	6	2%	5%	2	1%	1%	
IGN. RX. FRAG.		0%	0%		0%	0%	
MET. RX. FRAG.	0	0%	0%	22	7%	11%	
GLAUCONITE		0%	0%	0	0%	0%	
ACCESORY	0	0%	0%	0	0%	0%	
		0%			0%		
OPAQUES	0	0%		0	0%		
ORG.MATTER	38	13%		15	5%		
FE OXIDE	2	1%		12	4%		
MICRITE		0%			0%		
CA CEMENT	4	1%		11	4%		
SI CEMENT		0%			0%		
CLAY	50	17%		16	5%		
PYRITE		0%			0%		
PRIMARY POROSITY		0%			0%		
SECONDARY POROSITY	86	29%		57	19%		
TOTALS=	300	100%	120.0	300	100%	189.1	

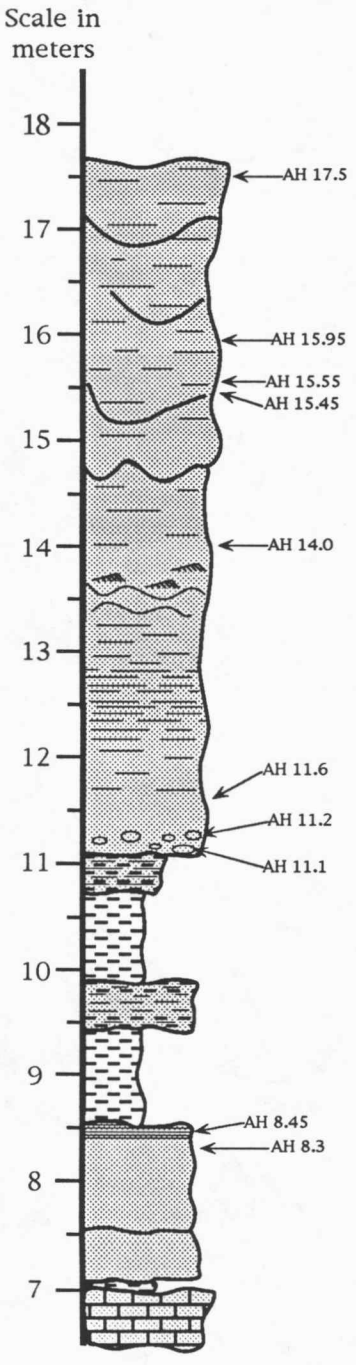
APPENDIX III

STRATIGRAPHIC COLUMNS

Key to stratigraphic columns symbols:



Section: Allin Hill
State: Kansas County: Montgomery
Location: SW, SW, sec. 32, T34S, R16E, west of Coffeyville, along US 169.



14.8-17.65m.
Finely-laminated, sandstone, with nested channels. Erosional contact with underlying unit. Top is massive with some plant remains.

11.1-14.8m.
Very fine-grained sandstone. Massive and thinly bedded (slabby), with shale chips, plant remains, planar, wavy, and ripple laminations. Pyrite and coaly concretions at the base. Sharp contact with underlying unit.

10.75-11.1m.
Thinly-laminated very fine-grained sandstone interbedded with silty shale. SS/Sh=3/1.

9.9-10.75m.
Clayey shale interbedded with fissile, silty shale.

9.45-9.9m.
Thinly-bedded, thinly-laminated, fine-grained sandstone. Plant remains and mica concentrated along bedding planes. Contact is gradational, grading upward from shaly sandstone, to massive sandstone, to shaly sandstone.

8.55-9.45m.
Fissile and poorly exposed clayey gray shale.

7.55-8.55m.
Massive, micaceous, Fe-oxide stained, fine-grained sandstone. Homogeneous at the base, thickly bedded at the top. Top 10 cm. are finely laminated.

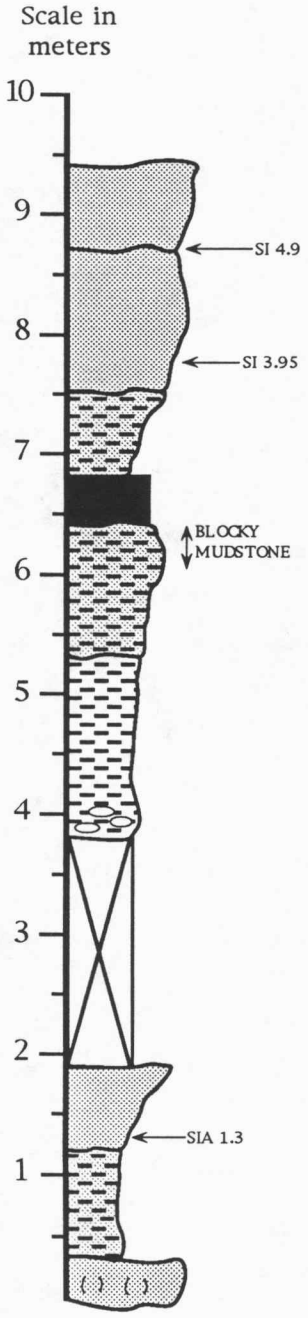
7.1-7.55m.
Massive, micaceous, thinly-bedded, fine-grained sandstone. Sharp contact with shale.

7.0-7.1 m.
Gray, clayey shale with Fe-oxide stains. Micaceous concentrations along bedding planes. Sharp contact with underlying unit.

6.5-7.0 m.
Limestone of the Cherryvale Fm., light gray and silty. Poorly exposed.

0-6.5 m.
Beds of Winterset Limestone to Nelly Bly Shale (not shown).

Section: South Independence
State: Kansas County: Montgomery
Location: NE, NE, SE, sec. 24, T33S, R15E



7.5-9.4m.
Slabby, massive, well-cemented, micaceous Fe-stained, fine-grained sandstone in gradational contact with silty shale. A contact surface occurs at 8.7 m.

6.8-7.5m.
Poorly exposed, silty shale in sharp contact with coal, Fe concentrations in layers. Siltier upwards.

6.4-6.8m.
Coal with sulfur and Fe concentrations along fractures. Plant structures preserved along bedding planes. Gradational contact with mudstone.

5.3-6.4m.
Highly weathered, Fe-oxide stained, silty shale. Organic matter and root casts increasing upwards. Top 35 cm. of unit is a poorly exposed blocky mudstone (underclay). Gradational contact with shale.

3.8-5.3m.
Fissile (chippy), poorly exposed, gray clayey shale. A layer of coaly concretions towards the base. Contact not exposed.

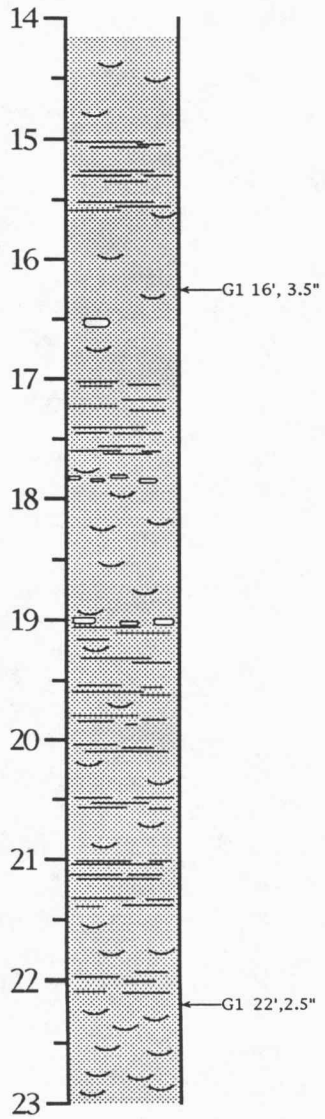
1.9-3.8m.
Covered Interval

1.2-1.9m.
Massive, blocky, micaceous, Fe-oxide stained, tightly cemented, fine-grained sandstone in gradational contact with silty shale.

0.30-1.2m.
Fissile, light-brown, silty shale in gradational contact with underlying sandstone. Poorly exposed.

0-0.30m.
Very fine-grained, massive, blocky sandstone, showing spheroidal weathering. Contact is not exposed.

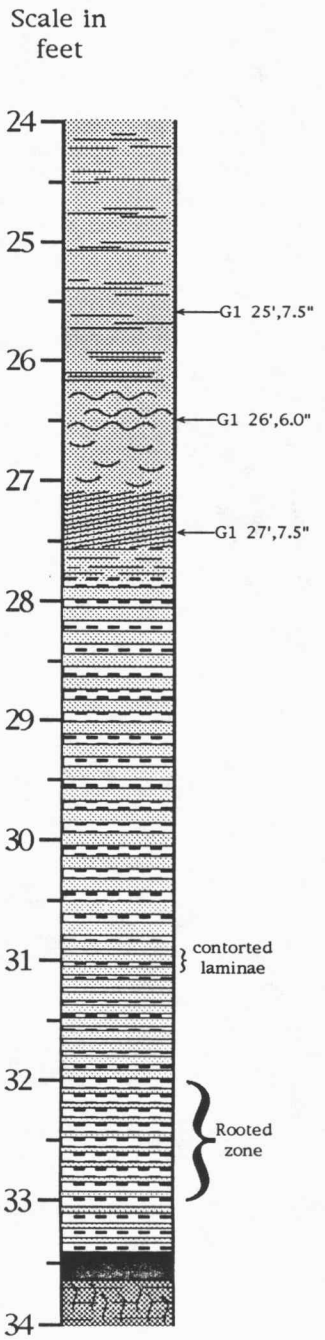
Gaddy # 1 Core
State: Kansas County: Montgomery
Location: NE, SE, SE, sec. 24, T31S, R16E



27',9.5"-14',2.0" ft
Fine-grained, micaceous, sandstone with scattered organic matter laminations. Some of the laminations are horizontal, or gently dipping while others are contorted and/or discontinuous. Organic matter content is higher towards the lower part. An area of heavy organic concentration is located from 26', 7.5" to 26', 2.5". Scattered fractures are stained with Fe-oxide. Some pyrite and shale chips (still soft) are present close to areas of high organic concentration. The unit is unfossiliferous and lies in gradational contact with the underlying unit. Carbonate cementation is present in the unit until 23',9.0".

Continued in next page.

Gaddy # 1 Core, continued.
State: Kansas County: Montgomery
Location: NE, SE, SE, sec. 24, T31S, R16E



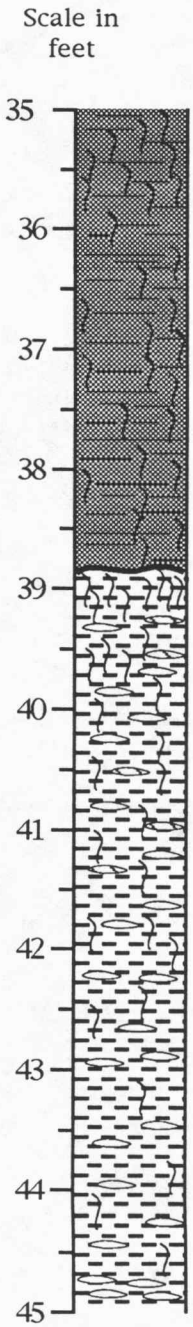
27', 9.5"-33', 5.0" ft
Interbedded siltstone and shale. Amount of siltstone and the thickness of the laminae increasing upwards. Spacing between laminae is rhytmic and decreasing upwards. Some of the laminae are contorted. Organic matter (plant fragments) is restricted to the lower part, mainly concentrated in a rooted zone (32', 11.5" -32', 2.5") where some of the fragments show pyritization. The unit is mottled at the base and is in sharp contact with the coal.

33', 5.0"-33', 8.0" ft.
Sulfurous coal. Poorly preserved, poorly recovered. Gap in core.

38', 10.0-33', 8.0" ft.
Medium to light gray, highly mottled, blocky mudstone. Some carbonaceous material and scattered organic matter are present. In sharp contact with underlying shale. Poorly preserved, poorly recovered. About 2' of gap in core.

Continued in next page.

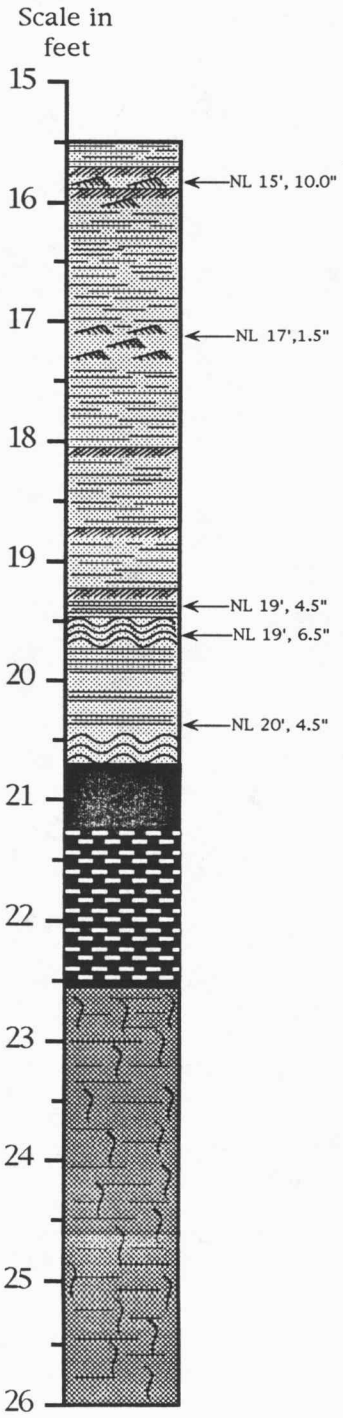
Gaddy # 1 core continued.
State: Kansas County: Montgomery
Location: NE, SE, SE, sec. 24, T31S, R16E



38', 10.0"-45', 0.0" ft
Unfossiliferous, mottled gray shale with silt lenses. Silt in lenses is gray, and sometimes rippled. The amount of lenses increases upwards as well as the mottling, and the degradation of the rock. Becomes blocky at the top.

45',0.0"-72',0.0"ft
Notstudied.

Joe Newland Core
State: Kansas County: Wilson
Location: NE, SE, SE, sec. 24, T31S, R16E



15',5.0"-20',9.5" ft.
Thinly-laminated, micaceous, Fe-oxide stained, organic-rich, fine-grained sandstone. Organic matter concentrated in laminae. In erosional contact with underlying coal. Parts of the coal are mixed in with the sandstone along contorted layers towards the base. Laminations increasing upwards from about 20'. Some ripple laminations, flaser bedding, and ractivation surfaces scattered within the sandstone. Grain size and cementation are constant throughout the sandstone.

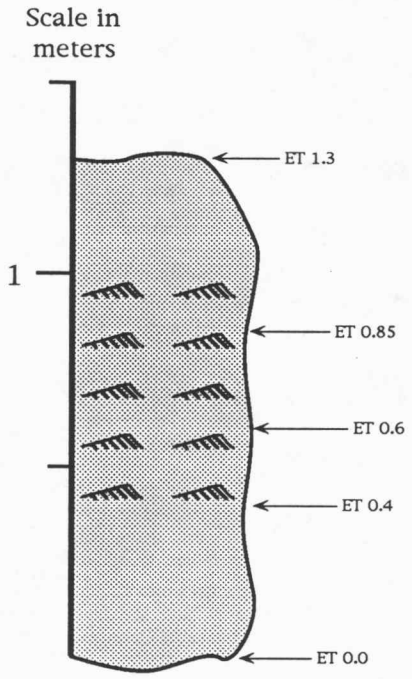
20',9.5"-21',3.5" ft.
Coal. Poorly preserved, poorly recovered. Some carbonates present along fractures. Sharp contact with underlying coaly shale.

21', 3.5"- 22', 6.5" ft
Fissile, organic-rich, coaly shale. Poorly preserved, and poorly recovered. Missing gap in core approximately 4.5".

22',6.5"-26',0.0"ft.
Light gray, silty, mottled, blocky mudstone. Well cemented and unfossiliferous. Progressively becoming darker and less cohesive upwards.

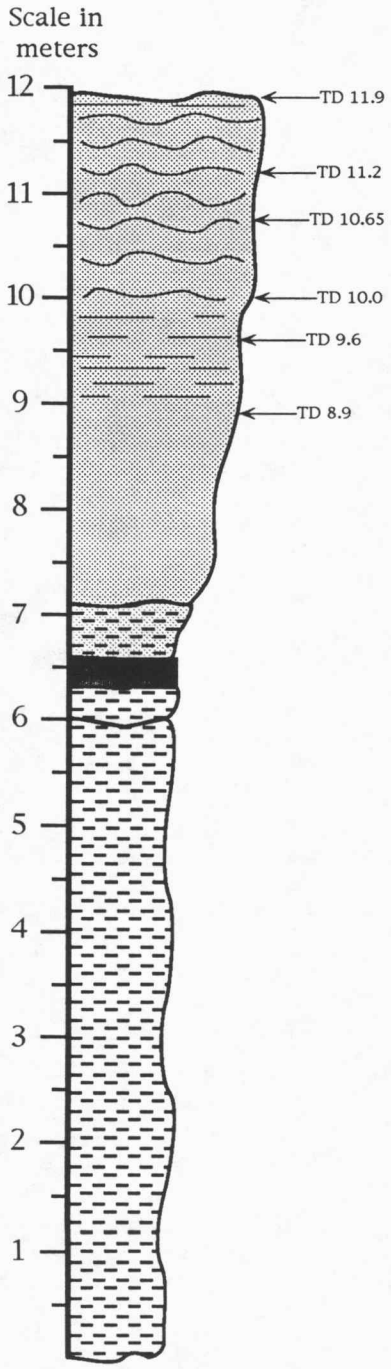
26',0.0"-56',0.0" ft.
Notstudied.

Section: East Thayer
State: Kansas County: Neosho
Location: SW, NW, sec. 20, T29S, R18S, west fork of Elk Creek.



0-1.3 m.
Thinly -bedded (slabby), micaceous, Fe-stained, fine-grained sandstone. Plant remains are present. The unit fines upward, showing ripple laminations towards the tops of individual slabs from 0.4 to 0.95 m. An overturned slab shows trace fossils and some finer sediments (mud) on the underside. Contact is not exposed.

Section: Thayer Dam
State: Kansas County: Neosho
Location: SW, NW, NW, sec. 30, T29S, R18E.



7.1 11.9 m.
Thinly-bedded, homogeneous, micaceous organic-rich, Fe-oxide stained, very fine-grained sandstone in gradational contact with shale-silty shale interbeds. Coarsening and grading upward into thinly-laminated, and contorted, better cemented sandstones. Contorted beds are lost towards the top.

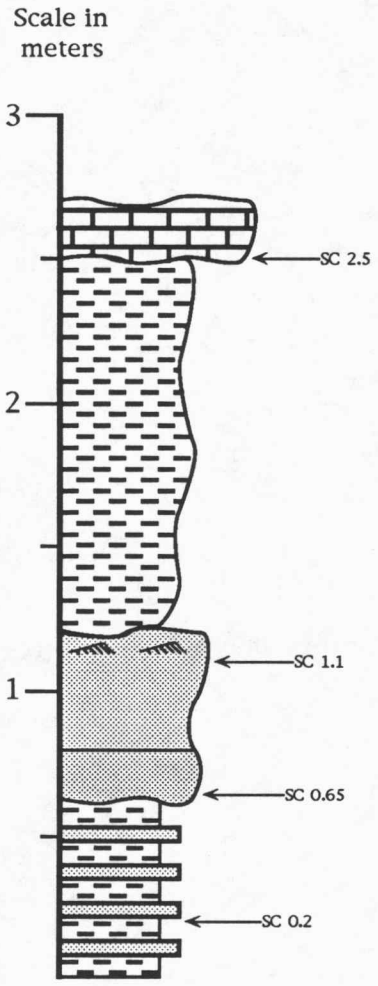
6.6-7.1
Fissile gray clayey shale grading upward into silty shale, to interbedded shale and siltstone. Gradational contact with underlying coal.

6.3-6.6
Fissile coal layer showing sulfurous concentrations along fractures. Organic plant structures are preserved along bedding planes. In gradational contact with mudstone.

6.0-6.3
Organic-rich (roots and plant material) blocky mudstone in gradational contact with underlying shale.

0-6 m.
Gray, fissile, clayey shale with Fe-oxide concentrations along fractures.

Section: South Chanute
State: Kansas County: Neosho
Location: SE, SE, sec. 10, T28S, R18E



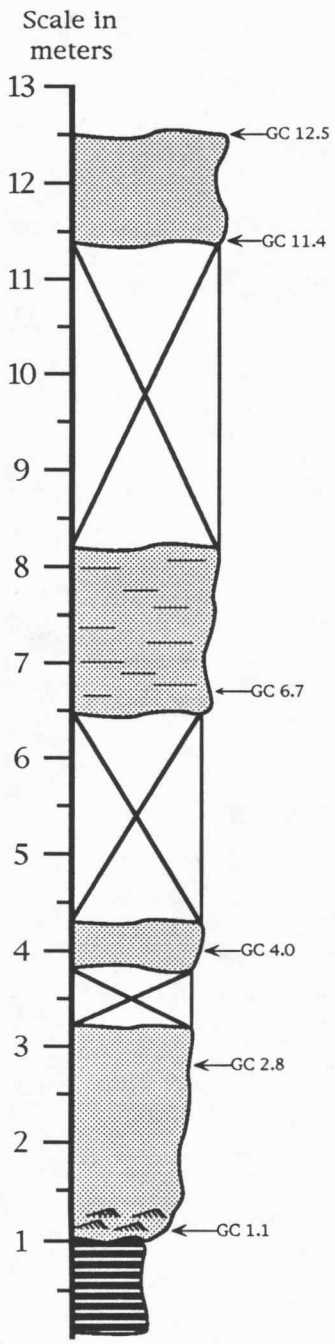
2.5-2.7 m.
Crinoidal limestone (Iola Limestone) in sharp contact with underlying shale. Bryozoans are also observed.

1.2-2.5 m.
Fissile, gray, clayey shale. Poorly exposed.

0.62-1.2 m.
Slabby, homogeneous, well-cemented, micaceous, fine-grained sandstone in sharp contact with underlying unit. A shale break at 0.8 m, separates the interval in two. Ripple laminations occur at the top of the interval.

0-0.62 m.
Interbedded sandstone and fissile silty shale. SS/Sh=3/1. Sandstone beds are micaceous, 2-3 cm thick, and showing Fe-oxide stains, and sparse planar laminations.

Section: Greenwood Cemetery
State: Kansas County: Neosho
Location: near c., E line, sec. 26, T27S, R18E



11.4-12.5m.
Slabby, micaceous, Fe-oxide stained, fine-grained sandstone. Poorly exposed.

8.2-11.4m.
Covered interval.

6.5-8.2 m.
Massive and slabby, micaceous, fine-grained sandstone. Sparse laminations, Fe-oxide stains and plant fragments. Poorly exposed.

4.3-6.5 m.
Covered interval.

3.8-4.3 m.
Massive, homogeneous, micaceous,very fine-grained sandstone. Poorly exposed.

3.2-3.8 m.
Covered interval.

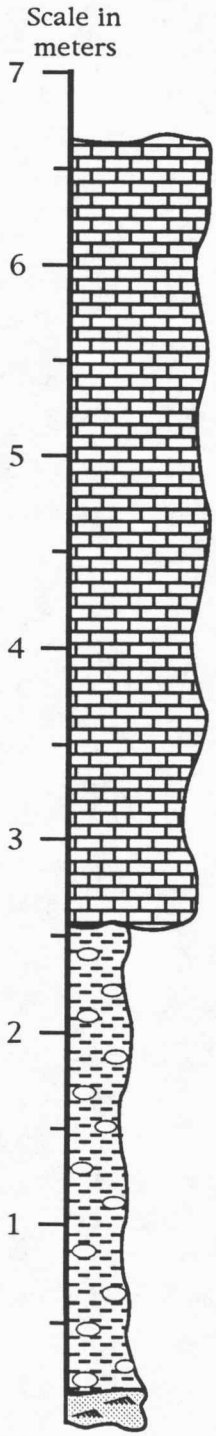
1.05-3.2m.
Massive, homogeneous, Fe-oxide stained, micaceous, fine-grained sandstone in sharp contact with redish clayey silt. Bottom of the sandstone is rippled, but massive upwards.

1.0-1.05m.
Unconsolidated, redish, clayey,silt. Poorly exposed (not shown).

0.05-1.0m.
Black, fissile, clayey shale.

0-0.05 m.
Covered interval.

Section: North Chanute
State: Kansas County: Neosho
Location: SE, SW, NE, sec. 33, T26S, R18E

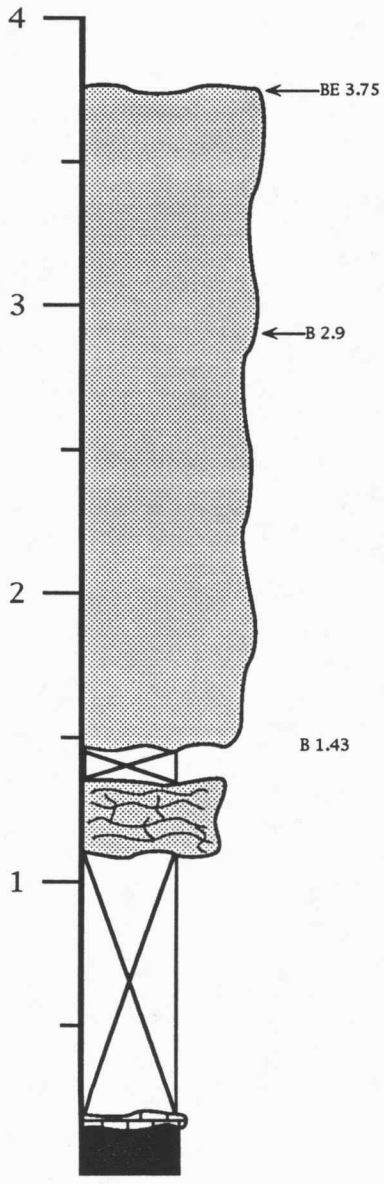


2.55-6.65m.
Crinoidal, micritic limestone, with scattered brachiopods and bryozoans in sharp contact with underlying shale. Highly recrystallized and blocky in appearance. Abruptly gradational surface at 3.85 m. (Iola Limestone).

0.15-2.55m.
Gray, fissile, clayey shale in gradational contact with the underlying siltstone. Large wood fragments and Fe-oxide concretions are present. Organic content and concretions are constant throughout the unit.

0-0.15m.
Extremely fissile, gray siltstone, with some organic content and ripples. Poorly exposed; contact is buried.

Section: Beagle
State: Kansas County: Linn, Miami co. line
Location: W line, NW, sec. 23, T19S, R22E



1.35-3.75m.
Very fine-grained, micaceous, Fe-oxide stained, slabby sandstone with organic matter. Individual beds are wavy, and 3-4 cm thick. Grain size and organic matter increase upwards.

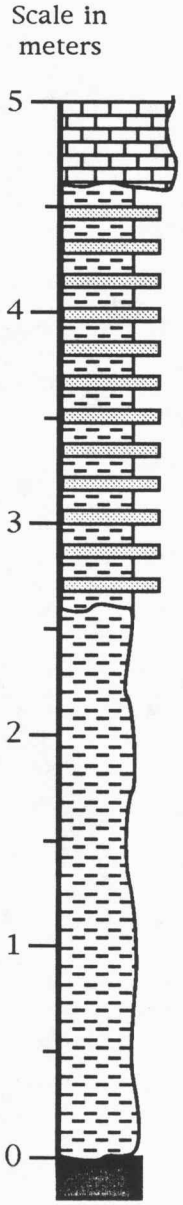
1.1-1.35m.
Mottled, fine-grained sandstone with organic matter.

0.20-1.1m.
Covered interval

0.15-0.20m.
Light gray limestone with organic matter in gradational contact with underlying coal.

0-0.15m.
Coal, poorly exposed.

Section: North Osawatomie
State: Kansas County: Miami
Location: SW, sec. 1, T18S, R22E



4.6 m.
Base of crinoidal limestone beds. Blocky appearance in sharp contact with underlying interval.

2.6-4.6 m.
Interbedded siltstone and shale. Poorly exposed, in gradational contact with underlying shale.

0-2.6 m.
Poorly exposed, gray,clayey shale with plant fragments (wood) in sharp contact with underlying coal.

?-0 m.
Coal with sulfur and Fe-oxide concentrations along fractures. Some pyrite is present and the organic structure of plant remains is preserved.

APPENDIX IV

MICROPROBE DATA

Table 4. Microprobe data of the Chanute Shale sandstones.

Sample ID	spot	CaO	MgO	MnO	FeO	SrO	SiO		CaCO3	MgCO3	MnCO3	FeCO3	SrCO3
		stoichiometric factors:											
		wt-%	wt-%	wt-%	wt-%	wt-%			mole-%	mole-%	mole-%	mole-%	mole-%
G1 22, 2.5	1	29.972	9.217	0.767	12.808	0.067	5.95		56.09	24.00	1.13	18.71	0.07
G1 22, 2.5	2	0.213	0.134	0.076	1.951	0.000	41.9		9.61	8.41	2.71	68.73	0.00
G1 22, 2.5	3	0.390	0.092	0.004	0.242	0.000	100		53.81	17.66	0.44	26.06	0.00
G1 22, 2.5	4	20.167	5.479	0.491	8.203	0.030	36.5		58.13	21.98	1.12	18.46	0.05
G1 22, 2.5	5	20.733	4.750	0.634	8.528	0.000	18.3		59.57	18.99	1.44	19.13	0.00
G1 22, 2.5	6	0.224	0.046	0.017	0.200	0.000	98.8		46.95	13.42	2.82	32.72	0.00
G1 22, 2.5	7	26.326	8.056	0.761	12.234	0.000	8.79		55.06	23.44	1.26	19.97	0.00
G1 22, 2.5	8	1.371	0.048	0.000	0.060	0.000	61.3		91.96	4.48	0.00	3.14	0.00
G1 22, 2.5	9	3.358	0.000	0.000	0.108	0.005	60.6		96.45	0.00	0.00	2.42	0.08
G1 22, 2.5	10	30.940	9.225	0.931	14.010	0.027	0.01		55.62	23.07	1.32	19.66	0.03
G1 22, 2.5	11	10.315	2.231	0.325	3.799	0.000	47.2		61.53	18.52	1.53	17.69	0.00
G1 22, 2.5	12	29.049	8.834	0.784	14.962	0.025	4.19		53.80	22.76	1.15	21.63	0.03
G1 22, 2.5	13	11.640	5.099	0.320	8.628	0.000	25.1		45.00	27.43	0.98	26.04	0.00
G1 22, 2.5	14	22.037	6.649	0.607	9.729	0.010	17.3		55.89	23.46	1.22	19.26	0.01
G1 22, 2.5	15	0.103	0.056	0.016	0.638	0.000	103		13.47	10.19	1.65	65.14	0.00
G1 22, 2.5	16	31.692	9.791	0.745	12.661	0.080	0.12		56.90	24.46	1.06	17.74	0.08
G1 22, 2.5	17	26.226	10.829	0.601	14.079	0.000	0.33		49.94	28.69	0.90	20.93	0.00
G1 22, 2.5	18	29.020	8.506	0.838	14.400	0.046	3.99		54.62	22.27	1.25	21.15	0.05
G1 22, 2.5	19	26.505	7.768	0.774	11.380	0.012	19		56.51	23.04	1.30	18.94	0.01
G1 22, 2.5	20	28.663	9.757	0.798	14.257	0.032	1.59		53.01	25.11	1.17	20.58	0.03
G1 22, 2.5	21	26.118	7.814	0.860	12.678	0.011	10.3		54.61	22.73	1.42	20.69	0.01
G1 22, 2.5	22	0.639	0.144	0.012	0.415	0.000	59.4		53.19	16.68	0.79	26.97	0.00
G1 22, 2.5	23	9.249	2.370	0.220	4.786	0.000	62.5		55.53	19.80	1.04	22.43	0.00
G1 22, 2.5	24	29.776	9.390	0.826	15.534	0.006	0.07		53.24	23.36	1.17	21.68	0.01

Table 4- continued.

Sample ID	spot	CaO	MgO	MnO	FeO	SrO	SiO		CaCO3	MgCO3	MnCO3	FeCO3	SrCO3
		stoichiometric factors:											
		wt-%	wt-%	wt-%	wt-%	wt-%			mole-%	mole-%	mole-%	mole-%	mole-%
G1 22, 2.5	25	28.092	10.137	1.037	15.963	0.026	0.04		50.42	25.32	1.47	22.37	0.03
G1 22, 2.5	26	16.673	4.158	0.475	11.703	0.000	40.9		50.90	17.66	1.15	27.88	0.00
G1 22, 2.5	27	27.973	8.441	0.715	11.433	0.062	8.81		56.85	23.87	1.15	18.14	0.07
G1 22, 2.5	28	29.844	9.369	0.843	13.250	0.022	2.12		55.35	24.18	1.24	19.18	0.02
G1 22, 2.5	29	0.072	0.033	0.014	0.308	0.000	74.1		17.81	11.36	2.74	59.47	0.00
G1 22, 2.5	30	31.165	9.593	0.859	12.533	0.075	0.2		56.75	24.30	1.24	17.81	0.07
G1 22, 2.5	31	1.163	0.277	0.028	0.356	0.000	99.6		62.99	20.87	1.20	15.05	0.00
G1 22, 2.5	32	27.621	10.567	0.749	12.474	0.027	2.17		52.80	28.11	1.13	18.61	0.03
G1 22, 2.5	33	5.327	1.454	0.017	2.493	0.000	84.7		56.92	21.62	0.14	20.79	0.00
G1 22, 2.5	34	30.096	9.239	1.036	13.133	0.036	0.57		55.63	23.76	1.51	18.95	0.04
NL 17, 1.5	1	30.795	9.777	0.844	13.851	0.058	0.06		55.05	24.32	1.19	19.33	0.06
NL 17, 1.5	2	0.030	0.044	0.000	0.171	0.000	101		12.63	25.77	0.00	56.18	0.00
NL 17, 1.5	3	0.058	0.255	0.000	0.695	0.000	40.8		5.85	35.80	0.00	54.74	0.00
NL 17, 1.5	4	0.049	0.078	0.000	0.136	0.000	86.4		18.49	40.96	0.00	40.06	0.00
NL 17, 1.5	5	0.829	0.254	0.000	0.310	0.000	46.5		58.55	24.96	0.00	17.09	0.00
NL 17, 1.5	6	0.448	0.197	0.000	0.201	0.000	32.4		51.73	31.65	0.00	18.12	0.00
NL 17, 1.5	7	0.000	0.000	0.000	0.000	0.000	0.12		-	-	-	-	-
NL 17, 1.5	8	28.004	17.305	0.198	2.108	0.010	3.56		55.23	47.49	0.31	3.25	0.01
NL 17, 1.5	9	0.055	0.124	0.005	0.255	0.000	45.6		12.56	39.39	0.90	45.44	0.00
NL 17, 1.5	10	0.078	0.153	0.000	0.579	0.000	67.9		9.93	27.10	0.00	57.54	0.00
NL 17, 1.5	11	0.233	0.599	0.001	1.706	0.000	47.8		9.35	33.43	0.03	53.41	0.00
NL 17, 1.5	12	11.479	4.057	0.209	6.003	0.000	10		52.21	25.67	0.75	21.31	0.00

REFERENCES CITED

Adler, F. J., coord., Lindberg Alan F., ed., 1987, Correlation of Stratigraphic Units of North America (COSUNA) Project, Mid-Continent Region, AAPG.

Arbenz, Kaspar J., 1989, The Ouachita System, *in* Bally, A. W., and Palmer, A. R., eds., The Geology of North America-An Overview: Boulder, Colorado, Geological Society of America, The Geology of North America, v. A., p. 371-396.

Bally, A. W., 1989, Phanerozoic basins of North America, *in* Bally, A. W., and Palmer, A. R., eds., The Geology of North America-An Overview: Boulder, Colorado, Geological Society of America, The Geology of North America, v. A., p. 397-446.

Bath, A. H., Milodowski, A. E, Spiro, B.,1987, Diagenesis of carbonate cements in Permo-Triassic sandstones in the Wessex and East Yorkshire-Lincolnshire Basins, UK: a stable isotope study *in,* Marshall, ed., Diagenesis of Sedimentary Sequences, Geological Society Special Publication No. 36, Blackwell Scientific Publications, p. 173-190.

Bjørlykke, K., 1984, Formation of Porosity: How important is it?, *in* McDonald and Surdam, eds., Clastic Diagenesis, AAPG Memoir 37, p. 277-286.

---------, 1988, Sandstone Diagenesis in Relation to Preservation Destruction and Creation of Porosity, *in* Chilingarian and Wolf eds., Diagenesis, I, Developments in Sedimentology 41, p. 555-584, Elsiever Press.

Blatt, H., 1979, Diagenetic Processes in Sandstones, *in* Scholle, P. A., and Schluger, P. R., Aspects of Diagenesis, SEPM Special Publication 26, Eastern and Rocky Mountain Sections SEPM, p. 141-158.

---------, 1982, Sedimentary Petrology, 1rst. ed., W. H. Freeman and Company, San Francisco, 557 p.

Boggs, S. Jr., 1987, Principles of Sedimentology and Stratigraphy, Merrill Publishing Company, 784 p.

Boles, J. R., 1978, Active ankerite cementation in the subsurface Eocene of southwest Texas, Contributions to Mineralogy and Petrology, v. 68, p. 13-22.

Boles, J. R., and Franks, S. G., 1979, Clay diagenesis in Wilcox Sandstones of southwest Texas; Implications of smectite diagenesis on sandstone cementation: Journal of Sedimentary Petrology, v. 49, p. 55-70.

Brenner, R L., 1989, Stratigraphy, petrology, and paleogeography of the upper portion of the Cherokee Group (Middle Pennsylvanian), eastern Kansas and northeastern Oklahoma, Geology Series 3, Kansas Geological Survey.

Brenner, R. L., and McHargue, T. R., 1988, Integrative Stratigraphy, Prentice Hall, p. 36-41.

Bucke, D. P., and Mankin, C. J., 1971, Clay-Mineral Diagenesis within interlaminated Shales and Sandstones, Journal of Sedimentary Petrology, v. 41, no. 4, p. 971-981.

Bunker, B. J., Witzke, B. J., Watney, W. L., and Ludvigson, G. A., 1988, Phanerozoic history of the central midcontinent, United States, *in* Sloss, L. L., ed., Sedimentary Cover-North American Craton; U. S.: Boulder, Colorado, Geological Society of America, The Geology of North America, v. D-2, p. 243-260.

Coleman, J. M., and Prior, D. B., 1982, Deltaic Environments of Deposition, *in* Scholle, P. A., and Darwin, S., eds., Sandstone Depositional Environments, AAPG Memoir # 31, p. 139-178.

Condra, G. E., 1949, The nomenclature, type localities and correlations of the Pennsylvanian subdivisions in eastern Nebraska and adjacent areas, Nebraska Geological Survey Bulletin (2nd series) 16, 67 p.

Davis, R. A. Jr., 1985, Coastal Sedimentary Environments, 2nd revised ed., Springer-Verlag, 716 p.

Eggleton, R. A, and Buseck, P. R., 1980, High resolution electron microscopy of feldspar weathering, Clays Clay Mineralogy, v. 28, p 173-178.

Fruit, David J., and Elmore, Douglas R., 1988, Tide and Storm Dominated Sand Ridges on a Muddy Shelf: Cottage Grove Sandstone (Upper Pennsylvanian), Northwestern Oklahoma., AAPG Bulletin, v. 72, n. 10, p. 1200-1211.

Haggiagi, Musa A., 1970, Stratigraphy and Environments of Deposition of the Chanute Shale (Pennsylvanian) in Southeastern Kansas, M. S. Thesis, University of Kansas.

Haworth, E., Bennett, J., 1908, General Stratigraphy of Kansas, Kansas University Geological Survey, v. 9, p. 57-121.

Haworth, E., Kirk, M. Z., 1894, A Geologic Section Along the Neosho River from the Mississippian Formation on the Indian Territory to White City, Kansas and along the Cottonwood River from Wyckoff to Peabody, Kansas University Quarterly, v. 2, p. 102-115.

Hay, R. L., 1966, Zeolites and zeolitic reactions in sedimentary rocks, GSA Special Paper 85.

Hayes, J, B., 1979, Sandstone Diagenesis-The Hole Truth, *in* Scholle, P. A., and Schluger, P. R., Aspects of Diagenesis, SEPM Special Publication 26, Eastern and Rocky Mountain Sections SEPM, p. 127-140.

Heckel, P. H., 1977, Origin of phosphatic black shale facies in Pennsylvanian cyclothems of midcontinent North America, AAPG Bulletin, v. 61, p. 1045-1068.

---------, 1979, Field Guide to Pennsylvanian Cyclic Deposits In Kansas and Nebraska, Ninth International Congress of Carboniferous Stratigraphy and Geology, Field trip No. 10, Pennsylvanian Cyclic Platform Deposits of Kansas and Nebraska, Guidebook Series 4, Kansas Geological Survey, The University of Kansas, p.1-49.

---------, 1980, Paleogeography of eustatic model for deposition of midcontinent Upper Pennsylvanian cyclothems *in* Fouch, T. D., and Magathan, E. R., eds., Paleogeography of west-central United States: SEPM, Rocky Mountain Paleogeography Symposium 1, p. 197-215.

---------, 1986, Sea-Level Curve for Pennsylvanian Eustatic Marine Transgressive-Regressive Depositional Cycles Along the Midcontinent Outcrop Belt, North America, Geology, v. 14, p. 330.

----------, manuscript in review, Revision of Missourian Stratigraphy in Kansas and Adjacent States, Kansas Geological Survey.

Hershey, H. G., Brown, C. N., Van Eck, O., and Northrup, R. C.,1960, Highway Construction Materials from the Consolidated Rocks of Southwestern Iowa, Iowa Highway Research Board Bulletin 15, 151 p., prepared by the Iowa Geological Survey.

Horne, J. C., Ferm, J. C., Caruccio, F. T., Baganz, B. P., 1978, Depositional Models in Coal Exploration and Mine Planning in the Appalachian Region, AAPG Bulletin, v. 62, p. 2379-2411.

Houseknecht, D., Wood, G., Jaques, R., Gresham, A., 1993, Influence of the Ozark Uplift on Pennsylvanian Dispersal Patterns, GSA Bulletin, Abstracts with programs, North-Central section, v. 25, n. 3, p. 26-27.

Kaiser, W. A., 1984, Predicting Reservoir Quality and Diagenetic History in the Frio Formation (Oligocene) of Texas, *in* McDonald and Surdam, eds., Clastic Diagenesis, AAPG Memoir 37, p. 195-216.

Klein, G., Willard, D. A., 1989, Origin of Pennsylvanian coal-bearing cyclothems of North America, Geology, v. 17, p. 152-155

Krauskopf, K. B., 1959, The Geochemistry of Silica in Sedimentary Environments, *in* Ireland, H. A., Silica in Sediments, SEPM Special Publication No. 7, p. 4-19.

Krumme, George W., 1981, Stratigraphic Significance of Limestones of the Marmaton Group (Pennsylvanian, Desmoinesian) in eastern Oklahoma, Oklahoma Geological Survey Bulletin 131, 71 p.

Meunier, A., and Velde, B., 1979, Weathering mineral facies in altered granites: The importance of local small-scale equilibria, Mineralogy Mag., v. 43, p. 261-268.

Mimran, Y., 1977, Chalk deformation and large scale migration of calcium carbonate, Sedimentology, v. 24, p. 333-360.

Moncure, G. K., Lahann, R. W., Siebert, R. M.,1984, Origin of Secondary Porosity and Cement Distribution in a Sandstone/Shale Sequence from the Frio Formation (Oligocene), *in* McDonald and Surdam, eds., Clastic Diagenesis, AAPG Memoir 37, p. 151-162.

Moore, R. C., 1936, Stratigraphic classification of the Pennsylvanian rocks of Kansas, Kansas Geological Survey Bulletin 22, 256 p.

----------,1948, Classification of Pennsylvanian Rocks in Iowa, Kansas, Missouri, Nebraska, and Northern Oklahoma, AAPG Bulletin, v. 32, n. 11, p. 2011-2040.

----------,1949, Divisions of the Pennsylvanian System in Kansas, Kansas Geological Survey Bulletin 83, 203 p.

Newell, N. D., 1935, The Geology of Johnson and Miami counties, Kansas, Kansas Geological Survey Bulletin 21, p. 7-150.

Oakes, M. C., 1952, Geology and Mineral Resources of Tulsa County, Oklahoma, Oklahoma Geological Survey Bull. 69, 234 p.

----------, 1959, Geology and Mineral Resources of Creek County, Oklahoma, Oklahoma Geological Survey Bulletin 81, p. 28-31.

Price, R. C., Mitchell, J. C., Ravn, R. L., 1985, Controls on Pennsylvanian Algal Mound Distribution in Mid-Continent North America, AAPG Bulletin, v. 69, n. 2, p. 298.

Rascoe, B. JR., and Adler, F. J., 1983, Permo-Carboniferous Accumulations, Mid-Continent U.S.A., AAPG Bulletin, v. 67, n. 6, p. 979-1001.

Schoewe, W. H., 1944, Coal Resources of the Kansas City Group, "Thayer" bed, in eastern Kansas, Kansas Geological Survey Bulletin, v. 52, Part 3, p. 81-118.

Schwartz, F. W., and Longstaffe, F. J., 1988, Ground Water and Clastic Diagenesis, *in* The Geology of North America, DNAG, v. O-2, Hydrogeology, p. 413-434.

Seevers, W. J., 1969, Geology and Ground-Water Resources of Linn County, Kansas, State Geological Survey of Kansas, Bulletin 193, University of Kansas Publications.

Siebert, R. M., , Moncure, G. K., Lahan, R. W., 1984, A Theory of Framework Grain Dissolution in Sandstones, *in* McDonald and Surdam, eds., Clastic Diagenesis, AAPG Memoir 37, p. 163-176.

Sloss, L. L., 1963, Sequences in the cratonic interior of North America, GSA Bulletin, v. 74, p. 93-114.

Stewart, G. F., 1975, Paleotectonic Investigations of the Pennsylvanian System In The United States. Part I: Introduction And Regional Analyses of The Pennsylvanian System, Kansas, Geological Survey Professional Survey, p. 125-156.

Tazaki, K. and Fyfe, W. S., 1986, Primitive Clay Precursors Formed on Feldspar, Canadian Journal of Earth Science.

Tucker, M. E, 1981, Sedimentary Petrology: an introduction to the origin of sedimentary rocks, 2nd. ed., Blackwell Scientific Publications, 260 p.

Udden, J. A., 1912, Geology and mineral resources of the Peoria quadrangle, Illinois, U. S. Geological Survey Bulletin 506, 1-103.

Wanless, H. R., and Shepard, F. P., 1936, Sea Level And Climatic Changes Related To Late Paleozoic Cycles, GSA Bulletin, v. 47, p. 1177-1206.

Watney, Lynn W., French, John, and Franseen, Evan K., 1989, Sequence Stratigraphic Interpretations and Modeling of Cyclothems in the Upper Pennsylvanian (Missourian) Lansing and Kansas City Groups in Eastern Kansas, Field guide 41st Annual Field Trip Kansas Geological Society, Kansas Geological Survey, The University of Kansas.

Weaver, C. E., 1989, Clays, Muds, and Shales, Developments in Sedimentology 44, Elsiever Press, 819 p.

Weller, J. M., 1930, Cyclical sedimentation of the Pennsylvanian Period and it's significance, Journal of Geology, v. 38, p. 97-135.

Welp, T. L, Thomas, L. A., and Dixon, H. R., 1957, A Correlation and Structural Interpretation of the Missourian and Virgilian Rocks Exposed Along the Middle River Traverse of Iowa, Iowa Academy of Science Procedures, v. 64, p. 418-420.